IMMUNOTHERAPEUTIC ACTION OF EXTRACELLULAR VESICLES
AND
EFFECTS OF TLR SIGNALING TO IMMUNE DYSFUNCTION OF SCI PATIENTS

A DISSERTATION SUBMITTED TO
THE GRADUATE SCHOOL OF ENGINEERING AND SCIENCE
OF BILKENT UNIVERSITY
IN PARTIAL FULFILLMENT OF THE REQUIREMENTS
FOR THE DEGREE OF
DOCTOR OF PHILOSOPHY
IN
MOLECULAR BIOLOGY AND GENETICS

By
Gözde Güçlüler
March 2017

Immunotherapeutic Action of Extracellular Vesicles and Effects of TLR Signaling to Immune Dysfunction of SCI patients

By Gözde Güçlüler

March, 2017

We certify that we have read this dissertation and that in our opinion it is fully adequate, in scope and in quality, as a thesis for the degree of Doctor of Philosophy.

İhsan Gürsel
(Advisor)

Tamer Yağcı

Kamil Can Akçalı

Özgür Şahin

Murat Alper Cevher

Approved for the Graduate School of Engineering and Science

Ezhan Karaşan

Director of the Graduate School of Engineering and Science

ABSTRACT

Immunotherapeutic Action of Extracellular Vesicles and Effects of TLR Signaling to Immune Dysfunction of SCI Patients

Gözde Güçlüler
Ph.D. in Molecular Biology and Genetics
Supervisor: İhsan Gürsel
March, 2017

The primary aim of this thesis is to extend the breadth of *in vivo* application of externally loaded exosomes as prophylactic or therapeutic carriers against disease treatment. Exosomes are secreted from all cells and could be purified from all bodily fluids; however, engineering of exosomes to carry specific ligands post-purification is a daunting task. Herein, we show that lyophilization of exosomes together with the biological cargo alone or in combination of CpG ODN motifs, model protein antigen ovalbumin or lipidic ligand alpha-galactosylceramide (αGC) followed by controlled reconstitution successfully internalizes these cargos within exosomes. Furthermore, the bioactivity of the loaded ligand(s) surpasses the unloaded free ligand activities. When tested *in vivo*, exosome incorporated ligand(s) proved to be significantly effective against model tumors such as E.G7 thymoma or established melanoma models. The mechanism behind this elevated immune activity is the ability of exosomes to be delivered to target cells and boost immune antigen dependent immune activation. Our *in vitro* findings revealed that encapsulation of CpG ODN into exosomes enhances immunostimulatory activity of CpG ODN than free form as evidenced by superior levels of cytokines like IL6, IL12 and Type-I and II interferons. This magnified immune activity might be partly due the increased APC activation observed as elevated CD86/MHCII surface marker expression. Immunization of C57/Bl6 mice with exosomal CpG ODN plus OVA induced strong Th1-biased anti-OVA response. Following thymoma induction in naive and OVA-immunized animals, >85% of exosomal vaccine treated mice cleared tumors whereas almost all naive animals were positive for tumor. This data suggests that CpG ODN encapsulation into exosomes improve immunostimulatory activity, provide better anti-OVA immunity thereby contribute effective tumor clearance in mice. A second aim of this thesis was to establish that it is feasible to load exosomes with more than two ligands. Next, invariant natural killer T (iNKT) cell ligand αGC was included within exosomes as the third element next to OVA and CpG ODN. Initial *in vivo*

studies revealed that exosomes containing αGC were significantly more potent in inducing antigen dependent immune responses in comparison to free form of CpG ODN, OVA and αGC. In therapeutic tumor vaccine model, two exosome injections (@d: 9 and d: 15) were done to B16-OVA tumor bearing animals and tumor regression was followed. Mice that had triple exosomal ligands significantly reduced tumors compared to mice treated with non-exosomal ligands. This study confirmed that exosomes with triple ligands could be effectively control established tumor development.

In this thesis, the elucidation of the involvement of extracellular vesicles (EVs) on the pathogenesis of autoimmune/autoinflammatory diseases was studied. The underlying mechanism in BD pathogenesis is still unclear. We found that one of the human cathelicidin group members, antimicrobial peptide LL37 along with EVs were elevated in active BD patients` plasmas. Strikingly, majority of plasma LL37 was associated with circulating EVs. We found that there was a strong correlation between i) LL37 level, ii) EV #/ml plasma and iii) cytokine production.

In the last part of this thesis, one of the possible mechanisms of immune dysfunction contributing to severe neurological deterioration of chronic spinal cord injured (SCI) patients was unearthed. We aimed to investigate whether there is a correlation between susceptibility to infections of chronic SCI patients within the context of impaired innate recognition of pathogen associated molecular patterns (PAMPs). Our data implicated that although there was no dysfunction of B cell, or $CD4^{+}$ Treg activity, but sensing TLR7 and TLR9 ligands by monocytes and pDCs were ablated in patients with SCI, leading to lower IFNγ and IP10 production along with co-stimulatory molecule expression, that could explain the immunological dysfunction in patient with SCI contributing to persistent complications.

Keywords: Extracellular vesicles, Microvesicles, Exosomes, Vaccine carrier, Anti-tumor therapy, Behçet's Disease, LL37, Spinal cord injury

ÖZET

Hücredışı Keseciklerin İmmünoterapötik Etkinlikleri ve TLR Yolaklarının Omurilik Hasarlı Hastalarda Görülen İmmün Disfonksiyona Etkileri

Gözde Güçlüler
Moleküler Biyoloji ve Genetik Bölümü, Doktora
Tez Danışmanı: İhsan Gürsel
Mart, 2017

Bu tezin temel amacı, dıştan yüklenmiş eksozomların hastalıklara karşı koruyucu ve terapötik taşıyıcılar olarak kullanımının *in vivo* uygulanabilirliğinin genişletilmesidir. Eksozomlar bütün hücreler tarafından salınmakta ve bütün vücut sıvılarından saflaştırılabilmektedir. Fakat saflaştırma sonrası eksozomların istenilen ligandlar ile yüklenmesi pek denenmiş bir yöntem değildir. Bu çalışmada, eksozomların kendi biyolojik kargolarının yanında CpG ODN dizinleri, model protein antijeni ovalbumin ve yağsı ligandlardan alpha-galactosylceramide (αGC) molekülü ayrı ayrı ya da birlikte kullanarak önce liyofilizasyonu yapılıp sonrasında da kontrollü rekonstrüksiyonu sonucunda bu kargoların eksozomlara başarılı bir şekilde yüklendiği gösterilmiştir. Eksozoma yüklenmiş ligandların immünolojik etkinliğinin yüklenmemiş serbest ligandların etkinliğinden daha yüksek düzeyde olduğu belirlenmiştir. *In vivo* çalışmalarda eksozoma yüklenmiş ligandların E.G7 timoma ve B16 melanoma tümör modellerinde oldukça etkili olduğu saptanmıştır. Gözlenen immün etkinlik artışının arkasındaki mekanizma, eksozomların hedef hücrelere kargoyu bozulmadan taşıyabilmesi ve antijene bağlı immün tepkinin gelişmesini sağlamasına bağlıdır. *In vitro* çalışmalar, CpG ODN'lerin eksozomlara yüklenmesiyle, serbest CpG ODN'lere göre immün uyarıcı etkinliğini artırdığını IL6, IL12, tip I ve II interferonlar gibi sitokinlerin yüksek seviyelerde salınmasını sağladığını gösterilmiştir. Bu artan immün etkinlik kısmen CD86/MHCII yüzey markörlerinin artışıyla gösterilen antijen sunum hücrelerin aktivitesindeki artıştan kaynaklanıyor olabilir. C57/B16 farelerin eksozomal CpG ODN ve OVA ile aşılanması güçlü bir anti-OVA Th1 tepkisine yol açmıştır. Aşılanmamış ve aşılanmış hayvanlarda timoma tetiklendiğinde, eksozomal aşı ile aşılanmış farelerin 85%'inde tümör gerilemişken, neredeyse bütün aşılanmamış hayvanlarda tümör gelişimi görülmüştür. Bu bulgular, CpG ODN'lerin eksozomlara yüklenmesiyle oluşan

immün uyarıcı mekanizmanın, güçlü anti-OVA bağışıklığı sağladığını ve farelerde anti-tümör tepkisini geliştirdiğini göstermektedir.

Bu tezin ikinci bir amacı, eksozomların ikiden fazla ligand ile yüklenmesinin uygulanabilir olduğunu göstermektir. İnvaryant doğal öldürücü T (iNKT) hücrelerinin ligandı αGC, eksozomlara OVA ve CpG ODN'lerin yanında üçüncü ligand olarak katılmıştır. Ön *in vivo* çalışmalar, αGC içeren eksozomların antijene bağlı immün tepkiye yol açmada ligandların serbest formlarina kıyasla çok daha etkili olduğunu ortaya çıkarmıştır. Terapötik tümör aşılaması modelinde, B16-OVA tümörü taşıyan hayvanlara 9. ve 15. günlerde iki eksozom enjeksiyonu yapılmış ve tümörlerde gerileme gözlenmiştir. Üç ligandla yüklenmiş eksozomlarla tedavi edilen farelerde eksozoma yüklenmemiş ligandlarla tedavi edilen farelere göre tümörlerde daha ciddi bir azalma görülmüştür. Bu çalışma, üçlü ligandlarla yüklenmiş eksozomların tümör gelişimini etkili bir şekilde geriletebildiğini ortaya koymuştur.

Bu tezde ayrıca, hücre dışı keseciklerin (EV) otoimmün ve otoinflamatuar hastalıkların patogenezindeki rolü araştırılmıştır. Behçet Hastalığı'nın (BH) patogenezinin altında yatan mekanizma hala belirsizdir. Çalışmalarımız, BH hastalarının plazmalarında EV'lerin yanısıra bir cathelicidin grubu üyesi antimikrobiyal peptid olan LL37'nin yüksek miktarda bulunduğunu göstermiştir. Çarpıcı bir şekilde, plazmadaki LL37'nin büyük çoğunluğunun dolaşımdaki EV'lerle asosiye olduğu tespit edilmiştir. Bu bağlantı hem EVlerin monositlere ve plazmasitoid dendritik hücrelere sevkiyatının artmasına, hem de IL1β, IL6, IP10, IFNα gibi sitokinlerin üretiminin işaret ettiği üzere immün aktivasyonunun tetiklenmesi ve sürdürülmesine aracılık etmekte, böylece şiddetli ve uzun süreli BH patolojisine katkıda bulunmaktadır. Çalışmalarımızda LL37 seviyesi, plazmadaki EV miktarı ve sitokin üretimi arasında güçlü bir korelasyon olduğu bulunmuştur.

Bu tezin son kısmında, kronik omurilik hasarlı hastalarda şiddetli nörolojik bozulmaya katkı sağlayan immün bozukluğun muhtemel bir mekanizması açığa çıkarılmıştır. Kronik omurilik hasarlı hastalarda enfeksiyona yatkınlık ile patojen ilişkili moleküler desenlerin (PAMP) tanınmasındaki bozukluklar arasında bir korelasyon olup olmadığı araştırılmıştır. Omurilik hasarlı hastalarda, B hücreleri ve $CD4^{+}$ Treg hücrelerinin etkinliğinde bir bozukluk olmamasına rağmen, monositler ve plazmasitoid dendritik hücreler tarafından TLR7 ve TLR9 ligandlarının tanınmasının işlevsiz olduğu, bunun da düşük IFNγ ve IP10 üretimi ile yardımcı uyaran molekül ifadesinde azalmaya yol açtığı belirlenmiştir. Bu mekanizma, omurilik hasarlı hastalardaki immünolojik bozukluğa bağlı kalıcı komplikasyonlara olan katkısını açıklayabilir.

Anahtar Kelimeler: Hücredışı kesecikler, Mikrokesecikler, Eksozom, Aşı taşıyıcı sistemler, Anti-tümor terapi, Behçet hastalığı, LL37, Omurilik hasarı

To my precious family…

Acknowledgements

First and foremost, I would like to express my gratefulness to my advisor Prof. Dr. İhsan Gürsel for his support, trust, patience and guidance. It was a privilege to be his student and learn the basis of being how to be a good scientist along with all the values he thought to me.

I would like to also thank to Prof. Dr. Mayda Gürsel deeply from my heart for supporting me in life and science based perspectives.

I would like to thank to my thesis committee members; Prof. Dr. Tamer Yağcı and Prof. Dr. Kamil Can Akçalı for sharing their experience, academic knowledge and guidance throughout the progress of my thesis project. Moreover, I am thankful to Assist. Prof. Dr. Özgür Şahin and Assist. Prof. Dr. Murat Alper Cevher for accepting to become my thesis jury members.

I want to share my gratefulness with all past and new members of Thorlab; Fuat Cem Yağcı, Arda Gürsel, Mehmet Şahin, İhsan Dereli, Yusuf İsmail Ertuna, Merve Deniz, Elif Senem Kayali, , Hakan Köksal, Begüm Yıldız, Özlem Bulut, Gizem Kılınç, Havva Özgen Kılgöz, Muzaffer Yıldırım, Gizem Tincer König, Kübra Almacıoğlu and Banu Bayyurt Kocabaş. Particularly, I would like to thank to Tamer Kahraman for his scientific support and friendship during my PhD studies in Thorlab. It was a privilege to work with these helpful and nice people. Also, I am thankful to MG Group members Bilgi Güngör, Esin Alpdündar and Cihan Ayanoğlu for their support and friendship.

I would like to also extend my gratitude to Assoc. Prof. Susanne Gabrielsson (from Karolinska Institutet, Stockholm, Sweden) for accepting me as a guest researcher to work in her group. Also, I want to thank to all members of Gabrielsson's research group especially to Pia Larssen for her support during and after my visit in Gabrielsson's laboratory in Karolinska Institutet.

It was a privilege to be a part of MBG family and work with amazing people. I believe that their friendship will remain in the rest of my life. I am thankful to Dilan Çelebi Birand, Merve Mutlu, Gülşah Dal Kılınç, Deniz Cansen Yildirim, Banu

Bayyurt Kocabaş, Ayşegül Örs, Özlem Tufanlı, Şeyma Demirsoy, Büşra Yağabasan, Füsün Doldur Ballı, Gurbet Karahan and Nilüfer Sayar Atasoy.

Particularly, I would like to thank to Defne Bayık and Verda Bitirim for their friendship with full of support and guidance. They never let me feel alone during this journey.

I want to share my thanks to MBG veterinarian Dr. Gamze Aykut for her help and guidance in animal experiments and technicians Abdullah Ünnü and Turan Dastandır for their support in technical issues.

I would like to share my gratefulness to Begüm Han Horuluoğlu for her precious friendship during all good and bad days. She will remain my best friend throughout of my life.

Finally, I want to thank to my parents Nurten and Sefa, my sister Gaye for their support, trust and guidance. Without their endless love, I couldn't accomplish to complete my PhD work. I hope I can always make them proud.

Contents

List of Figures

List of Tables

Abbreviations

αGC	alpha-Galactosylceramide
aBD	active BD
AFM	Atomic Force Microscopy
AICD	Activation induced cell death
AIM-2	Absent in melanoma 2
allo	Allogeneic
ALP	Alkaline phosphatase
AnV	Annexin-V
APC	Antigen presenting cell
ATP	Adenosine three phosphate
BD	Behçet's Disease
BSA	Bovine serum albumin
CCL	C-C motif chemokine ligand
CD	Cluster of differentiation
CeA	Carcinoembryonic antigen
CFSE	Carboxyfluorescein succinimidyl ester
DC	Dendritic cell
DIC	Differential interferance contrast
DLS	Dynamic Light Scattering
DNA	Deoxynucleic acid
EDTA	Ethylenediamine tetraacetic acid
EGFR2	Epidermal growth factor receptor 2
EGFRvIII	Epidermal growth factor receptor variant III
EV	Extracellular vesicles
FACS	Flourescence assosicated cell sorting
FasL	Fas ligand
gp100	Glycoprotein 100
GvHD	Graft versus host disease
HRP	Horseradish peroxidase

ICAM1	Intercellular adhesion molecule 1
IFN	Interferon
Ig	immunoglobulin
IL	Interleukin
IP-10	Interferon gamma-induced protein 10
iBD	inactive BD
L1CAM	L1 cell adhesion molecule
LEAF	Low Endotoxin, Azide-Free
LPS	Lipopolysaccharide
MART1	Melanoma antigen recognized by T cells 1
MCP-1	Monocyte chemoattractant protein-1
MDA-5	Melanoma differentiation-associated protein 5
MD-DC	Monocyte derived DC
MDSC	Myeloid-derived suppressor cell
MHC	Major histocompatibility complex
miRNA	MicroRNA
MMP	Metalloproteinase
mRNA	messenger RNA
MSC	Mesenchymal stem cell
MSC-EV	Mesenchymal stem cell derived EV
MV	Microvesicle
MVB	Multivesicular bodies
MyD88	Myeloid differentiation primary response 88
NK	Natural killer
NKG2D	Natural killer group 2D
NS	Not significant
ODN	Oligodeoxynucleotide
OVA	Ovalbumin
PBMC	Peripheral Blood mononuclear cell

PBS	Phosphate buffered saline
pDC	Plasmocytoid dentritic cell
PDGF	Platelet-derived growth factor
PMV	Platelet derived MV
PNPP	p-nitrophenyl phosphate
PS	Phosphatidylserine
RA	Rheumatic arthritis
RANTES	Regulated on activation, normal T cell expressed and secreted
RNA	Ribonucleic acid
RT	Room Temperature
siRNA	small interfering RNA
SLE	Systemic lupus erythematosus
SSc	Systemic sclerosis
TF	Tissue factor
TGFβ	transforming growth factor β
Th	T-helper
TLR	Toll-like receptor
TMB	3,3′,5,5′-Tetramethylbenzidine
TNFα	Tumor necrosis factor α
Treg	Regulatory T cell
TSG101	Tumor susceptibility gene 101
VEGF	Vascular endothelial growth factor

Chapter 1

Introduction

1.1. Extracellular Vesicles

Secretion of membrane-enclosed vesicles to the extracellular environment has been reported many decades ago. Membrane vesicles are secreted into the extracellular environment by almost all cell types from different organisms from eukaryotic to prokaryotic and this process has gained an important role since they have been found as key players in several cellular activities from cell-to-cell signaling to regulation of immune responses. It is possible to isolate extracellular vesicles (EVs) from any bodily fluids such as blood, saliva, urine, breast milk, amniotic fluid, ascites, cerebrospinal fluid, and semen. These EVs differ from each other in their biogenesis, size and biological functions and they are named as apoptotic vesicles, membrane particles, ectosomes, microvesicles and exosomes according to their distinctive features [1].

1.1.1. Types of extracellular vesicles

Starting from 1970s, presence of EVs outside of the cells including solid tissues, biological fluids, tumor cells and platelets were documented by several groups [2-7]. This group of vesicles was first shown to be released by cells directly outward budding of the plasma membrane (PM). In 1980s, a new EV secretion pathway was proposed describing the formation of vesicles approximately 50 nm in diameter initially within multivesicular bodies (MVBs) and release following fusion of MVBs with the PM [8, 9]. Then, in 1987, the term exosomes were first mentioned by Johnstone et al. to describe the formation and secretion of the EVs originated from endosomal pathway [10]. Today, it is known that EVs are heterogeneous populations composed of different types of vesicles classified according their sub-cellular origin and size (Fig 1.1).

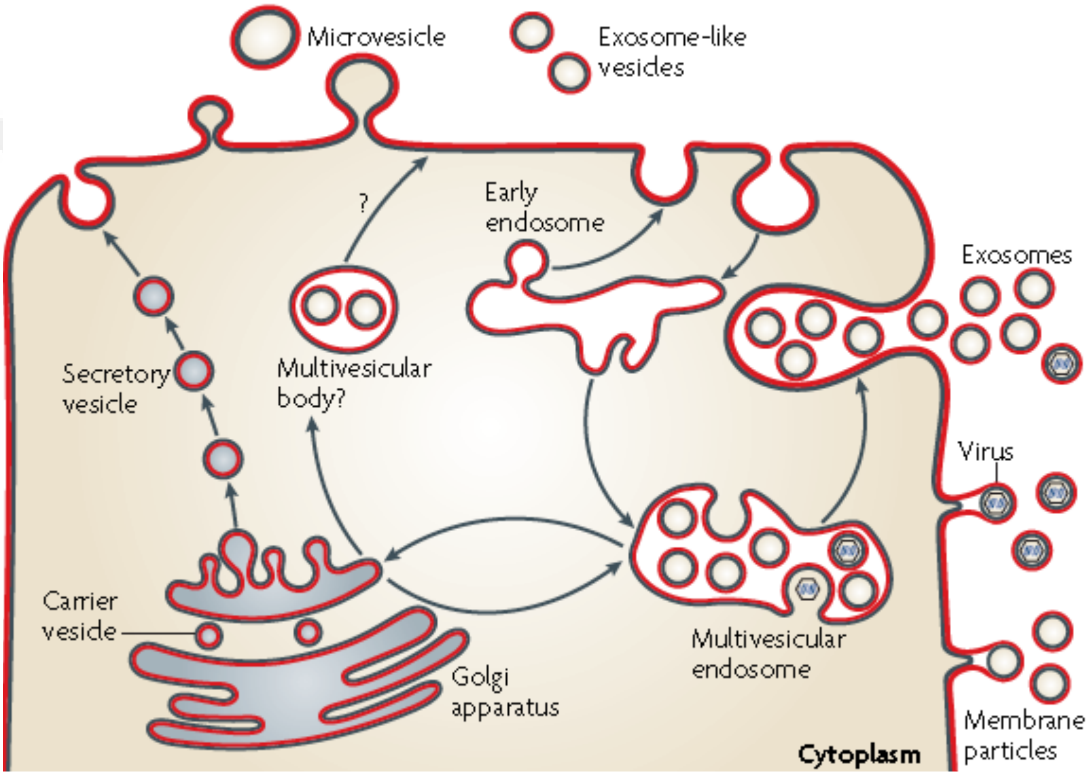

Figure 1.1. Different types of EVs secreted from cells.
There are different types of EVs depending on their formation mechanism and size. EVs can be formed by direct outward budding of PM like microparticles or by fusion of MVBs with the PM leading to release of vesicles called exosomes (adopted from [20]).

EVs are in the size range between 150-1000 nm and formed by direct budding from PM. They are nomenclatured with the terms ectosomes, shedding vesicles, microparticle and microvesicles according to their cell origin and sizes [11]. On the other hand, the term exosome is used for the vesicles with smaller size range between 30 and 100 nm formed within MVBs [5]. EVs are composed of lipid bilayer enclosing proteins and RNA as cargo proteins. They have a great impact on cell-to-cell communication as they are internalized by recipient cell via receptor-ligand interaction or by endocytosis and/or phagocytosis or even fuse with the target cell's membrane. These effects of EVs are dependent on the state of the cells that they are originated from and their cargo as it is proposed that they carry functional genetic materials such as mRNA, miRNA as cargo molecules [1, 11, 12].

1.1.2. Biogenesis of EVs

The formation of MVBs is a highly dynamic process from start to end along with involvement of internalization and recycling of membrane compartments [11, 13]. In this process, early endosomes generated by inward budding of the PM mature into the late endosomes; intracellular ligands and cellular compartments accumulate intraluminal vesicles (ILV) formed by inward budding of endosomal membrane changing the definition of endosomes to MVBs [14].

In general, MVBs are destined to fusion with the lysosomes to degrade the endosomal contents such as lipids, proteins and cytosol. On the other side, the fate of some MVBs, bearing tetraspanin molecule CD63, LAMP1 and LAMP2 (lysosomal-associated membrane proteins 1 and 2), can be released from the cells by fusion of MVBs with the PM. These different pathways for MVB formation propose that there are different subpopulations of MVBs within a cell. MVBs can differ in their morphology depending on the appearance and the size of the ILVS that they enclose [1, 15, 16].

There are two mechanisms proposed how ILVs are formed in MBVs (Fig 1.2). Endosomal sorting complex required for transport (ESCRT)-dependent mechanism is the best described explanation of the highly dynamic process of ILV formation. ESCRT is composed of almost thirty proteins that assemble into 4 different complexes ESCRT-0, I, II and III associated with several proteins such as ALIX, VTAI and Tsg101 [17]. All these complexes have different role in endocytic pathway including recognition and sequestration of transmembrane proteins in the endosomal membrane, membrane deformation into sorted cargo and vesicle excretion [17].

There are also evidences showing that ILVs and MVBs can be formed in an ESCRT-independent mechanism. This is proposed by different studies showing inactivation of four ESCRT complexes does not abrogate the formation of ILVs and MVBs [18]. These findings indicate that ILVs and MVBs can be generated by both ESCRT-dependent and independent mechanisms. However, this different mechanistic formation can lead to different consequences in the release yield and composition of EVs [19].

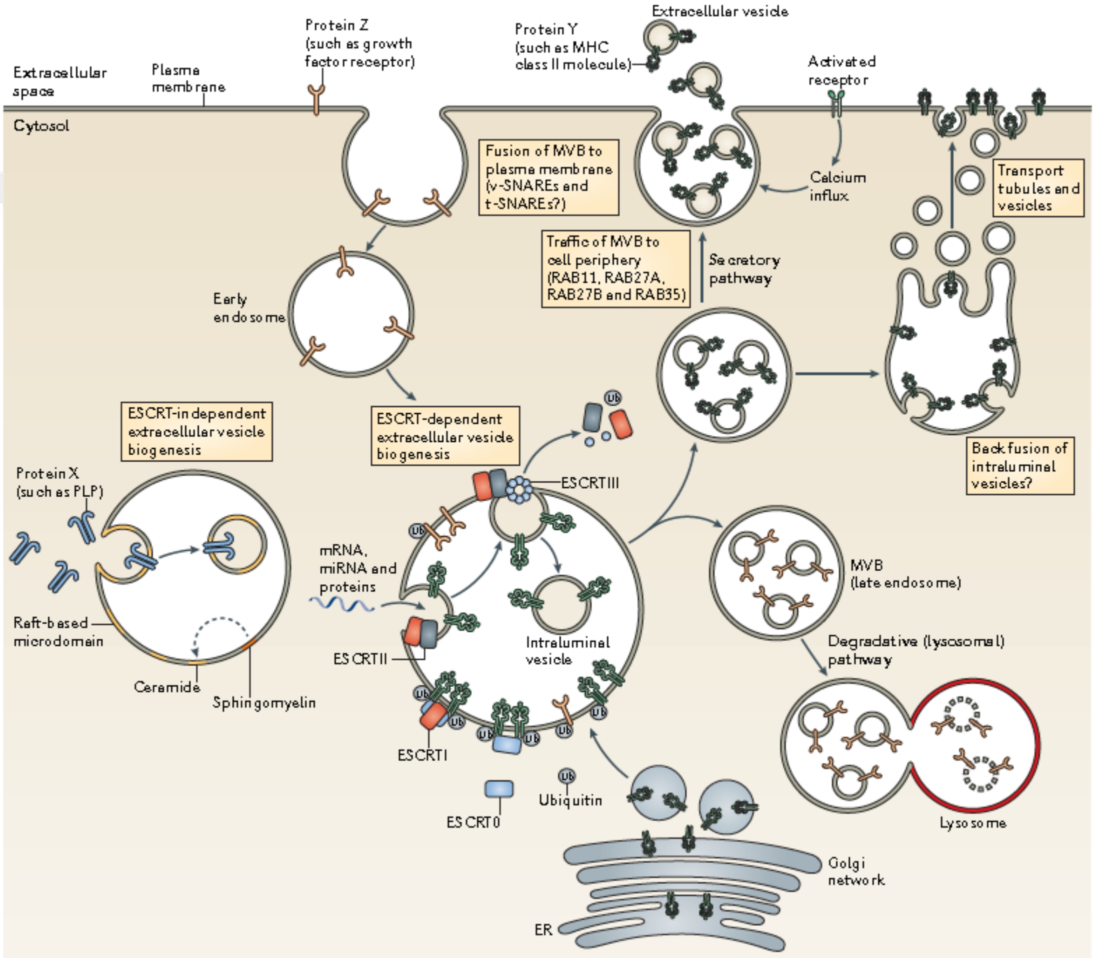

Figure 1.2. Biogenesis mechanisms of extracellular vesicles.

EVs are generated by ESCRT-dependent or independent pathways (adopted from [21]).

1.1.3. Composition and cargo of EVs

Although PM-derived EVs and exosomes have similar biogenesis pathways, they show distinctive physicochemical and molecular features (Fig 1.3). When their properties are compared, exosomes bear the hallmarks of ILVs and their composition is more likely closer to endosomal composition, whereas EVs are tend to show more PM characteristics [1]. Since exosomes are derived from the ILVs of which size range between 30 and 100 nm, exosomes released following MVB fusion with the PM would have a slightly larger size reaching to maximum 150 nm. In contrast, size of EVs released to the extracellular milieu following direct outward budding of PM can diverse between 150 nm and 1000 nm [20]. Sedimentation of exosomes and EVs is also different due to their different size ranges. While exosomes can be isolated by ultracentrifugation at 100000xg, larger vesicles should be isolated at lower speed from 10000xg to 50000xg [22, 23, 24]. In addition to ultracentrifugation, using sucrose gradient would be another alternative for isolation of exosomes that have density between 1.13 and 1.19 g/ml in sucrose [22]. Since studies showed that populations obtained by ultracentrifugation are composed of heterogeneous vesicles, each fraction should be characterized separately.

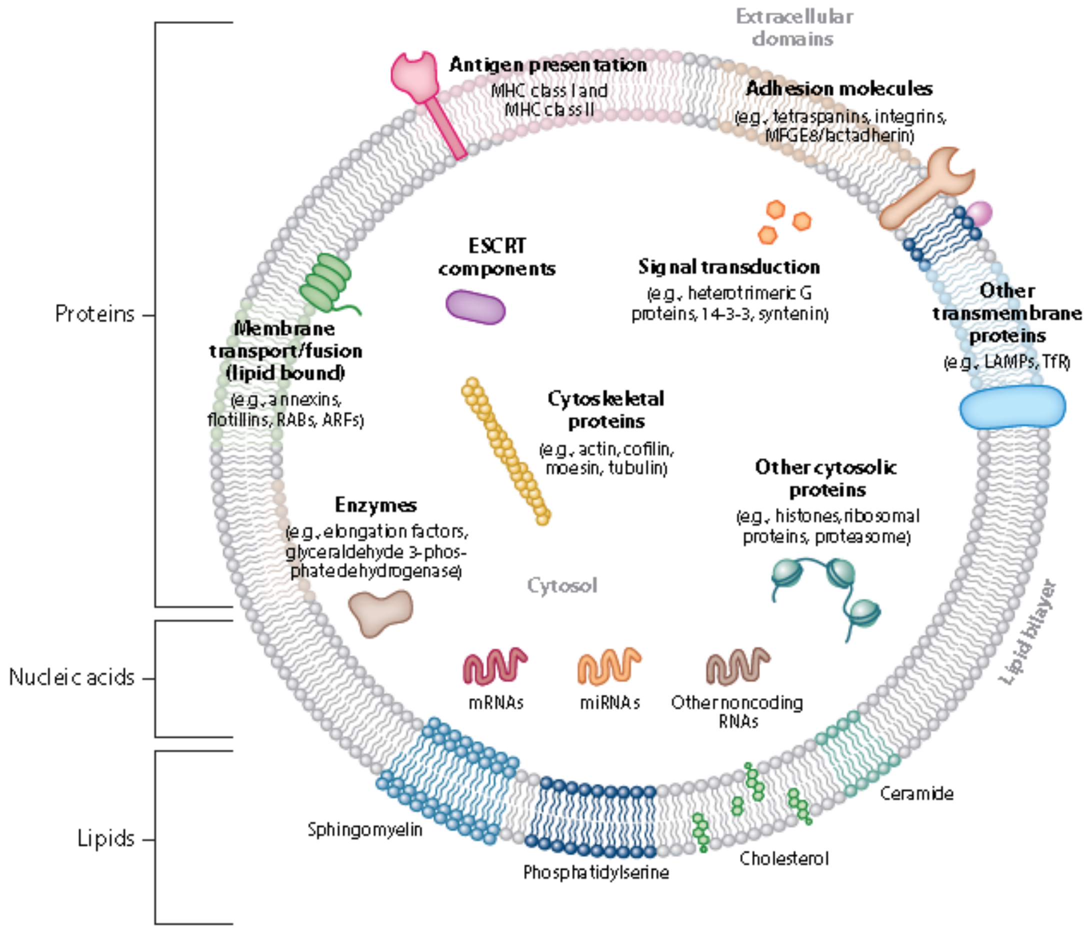

Figure 1.3. Composition of extracellular vesicles.

EVs are generated by ESCRT-dependent or independent pathways (adopted from [1]).

Exosomes contain biological contents as proteins, lipids and genetic materials. However, it has been shown that these contents are specific set of proteins, RNAs and lipids [21, 25]. Almost all exosomes are enriched in cytoplasmic proteins such as tubulin, actin, annexins and Rab proteins that can be find in the surface or in the lumen of exosomes [26]. Proteins associated with MVB formation such as Alix and Tsg101 are enclosed by exosomes [27, 28]. In 1998, it was found out that tetraspanins (CD63, CD81, CD82, CD53, CD37) were highly enriched on exosomes secreted from human B cells [29]. Other studies also showed that exosomes from other sources contain tetraspanin molecules [30]. Exosomes from different cell types also have been shown to carry Hsp70 and Hsp90 heat-shock proteins [10, 31]. Studies revealed that exosomes secreted from B cells carry MHC class I and MHC class II molecules [16, 32]. Exosomes have proteins on their membrane associated lipid rafts and also their membrane is enriched in cholesterol, sphingomyelin and hexosylceramides. Saturated and monounsaturated fatty acids also exist in exosomes [26]. In addition to their protein and lipid contents, they enclose genetic materials as mRNA and miRNA. This was first discovered in 2004 from blood of Hepatitis C virus (HCV) infected individuals that the virus envelope proteins were associated with exosomes [33]. It was also shown that mRNAs and miRNAs are transferred between cells via exosome-mediated mechanism (24). Following studies supported the existence of these genetic materials in exosomes from different cell types and body fluids [34-36]. Moreover, it has been revealed that exosomes also contain various types of small noncoding RNA molecules such as structural RNAs, tRNA fragments and small interfering RNAs [37, 38]. It is important to identify the exosome cargo by biochemical and biological techniques, since this kind of discovery elicits the understanding of the mechanisms associated with the exosomes in physiological and pathological conditions.

When PM derived EVs such as microvesicles are investigated, it has been documented that they share similar characteristics with exosomes. However, the most substantial difference of MVs from exosomes, apart from their larger size, is that they have similar surface composition to the cells that they are originated from.

Both exosomes and PM derived EVs have exposed phosphotidylserine (PS) on their surface. PS is a negatively charged molecule that tends to be located in the inner leaflet of the lipid bilayer in live cells in the presence of ATP by flippase [39, 40]. This feature makes it possible to identify the EVs by Annexin-V (AnV) staining [41]. Characteristics of EVs are summarized in Table 1.1. These physical and biochemical characteristics of exosomes and PM-derived EVs provide EV researcher to differentiate between different types of EVs.

Table 1.1. Differential characteristics of EVs [42].

	Exosome	Ectosome Microparticle (MP) Microvesicles (MV)	Others Apoptotic bodies (AP) Large vesicles (LV)
Size	30-100 nm	100-1000 nm	AB: 1-4 μM LV: 2-50 μM
Origin	MVB fusion with PM	Budding from PM	Budding from PM
Markers	Tetraspanins ((CD9, CD63, CD81) Alix, TSG101, HSP70)	Annexin V, Integrin, Selectin, CD40 ligand, metalloproteinase	AB: Annexin V, DNA, Caspase 3, Histones LV: Annexin V, ARF6, GAPDH
Isolation method	Ultracentrifugation (100000xg)	Ultracentrifugation (10000–50000xg)	Ultracentrifugation (6000–10000xg)

1.2. Role of EVs in Different Physiological Conditions

When EVs were first identified during monitoring of the loss of transferrin receptor, they were thought as just cell debris [8, 9]. However, when Raposo et.al. found out that Epstain-Barr virus (EBV) transformed B cell lines derived exosomes are enriched by MHC class II molecules and can present antigens to T cells [12], several important functions were started to be defined for EVs. It has been reported that EVs play crucial roles in vital cellular events from cell-to-cell communication to modulation of immune responses via transferring their cargo molecules. However, there is a great effort exposing the involvement of MVs to the pathogenesis of several diseases.

1.2.1 Modulation of immune responses by EVs

Since studies showed that EVs enclose both antigenic peptides and peptide-MHC complexes, they were thought that EVs could induce the immune activation [43]. It was revealed that exosomes isolated from tumor cells lines or patients' tumors have tumor antigens and *in vitro* settings showed that they trigger T cell activation when there is DCs in the environment [44, 45]. The most common antigens carried by tumor derived exosomes are transmembrane proteins (human EGFR2, carcinoembryonic antigen CeA) or endosomal components such as MART1, GP100 and tyrosine-related protein 1 of the cells that exosomes are originated from.

In addition to activation of immune responses by antigens, EVs can directly activate T cells by peptide-MHC class complexes displayed on their surface, too. Numerous studies documented that exosomes derived from DCs trigger cytotoxic T cell activation even if they are alone or incubated with MHC Class I expressing DCs [46-49]. This suggests that exosomes carry physiologically functional MHC class I molecules. However, studies with immature and mature DCs pointed out that mature DC-derived exosomes are more potent in inducing T cells then those derived from immature DCs, since they carry co-stimulatory molecules [50]. However, the only way to activate $CD8^+$ T cells with exosomes derived from tumor cells is to incubate cells with exosomes in the presence of DCs having the right MHC haplotype [44,45].

In addition to presence of MHC Class I molecules, exosomes isolated from APCs could also carry a large amounts of MHC Class II molecules [16, 51]. It was shown that these exosomes can transmit peptide-MHC Class II complexes to the DCs lacking MHC Class II molecule and then these DCs can trigger antigen specific $CD4^+$ T cells [52, 53]. Like $CD8^+$ T cell activation, exosomes derived from immature DCs are more potent activators of $CD4^+$ T cells [52, 54]. Not only exosomes, PM derived microvesicles derived from mature DCs can also induce activation of allogeneic T cells via transfer of MHC molecules to DCs [55].

Immune activating properties of vesicles secreted from other cell types have been reported, too. It was shown that platelet-derived exosomes trigger proliferation, survival and chemotaxis of hematopoietic cells [56]. Moreover, these exosomes were shown to be functional in induction of pro-inflammatory cytokine secretion from monocytes and activated B cells through CD40L present in exosomes [57, 58]. Furthermore, it was determined that EVs derived from macrophages infected with pathogens such as Mycobacterium tuberculosis, *Salmonella enterica subsp. enterica*, *serovar Typhimurium* or *T. gondii* carry microbial antigens and they induce activation of both $CD4^+$ and $CD8^+$ T cells in *in-vitro* and *in-vivo* settings [58, 59]. It was also documented that B- and T-cells can be activated by pro-inflammatory exosomes derived from cell cultures infected by *Mycoplasma orale* and *Mycoplasma arginini* [60].

Studies also showed that EVs derived from cells can also exhibit immune suppressive profile [43]. Especially tumor derived exosomes were identified with immune suppressive characteristics. It was shown that EVs secreted from tumor cells of patients provide immune escaping by CD95L presence on their surface via triggering T cell apoptosis [61]. Also, exosomes isolated from tumors inhibit cytotoxic profile of T and natural killer (NK) cells [62, 63]. It was shown that this inhibitory capacity of tumor derived exosomes on NK and $CD8^+$ T cells could be correlated with the presence of NK2GD ligands and transforming growth factor-β (TGF-β) on the membrane of exosomes [63, 64]. Moreover, exosomes can trigger activation of regulatory T cell (Treg) signaling pathways and thus prevent interleukin 2 (IL2) mediated T cell proliferation [64]. Moreover, exosomes derived from tumor cells can induce generation of myeloid-derived suppressor cell (MDSC) because of activated Treg signaling by TGF-β dependent pathway attenuating the differentiation of myeloid precursors to DCs [65-67]. Collectively, tumor derived vesicles can play crucial role in the modulation of immune responses with dual activation mechanisms.

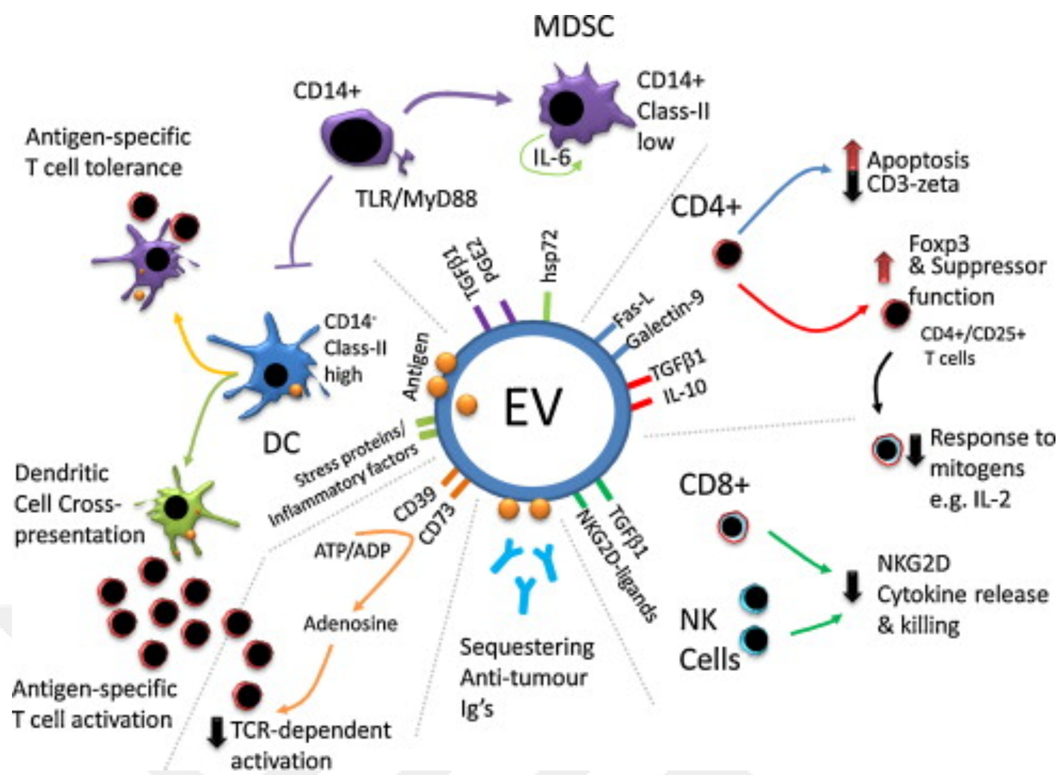

Figure 1.4. EVs modulate immune responses.

These include transmission of tumor-antigens to dendritic cells (DC), which may cross-present these to T cells, or may tolerize T cells in an antigen specific manner. EV-antigens may sequester antibodies, impacting antibody-dependent killing of tumor cells. Differentiation of myeloid (CD14+) cells to functional antigen presenting cells is inhibited by EV supporting the generation of myeloid derived suppressor cells (MDSC). T lymphocytes may undergo apoptosis, or downregulate functionally important receptors, and a subset of CD4^{+}CD25-high cells may be induced into regulatory cells, that suppress proliferation to mitogenic stimuli. NK cell functions may also be impaired through loss of activating surface receptors. (adopted from [68]).

Other than activating properties of immature DC derived exosomes, they also exhibit tolerogenic effect on cells. In a mouse septic shock model, it was shown that CD95L or IL10 harboring DC derived exosomes could reduce the inflammation mediated by macrophages [69, 70]. Moreover, tumor derived exosomes were shown suppressing immune responses in the absence of co-stimulatory molecules and promoting tumor development in mice vaccination model with exosomes [62]. Studies showed that exosomes isolated from Treg cell mediate immune suppression due to the presence of CD73 [30]. These exosomes decrease the antigen presenting function of DCs thus led to suppression of cytotoxic activity of $CD8^+$ T cells. In addition, presence of CD25 and CTLA-4 molecules on exosomes secreted from Tregs suggests that the suppression of CD4+ and CD8+ T cell activities by Treg derived exosomes could be mediated by CTLA-4 dependent pathway [71].

Collectively, both *in vitro* and *in vivo* findings propose that EVs can play dual role in the modulation of immune responses (Fig 1.5). Depending on the state of the donor cells, exosomes encounter different compositions leading to activation of different immunological pathways in the recipient cells.

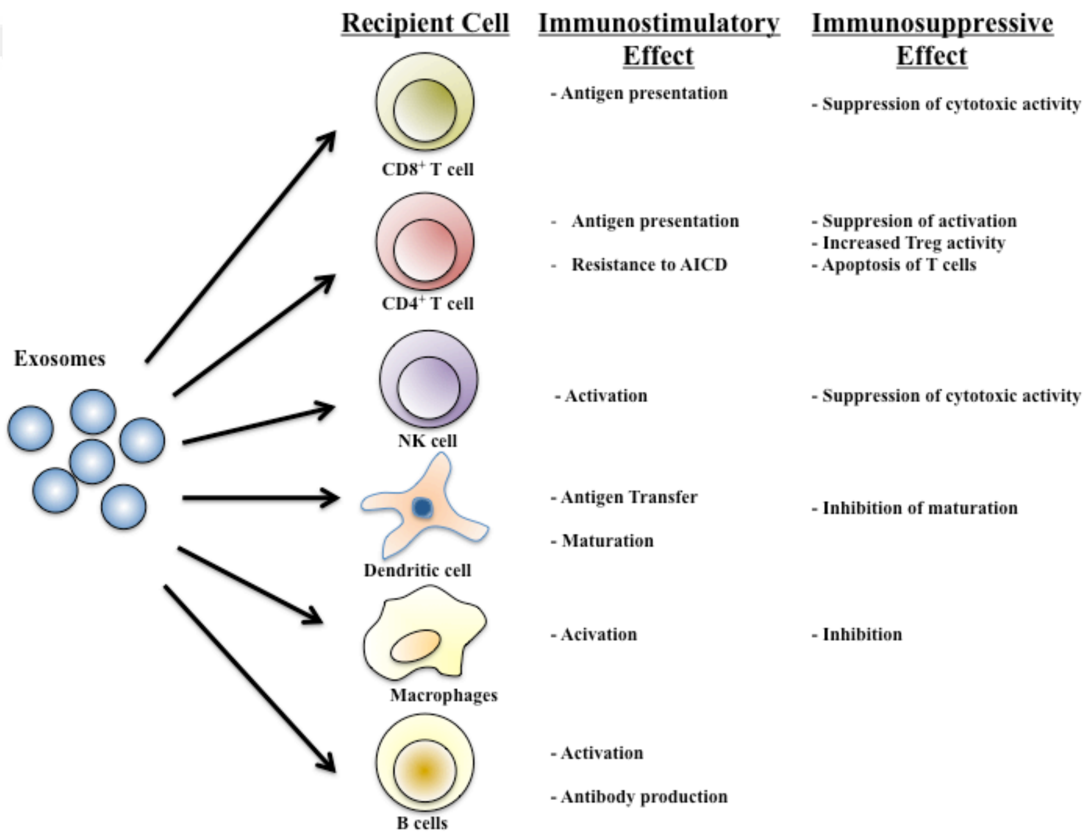

Figure 1.5. Representative modulatory effects of exosomes on immune cells.

Exosomes induce immunostimulatory and immunosuppressive pathways depending on the cells they are originated from. (Adopted from [72]).

1.2.2. Role of EVs in disease pathogenesis

1.2.2.1. EVs in cancer

EVs secreted from tumor cells play critical roles in communication between tumor and stromal cells even between distant microenvironments. They regulate invasion, angiogenesis, coagulation and immune suppression of tumors [73].
Active communication between neighbor cells and their microenvironment is crucial for during primary tumor formation. Tumor cells were identified with critical roles in cell-to-cell communication between tumor cells and their surrounding counterparts.

During primary tumor formation, oncogenic molecules are transferred between tumor cells by tumor-secreted EVs. It was shown that microvesicles derived from EGFRvIII expressing glioma cells were shown expressing EGFRvIII and they transmit this molecule to other malignant cells [74]. Following internalization of EVs by the recipient cells, mitogen-activated protein kinase (MAPK) and protein kinase B (PKB/Akt) are activated by EGFRvIII which triggering cancer growth [75]. EVs derived from tumors do not affect only other tumor cells, they also trigger different signaling pathways in adjacent stromal cells like fibroblasts and endothelial cells. It was shown that glioblastoma-derived microvesicles advocate proliferation of endothelial cells and growth of primary tumors as they transmit their cargo molecules mRNA, miRNA and angiogenic [35]. Pancreatic cancer-derived exosomes were also shown that they induce expression of angiogenic proteins in endothelial cells expressing tetraspanin 8 [76]. Contribution of tumor derived exosomes to tumor growth, vascularization and invasion was determined by fibroblast to myofibroblast transition mediated by TGF-β expressing tumor derived exosomes [77, 78]. Exosomes derived from breast cancer were shown promoting TGF-β expression, vascular endothelial growth factor (VEGF), stromal cell-derived factor 1 (SDF-1), and C-C motif chemokine ligand 5 (CCL5) in adipose tissue derived mesenchymal stem cells [79].

In addition to tumor derived vesicles, stromal cell derived exosomes can also induce the tumor growth. It was shown that tumor motility and invasion can be advocated by breast-cancer-associated fibroblasts by activation of the Wnt-planar cell polarity

(Wnt-PCP) signaling cascade [80]. These data suggest that the role of EVs in tumorigenesis is bidirectional between tumor cells and their microenvironment.

Studies showed that extracellular matrix (ECM) remodeling influence the tumor invasion. This influence was shown to be promoted by the contribution of tumor derived EVs. Exosomes secreted from tumor cells having fibronectin were shown to induce cell motility [81]. It was documented that microvesicles from tumor cells transfer EMMPRIN to fibroblasts and induces the MMP production leading to tumor metastasis [82]. EVs derived from endothelial cells stimulated with VEGF and fibroblast factor 2 (FGF-2) triggered tumor invasion via initiating proteolysis [83].

Thrombotic complications are one of the major causes leading death in cancer patients [84]. Recognition of cancer cells by immune system is hampered in case of coagulation and platelet accumulation at tumor location and tumor growth and metastasis is promoted [85]. It was shown that microvesicles associated with coagulation are derived from platelets, inflammatory cells, and cancer cells [86]. In cancer patients, it was found out that increased risk of coagulation is strongly associated with elevated levels of circulating microvesicles expressing tissue factor (TF) thrombosis [86-88]. Microvesicles derived from pancreatic cancer cells were shown containing physiologically active F- and P-selectin glycoprotein ligand 1 (SELPLG). When these vesicles are delivered to injury site, they induce the inhibition of bleeding [87]. Collectively, these data propose that tumor derived EVs play important roles in coagulation promoting progression and metastasis of tumor [87, 88].

Accumulating evidences also showed that tumor derived EVs play modulatory role in immunosuppression that leads to progression of cancer. It was shown that tumor derived microvesicles carrying Fas ligand or TRAIL induces apoptosis of immune cells [89, 90] Tumor derived exosomes were also determined that they can suppress the cytotoxic activity of NK cell [91].

1.2.2.2. EVs in inflammatory diseases

Accumulating evidences suggest that EVs do not only play important role in tumor formation, they also influence the progression of inflammation involving in communication between the infected cells and interaction between host cells and bacteria [92].

It has been the most investigated question whether EVs can trigger or provide the maintenance of pathological autoimmune response as a target of autoreactive recognition. It was shown that EVs enclose several autoantigens such as HSPs, histones, and α-enolase [93]. Moreover, EVs were identified with a potential role in rheumatoid arthritis (AR), since it was found out that they carry citrullinated proteins (CD5 antigen-like precursor and fibrinogen components) [94, 95]. Studies with RA patients showed that immune recognition is mediated by antigens associated with EVs. RA pathogenesis is promoted by formation of pro-inflammatory immune complexes between large microvesicles derived from synovial fluid of patient with RA with citrullinated protein-specific, vimentin-specific and fibrinogen-specific autoantibodies [94].

RA associated EVs are particularly microvesicles originated from platelets (PMV). It was shown that level of PMVs is elevated in patients with RA compared to healthy individuals. Moreover, elevated number of PMVs in circulation inflammatory joints is strongly associated with disease severity [95-99]. In RA studies, disease progression is mediated by pro-inflammatory cytokines carried by PMVs [100]. Also, microvesicles of RA patients contributes to cardiovascular comorbidities [99, 102]. Of note, microvesicles isolated from synovial fluids of patients with RA were shown to induce inflammatory cytokine and chemokine production such as IL8, IL6, CCL5 (also known as RANTES), CCL2 (also known as MCP1), vascular endothelial growth factor A (VEGF) and intercellular adhesion molecule 1 (ICAM-1) by cultured synoviocytes [103]. PMVs also trigger synoviocyte activation.

Besides RA, PMV level was found elevated in patients with systemic lupus erythematous (SLE) [104, 105]. However, none of the studies with SLE patients show any correlation between the elevated PMV number and disease severity [98].

On the other hand, studies showed that increased number of circulating EVs contributes to thrombosis and induces cardiovascular risk in SLE patients. Studies showed that the composition of EVs in SLE were different from the EVs from RA, systemic sclerosis (SSc) and healthy individuals. They were shown to have immunoglobulins, complement and other opsonizing molecules [105]. EVs from patients with SLE were also found correlated sustained inflammation and disease pathogenesis similar to RA pathogenesis [106].

Also, elevated numbers of EVs were documented in patients with systemic sclerosis (SSc) mediating contribution of activated cell populations to pathogenesis [107] Endothelial cell apoptosis which has been suggested to be a primary pathogenic event in SSc might be substantially modulated by high concentrations of circulating EVs [108].

1.3. Application of EVs

1.3.1 Diagnostic and prognostic application of EVs

EVs are secreted from almost cell types and it is possible to isolate them from all bodily fluid such as plasma, serum, saliva, urine. Biological cargo and composition of EVs can differentiate according to the physiological condition of the cell that they are originated from. As it was mentioned above, EVs contributes to pathogenesis of several diseases like cancer and inflammatory diseases, there are several studies investigating whether EVs can be used as diagnostic marker for diseases.

There are accumulating evidences revealed that levels of microvesicles are elevated in malignant effusions, serum, and urine from cancer patients [8]. Moreover, the prognosis and survival of cancer patients were shown to be strongly associated with different levels of platelet derived microvesicles [109, 110]. Microvesicles enclosing tissue factor (TF) or mucin were determined as diagnostic marker for adenocarcinomas [111]. These evidences suggest that MVs can be considered as potential diagnostic molecules for several cancer types due to their specific composition.

In addition to protein composition, MVs from patients with cancer were shown carrying specific mRNA and miRNA molecules. It was shown that oncogenic mRNA molecules HER-2/neu and MAGE-1 HER-2/neu were highly expressed in MVs from patients with gastric cancer [112]. Of note, it was also revealed that MVs from glioblastome patients had cancer specific mRNA and miRNA [35].

Morphology of MVs can be also used as a diagnostic marker as it was evidenced by the comparison of MVs from patients with prostate cancer and healthy individuals by electron microscopy. This study showed that urine of the prostate cancer patients contains cup-shaped exosomes whereas healthy urine has prostasomes [113].

In another study, it was shown that size of the MVs in plasma of patients with preeclampsia changes in addition to the elevated number [114].

Collectively, MVs can be used as diagnostic markers by analysis of them in three classes as following; i) MV quantity, (ii) MV protein composition, and (iii) MV miRNA or mRNA composition [115].

1.3.2. Therapeutic application of EVs as delivery tools

EVs play important roles in cell-to-cell communication and modulation of immune response due to their differential composition and capability of transferring cargo molecules. These evidences suggest that particularly exosomes are potential therapeutic agents due to their stable structures.

EVs can be used to modulate immune responses in pathological conditions such as autoimmune and inflammatory diseases depending on the state of origin cells. Particularly, EVs derived from mesenchymal stem cells (MSC) (MSC-EVs) are the most extendedly investigated population among EVs for therapeutic and regenerative purposes [116]. In an experimental acute injury study, it was shown that tubular injury was prevented via transmission of anti-apoptotic signals by MSC-EVs [117, 118]. Moreover, it was shown that levels of EVs are increased in MSC rich fragments and they provided the protection against tissue destruction [117]. In another study, it was shown that M2 type macrophage polarization could be mediated by MSC-EVs [119]. Furthermore, inhibitory effect of MSC-EV on NK cells was shown in patients with graft versus host disease (GvHD) [120].

Due to their immunosuppressive activity, Tregs are widely studied to prevent graft rejection. However, studies revealed that inflammatory environment inhibits immunosuppressive activity of Tregs following administration [121]. Since exosomes derived from Tregs are more resistant to inflammatory environment and they retain their immunosuppressive profile, there are several studies trying to utilize Treg exosomes in prevention of graft rejection. In one of them, it was shown that survival and function of kidney transplants was elevated following adoptive transfer of exosomes derived from Treg [122].

EVs derived from mature DCs activate T cells when expressing appropriate MHC class molecules and co-stimulatory molecules on them. It was shown that vesicles isolated from DCs pulsed with tumor antigen significantly contributed to tumor specific T cell response mediated tumor clearance in mice [123]. In couple of clinical trials, EVs having tumor-associated peptides were isolated from monocytes-derived DCs of patients were used for anti-therapeutic treatment of melanoma and non-small cell lung carcinoma [124-126]. In another study, it was found out that when monocyte derived DCs were treated with IFNγ, EVs from these cells were shown having more improved stimulatory activity due to elevated amount of CD40, ICAM1, and B7 molecules. According to this finding, EVs derived from tumor antigen pulsed IFNγ-matured MD-DCs were used for the treatment of non-small lung carcinoma in phase II clinical trial [127]. Collectively, these findings strongly support the attempts to develop therapeutic strategies using EVs isolated from appropriate cell type at an appropriate state.

In addition to use of EVs in therapeutic applications as they are isolated, there are also studies showing it is possible to modify exosomes to deliver different types of therapeutic agents to the cells [128]. Accumulating evidences point out that exosomes can deliver their cargo in an intact form to the recipient cells and modulate several cellular activities [34, 129, 49, 25, 130]

Two main strategies have been developed so far for utilization of exosomes as drug delivery systems. One of them is *in vitro* loading which required encapsulation of molecule of interest into exosomes via membrane breaching [131, 132] or physical entrapment [133, 134]. *In vitro* loading strategy was first introduced by mixing exosomes isolated from EL-4 cells with curcumin at room temperature. It was shown that encapsulation into exosomes increased the anti-inflammatory effect of curcumin [133]. Moreover, this complex was investigated in another study and it was revealed that curcumin encapsulated into exosomes mediated LPS-induced brain inflammation passing through the blood-brain barrier [134]. It was also documented that siRNA and miRNA molecules could be also loaded into exosomes with similar approach and their encapsulation into exosomes involves in the tumor clearance [135, 136]. On the other hand, *in vivo* loading approach suggests that cells fed or stably transfected with the molecule of interest secrete exosomes expressing these molecules [137, 138]. Both techniques have limitations regarding to the loading of any molecule on demand with high yielding efficiency.

1.4. Immunostimulatory ligands

1.4.1. CpG ODN and their applications

Bacterial DNA is known inducing activation of immune cells. It was shown that this activation capacity is due to the sequences of unmethylated CpGs flanked by two purines and two pyrimidines on 5' and 3' side, respectively [139]. The frequency of CpG sequences in mammalian DNA is 20-fold less than bacterial DNA, thus the immune suppression capacity by methylation is less observed. This difference between mammalian and bacterial DNA ended up with development of an evolutionary conserved recognition system that discriminates self and non-self-bacterial DNA by Toll-like receptor 9 (TLR9) [140].

Synthetic ODNs mimicking bacterial DNA were first identified with immune activation function due to their sequences containing CpG motifs in 1992 (Yamamoto 1992). They induce secretion of pro-inflammatory and T-helper (Th) 1 biased cytokines [141]. All CpG ODN types contain at least 8 base pair and at least one unmethylated CpG motif flanked by two 5' purines (Pu) and two 3' pyrimidines (Py) to be functional in immune stimulation in mice [139]. However, human PBMCs are less responsive to CpG ODNs that stimulates mice immune cells [142].

There are 2 mainly types of CpG ODNs as D-type and K-type which are also known as A and B type. There is also a recent type of CpG ODN called C-class. K-type

ODNs can have more than one CpG motif that makes them more potent immunostimulatory, whereas D-type ODNs can form nanoparticle like structures since they have poly G tail [142]. Due to these structural differences, their fate and action mechanisms also differ. D-type ODNs are recognized by TLR9 on early endosomes and entrapped in early endosomes upon internalization in human pDCs. Then, they activate MyD88 dependent signaling cascade and trigger innate immune responses via inducing type-I IFN secretion [143]. In contrast to D-type ODNs, K-type ODNs are relocated in late endosomes and they activate adaptive immunity through DC generation [144]. In Fig 1.5, sub-cellular localization and immunostimulatory action of D- and K-type CpG ODNs are represented.

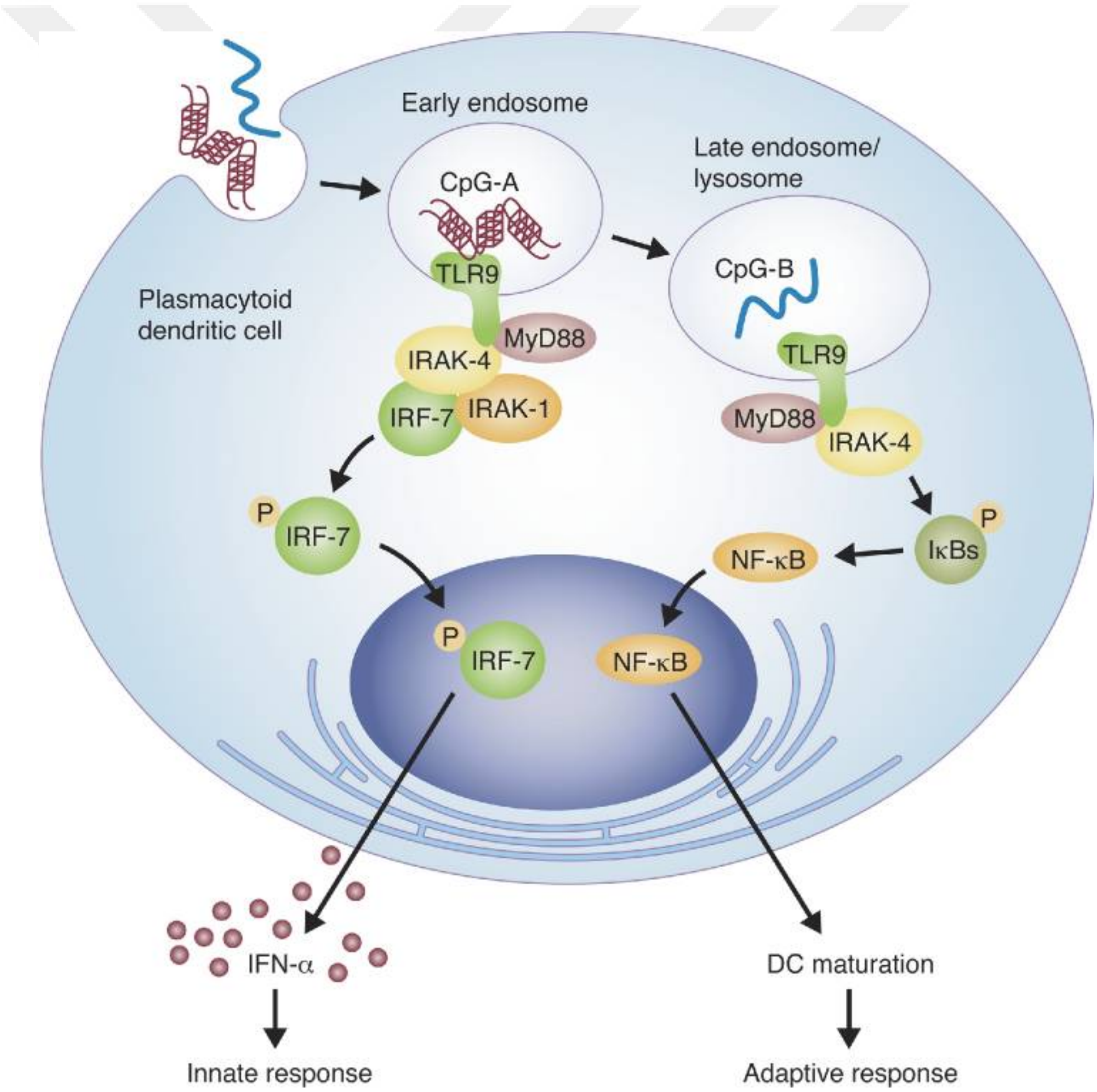

Figure 1.6. Activated signaling pathways upon recognition of CpG ODNs.

D-type ODNs are localized into early endosomes, whereas K-type ODNs are transferred to the late endosomes. Due to their structural differences, they activate different signaling pathways. (Adopted from [145]).

TLR9 ligands CpG ODNs have a great potential to be used as vaccine adjuvants, since they are capable of alarming immune system through activation of both innate and adaptive immunity. Upon recognition, they activate immune cells directly and also triggering signaling cascades that starts production of inflammatory cytokines. It has been shown that CpG ODNs directly activates human B cells and pDCs [146]. Their indirect effect is observed in maturation and proliferation of macrophages, T cell and NK cells [145]. They also activate APCs via upregulating co-stimulatory molecule expressions such as MHC class II, CD80, CD86 and CD40 [139, 148, 149]. Moreover, they induce humoral immunity by activating B cells that produces IgM along with IL10 and IL6 [150]. Of note, they are characterized by inducing secretion of IL12 and IFNγ as member of Th1 biased immunity from pDCs. It was also shown that pDCs start to produce several cytokines including IL6, IL-1β, IL18 and TNFα upon activation by CpG ODNs [151].

Due to their profound immune stimulatory capacity, CpG ODNs are studied as strong candidates for clinical use against cancer, protective agent against infectious diseases, as novel vaccine adjuvants and anti-allergic therapeutic agents to restore Th2 dominant immune response (Fig 1.6). Clinical studies showed that utilization of CpG ODNs in vaccines as adjuvant elicited antibody mediated immune responses against several pathogens such as influenza virus, anthrax, leishmania, measles virus, orthopox virus, tetanus toxoid and lymphocytic choriomeningitis virus [151-154], However, there are obstacles in their *in vivo* applications due to serum protein adsorption and nuclease attack.

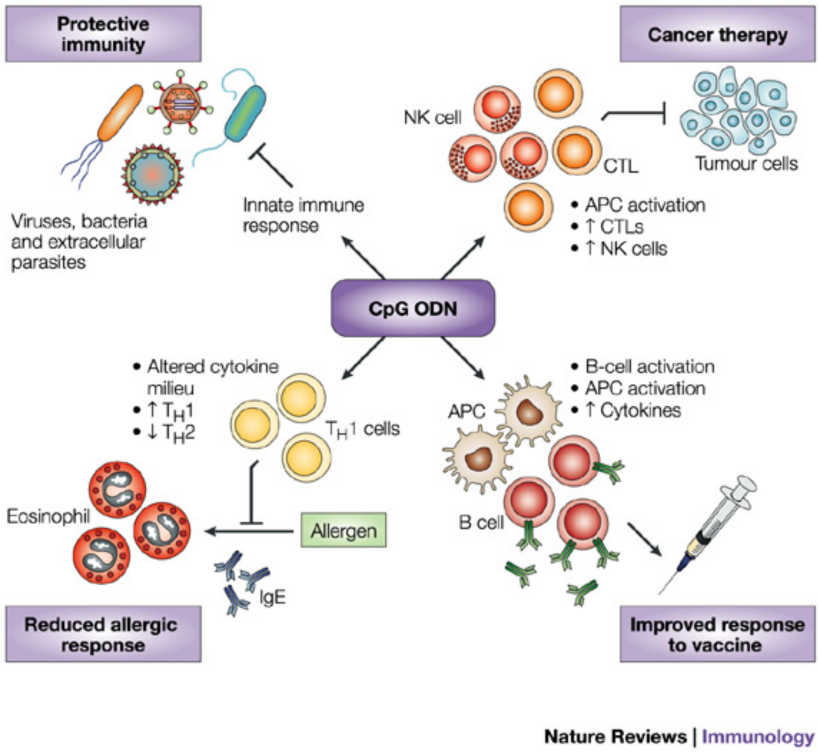

Figure 1.7. Potential therapeutic uses of CpG ODNs. (Adopted from [141]).

1.4.2. α-Galactosylceramide

Invariant natural killer T (iNKT) cells are a specialized T cell subset that recognizes self and bacterial lipid antigens presented by monomorphic MHC class I-like CD1d expressed by antigen presenting cells (APC) [155, 156]. Following activation with lipid antigen, iNKT cells play a dual role as both protective and pathogenic, by mediating both innate and adaptive immunity [157]. Alpha-galactosylceramide (αGC) is a glycolipid ligand for both murine and human iNKT cells and it induces rapid activation of iNKT cells *in vivo* leading to Th1, Th2 and Th17 specific cytokines production (IFN- γ, IL-4 and IL-17, respectively) that can mediate the immune responses against pathogens and tumors [158-161]. Due to profound role of iNKT cells in activation of immune system, there are several studies trying to explore their role in health and disease conditions using αGC in several animal models and human trials [156, 162]. According to pre-clinical trials, following activation, iNKT cells starts to produce IFNγ at earlier time points and then they trigger secretion of IFNγ from NK cells and IL12 from DCs [163]. After these encouraging findings, αGC has been tested in clinical trials for treatment of cancer patients. Surprisingly, none of these trials ended up with successful outcomes [164]. The underlying reasons behind these failures were thought to be correlated with low number of iNKT cells in patients or anergy upon multiple administration αGC [165, 166]. However, other studies showed that dendritic cells and B cells could efficiently activate iNKT cells bypassing iNKT cell unresponsiveness [167-169]. In addition to human studies, there are several studies showing potent anti-tumor activity of αGC when presented by DCs to iNKT cells in cell based mouse models [170]. DCs expressing mammary tumor–associated Ag Her-2 and loaded with αGC were shown that they could trigger anti-tumor responses. Moreover, the activity of these DCs was amplified upon combination with gemcitabine overcoming the immunosuppression [171]. In different mouse tumor models, DC based strategies were used to increase the anti-tumor activity of αGC in both preventive and therapeutic settings [172]. It was shown that DCs expressing OVA along with CCL21 via genetically modification could efficiently demolish OVA-expressing tumors [173].

In addition to cell-based techniques, there are some efforts to elicit the iNKT cell-dependent anti-tumor immunity via delivery of αGC by using biodegradable vectors. This approach suggests that encapsulation of αGC into nanovectors smaller than 1 mm can be superior to soluble αGC increasing uptake by APCs and avoiding side effects. It has been reported that silica microspheres coated with αGC containing lipid bilayers were targeted to DCs and macrophages [174, 175]. It has been also documented that PLGA (poly(lactic-co-glycolic acid)) can be also used to activate iNKT cells through APC uptake [176, 177].

Overall, the potential of iNKT cells to be as an important actor and the adjuvant properties of αGC in the eradication of malignancies cannot be underestimated. However, clinical trials have been showed that there is a necessity to develop new innovative approaches to pronounce the anti-tumor potential of iNKT cells and use of αGC.

1.5. Behçet's Disease and Pathogenesis

Behcet's disease is a chronic inflammatory disorder of which etiology is unknown. It was first characterized by recurrence of skin and mucosal lesions such uveitis, oral and genital ulcers by Turkish dermatologist Hulusi Behçet in 1937 [178]. Today, BD is known as a multisystem disease with vascular, articular, gastrointestinal, neurologic, urogenital, pulmonary and cardiac involvement [179].

BD is a disease mainly restricted to a distinct geography especially in Middle Eastern to the Far East and the Mediterranean countries [180]. Onset age of the disease is usually around the third or fourth decade of life [181]. Although the incidence percentage between genders is similar; progression of BD is more severe in men [182]. Frequency of the disorder and individual symptoms are directed by environmental factors in addition to genetic background. Although etiology of BD is not clear, it is known that geographic distribution of human leukocyte antigen (HLA)-B51 is strongly associated with the disease susceptibility [183]. Patients with BD could have high risk of having blindness, physical disability, cognitive impairment, and increased mortality [182].

Several studies showed that HLA-B51 is the main genetic factor underlying the BD susceptibility in many populations [183, 184]. However, BD is less observed in some areas with similar HLA-B51 frequency or frequently observed in HLA-B51 negative populations [185]. This suggests that in addition to contribution of HLA-B51, there are other genetic and unknown environmental factors that lead to BD pathogenesis. According to a genome-wide association study (GWAS), HLA-A*26 allele was identified as a second major susceptibility genetic factor for BD [186]. Polymoprhism in the genes encoding IL10, IL23 receptor, IL12 receptor-β and STAT4 was fount to be responsible for the increased BD incidence in Turkish, Japanese and Korean populations [187, 188]. Involvement of these genes in production of cardinal proteins for Th1 and Th17 biased immunity suggests that immune responses have a pivotal role in the development of BD [188]. Levels of pro-inflammatory cytokines such as IL1, IL6, IL8, IL10, IL12, IL15, IL18 and TNFα were shown to be strongly elevated in BD patients suggesting the contribution of different immune cells to the BD pathogenesis [189, 190]. $CD4^+$ T cells were identified as the predominant cell type in the lesions of patient with BD. Moreover, in the same study, Th-1 biased immunity was triggered following skin injury of BD patients via IL12 mediated IFNγ production by $CD4^+$ T lymphocytes [191]. Other studies also documented that BD patients had elevated levels of IL-1β and IL6 cytokines that are important for T lymphocytes differentiation into Th17 cells and this suggests that Th17 cells could play important role in BD pathogenesis [192-194]. A study group attempted to compare the serum levels of IL-8, IL-18, IFN-α2a, IL-6, IFN-γ, CXCL10, CXCL11, CXCL9, and SAA between patients with BD and healthy individuals. They found out that BD patients had significantly increased serum levels of IL-8, IL-18, IFN-α2a, and IL-6 and less CXCL11 compared to healthy controls. More importantly, this elevated cytokine trend was strongly correlated with the disease severity as active BD patients had higher levels of cytokines [195]. Although pathogenesis of BD is very complex and it is still unclear, it is known that the profound correlation between the genetic background and activation immunity are responsible for increased risk of BD. Understanding the underlying mechanisms that links these factors can lead to discovery of effective therapeutic strategies for BD.

1.6. Spinal Cord Injury and Disease Pathogenesis

Spinal cord injury (SCI) is a dramatic and devastating neurological condition caused by damage to the spinal cord leading to transient or permanent loss of motor, sensory and autonomic functions. In addition to impairment of motor skills, numerous metabolic and immune system complications are identified after SCI that affect the quality of life and end up with mortality [196, 197].

The most predominant causes of SCI are motor vehicle collisions (46%), falls (22%), violence (16%) and sports-related injury (12%) [198]. Although its etiology differs between countries, ethnicities, age and gender, its traumatic effects on physiological, social and socioeconomic conditions are the universal outcomes [199]. Annual incidence of SCI is 15-52.5 cases per million occurring mostly in healthy individuals 80% being male between 15 to 35 years of age. Following SCI, patients are left tetraplegic (53%) or paraplegic (42%) depending on the level of injury and severity of sensorimotor dysfunction [198]. Estimated treatment cost of SCI is $9.7 billion per year [200]. The highest mortality rate is observed in patients with higher injury and first year after the injury. Although there are several studies and investments regarding to the treatment of SCI, life expectancy has not improved for the last 30 years. Following systemic complications due to the impairment in the immune system are strongly associated with morbidity and mortality [199]. Pulmonary, cardiovascular and infectious sources are the most leading causes of death in SCI patients [201]. It is important to understand the pathophysiology of SCI to develop effective treatment strategies to increase the quality of life and avert the high mortality incidence.

SCI has a biphasic pathophysiology determined by primary and secondary injury mechanisms. Primary phase is the mechanical injury determines the neurological grade of the patients on admission and it is used as a prognostic marker. Secondary phase follow primary phase as the occurrence of vascular dysfunction, edema, ischemia, excitotoxicity, electrolyte shifts, free radical production, inflammation, and delayed apoptotic cell death [202]. Neurological deficiencies are observed subsequently the first mechanical injury. However, the consequence of the secondary injury phase is a long period of tissue destruction. Most of the understanding about SCI pathophysiology has been obtained from the animal studies since it is difficult to study with human postmortem tissues. To develop effective treatment strategies and to precede a successful management period thought out of patients' life, it is important to understand the pathophysiology of the SCI [203].

Clinical data reveal that SCI is followed by systemic complications due to serious immunological impairment [204, 205]. Immune dysfunction following SCI increases the risk of infection; moreover, predominantly pulmonary, gastrointestinal and urinary tract infections are one the main reason for re-hospitalization of patients with SCI and death in the post-acute phase of injury [206-208]. Moreover, progression of neurological responses after injury tends to get less functional is strongly associated with infections according to the clinical studies [209-211]. It has been shown that neutrophil phagocytosis, natural killer (NK) cell cytotoxicity and T cell activation was reduced in SCI patients compared to healthy controls, proposing that innate and adaptive immunity might be subjected to a suppression mechanism after SCI [212-214]. Moreover, this immune suppression profile could be dependent on the level of injury since there is a decentralized sympathetic outflow after damage at mid-thoracic or higher levels [215-216]. When SCI patients with tetraplegia and paraplegia are compared, it was shown that in contrast to reduced phagocytosis, changes in cytotoxic activity of T and NK cells were not level-dependent [213, 217]. In addition to clinical data, experimental models revealed that impairment in B cell functions could be level-dependent [218]. These data propose that SCI can cause in immune dysfunction that could prevent the development of a protective immune responses to infections. To develop strategies for better management of SCI, it is important to understand the mechanisms underlying this immune suppression.

1.7. Aims of this thesis

EVs are unique heterogeneous population secreted from all cell types to the extracellular milieu. They were identified with critical roles in the distant cellular communication and immune response modulation. The underlying reason for these effects are due to their cargo compositions and capability of internalization by target cells thereby achieving delivery of molecules such as DNA, RNA, peptides, proteins and lipids to target cells. There are several studies showing that EVs particularly microvesicles contributes the establishment of health and aggravation of disease progression. Considering these profound features of EVs, recently they are tremendous scientific efforts attempting to develop them either as diagnostic or therapeutic agents.

To this end, this thesis aimed to develop exosomes as vaccine/drug delivery system and apply them either in prophylactic or therapeutic cancer vaccine applications. Lyophilization of cell line derived exosomes was achieved. Encapsulation of different biological ligands (either alone or in combination) ranging from nucleic acid ligand, CpG ODN, protein antigen OVA and/or lipidic ligand αGC was accomplished. Physical and functional characterization of exosome loaded ligands were conducted either by instrumental analyses such as AFM, or DLS, or from cell stimulation assays. Contribution of E.G7 derived exosomes loaded with CpG ODN to the tumor clearance in a prophylactic therapeutic model was evaluated following immunization mice. To demonstrate that loading of exosomes with more than two reagents is more beneficial for immune therapy, next, addition of iNKT cell ligand, αGC together with OVA and CpG ODN was investigated. Superior immunostimulatory capacity of exosomes encapsulated with three different molecules was first tested *in vivo* on mice where animals were fed with BrdU containing water for 7 days. Contribution of CpG ODN and aGC to eradicate established tumor B16 melanoma tumor bearing mice were treated with exosomes harboring triple ligands.

Next, the involvement of exosomes to disease progression was investigated in Behcet`s Disease plasmas. Here the aim was to delineate the contribution of EVs to BD pathogenesis and we attempted to unearth the ability of EVs to sustain and exacerbate BD activity and severity. Initial efforts were put to characterize circulating EVs identity from blood plasma. Then, change in the EV levels of patients with different BD activity was investigated and compared to healthy individual EV levels. Contribution of elevated numbers of EVs in patients to disease pathogenesis, healthy PBMCs were stimulated to demonstrate that EVs isolated from BD patients are indeed pathogenic in character. The mechanism of this augmented EV immune activity was then identified by detecting the LL37 levels in i) plasma and their associated amounts that co-exist together with EVs. Lastly, contribution of LL37-associated EV activity was identified using either healthy or BD EVs.

The last part of this thesis is not directly related to EV work. Here, the contribution of innate recognition of pathogen associated molecular patterns (PAMPs) to the sustained immune dysfunction seen in chronic SCI patients was studied. In this context, response of SCI patients' PBMCs to different immune stimulatory ligands compared to those from healthy individuals via *in vitro* stimulations was evaluated. Impairment in TLR7 and TLR9 responses to R848 and CpG ODN stimulation was demonstrated at protein and cellular level. The underlying mechanism of SCI immune dysregulation leading to persistent chronic infections that could lead to death in many instances, were explored.

Chapter 2

Materials and Methods

2.1. Materials

2.1.1. Cell culture media and general solution components

FBS (Catalog #S18G-050) was purchased from Biowest. 1x PBS (Catalog # 14190-250) and RPMI-1640 medium without HEPES (Catalog # 21875-034) were supplied from ThermoFisher Scientific. Sodium Pyruvate (100 mM; Catalog # BE13-115E), HEPES (1M, Catalog # BE17-737E), nonessential amino acids (100x, Catalog # BE13-114E) and Penicillin-Streptomycin (10000 units/ml Penicillin and 10000 μg/ml Streptomycin; Catalog # DE17-602E) were purchased from Lonza. BSA (Catalog # 10735094001) was purchased from Roche.

Complete RPMI-1640 were prepared by adding 5 ml from Sodium Pyruvate, HEPES, nonessential amino acids, Penicillin-Streptomycin and different amounts of FBS (heat-inactivated at 55°C for 1 hour). For each experiment, FBS percentage of the media was specified in Methods Section.

2.1.2. Ligands

Exosomes were loaded with TLR9 and iNKT cell ligands. D-type CpG ODN as TLR9 ligand (ID: D35 sequence, Alpha DNA, 5'ggTGCATCGATGCAGGGGgg-3', lower letters represent phosphodiester linkages, capital letters phosphorothioate linkages) and iNKT cell ligand α-Galactosylceramide (KRN7000 αGC, Avanti, Catalog # 260377) were used during single, dual or triple reagent encapsulation experiments.

2.1.3. ELISA reagents

Specificities and concentrations of coating antibodies, biotinylated detection antibodies and recombinant protein standards for ELISA studies were shown in Table 2.1.

Table 2.1. ELISA reagents and their working concentrations.

Antibodies	Company	Catalog #	Clone	Concentration
Anti-human IL6	Biolegend	501102	MQ2-13A5	2μg/ml
Biotin Anti-human IL6	Biolegend	501202	MQ2-39C3	0.5μg/ml
Human recombinant IL6	Biolegend	570802	N/A	1000-0.98ng/ml
Anti-human IL10	Biolegend	506802	JES-19F1	4μg/ml
Biotin anti-human IL10	Biolegend	501502	12G8	0.5μg/ml
Human recombinant IL10	Biolegend	571004	N/A	250-0.25ng/ml
Anti-human IFNγ	Biolegend	507502	MD-1	5μg/ml
Biotin anti-human IFNγ	Biolegend	502504	4S.B3	0.5ug/ml
Human recombinant IFNγ	Biolegend	570202	N/A	500-0.49ng/ml
Anti-human IFNα	MabTech	3425-1a-20	MT1/3/5	2μg/ml
Biotin Anti-human IFNα	MabTech	B-558269	MT2/4/6	1μg/ml
Human recombinant IFNα	MabTech	3425-1A-20	N/A	20-0.02 ng/ml
Anti-human IP10	BD	555046	4D5/A7/C5	2μg/ml
Biotin Anti-human IP10	BD	555048	6D4/D6/G2	0.5μg/ml
Human recombinant IP10	BD	551130	N/A	100-0.08ng/ml
Human LL37 ELISA kit	HyCult	HK321-02	N/A	Coating Ab; Pre-coated Tracker Ab; not-known SA-HRP; 1:1000 dilution Standard; 100 ng/ml
Anti-mouse IFNγ	MabTech	3321-1a-20	MD-1	5μg/ml
Biotin anti-mouse IFNγ	MabTech	3321-1a-20	4S.B3	0.5ug/ml
Anti-mouse IL-6	Biolegend	504502	MP5-20F3	4 μg/ml
Anti-mouse IL-6 Biotin	Biolegend	504602	MP5-32C11	0.5μg/ml
Mouse recombinant IL-6	Biolegend	563401	N/A	1:1000 dilution
Anti-mouse IL-12	Biolegend	505202	C15.6	4 μg/ml
Anti-mouse IL-12 Biotin	Biolegend	505302	C17.8	0.5μg/ml
Mouse recombinant IL-12	Biolegend	563401	N/A	400 ng/ml
anti-mouse OVA	Nordic Biosite	AMB-7083	3G2E1D9	1:10000 dilution
anti-mouse IgG HRP	Southern BioTech	1030-05	1030-05	1:2000 dilution
Anti-mouse IgG-ALP	Southern BioTech	1030-04	N/A	1 μg/ml
Anti-mouse IgG1-ALP	Southern BioTech	1070-04	N/A	1 μg/ml
Anti-mouse IgG2c-ALP	Southern BioTech	1079-04	N/A	1 μg/ml
SA-ALP	MabTech	3310-8	N/A	1:1000 dilution
PNPP	Thermo	34047	N/A	1 tablet/5ml

2.1.4. Western blot antibodies and solutions

Specificities and concentrations of primary and secondary antibodies, used in western blot studies were shown in Table 2.2.

Table 2.2. Western blot reagents and their working concentrations

Antibodies	Company	Catalog #	Western Blotting Dilution
Alix (3A9)	Cell Signaling Technology	2171	1:1000
Tsg101	Santa Cruz	sc-7964	1:1000
Grp94	Cell Signaling Technology	2104	1:1000
anti-mouse IgG HRP	Cell Signaling Technology	7076P2	1:10000
anti-mouse IgG HRP	Santa Cruz	sc-2031	1:10000
anti-rabbit IgG HRP	Cell Signaling Technology	7074P2	1:10000

RIPA buffer used before loading samples to the gels were prepared freshly by mixing 75 µl 2M NaCl, 50 µl 1M Tris-HCl (pH=8), 10 µl NP-40 (Abcam, Catalog # ab142227), 10 µl 10% SDS and 815 µl ddH_2O. Before the homogenization protocol, 10 µl protease inhibitor (100x, Calbiochem, Catalog # 539131) was added to the solution.

Tris-glycine gels were used to run proteins. 5% stacking gel was prepared by mixing H_2O, acrylamide mix (Sigma, Catalog #A3574), 1M Tris-HCl (pH=6.8), 10% SDS and 10% ammonium persulfate in desired amounts. To prepare 10% resolving gel, same solutions were mixed in appropriate amount except 1M Tris-HCl. Instead of it, 1.5 M Tris-HCl (pH=8.8) was used.

10x running buffer was prepared by dissolving 30.3 g Tris base (Sigma-Aldrich, Catalog # 77-86-1, 28), 144.1 g glycine (Santa Cruz, Catalog # sc-29096), 100 ml 10% SDS in 800 ml ddH_2O. Then, the pH was adjusted to 8.3. The buffer was stored at room temperature and diluted to 1x with ddH_2O before using.

10x TBS buffer was prepared by dissolving 12g Tris base and 80g NaCl in 800 ml H_2O. Then, the volume was filled up to 1 L with H_2O. For washing membranes, 10x TBS was diluted to 1x and 3 ml Tween-20 was added to prepare TBS-T.

To prepare transfer buffer used in the wet transfer, 6 g Tris base, 28 g glycine and 400 ml methanol (Sigma-Aldrich, Catalog # 24229) was mixed and stored at +4°C for 1 hour. Then, 1600 ml cold ddH_2O was added.

For blocking membranes, blocking buffer was prepared by dissolving 2.5 g non-fat milk powder in 20 ml TBS-T and stored at +4°C.

2.1.5. Flow cytometry antibodies

Fluorescence conjugated antibodies and isotype controls are shown in Table 2.3. All antibody concentrations were adjusted to 1 μg/ml final concentration and DimerX was used 2.5 μl/sample throughout all staining protocols.

Table 2.3. Specificities of the FACS antibodies

Antibodies	Company	Catalog #	Clone
Anti-human CXCL IP10-PE	Biolegend	519502	D34D6
Anti-human CD14-FITC	Biolegend	325604	HCD14
Anti-human CD83-PE	Biolegend	305308	HB15e
Anti-human HLA-DR-FITC	Biolegend	307604	L243
Anti-human CD4-PE	Biolegend	317410	OKT4
Anti-human IFNγ-FITC	Biolegend	506504	B27
Anti-human CD9-PE	Biolegend	312106	HI9A
Mouse IgG1-PE	Biolegend	40011	MOPC-21
Anti-human CD63-PE	Biolegend	353004	H5C6
Annexin V-PE	Biolegend	640908	N/A
Anti-mouse CD81-PE	Biolegend	104906	Eat-2
Anti-mouse CD9-FITC	Biolegend	124808	MZ3
Human/Mouse-CD11b-PE	Tonbo biosciences	50-0112-U100	M1/70
Anti-mouse H2Kd-PE	Biolegend	116607	SF1-1.1
Anti-mouse I-A/I-E-PE	Biolegend	107608	M5/114.15.2
Anti-mouse CD1d-PE	Biolegend	123509	1B1
Anti-mouse/human CD45R/B220	Biolegend	103210	RA3-6B2
Anti-mouse Ly-6G	Biolegend	127606	1A8
Anti-mouse CXCR5-PE/Cy7	BD Biosciences	560617	2G8
Anti-mouse PD-1-APC	Biolegend	135209	29F.1A12
Anti-mouse CD4-APC/Cy7	Biolegend	100414	GK1.5
Anti-mouse TCR-β-Pacific Blue	Biolegend	109226	H57-597
Anti-mouse B220-Brilliant Violet 605	BD Biosciences	563808	RA3-6B2
Anti-mouse B220-PerCp/Cy5.5	Biolegend	103235	RA3-6B2
Anti-mouse CD3-PE/Cy7	BD Biosciences	560591	17A2
Anti-mouse γδTCR-β-APC	Biolegend	118115	GL3
Anti-mouse CD8a-Brilliant Violet 605	Biolegend	100743	53-6.7
Anti-mouse CD4-PE	Biolegend	105111	RM4-5
Anti-mouse CD8a-PE/Cy7	Biolegend	100722	53-6.7
Anti-mouse NK1.1-APC/Cy7	Biolegend	108724	PK136
Anti-mouse CD21-PerCp/Cy5.5	Biolegend	123416	7.00E+09
Anti-mouse CD23-PE	Biolegend	101607	B3B4
Anti-mouse CD95-PE/Cy7	BD Biosciences	557653	Jo2
Anti-mouse CD138-APC	Biolegend	142506	281-2
Anti-mouse GL7-Pacific Blue	Biolegend	144614	GL7
Anti-mouse IFNγ-PE/Cy7	Biolegend	505826	XMG1.2
SIINFEKL Pentamer-PE	ProImmune	93	N/A
Unconjugated DimerX	BD Biosciences	557599	N/A
Rat IgG2b-PE	Biolegend	400607	RTK4530
Armenian Hamster IgG-PE	Biolegend	400907	HTK888
Rat IgG2a-FITC	Biolegend	400505	RTK2578

2.2. Methods

2.2.1 Patients and Controls

2.2.1.1 SCI patients and controls

SCI patients were obtained from PMR Department of Turkish Armed Forces Rehabilitation Center in Gülhane Military Medical Academy and the same hospital employee involved as healthy controls. Patients were included in this study if they met the criteria as following: i) having neurologically complete spinal cord injury (AIS A, Based on American Spinal Injury Association, Atlanta, GA, USA) occurring 6 or more months prior to the study, ii) injury level above T6, iii) being older than 18 years old. Patients who had fewer in 7 days before study; current pressure ulcers; vaccine therapy in the last three months; substances that affect the immune system such as corticosteroids, alcohol and chemotherapies in the last nine months were not included in the study. In addition to the evaluation of these criteria, all patients were particularly examined based on American Spinal Injury Association (ASIA) protocol. This study was approved by Keçiören Training and Research Hospital Ethical Committee with the decision number 249 on 13.03.2013 and written informed consent was provided by each subject. For this study, venous blood samples from 17 SCI patients and 13 healthy control was collected into transfer tubes treated with EDTA under non-fasting conditions between 7:00-8:00 am. Detailed information about age, sex and hematological characteristics of SCI patients and healthy controls were represented in Table 2.4 and Table 2.5.

Table 2.4. Baseline characteristics of the patients and control group.

	SCI Patients (n=17)	Healthy Controls (n=13)	p
Age (median, (min-max))	37.0 (21.0-45.0)	29.0 (24.0-49.0)	0,14*
Sex (%male; %female)	82.4; 17.6	53.8; 46.2	0,09**
Months from injury (median, (min-max))	72.0 (10.0-288.0)	NA	
Etiology (%)			
Motor vehicle collisions	47.0	NA	
Fall from an elevated height	29.4	NA	
Gunshot wound	11.8	NA	
Diving into shallow water	11.8	NA	

Abbreviation: NA, not applicable, * Mann-Whitney U test, **Chi-square test

Table 2.5. Hematological characteristics of the patients and the control group.

Blood variable	SCI patients	Healthy control	p
Hemoglobin (g/dL)	12.9±1.2	14.1±1.4	>0.05*
Erythrocytes ($X10^6/\mu L$)	4.5±0.4	4.8±0.3	>0.05*
Thrombocytes ($X10^3/\mu L$)	255.8±43.7	269.8±79.5	>0.05*
Leukocytes ($X10^3/\mu L$)	6.3±1.1	6.9±2.3	>0.05*
Leukocytes subsets ($X10^3/\mu L$)			
Lymphocytes	2.4±0.6	2.4±0.9	>0.05*
Neutrophils	3.2±0.8	3.6±1.4	>0.05*
Eosinophils	0.2±0.1	0.2±0.1	>0.05*
Monocytes	0.5±0.1	0.5±0.1	>0.05*

* Mann-Whitney U test

2.2.1.2. BD patients and controls

The patients were diagnosed with BD according to the International Study Group criteria for Behçet's disease were recruited from the Department of Rheumatology in Gülhane Military Medical Academy. Their clinical statuses were represented in Table 2.6. Exclusion criteria were having hypertension, diabetes mellitus, renal disease or a previous history of coronary artery disease or myocardial infarction. Patients having two and more clinical characteristics such as; oral ulcers, genital ulcers, papulopustular or pseudo-follicular cutaneous lesions, active vascular disease and active ocular involvement were defined as active BD patients. Inactive disease inclusion criteria were showing no symptoms related with BD at the time of sampling and receiving medication for at least 1 month. Patients were classified into categories if they have different organ involvement as i) mucocutaneous, ii) ocular, and iii) vascular. For this study, venous blood samples were drawn under non-fasting conditions from 72 BD patients (Active; n=35, Inactive; n=37) and 22 healthy control individuals. Age and sex distributions of patients and healthy participants and clinical status of patients were shown in Table 2.6. Written informed consent form was obtained from each participant and the study protocol was approved by the Institutional Review Board.

Table 2.6. Clinical evaluations of the BD Patients.

	Healthy (n=22)	**Inactive BD (n=37)**	**Active BD (n=35)**
Sex (M)	22	37	35
Age (year, mean±SD)	22±5	22±5	19±6
Disease Duration (year, mean±SD)	N/A	11±5	8±2
Disease Progression			
Mucosa	N/A	9	16
Vein	N/A	12	7
Eye	N/A	16	12
Treatment			
Colchicine	N/A	21	24
Azathioprine	N/A	14	11
Cyclophophamide	N/A	2	0

2.2.2. Cell Culture and Animals

2.2.2.1. Isolation of PBMCs and plasma from peripheral blood

To isolate PBMCs, lymphocyte separation medium (Lonza, Catalog # 17-829E) was added at the bottom of into falcon tubes and 1.5 times more volume of blood samples were slowly layered onto lymphocytes separation medium. Then, they were centrifuged at 600xg for 30 minutes at room temperature with break off. After the centrifugation, three layers were obtained. The top phase as plasma was transferred into a new tube to be further used for EV isolation as it is explained in section 2.3.2. The cloudy part as lymphocytes between plasma and lymphocytes separation medium was gently transferred to new falcon tubes by sterile Pasteur pipette. Lymphocytes were washed for two times via centrifugation at 600xg for 10 minutes with the addition of complete 2% FBS supplemented complete RPMI-1640 media. At the end, the supernatant was discarded and the cells were resuspended in 5% FBS supplemented complete RPMI-1640 media. Cell number was counted by BD Accuri 6 Flow Cytometry (BD Biosciences).

2.2.2.2. Animals

For all ex-vivo and *in vivo* experiments except *in vivo* proliferation study, 6-8 weeks old female C57Bl/6 mice were maintained in the Bilkent University Animal Housing Facility of the Department of Molecular Biology and Genetics. Mice used in *in vivo* proliferation experiment were kept at the Karolinska Institutet's animal facility. Housing conditions for all mice were at 22°C with 12 h light and 12 h dark cycles and provided with unlimited access of food and water. All experimental procedures were approved by the animal ethical committee of Bilkent University (Bil-AEC/Protocol#2011/31, Bil-AEC/Protocol#2012/19, Bil-AEC/Protocol# 2014/31, Bil-AEC/Protocol# 2016/2).

2.2.2.3. Preparation of single cell suspension from mice spleens

C57Bl/6 or OT1 mice were sacrificed by cervical dislocation and spleens were removed into 2-3ml of ice-cold complete RPMI 1640 supplemented with 2% FBS until starting preparation of single cell suspension. Then, spleens were smashed either with the back of a syringe plunger in a 60x15 mm cell culture petri dish or 0.70 µm filters in order to get rid of adipose and connective tissue. Cells were transferred to 15 ml falcon tubes by adding warm 2% FBS supplemented complete RPMI 1640 up to 14 ml and centrifuged at 300xg for 7 minutes at room temperature. Following centrifugation, supernatant was discarded and the cells were washed at the same conditions. Then, cells were resuspended within 1 ml of 5% FBS supplemented complete RPMI 1640 and counted with hemocytometer.

2.2.2.4. Culture of RAW264.7 murine macrophage cells for supernatant collection

Murine macrophage like cell line RAW264.7 and murine E.G7 thymoma cell line were purchased from ATCC (ATCC® TIB-71™). Cells were cultured in 5% FBS supplemented complete RPMI-1640 media. All media components were either centrifuged at 100000xg for 18 hours or filtered through 0.2 µm filters before use in order to eliminate all particles that could interfere with the exosomes isolated from the cell culture supernatants. For culturing RAW264.7 cells, $1x10^7$ cells were seeded into 145x20 mm cell culture petri dishes in 10 ml media and incubated at 37°C 5% CO_2 for 2-3 hours until all cells attached to the petri dish surface. Then, culture media was removed and replaced with 30 ml of fresh media. When the cells reached to 90-95% confluence, media was collected for exosome isolation. For E.G7 cells, $2.5x10^5$/ml cells were cultured in 50 ml media for 2-3 days until cell concentration reached to $1x10^6$/ml. Then, media was collected for exosome isolation. Cells were prepared as described above to collect cell culture supernatant for another round of exosome isolation.

2.2.2.5. Preparation of PECs

To evaluate the effect of intraperitoneal injected non-lyophilized and lyophilized exosomes on peritoneal immune cells, 5% of 2.5ml thioglycolate (Sigma Aldrich, Catalog # T9032-1) was intraperitoneally injected to C57Bl/6 mice and they were kept in the animal facility for 5 days. 4 hours before sacrificing mice, they were intraperitoneally injected with 30µg of non-lyophilized and lyophilized exosomes. Then, PECs were collected by injecting and recollecting of 10 ml of ice-cold 2% FBS supplemented RPMI media into euthanized mice. Recovered media was centrifuged for 2 times with warm 2% FBS supplemented complete RPMI-1640 at 300xg for 7 minutes. At the end, cell pellet was resuspended with 5% FBS supplemented complete RPMI-1640 and counted with BD Accuri 6 Flow Cytometry. 10^6 cells were fixed and stored at +4°C until they were stained with macrophage, B cell and neutrophil specific mouse antibodies.

2.2.2.6. Cell counting

For human PBMC and mouse splenocytes studies, cells were counted by BD Accuri C6 flow cytometer. In brief, 20 µl from single cell suspension of cells prepared within 1 ml complete RPMI-1640 and then were added into 10 ml of Isoton II Diluent Buffer (Beckmann Coulter, Catalog # 8546719) and 2-3 drops of Zap-Oglobin II Lytic Reagent (Beckmann Coulter, Catalog # 7546138) were added into the solution to burst red blood cells. 20 µl from this solution was acquired by BD Accuri 6 Flow Cytometry. Live cells were gated excluding cell debris and apoptotic cell population. Total cell number was calculated according to the formula given below.

$$\text{Total Cell \#} = \left(\frac{\text{Counted Cell \#}}{\text{Used Volume } (\mu\text{l})}\right) \times 500 \text{ (Dilution Factor)} \times 1000 \text{ (Volume } (\mu\text{l}))$$

RAW264.7 and E.G7 cells were counted by hemocytometer. 10 µl from 1 ml single cell suspension was 10 times diluted with fresh media and then mixed with Trypan Blue (Lonza, Cat#17-942E) at 1:1 ratio in order to eliminate dead cells during counting. 10 µl from this 20 fold diluted cell suspension were transferred onto hemocytometer. The hemocytometer was placed under the microscope and it was adjusted to count the cells settled in the area framed by the bold red squares (0.1mm^3/each) represented in Figure 2.1. The total cell number was calculated from counted cell number according to following formula;

$$\text{Total Cell \#} = \left(\frac{\text{Counted Cell \#}}{4}\right) \times 10^4 \times 10(\text{Dilution Factor}) \times (\text{Volume})$$

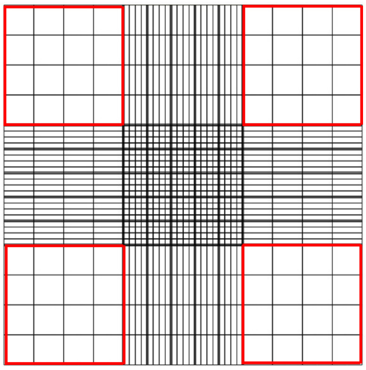

Figure 2.1. Representative picture of grids in hemocytometer. Cells residing within the red squares were included in the counting.

2.2.3. Isolation of EVs and Exosomes

2.2.3.1. Isolation of exosomes from cell culture

Following supernatant collection from cultured cells, they were centrifuged at 1500xg for 10 minutes at room temperature in order to get rid of any other contaminants such as remaining cells and cell debris. Supernatants were transferred to new falcon tubes and they were snap-frozen in liquid nitrogen and kept at -80°C for exosome isolation at a later timer. Before starting exosome isolation protocol, exosome containing supernatants were slowly thawed by overnight incubation at +4°C and then they were vortex strongly in order to dislodge any vesicle aggregation or detach the proteins bound to exosomes while they were kept at -80°C and during thawing step in the fridge. Supernatants were transferred to ultracentrifugation tubes (Beckmann Coulter) to be centrifuged at 10000xg for 10 minutes at +4°C in order to remove any other large particles. Following this step, the supernatant was transferred to new ultracentrifuge tubes and volume was completed up to 35 ml with $Ca^{2+/}Mg^{2+}$ free 1x PBS if necessary and they were centrifuged at 30000xg for 30 minutes at +4°. The aim of this centrifugation step was to sediment microvesicles. After pelleting microvesicles, supernatant was collected and passed through 0.2 µm filter to ensure that all larger particles were eliminated. Then, filtered supernatants were transferred to a new ultracentrifuge tube and $Ca^{2+/}Mg^{2+}$ free 1x PBS was again used for the completion of the volume up to 35 ml. Supernatants was centrifuged at 100000xg for 90min at +4°C. At the end, supernatant was discarded and the pellet was gently resuspended within 1 ml of 1x PBS. Then, the volume was completed up to 35 ml with 1x PBS to wash exosome pellet by ultracentrifugation at 100000xg for another 90min at +4°C. Following washing step, supernatants were aspirated and the exosomes as pellet was resuspended within desired volume of $Ca^{2+/}Mg^{2+}$ free 1x PBS stored at +4°C for further use.

2.2.3.2. Isolation of EVs from peripheral blood plasma

After separating plasma from peripheral blood, another centrifugation step at 1500xg for 10 minutes at room temperature was performed in order to get rid of any other cell contaminants. Supernatants were collected and immediately snap-frozen in liquid nitrogen and maintained at -80°C until EV isolation. Before starting EV isolation, EV containing supernatants were taken out from the -80°C and left to be thaw slowly at +4°C overnight. Just before starting centrifugation, supernatants were vigorously vortexed in order to resolve any clumping structures composed during snap-frozen or thawing. Then, samples were transferred to ultracentrifuge tubes (Beckmann Coulter) and if it was necessary their volumes were adjusted with the addition of PBS-citrate buffer (10 mM tri-sodium citrate PBS @ pH=7.4). Supernatants were centrifuged at 10000xg for 10 minutes at +4°C. Following centrifugation, supernatant was transferred into new ultracentrifuge tubes and the pellet was discarded as it was either remaining cell debris or other contaminating vesicles. Supernatants were centrifuged at 100000xg for 90 minutes at +4°C. At the end of this step, supernatant was discarded and EVs pelleted at the bottom of the tubes were resuspended within $Ca^{2+/}Mg^{2+}$ free 1x PBS to be centrifuged at 100000xg for another 90 minutes at +4°C. Following centrifugation, EVs were collected at the bottom of the tubes and resuspended within Ca^{2+}/Mg^{2+} free 1x PBS. EVs were stored at +4°C for further use.

2.2.3.3. Purification of EVs by sucrose cushion

Following purification of EVs from peripheral blood plasma, EVs were resuspended within 2 ml of 1x PBS and layered onto 30% (w/v) sucrose solution in 15 ml ultracentrifuge tubes. Centrifugation at 100000xg for 2 hours at 4°C were performed and different layers were obtained at the end of this centrifugation. From these layers, 3-4 ml of supernatants as EV containing top layer were collected and transferred into ultracentrifugation tubes. Volume was filled up to 35 ml with 1x PBS and again centrifuged at 100000xg for 2 hours. EVs were pelleted at the bottom of the ultracentrifugation tubes and this pellet was resuspended within 150 µl 1x PBS for further analysis.

2.2.3.4. Purification of EVs by size exclusion chromatography

Size exclusion chromatography (SEC) was performed to purify and further analyze exosomes in the blood plasma. 1-1.5 ml of plasma samples from BD patients or healthy subjects diluted with 1x PBS up to 2 ml were centrifuged at 10000xg for 20 minutes in order to get rid of any contaminants such as debris and precipitates. Following centrifugation, collected supernatants were filtered through 0.22 µm filters and subsequently loaded on a HiPrep 16/60 Sephacryl S-400 HR SEC column (GE Healthcare, Uppsala, Sweden) with a 120 ml bed volume connected to an ÄKTA FPLC system (GE Healthcare). Elution was obtained by the separation at 0.5 ml/min flow rate using PBS and the chromatogram was recorded using absorbance at 280 nm and 2 ml fractions were collected. After separation, indicated fractions were pooled and concentrated using ultracentrifugation as described above.

2.2.3.5. Determining protein concentration of exosomes

Protein concentration of EVs and exosomes was determined by using Pierce™ BCA protein assay kit (ThermoFisher Scientific, Catalog # 23225). Manufacturer's protocol was performed as described in the following. BSA standards dilutions were prepared between 1.96-2000 µg/ml (10 times 2 times dilution by using 1x PBS) and exosomes were diluted for 4 fold with 1x PBS. All these preparations were added into 96-well plate and mixed with working reagent 1:8 volumetric ratios. Samples were incubated at 37°C for 30 minutes and then 15 minutes at room temperature. Then, the absorbance of the BSA standards and exosomes were measured at 562 nm by spectrophotometer (Synergy HT, Biotek). The concentration of samples was determined by BSA standard curve.

2.2.4. Characterization of Exosomes

2.2.4.1. Bead based flow cytometry technique to determine the specific EV and exosomal markers

The presence of the specific markers on EVs and exosomes can be confirmed by bead-based flow cytometry technique that confirms the existence of vesicles in the isolated solutions.

In order to detect exosomes isolated from RAW264.7 cell supernatants via this technique, carboxyl modified latex beads (Life Technologies, Catalog # C37282) were conjugated to LEAF purified anti-mouse CD81 antibody and the experimental set up was briefly explained below. 10µl latex beads were incubated with 10 µg of LEAF purified anti-mouse CD81 antibody and incubated at room temperature for 10 minutes. Then, volume was filled up to 500 µl with 1x PBS and bead-antibody mix was incubated overnight at room temperature by continuous rotating shaking. Following incubation, bead-antibody mix was washed by 13000xg centrifugation for 10 minutes. After discarding the excess supernatant, beads were blocked with 5% BSA containing 1x PBS for 4 hours at room temperature by rotating. Following blocking, beads were washed with 1x PBS twice and anti-mouse CD81 conjugated beads were resuspended within 1% BSA containing 1x PBS to be stored at 4°C until they were used for further analysis. In order to analyze the specific molecules on exosomes, 1 µg protein containing exosomes were mixed with 1 µl anti-mouse CD81 conjugated bead and incubated at room temperature overnight. After washing step, they were incubated with 100 µl of solutions containing either anti-CD9-FITC, anti-CD81-PE, anti- CD11b-PE, anti- MHCI-PE, anti-MHCII-PE or anti-CD1d-PE in FACS buffer and their corresponding isotype controls for 30 minutes at room temperature. They were washed and resuspended in 150 µl 1X PBS and then analyzed by BD Accuri C6 flow cytometer.

In order to evaluate the presence of cardinal EV markers on EVs isolated from human plasma, same protocol explained above for exosomes were performed. In this experimental setting, LEAF purified anti-human CD63 antibody was used to coat the carboxyl modified beads instead of LEAF purified anti-mouse CD81. To detect the presence of specific EV markers, EV coated CD63 conjugated beads were resuspended within 100 µl of solutions containing anti-CD9-PE, CD63-PE antibody or Annexin V-PE in FACS buffer.

2.2.4.2. Western blot for determining the presence of exosomal markers

Exosomes were mixed with RIPA lysis buffer 1:1 volume ratio and sonicated for 15 minutes and then vortexed for 15 seconds at the end of every 5 minutes. Then, protein concentration of exosomes was determined by using Pierce™ BCA protein assay kit as described in Section 2.2.2.5. Loading samples were prepared by mixing 25 µg of exosomes with 4x loading dye and RIPA lysis buffer to the final volume of 40 µl. Following incubation of loading samples at 95°C for 5 minutes, samples were added into the gel. For this study, 5% stacking and 10% resolving gel were used. After running the proteins, they were transferred to PVDF membranes that were activated in absolute methanol with wet transfer technique using 1x transfer buffer. 100 volts were applied for 90 minutes in order to perform the wet transfer. After the transfer, PVDF membranes were blocked with 5% non-fat dry milk containing 1x PBS-T at +4°C overnight. Blocked membranes were washed 3 times in 1x PBS-T for 10 minutes. Then, membranes were incubated with primary antibodies as Alix, Tsg101 or Grp94 prepared in 5% non-fat dry milk containing 1x PBS-T with 1:1000 dilution at +4°C overnight. Following primary antibody incubation, membranes were washed and incubated with 1:10000 diluted secondary antibodies 5% non-fat dry milk containing 1x PBS-T at room temperature for 1 hour. Membranes were developed using chemiluminescent detection kit, ECL+ (Amersham, UK) according to the manufacturer's protocols and visualized by Amersham Imager 600 (GE, Amersham).

2.2.4.3. Size distribution analysis of exosomes by AFM

In order to analyze size of exosomes, atomic force microscopy (AFM) was used. 10 µl of exosome solution was layered onto mica slides and then left to be dried. Mica slides were placed into AFM XE-100E model AFM (PSIA with XEI 1.6 software incorporated) and 1x1 µm areas were scanned in non-contact mode.

2.2.4.4. Size distribution analysis of EVs by DLS

Dynamic light scattering (DLS) was used determine the size distribution of EVs isolated from human plasma. 1x PBS was used to dilute EV solutions 100x. Diluted solutions were transferred to folded capillary zeta cells (Malvern Ins.). Zetasizer Nano ZS (Malvern Instruments, Worcestershire, UK) was used to determine the hydrated size of EVs.

2.2.5. TLR9 and iNKT Ligand Loading within Exosomes

30 µg of exosomes were mixed with 5 µg OVA, 10 µg ODN and 0.3 µg αGC. They were immediately snap-frozen in liquid nitrogen and lyophilized overnight in VirTis Bench Top K Freeze Dryer (SP Industries, New York, USA). Following this incubation period, powder mixture of exosomes and ligands were obtained and ligands were encapsulated into exosomes via controlled rehydration process by adding nuclease free H_2O in a 1:10 ratio of original solution volume. Then, this rehydrated mixture was vortexed for 15 seconds every 2 minutes during 20 minutes.

Following, $Ca^{2+/}Mg^{2+}$ free 1x PBS in same amount of H_2O used in the beginning of rehydration process was added and mixture was incubated at room temperature for 10 minutes. Then, mixture was vortexed for 15 seconds at half speed. Controlled rehydration process was completed with the addition of Ca^{2+}/Mg^{2+} free 1x PBS to adjust the desired concentration of ligand encapsulated exosome solution. Exosome solution was maintained at +4°C until use.

2.2.6. Cell Stimulation Studies

2.2.6.1. Stimulation of mouse splenocytes with free and exosomal CpG ODN

For IL6 ELISA study, mice splenocytes ($2.5x10^6$/ml) were stimulated with two different concentrations (0.4-and 2 μM) of free CpG ODN and exosomal counterparts for 8-, 16-, 24- and 48 hours. At the end of indicated time points, cell supernatants were collected for ELISA study.

For IL12 and IFNγ ELISA studies, mice splenocytes ($2.5x10^6$/ml) were stimulated with 4 different concentrations (0.1-, 0.3-, 1- and 3 μM) of free CpG ODN and E.G7 exosomal counterpart for 24 hours. At the end of indicated time points, cell supernatants were collected for ELISA study.

CD86/MHCII surface marker staining was performed on mouse splenocytes stimulated with 0.4 μM of free CpG ODN and E.G7 exosome loaded counterpart for 24 hours.

2.2.6.2. Stimulation of OT1 mice splenocytes with exosomal TLR9 and iNKT ligands

Spleens were collected from OT1 mice of which T cells are OVA-specific in order to evaluate the activator capacity of exosomal OVA+ODN+αGC in *in vitro*. After preparation of single cell suspension from spleens, cells were counted and $50x10^6$ cells/ml was labeled with 2.5 μM CFSE (Life Technologies, Catalog # C34554) for 10 minutes at 37°C. Labeling was stopped by adding complete media and centrifugation with 1x PBS for 3 times. CFSE labeled cells were co-cultured with 1- and 5µg/ml of exosomes for 5 days in CO_2 incubator. Following 5 day-incubation, cells were transferred to V-bottom 96-well plate and stained with antibodies.

2.2.6.3. Stimulation of SCI patients and healthy control PBMCs with different immunostimulatory ligands

$2x10^5$ PBMCs were seeded onto 96-well-plate in 200 µl final volume and they were treated with 5 µg/ml R848 (Enzo, Catalog # ALX-420-038-M025), 3µM D-type CpG ODN or 5 µg/ml PHA-1 µg/ml LPS (Roche, Sigma, Catalog # L-2880) for 24 hours and cell supernatants were collected to assess human IL6, IL10, IFNα, IFNγ and IP10 cytokine levels by ELISA assay.

In order to perform IFNγ and IP10 intracellular cytokine stainings, $1x10^6$ PBMCs in 1 ml were incubated either with 5 µg/ml R848 or 3 µM D35 for 12 hours and after addition of 10 µl/ml Brefeldin A onto each sample, the cells were incubated 8 more hours. In order to determine the T-cell function of PBMCs, 10^6 PBMCs/ml were incubated with 10 ng/ml PMA (Sigma, Catalog # P1585), 0,5 µM Ionomycin (Sigma, Catalog # I9657-1MG) and 10 µg/ml Brefeldin A (Biolegend, Catalog # BA6542-5mg) for 6 hours for further IFNγ and IP10 intracellular cytokine staining.

PBMCs ($1x10^6$) from healthy and SCI donors were treated either with R848 (5µg/ml) or D35 (3µM) in 1ml final volume of media for 24 hours in order to determine CD83/HLA-DR expression of human PBMCs by FACS analysis.

2.2.7. Flow Cytometry Studies

2.2.7.1. Intracellular cytokine staining

2.2.7.1.1. Intracellular cytokine staining of human PBMCs

Cells were incubated with the respective ligands indicated in Section 2.2.6.1 in order to determine the secretion of IFNγ and IP10 cytokines at cellular level. Following stimulation, cells were pelleted by centrifugation and resuspended within 100 µl fix and perm medium A (Invitrogen, Catalog # GAS001S100) and incubated in dark at room temperature for 15 minutes. Fixed cells were washed twice adding 2 ml of PBS-BSA-Sodium azide buffer. Following washing step, cells were resuspended within 50 μl fix and perm medium A (Invitrogen, Catalog # GAS002S-100) containing either anti-IFNγ-FITC and anti-CD4-PE cocktail or anti-CD14-FITC and anti-IP10-PE. Specificities and concentrations of each antibody used for staining were listed in Table 2.3. After 30-minute incubation in dark, cells were washed twice and resuspended in 500 μl PBS-BSA-Sodium azide buffer, transferred to FACS tubes and analyzed in BD Accuri 6 Flow Cytometry.

2.2.7.1.2. Intracellular cytokine staining of murine splenocytes

After incubating spleen cells with 50 ng/ml Phorbol-12- myristate 13-acetate (PMA, Sigma Aldrich, Catalog # P1585), 500 ng/ml Ionomycin (Sigma Aldrich, Catalog # I9657-1MG) and 1 μg/ml Brefeldin A (Sigma Aldrich, Catalog # BA6542-5mg) in complete media for 4 hours, cells were washed at 400xg for 2 minutes twice. Cells were resuspended within 50 μl 1x PBS containing DimerX and Fc Block. Following incubation on ice in dark for 30 minutes, cells were washed with 1x PBS. 50 μl 1x PBS containing B220-FITC, NK1.1-PerCp/Cy5.5, CD4-PE, TCRβ-Pacific Blue and B220-Brilliant Violet 605 were added onto cells and they were incubated on ice in dark for 30 minutes. Specificities and concentrations of each antibody used for staining were listed in Table 2.3. After repeating the washing steps. 50 μl fix/permeabilization buffer (Biolegend, Catalog # 421402) were added and cells were again incubated on ice for 30 minutes. Then, 1:10 diluted 100 μl permeabilization were added and cells were centrifuged at 400xg for 2 minutes. Following removal of the supernatant, 1:200 diluted 50 μl IFNγ antibody was added onto each ell and it was incubated on ice for 30 minutes in dark. Cells were washed again with permeabilization buffer and resuspended within 150 μl PBS-EDTA. Cells were transferred to FACS tubes and acquired by BD LSR Fortessa III (BD Biosciences).

2.2.7.2. Staining of Cell Surface markers

2.2.7.2.1. CD83/HLA-DR staining of human PBMCs

After incubating human PBMCs from healthy and SCI donors either with R848 (5μg/ml) or D35 (3μM) for 24 hours, fixation and washing steps were followed as they were described in Section 2.7.1.1. Cells were stained with anti-CD83-PE and anti-HLA-DR- FITC Ab. Following washing, cells were resuspended in 500 μl PBS-BSA-Sodium azide, and analyzed in BD Accuri 6 Flow Cytometry.

2.2.7.2.2. Surface marker staining of CFSE labeled murine splenocytes

After incubating OT1 mice spleen cells with exosomal ligands for 5 days, cells were transferred to V-bottom 96-well plate after a very well performed up and down pipetting. Then, cells were centrifuged at 400xg for 4 minutes and resuspended within 150 μl 1x PBS. Following another round of centrifugation at 400xg for 4 minutes, cells were resuspended within 50 μl 1x PBS containing 1:100 diluted Fc Block and incubated on ice in dark for 30 minutes. Cells were washed and CD4-PE, B220-PE/Cy7, CD44-APC, CD8a-APC/Cy7, TCRβ-Pacific Blue containing 50 μl 1x PBS was added onto each well. Specificities and concentrations of each antibody used for FACS analyses were listed in Table 2.3. After incubating on ice for 30 minutes, cells were washed twice and resuspended within 150 μl 1x PBS for analysis by BD LSR Fortessa III (BD Biosciences).

2.2.7.2.3. Surface marker staining of PECs

After collecting mice PECs, cells were fixed as it was described in Section 2.2.2.5. Then, 1:100 diluted Fc block containing 25 μl 1x PBS was added onto the cells and incubated on ice for 5 minutes. Following Fc block incubation, 25 μl 1x PBS containing CD11b-PE, Ly-6G-FITC or B220-PE/Cy5 were added and incubated for 30 minutes on ice in dark. Then, cells were washed twice and resuspended within 150 μl 1x PBS to be analyzed by BD Accuri 6 Flow Cytometry.

2.2.7.3. BrdU staining

Spleen cells were washed by centrifugation at 400x g for 2 minutes. Then, cells were incubated either with Live/Dead (1:1000 diluted) and Fc Block (1:100 diluted), Live/Dead (1:1000 diluted), Fc Block (1:100 diluted) and SIINFEKL pentamer (Table 2.3.) or Live/Dead (1:1000 diluted), Fc Block (1:100 diluted) and DimerX (Table 2.3.) for 30 minutes in dark on ice. Following washing cells, surface staining was done by incubating cells with 50µl of antibody mix for 30 minutes on ice in dark. To determine the BrdU incorporation by T helper cells, a fraction of cells which were incubated with only Live/dead and Fc Block first, were stained with CD44-PE, CXCR5-PE/Cy7, PD-1-APC, CD4-APC/Cy7, TCRβ-Pacific Blue and B220-Brilliant Violet 605. Another set of these cells were incubated with CD25-PerCp/Cy5.5, CD23-PE, CD95-PE/Cy7, CD138-APC, GL7-Pacific Blue and B220-Brilliant Violet 605. To determine the OVA-specific cytotoxic T cell proliferation, the remaining fraction of cells which were treated with Live/dead, Fc Block and SIINFEKL pentamer-PE cocktail, were further incubated with B220-PerCp/Cy5.5, CD3-PE/Cy7, γδTCR-APC, CD44-Pacific Blue and CD8a- Brilliant Violet 605. Cells, which were incubated with Live/dead, Fc Block and DimerX, first, stained with CD4-PE, CD8a-PE/Cy7, NK1.1-APC/Cy7, TCRβ-Pacific Blue and B220-Brilliant Violet 605. Specificities and concentrations of each antibody used for FACS analyses were listed in Table 2.3. Next, 1x PBS was added onto cells and they were washed again. According to the manufacturer's protocol for BrdU staining (BD Biosciences, catalog # 559619), 50µl of Cytofix/Cytoperm buffer was added onto cells and incubated for 15 minutes on ice. Following washing step with the addition of BD Perm/wash buffer at 400xg, cells were resuspended within 50 µl of Cytofix/Cytoperm. buffer and incubated on ice for 10 minutes. Then, cells were washed by adding 100 µl Perm/Wash buffer. Following washing, 50 µl of Cytofix/Cytoperm. was added and it was incubated on ice for 5 minutes. After repeating washing step, 100 µl of DNase was added onto cells and they were incubated at 37°C for 1 hours. Then, cells were washed and resuspended within 150 µl 1x PBS to perform the FACS analysis by BD LSR Fortessa III.

2.2.8. ELISA Studies

2.2.8.1. Cytokine ELISA

50 µl of antibodies specific for human IL6, IL10, IFNα, IFNγ and IP10 were coated onto Immulon2HB 96-well plates and incubated for 4 hours at RT or overnight at +4°C. Specificities and concentrations of each antibody used for ELISA analyses were listed in Table 2.1. 1x PBS-5% BSA were used to block plates for 2 hours at room temperature. Then, plates were washed 5 times with 1x PBS-0.025% Tween 20. Following washing step, the wells were covered with 50 µl from cell supernatants and recombinant standard proteins (Table 2.1) in duplicates were layered via serial dilutions (1/2x dilution, 11 series). After incubation of supernatants and recombinant proteins at +4°C overnight, washing step was followed and biotin-labeled anti-cytokine antibodies (Table 2.1) were added for 2 hours of incubation at room temperature. 1:1000x diluted Streptavidin-Alkaline Phosphatase (SA-ALP) was added after washing the plates and incubated for 1 hour at room temperature. ELISA plates were washed and developed by adding 1:5000x diluted Phosphatase substrate (PNPP). Optical density values for samples and standard cytokines were detected on a ELISA reader (Spectramax, Molecular Devices) at 405nm.

2.2.8.2. Anti-OVA IgG ELISA

MaxiSorp plates were coated with 50 µl of 10 µg/ml OVA diluted in 1x PBS and incubated at +4°C for overnight. Same blocking and washing steps performed during cytokine ELISA explained in Section 2.2.8.1 was repeated and then 10x diluted mice blood sera were layered onto coated and blocked first wells. Then, blood sera were transferred to wells at the vertical axis via 4x dilution with a 50 µl of final volume in each well. Following incubation at +4°C for overnight, plates were washed and 50 µl of 1:2000 diluted ALP conjugated anti-mouse IgG, IgG1 or IgG2c antibodies were added onto the cells and incubated for 2 hours at room temperature. Specificities and concentrations of each antibody used for ELISA analyses were listed in Table 2.1. After washing, PNPP substrate was added and development of yellow color was read by ELISA reader at 405 nm.

2.2.8.3. Anti-OVA ELISA

In order to determine the OVA presence on RAW264.7 exosomes encapsulated with OVA, 5 μg/ml of exosome were layered onto 96-well ELISA plates along with 3x diluted OVA with starting concentration of 1 μg/ml as standard control. Exosome samples and OVA standards were incubated at +4°C for overnight. Then, plates were washed and 50 μl of 1:1000 diluted anti-OVA were layered onto each well for 2 hours of incubation at room temperature. Following washing plates, 1:2000 diluted anti-mouse IgG-HRP as secondary antibody was added onto the wells. Following 1 hour incubation at room temperature, plates were washed and then developed adding TMB solution 3, 3', 5, 5'-tetramethylbenzidine (TMB) (Biolegend, Catalog # 421101) according to the manufacturer's protocol. Reaction was stopped by adding 1M H_2SO_4. The plates were read at 450 nm using Multilabel Reader (Enspire 2300 Perkin Elmer).

2.2.9. ELISPOT

PVDF membrane plates (Millipore) were activated with 95% ethanol and coated with 10 μg/ml IFNγ antibody for overnight at +4°C. Then, plates were blocked and $2x10^5$ spleen cells collected from mice, which injected with intraperitoneally with 5 μg OVA, 10μg ODN and 0.3μg αGC or their encapsulated forms into 30 μg of exosomes, were seeded onto each well along with only medium, 2 μg/ml OVA protein (Sigma Aldrich, Catalog # A5503), 2 μg/ml SIINFEKL (Innovagen, Catalog # SP-O257-1) 2 μg/ml $OVA_{323-339}$ peptide (Innovagen, Catalog # SP-O323-1), 2 μg/ml OVA or 2 μg/ml Concanavalin A (Sigma Aldrich, Catalog # C2272). Following incubation at 37°C for 22 hours, supernatants were removed and plates were washed with plate washer. 100 μl of 1:1000 diluted biotinylated antibody in 0.5% FCS-PBS was added onto cells and incubated at room temperature for 2 hours. Following washing step, 100 μl of 1:1000 diluted SA-ALP in 0.5% FCS-PBS was added onto cells and incubated at room temperature for 2 hours. In order to develop the ELISPOT plate, 100 μl of BCIP substrate was added onto the wells and development was stopped by rinsing the plate with tap water. Plates were kept in the dark at room temperature overnight. Spots were counted with Biosys Elispot Reader.

2.2.10. *In vivo* Studies

2.2.10.1. Immunization and E.G7 challenge study

Adult male C57BL/6 mice (8/group) were injected intraperitoneal with PBS, $3x10^7$ E.G7 exosomes and encapsulated form of $3x10^7$ E.G7 exosomes with ODN (15µg) 3 times with 14 and 21 days apart. One week after booster injection, mice were bled and serum was used to test anti-OVA IgG responses. At day 35, mice were subjected to second booster injection. At day 47, mice were tail bled and sera was maintained at -20°C for further anti-OVA IgG studies.

At day 54, $5x10^6$ E.G7 cells were injected to mice immunized mice subcutaneously. Tumor development was observed and tumor sizes were measured every day after following palpable tumor formation. At day 70, mice were tail bled and they were sacrificed.

2.2.10.2. *In vivo* cell proliferation study

C57Bl/6 mice were intraperitoneally injected either with mixture of 5 µg OVA, 10µg ODN and 0.3µg αGC or their encapsulated forms into 30 µg of exosomes. Mice were fed with 0.8 mg/ml 5-bromo-2´-deoxyuridine (BrdU, Sigma, Catalog # B5002) in drinking water supplemented with 2.5% sugar for 7 days. At day 7, mice were sacrificed, blood was collected from the heart to separate the sera. Then, sera were stored at -20°C for further analysis of anti-OVA IgG responses. Spleens were collected for ELISPOT, BrdU staining and intracellular cytokine staining experiments.

2.2.10.3. Tumor therapy study

Female C57Bl/6 mice were subcutaneously injected with $5x10^6$ OVA expressing B16-F10 cells in day zero at the shaved back of the mice. Tumor development was observed and at day 9 when tumors became palpable and measurable, mice were intraperitoneally injected with mixture of 5 µg OVA, 10 µg ODN and 0.3 µg αGC or their encapsulated counterparts into 30 µg of exosomes. Before repeating this treatment at day 15, mice were bled tail and sera was kept to further perform anti-OVA IgG ELISA. Tumor development was observed until the tumor sizes reached to 2000 mm^3 and then mice were sacrificed.

2.2.11. Statistical Analysis

All statistical analyses for studies carried out for SCI and αGC project were performed using GraphPad Software (GraphPad Inc.).

For SCI project, all continuous variables were presented as mean and standard deviation. Categorical data was presented using number and percent. Categorical variables were compared with the X2 test. $p<0.05$ was significant.

Mann-Whitney U test, Wilcoxon test and Kruskal-Wallis was used for comparison of between group results. Two-way ANOVA with Bonferroni's correction was used for comparison of within-group results. Categorical variables were compared with the X2 test. $p<0.05$ was significant.

All data analyses for BD project were performed using Sigma Stat 3.5 (Systat Software Inc.) program. Significance between active BD, inactive BD and healthy groups were tested by one-way ANOVA. Student's t-test was performed in order to determine significance between sub-groups of active BD vs inactive BD. $p \leq 0.05$ was set to be statistically significant.

Chapter 3

Results

PART-I: Utilization of Exosomes as a Prophylactic Anti-Cancer Vaccine

3.1. Use of CpG ODN Loaded Exosomes as a Potential Anti-cancer Therapeutic Agent

3.2.1. Encapsulation into exosomes increases immunostimulatory activity of CpG ODN

Exosomes isolated from OVA expressing E.G7 cell line supernatants were encapsulated with CpG ODN via lyophilization technique. Following controlled rehydration of powder, CpG ODN encapsulation was successfully obtained. Next, spleen cells were stimulated either with two different doses (0.4 and 2 μM) of free or exosome encapsulated CpG ODN for 8-48 hours to investigate the kinetics of stimulation. IL6 production from stimulated cell supernatants revealed that encapsulation of CpG ODN into E.G7 exosomes led to accelerated and magnified IL6 production even at low CpG ODN dose (Fig 3.1A). Over 50ng/ml IL6 was produced by 48h stimulation compared to undetectable IL6 level for non-encapsulated CpG ODN. Dose sparing effect of exosomes was further tested on mouse splenocytes. Four different doses of free CpG ODN (0.1, 0.3, 1.0 and 3.0 μM) or exosome loaded counterparts were incubated with splenocytes for 24h. IL12 and IFNγ secretion levels suggested that exosome loaded CpG ODN improved both IL12 and IFNγ in a dose dependent manner (Fig 3.1B and 3.1C). This induction capacity was much pronounced at lower doses.

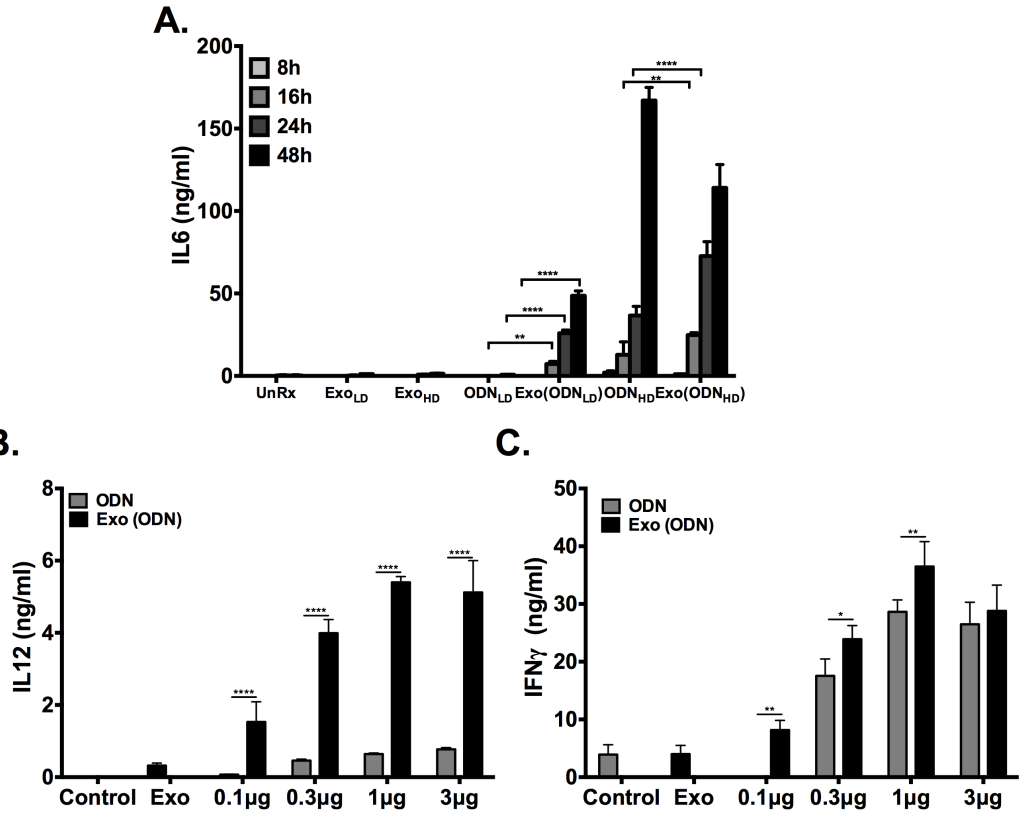

Figure 3.1. Immunostimulatory activity of CpG-ODN is elevated upon encapsulation into exosomes.

Splenocytes were stimulated with different doses of free or exosomal form of CpG for 8-48 hours for IL6, 24 hours for IL12 and IFNγ. Bar graphs represent (A) IL6, (B) IL12 and (C) IFNγ production detected by ELISA from cell supernatants. Statistical significance was tested by Student's t test. *, $p<0.05$; **, $p<0.001$; ****, $p<0.0001$. (LD: Low Dose, 0.4 μM and HD: High Dose, 2 μM).

3.1.2. Exosomal CpG ODN activates APCs

IFNα is a cardinal cytokine oh which secretion is specifically induced by D-type ODN. Following observation of enhanced immunostimulatory activity of CpG ODN within exosomes, IFNα production in mouse was investigated. With this aim, mouse splenocytes were stimulated with two different doses of free or exosomal form of CpG ODN (0.4 and 2.0 μM) for 24 hours and then intracellular IFNα staining was performed. FACS analysis indicated that exosome loaded CpG ODN elicited significantly higher IFNα production from mouse pDCs at low CpG ODN dose (Fig

3.2A and 3.2B). Furthermore, the surface marker expression levels of APCs following stimulation either with free or exosomal CpG ODN revealed that CpG ODN in exosome were more effective APC activator than free counterpart. Since their surface marker expression ($CD86^+/MHCII^+$) cells were significantly higher in response to exosomal CpG ODN than the free form (Fig 3.2C). Collectively, this data show that encapsulation into exosomes enhances the immunostimulatory activity of CpG ODN and this could be due to elicited activation of APCs.

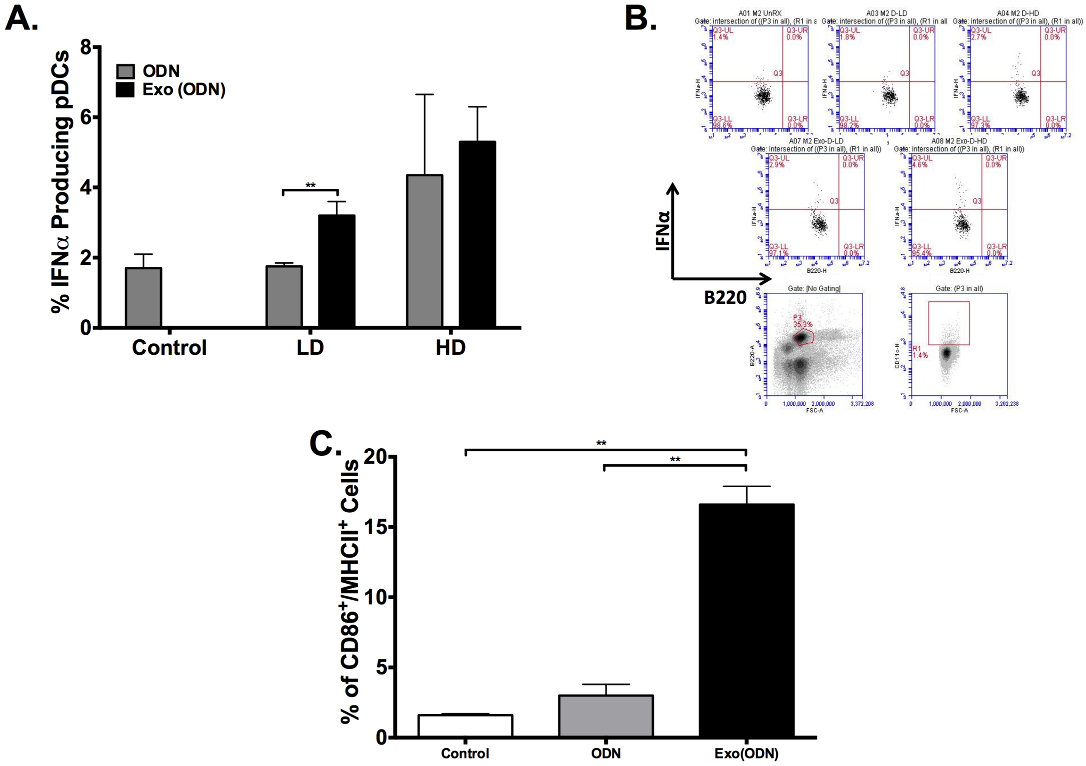

Figure 3.2. Exosomal CpG ODN enhances CpG ODN mediated immune activation.

Mice splenocytes were stimulated with 0.4 and 2.0 μM of free or exosomal CpG ODN for 24 hours. (A) Bar graph represents percent of IFNα producing pDCs ($B220^+/IFN\alpha^+$). (B) Representative dot-plots showing gating strategy of mouse pDCs. (C) Splenocytes were stimulated with 0.2 μM dose of free or exosomal CpG for 24 hours and stained for CD86/MHCII double positive cell. Bar graph shows double positive cell percentages following treatments. Student's t test was used to determine the statistical significance. **, p<0.001

3.1.3. CpG ODN encapsulated into exosomes triggers Th1-biased anti-OVA immunity and prevents tumor formation.

Mice (C57/Bl6) were injected ip. either with plain or CpG ODN loaded exosomes (@ week:0 and week:2, 15µg CpG ODN/mouse/injection, Fig 3.3A). After 1st booster injection, anti-OVA IgG responses from sera were studied and results showed that 2 injections were not sufficient to induce detectable anti-OVA IgG titers. Therefore @ week:5 animals were re-boosted with the same formulations. Then, 12 days later animals were tail bled to check the anti-OVA IgG responses. Results showed that mice injected either with plain or CpG ODN loaded exosomes induced Th1 biased immunity (Fig 3.3B). 20 days after second booster injection, mice were inoculated with E.G7 cells and tumor development was followed until week:10. At week 10, mice were tail bled and sacrificed. Anti-OVA responses from the sera suggested that mice immunized with CpG ODN encapsulated exosomes had improved anti-OVA response (Fig 3.3C). Moreover, exosomal CpG ODN prevented the tumor formation (Fig 3.3D).

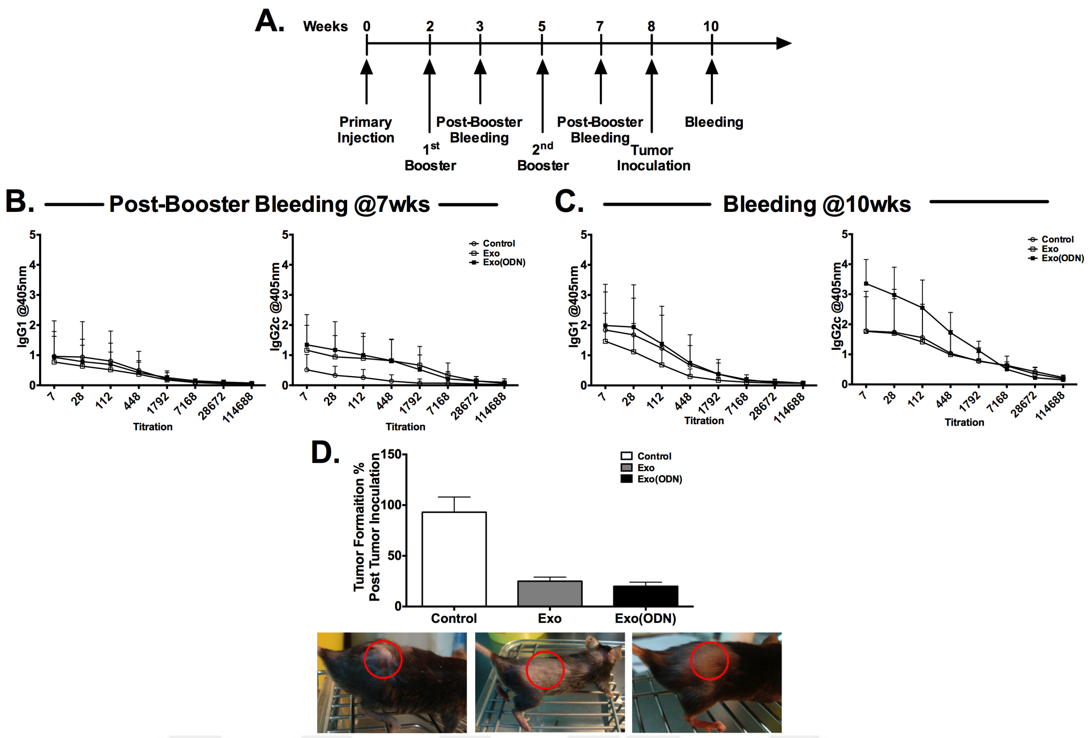

Figure 3.3. Exosomal CpG ODN immunization promotes Th1 biased immunity and tumor clearance.

(A) Immunization schedule of mice (8 mice/group) injected either with $3x10^7$ exosomes or 15 µg CpG ODN loaded exosomes, then challenged with E.G7 thymoma cells. Average anti-OVA IgG1 and IgG2c titers at (B) 7 weeks and (C) 10 weeks. (D) Bar graphs represent percentage of tumor formation in each group following immunization and representative images of mice with EG7 tumors were shown.

PART-II: Utilization of Exosomes as a Therapeutic Anti-Cancer Vaccine

3.2. Inclusion of αGC and CpG ODN within Exosomes Contribute to Immunogenicity of Cancer Vaccine

3.2.1. Exosomes isolated from RAW264.7 cells retain their exosomal properties after lyophilization.

Treating established tumors is clinically more relevant although more challenging. We next embarked on this task. In addition to OVA plus CpG ODN, we wished to load αGC. But initial experiments were focused on the evaluation of the possible harmful effects of lyophilization process on the generated exosomes. To identify changes on physical structure or vesicle membrane integrity of exosomes non-lyophilized and lyophilized exosomes isolated from macrophage-like murine cell line, RAW264.7, were assessed for the expression of surface marker distribution by flow cytometry, identification of exosome-specific proteins by western blot and average vesicle size distribution by AFM. Non-lyophilized and lyophilized exosomes from 5 different batches of RAW264.7 cell culture supernatants were coupled onto anti-CD81 conjugated latex beads and stained against CD81, CD11b, H-2Kd and I^A/I^E, CD1d and CD9 surface proteins. Flow cytometry analysis showed that lyophilized exosomes retained cardinal exosomal markers such as CD81 and CD9 as well as other markers carried by non-lyophilized exosomes (Fig 3.4A, Fig A1A and A1B). Furthermore, as it was shown in Fig 3.4B, the expression level of Alix and Tsg101 proteins, of which existence identifies the vesicles as exosomes, were indistinguishable between non-lyophilized and lyophilized exosomes. In order to determine the effect of lyophilization process on exosome size distribution, non-lyophilized and lyophilized exosomes were analyzed in dried state by AFM. Images shown in Fig 3.4C shows that size of the exosomes were significantly increased after lyophilization. In addition, we wanted to investigate if non-lyophilized and lyophilized exosomes behave differently when they are intraperitoneally injected to the mice regarding uptake by peritoneal cells. For this purpose, mice treated with thioglycolate for 4 days were intraperitoneally injected with PKH-26 labeled non-lyophilized and lyophilized exosomes. Four hours later, mice were sacrificed and PECs were recovered for analysis by flow cytometry. Cells were stained with macrophage, neutrophil and B cell specific antibodies and PKH-26 positive cells were gated. Flow cytometry analysis revealed that the level of uptake of non-lyophilized or lyophilized exosomes by peritoneal cells were similar (Fig A2). Collectively, these findings confirmed that lyophilization process does not induce any detrimental changes on exosome bilayer structure or integrity and internalization kinetics were unaltered after lyophilization.

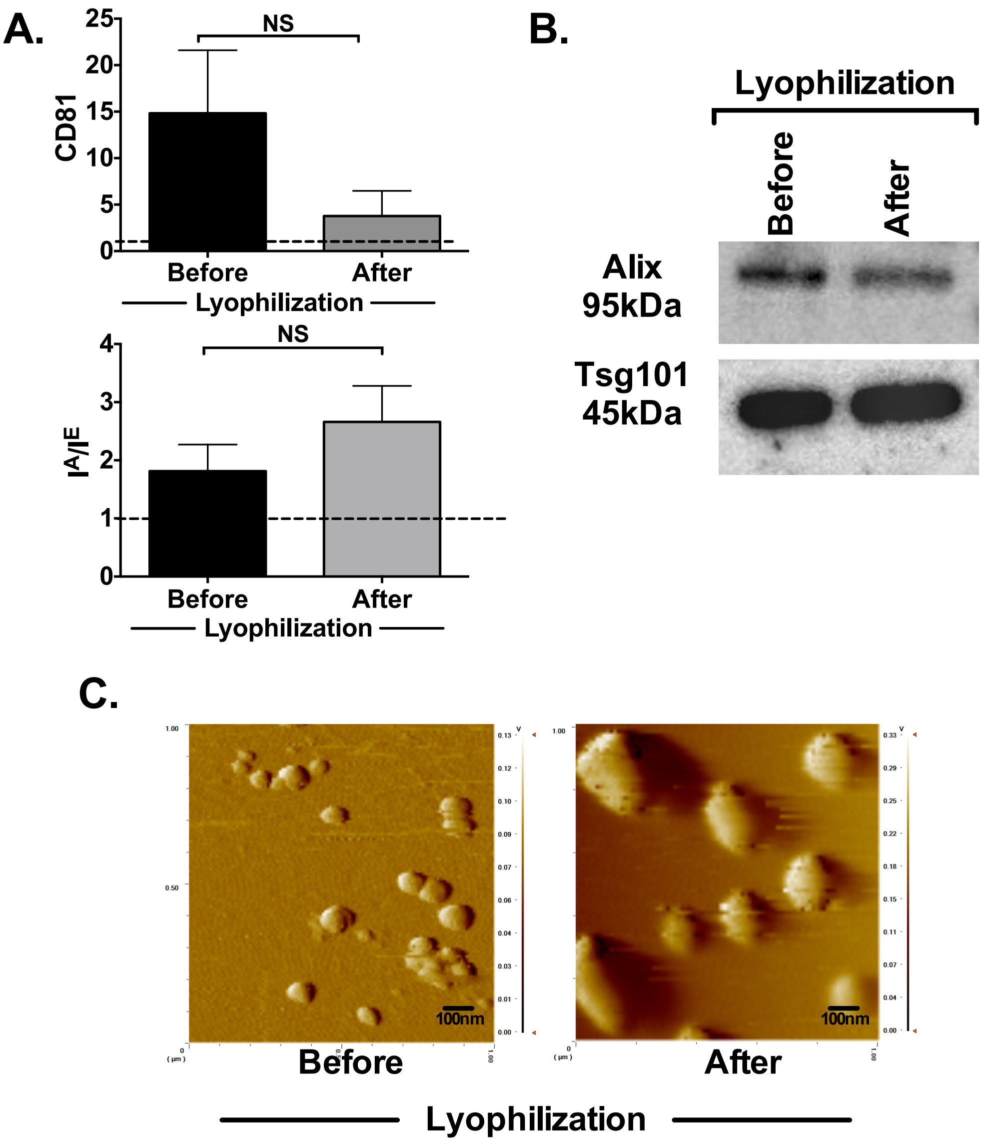

Figure 3.4. Characterization of exosomes isolated from RAW264.7 cell line.

(A) Non-lyophilized and lyophilized exosomes coupled to anti-CD81 conjugated beads were phenotyped via FACS analysis. Bar graphs represent the MFI ratio of the antibody to its specific isotype. Statistical significance was tested using Wilcoxon test. P value is 0.0625. (B) 25 μg of proteins isolated from non-lyophilized and lyophilized exosomes were analyzed by western blot to test the presence of Alix and Tsg101. (C) AFM topography images from 1μm^2 showing size distribution of non-lyophilized and lyophilized exosomes.

3.2.2. Lyophilization is a more effective loading technique than feeding and moreover it enables to load exosomes with more than two molecules.

Since we established that lyophilization is not detrimental to purified exosomes, we next checked whether this approach is more feasible than conventional cell feeding approach. It is important to note that ligands such as CpG ODNs could not be fed to cells if the aim is to include CpG ODNs within exosomes. If CpG ODN receptor is expressed by the target cell expected to secrete CpG containing exosomes, this will stimulate the cell rather than include the ligand within secreted exosomes. First, RAW264.7 cells were fed with OVA protein (1mg OVA/10^6 RAW cells) for 24 hours and then exosomes were purified from culture supernatants. In another batch, exosomes were first isolated from non-OVA treated RAW264.7 cells and 5 μg OVA protein was encapsulated via lyophilization into 30 μg exosomes. Then, these batches were immunoblotted against OVA protein. Western blot images shown in Fig 3.5A revealed that only exosome loaded OVA via lyophilization gave strong OVA signal. Moreover, anti-OVA ELISA confirmed that exosomes loaded with i) OVA, ii) OVA+ODN and iii) OVA+ODN+αGC (OVA: 5ug, CpG ODN: 10ug, and αGC: 0.3 μg within exosomes) via lyophilization expressed similar levels of OVA on the surface (Fig. 3.5B).

The immunological functionality of these constructs was then tested using OT1 mice spleen cells. For the *in vitro* T-cell proliferation assay, spleen cells were first labeled with CFSE, and then they were stimulated with 3 different exosomal constructs as mentioned above. Cells treated with 1 and 5 μg exosome containing (CpG ODN+OVA+αGC) induced significant OVA specific T-cell proliferation (Fig. 3.5C)

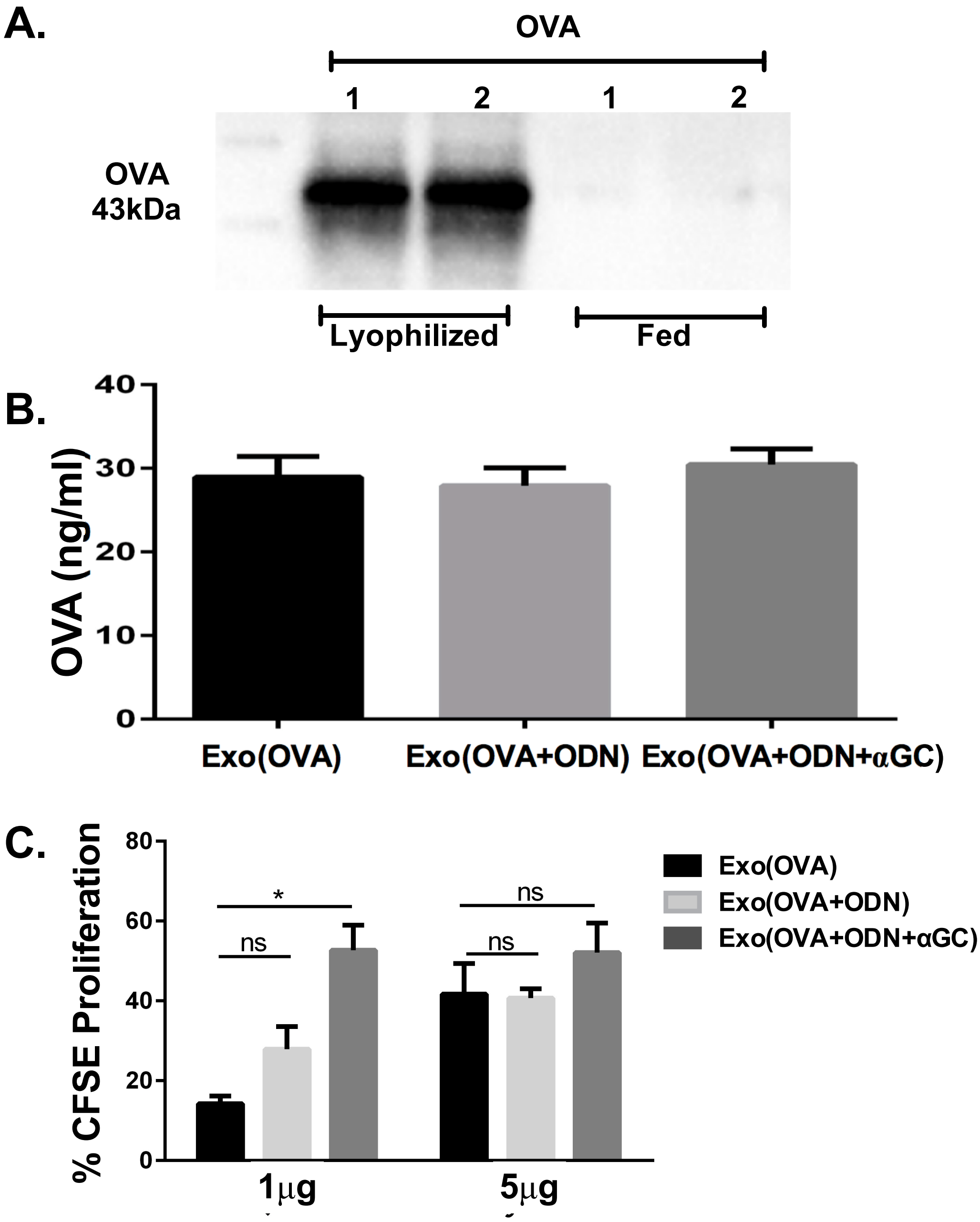

Figure 3.5. Exosomes can be loaded with different antigens and adjuvant at the same time.

(A) Western blot image showing OVA signal from exosomes either loaded via lyophilization or fed onto cell culture media. (B) OVA amount on exosome surface analyzed by ELISA. (C) Bar graph representing the percentage of proliferated OVA-specific T-cells from OT1 mice splenocytes stimulated with 1 and 5 μg concentrations of OVA, OVA+ODN and OVA+ODN+αGC loaded to RAW264.7 exosomes via lyophilization.

3.2.3. Encapsulation of D-type CpG ODN and αGC into exosomes induces OVA specific T-cell proliferation.

In vitro studies proved that lyophilization technique did not affect the exosomes and moreover by the help of this approach it was possible to encapsulate exosomes with antigens and immunostimulatory molecules. To assess the *in vivo* immunological responses, mice were intraperitoneally injected wither with mixture of 5μg OVA+10μg ODN+0.3μg αGC or their counterparts encapsulated into exosomes via lyophilization. After feeding mice with BrdU in drinking water for 7 days, flow cytometry analysis showed that both proliferated $CD4^+$ and $CD8^+$ T cell percent were significantly increased in response to exosomal form of antigens and adjuvant than the mixture form (Fig 3.6A and 3.6B, Fig A3.A and A3.B). Strikingly, mice injected with exosomal antigens and adjuvant had approximately 7.5-fold higher number of OVA specific $CD8^+$ T cell number compared to control group at the end of 7 days, whereas there was no significant increase in antigen specific cytotoxic T cell number in mice injected with free formulation (Fig 3.6C and 3.6D). Furthermore, exosomal formulation injection significantly induced proliferation of OVA specific $CD8^+$ T cells (Fig 3.6E). Exosomal OVA+ODN+αGC did not have additive effect only on proliferation of helper and cytotoxic T cells, this formulations also induced significant proliferation of splenic iNKT and γδ-TCR^+ T cells than control group (Fig 3.6F and 3.6G, Fig A3.C, Fig A3.D and FigA3.E).

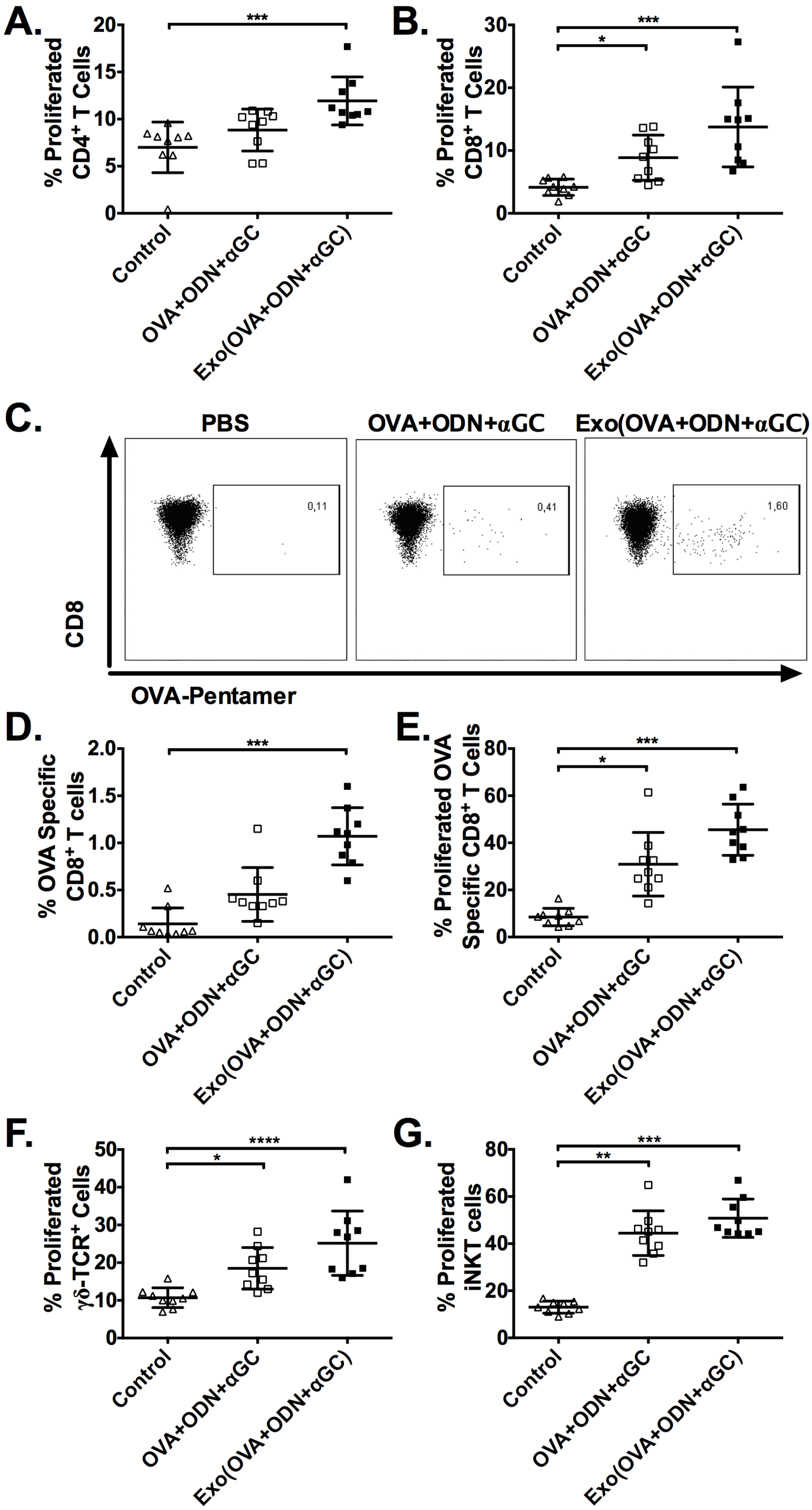

Figure 3.6. Exosomal CpG ODN and αGC induces OVA specific T cell proliferation.

Mice were injected intraperitoneally either with free or exosomal form of OVA+ODN+αGC. Mice were fed with BrdU in drinking water for 7 days and sacrificed. Proliferation of splenic T cells was analyzed by FACS according to the BrdU signal positivity. (A) Proliferated $CD4^+$ T cells (defined as live cells, $B220^-$, $TCR\beta^+$, $CD4^+$). (B) Proliferating $CD8^+$ T cells (defined as live cells, $B220^-$, $TCR\beta^+$, $CD8^+$). (C) Representative FACS analysis plots of one mouse from each group injected with PBS, OVA+ODN+αGC or Exo(OVA+ODN+αGC) (D) Percentage of OVA specific $CD8^+$ T cells (E) Proliferated OVA specific $CD8^+$ T cells (defined as live cells, $B220^-$, $TCR\beta^+$, $pentamer^+$, $CD8^+$). (F) Proliferated γδ-TCR^+ cells (defined as live cells, $B220^-$, $CD3^+$, γδ-TCR^+), (G) Proliferated splenic iNKT cells (defined as live cells, $B220^-$, $TCR\beta^+$, $DimerX^+$). Statistical significance was tested using Kruskal-Wallis test. *, p<0.05; **, p<0.001; ***, p<0.001; ****, p<0.0001.

3.2.4. Antigen specific T cell responses and antibody production are more pronounced by ODN and αGC loaded into exosomes than their free form.

Splenocytes from mice injected either with free or exosomal form of OVA+ODN+αGC were re-stimulated either with OVA protein or MHC-I/II specific OVA peptide to investigate antigen specific T cell responses. IFNγ ELISPOT study showed that free form of OVA+ODN+αGC was less potent in inducing antigen specific T cell responses than the exosomal formulation (Fig 3.7A, 3.7B and 3.7C). Strikingly, number of germinal center B cells was significantly higher in mice injected with exosomal form of antigens and adjuvant than the groups injected with PBS or free formulation (Fig 3.7D, Fig A4A and Fig A4B). In concordance with this data, OVA specific antibody production was more pronounced in response to exosomal antigens and adjuvant (Fig 3.7E).

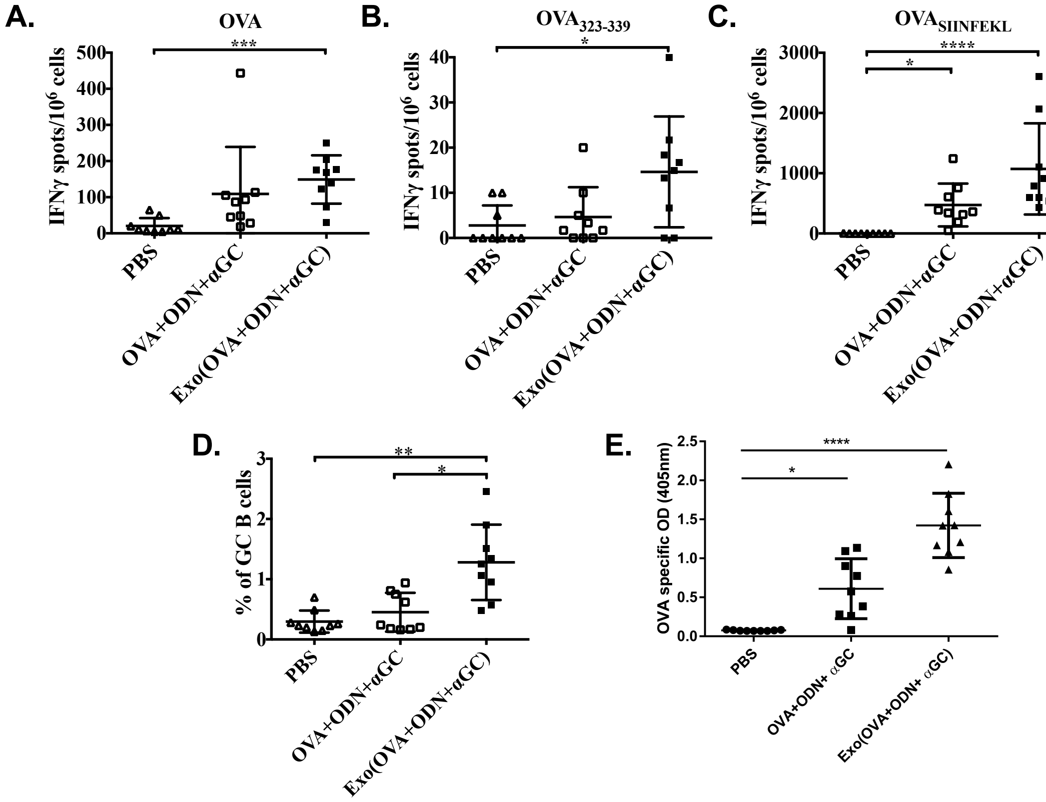

Figure 3.7. Antigen specific T-cell responses and antibody production are more pronounced by CpG ODN and αGC loaded into exosomes than their free form. IFNγ ELISPOT assays were conducted stimulating splenocytes with (A) Ovalbumin (OVA), (B) CD4 peptide (323-329), (C). CD8 peptide (SIINFEKL). (D) Graph showing the analysis of splenic germinal center B cells (defined as live cells, B220$^{+,}$ CD95^{+}, GL7^{+}). (E) OVA specific IgG production was determined by ELISA. Statistical significance was tested by using Kruskal-Wallis test. *, p<0.05; **, p<0.001; ***, p<0.001; ****, p<0.0001.

3.2.5. Therapeutic exosome vaccine harboring OVA+CpG ODN+αGC significantly regresses established tumors.

After showing exosomes loaded with OVA+ODN+αGC had more pronounced effect on cell mediated and humoral immunity, we decided to investigate whether this exosomal formulation can be effective in a therapeutic experimental set up. With this purpose, mice were injected with OVA expressing melanoma cell line B16-F10 and when tumors were palpable they were intraperitoneally treated with 30 µg exosomes loaded with 5 µg OVA 10 µg CpG ODN or 0.3 µg αGC or mixture of the antigens and adjuvant twice 6 days apart (Fig. 3.8A). When tumor volumes were followed, it was observed that mice injected with exosomal formulation had delayed tumor growth compared to those injected with only PBS or free form of antigens and adjuvant (Fig 3.8B). As it is shown in Fig 8C, only 5 days after the first injection, mice had significantly higher anti-OVA IgG responses to exosomal OVA+ODN+αGC (i.e. Ig titers were tested @ d-14, and IgG2c/IgG1>1.33). When these animals were followed over a month, we observed that while 100% of mice that received exosome therapy were alive, the rest of the animals were sacrificed due to high tumor volume (Fig. 3.8D).

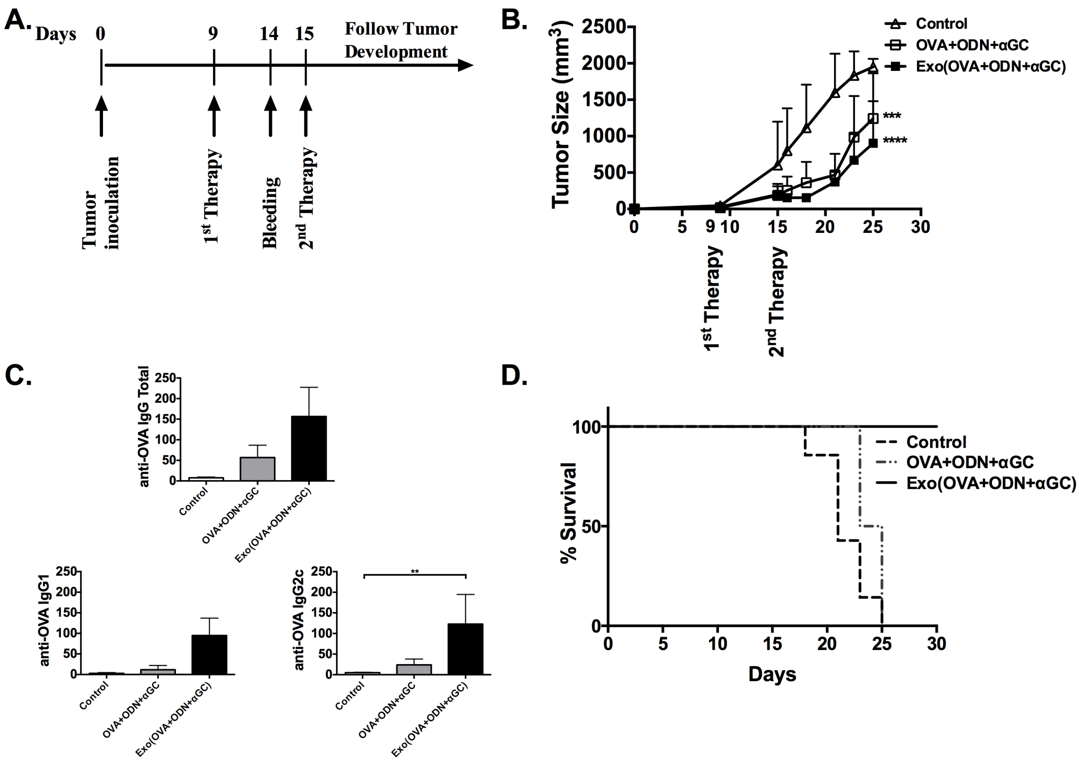

Figure 3.8. Exosomal antigens and adjuvant contributes prevention of tumor development and survival.

(A) Therapy schedule of mice (8 mice / group) inoculated with B16 melanoma cells. (B) Line graph shows average tumor volumes of mice following B16 cell inoculation at d:0. (C) End-point average anti- OVA total IgG, IgG1 and IgG2C responses of mice after 1st Rx, at d:14) Line graph showing survival rate of mice. **, p<0.01; ***, p<0.001; **** p<0.0001.

PART-III: Role of EVs in Behçet's Disease Pathogenesis

3.3. Role of LL37 Associated Plasma Extracellular Vesicles in Behçet's Disease

3.3.1. Vesicles isolated from plasma possess all universal EV characteristics.

EVs purified from healthy controls' and patients' blood plasma by ultracentrifugation were subjected to bead-based flow cytometry, western blot and DLS analysis to investigate whether EVs from plasma have the cardinal exosomal markers and are purified within expected size range. Western blot images shown in Fig 3.9A revealed that EVs from plasma had Alix and Grp94 proteins. Moreover, bead-based flow cytometry analysis revealed that EVs carry CD9 and CD63 in addition to PS residing on the surface indicated by Annexin V signal (Fig 3.9B). The DLS analysis was performed to analyze size distribution of EVs. The size of EVs isolated from plasma of both healthy controls and patients were within expected range (between ~30-700 nm, Fig 3.9C). Collectively, these data demonstrate that vesicles purified from blood plasma throughout this study fulfill the criteria that identify the vesicles as EVs.

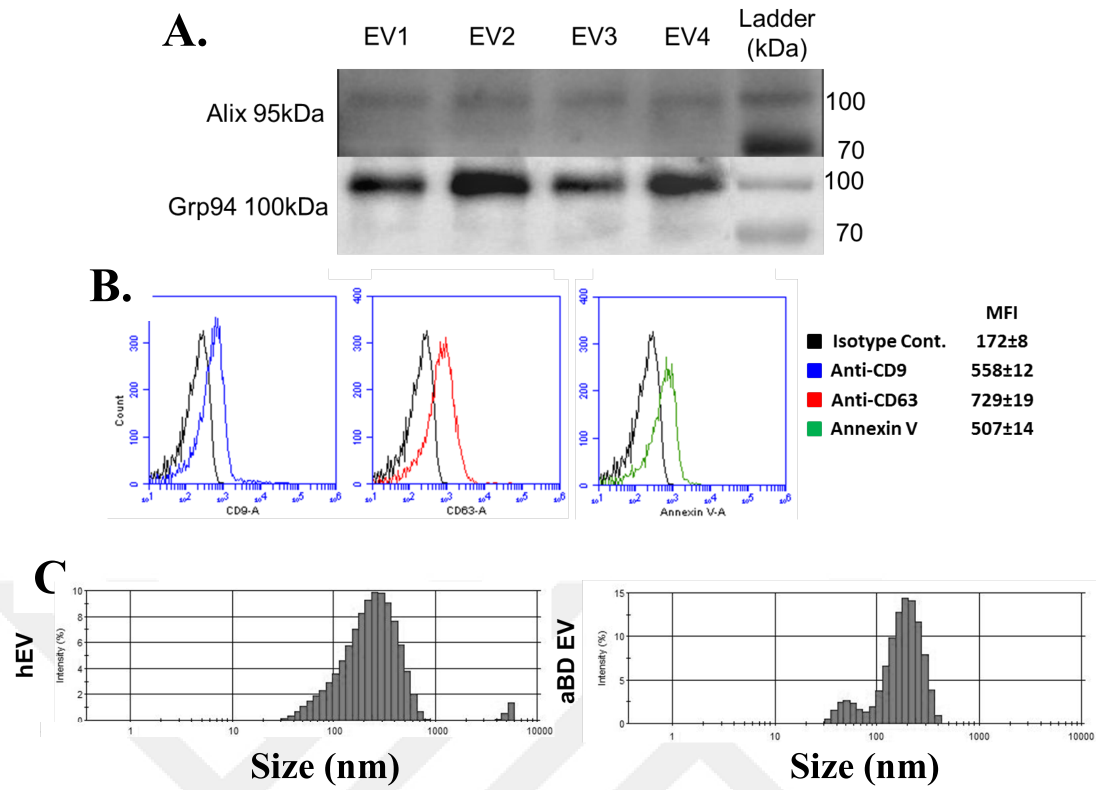

Figure 3.9. EVs isolated from plasma carry exosomal markers and their size is in expected range [219, 220].

(A) 25µg of EV protein was analyzed by western blot to determine presence of Alix and Grp94. Western blot images show expression of Alix and Grp94 proteins. (B) Flow cytometry plots represent the mean fluorescence intensity of CD9, CD63, Annexin V and their corresponding isotype controls on EVs associated with anti-CD63 conjugated beads. (C) DLS plots show the size distribution of EVs from healthy control (upper panel) and patient (lower panel) plasmas.

3.3.2. BD patients have higher numbers of plasma EVs

Isolated EVs were counted by flow cytometry in order to investigate whether there is any discrepancy in EV numbers of healthy controls and BD patients and it can be correlated with the disease severity. First, a gating strategy was optimized using binding buffer as negative control and co-incubating EVs with 1.1 µm beads (Fig 3.10A). Using this gating strategy, Annexin V FITC labeled EVs were counted by FACS. When concentrations of total plasma EV (number of EV/ml plasma) between healthy controls and patient groups were compared, it was revealed that number of active BD ($3.9 \pm 0.77 x 10^5$) and inactive BD ($2.05 \pm 0.46 x 10^5$) EVs were significantly higher than the healthy EVs ($0.78 \pm 0.25 x 10^5$). Moreover, active BD patients had more EVs in plasma than both inactive BD patients and healthy controls. In addition, active BD EVs were approximately 2 fold higher than the inactive BD EVs and this elevated trend in EV numbers were consistent between the sub-patient groups with different organ involvements (Fig 3.10B).

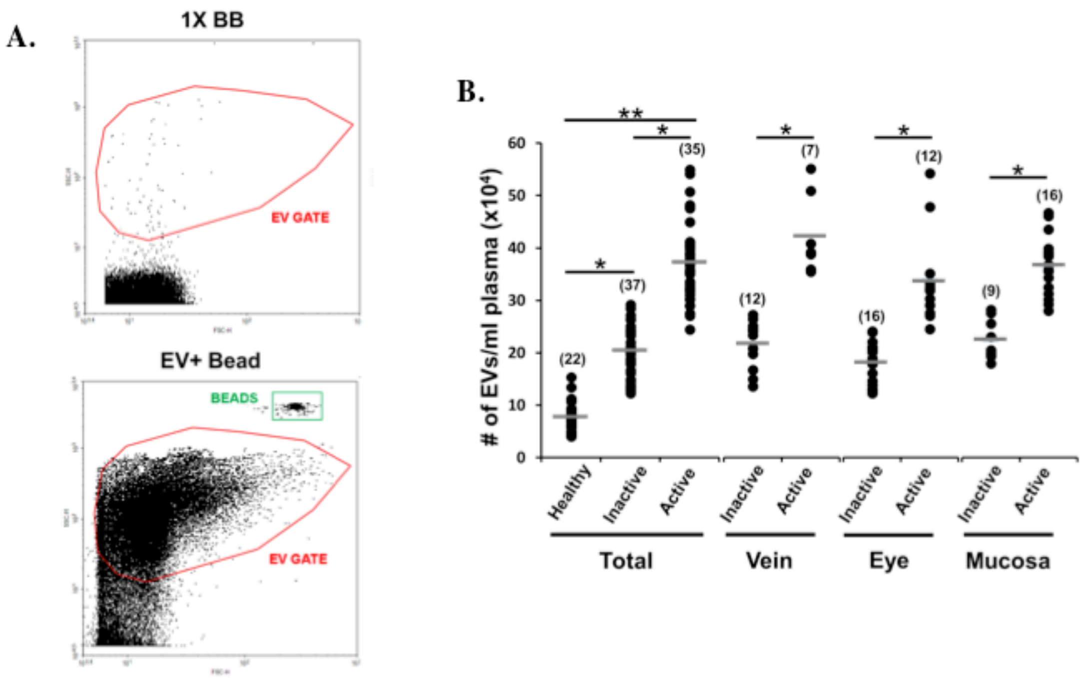

Figure 3.10. Total EV concentration is highly elevated in BD and majority of EVs is originated from platelets [219,220].

(A) Dot plots represent gating strategy to discriminate EV population from any contaminating particles and electrical noise during FACS Calibur analyses. Dot-plot image of binding buffer was used as a negative control (Upper Panel) and EVs were co-incubated with 1.1 μm control beads (Lower Panel). (B) EVs isolated from plasma were stained with Annexin V-FITC. Dot plots represent the number of EVs per ml plasma calculated according to Annexin V-FITC signal. * $p<0.01$ and ** $p<0.001$ for comparison groups based on student's t-test analyses of healthy vs. inactive BD, healthy vs. active BD and inactive BD vs. active BD. NS indicates not-significant.

3.3.3. Internalization of EVs by PBMCs induces IL6 production

After showing that EV number was increased especially in active BD plasma, we decided to investigate whether there was a correlation between this increment and immune activation observed in BD patients. In order to investigate this correlation, lipophilic CM-Dil dye was used to label EVs. Healthy PBMCs were incubated with labeled EVs isolated from BD patients' plasma at 37°C. As it is represented in Fig 3.11A, photomicrographs showed the internalization of EVs with the cells. Moreover, it was shown that this association was not due to any non-specific binding since incubation of labeled EVs with cells at +4°C abrogated cellular staining (Fig 3.11A, middle panel). Also, only CM-Dil dye pellet incubation with cells showed no non-specific dye binding to the cells (Fig 3.11A, lower panel). In next step, we aimed to evaluate whether EVs from BD patients could have a role in immune activation in different disease activity condition. With this purpose, healthy PBMCs were incubated with EVs purified from healthy controls, inactive or active BD patients for 12 hours. Cytokine ELISA study from cell supernatants revealed that active BD patients' EVs induced significantly higher IL6 than the inactive BD patients' EVs, where as healthy EVs induced very low amounts of IL6 production (Fig 3.11B).

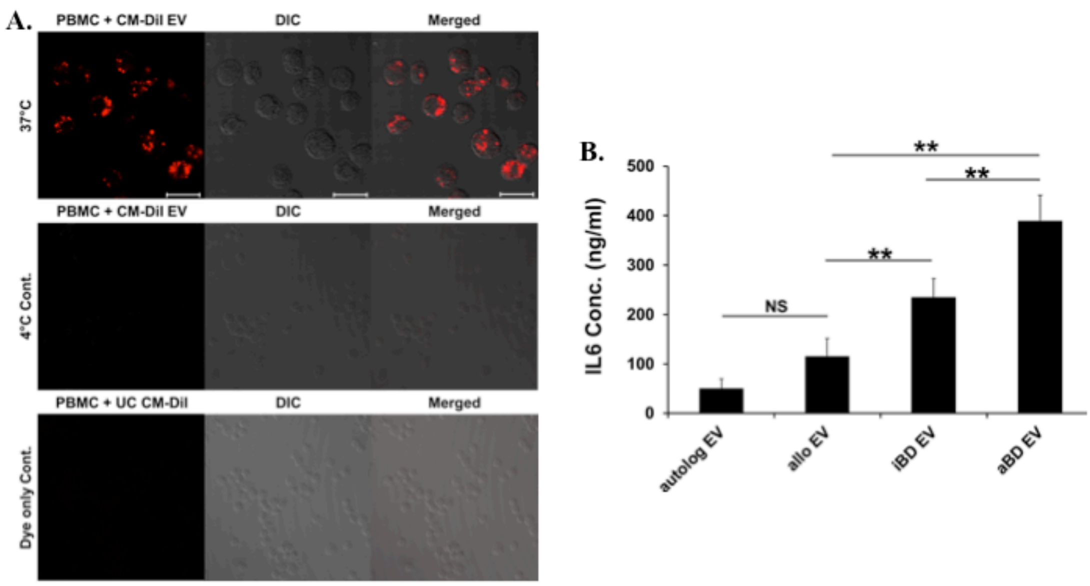

Figure 3.11. BD patients' EVs are internalized by cells and induce IL6 production [219, 220].

(A) Healthy PBMCs were incubated with BD patients' EVs for 8 hours in different conditions. Photomicrographs represent the incubation of EVs with PBMCs at 37°C (Upper Panels), +4°C (Middle Panels) and incubation of CM-Dil dye pellet with PBMCs. Left panels show CM-Dil positive signal, middle panels show DIC images and right panels show merged signals (Scale bar=20 µm). (B) Healthy PBMCs were incubated with at a cell:EV ratio of 1:2 for 12h. IL6 production was determined from the culture supernatants by ELISA. (autolog EV; autologous EVs from healthy donor; allo EV; allogeneic EVs from healthy donor; iBD EV; inactive BD EVs and aBD EV; active BD EVs). n=12 samples, ** $p<0.001$ for all comparisons.

3.3.4. Elevated levels of plasma LL37 in BD patients induces IL6 cytokine production and most of it is associated with EVs

We showed that EVs number was elevated in disease condition especially in active BD patients and this elevated number of EVs had an accelerated impact on immune activation in BD. To determine the EV-associated factor that induced the immune activation, we sought to analyze the plasma level of LL37 that is an anti-microbial peptide that is known associated with the pathogenesis of several autoimmune diseases. To achieve this, LL37 concentration in plasma, EV-depleted plasma (Plasma-EV) and EVs isolated from healthy controls, inactive and active BD patients were determined by ELISA. Compared to healthy individuals (39±8 ng/ml), both inactive BD (80±11 ng/ml) and active BD (207±16 ng/ml) patients had significantly higher levels of LL37 in plasma samples (Fig 3.12A). Following centrifugation, EV pellets were further purified with sucrose cushion and LL37 ELISA was performed on collected fraction to determine the LL37 concentration associated with EVs. LL37 concentration in active BD EVs was significantly higher than inactive BD EVs or healthy plasma EVs (Fig 3.12B, left panel). Furthermore, EVs from active BD patients purified with sucrose cushion had significantly higher induction capacity of IL6 secretion than the inactive BD EVs and healthy EVs (Fig 3.12B, right panel). To further demonstrate that immune activation was induced by LL37 association with EVS not any LL37 aggregates, plasma from healthy and aBD donors were purified with size exclusion chromatography. 3 different SEC fractions were obtained and each of them were subjected to bead based flow cytometry analysis to the detect presence of CD9 and CD63 in these fractions (Fig 3.12C). As it was expected, in fraction one the presence of CD9 and CD63 were significantly higher than the other fractions (Fig 3.12D and FigA5). When three different fractions collected from SEC were subjected to determination of LL37 concentration and IL6 production induction capacity, ELISA studies showed that there was no LL37 signal in any healthy fractions, whereas fraction #1 had significantly higher LL37 concentration from active BD patients (Fig 3.12E). Moreover, fraction #1 of active BD patients were induced significantly more IL6 secretion from healthy PBMCs (Fig 3.12F). These results confirmed that induced cytokine production was not due to any LL37 contamination in the plasma, it was strongly correlated with the association between LL37 and EVs.

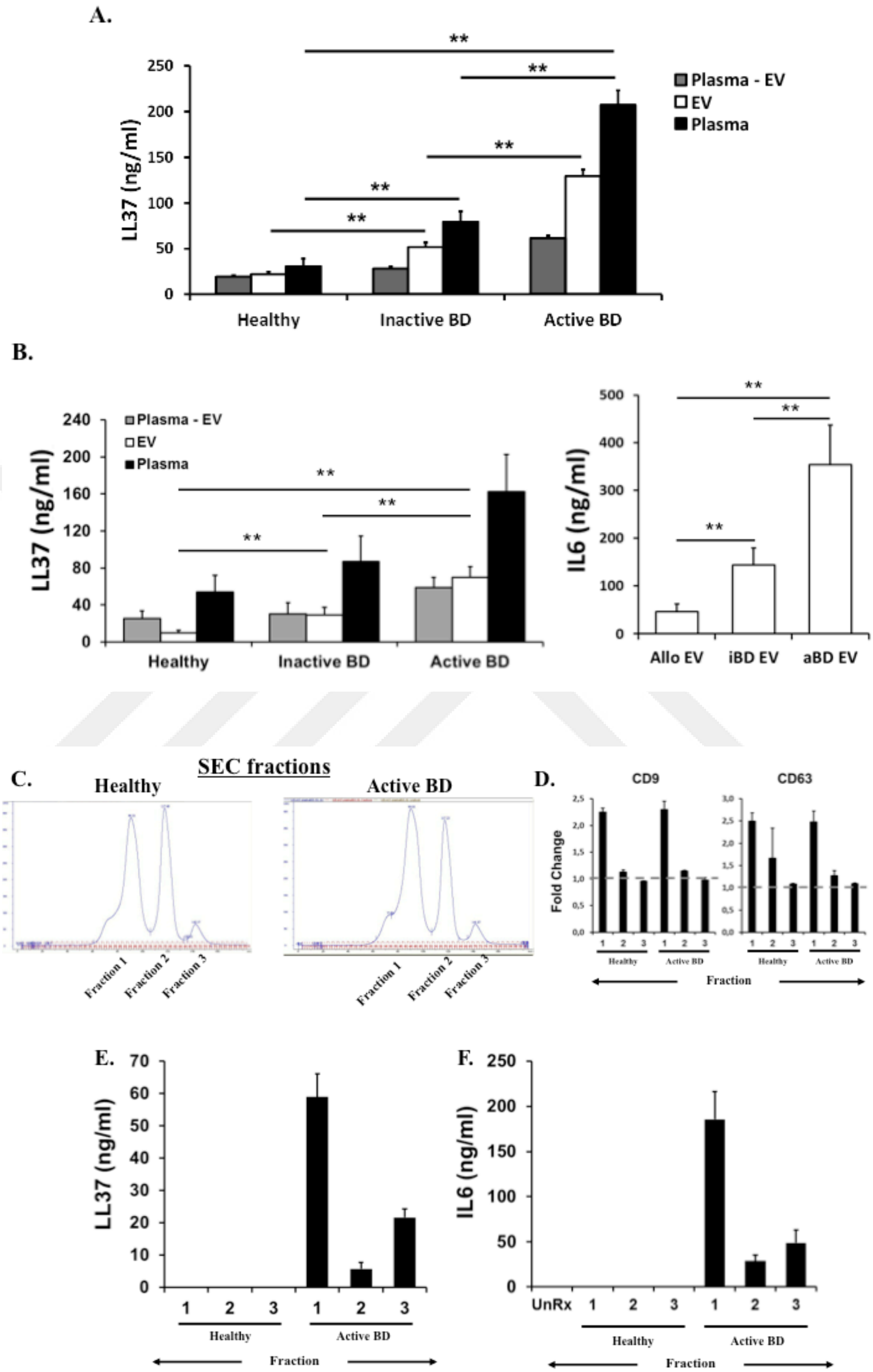
A.
**
**
**
**
**
Plasma - EV
EV
Plasma
LL37 (ng/ml)
250
200
150
100
50
0
Healthy
Inactive BD
Active BD
B.
240
200
160
120
80
40
0
LL37 (ng/ml)
Plasma - EV
EV
Plasma
**
**
**
Healthy
Inactive BD
Active BD
500
400
300
200
100
0
IL6 (ng/ml)
**
**
**
Allo EV
iBD EV
aBD EV
C.
SEC fractions
Healthy
Active BD
Fraction 1
Fraction 2
Fraction 3
Fraction 1
Fraction 2
Fraction 3
D.
CD9
CD63
Fold Change
Healthy
Active BD
Healthy
Active BD
Fraction
E.
70
60
50
40
30
20
10
0
LL37 (ng/ml)
1
2
3
1
2
3
Healthy
Active BD
Fraction
F.
250
200
150
100
50
0
IL6 (ng/ml)
UnRx
1
2
3
1
2
3
Healthy
Active BD
Fraction

Figure 3.12. LL37 plasma level is highly elevated in BD patients' plasma and it is associated with EVs [219, 220].

(A) Bar graphs represent the LL37 concentrations (ng/ml) in EV depleted plasma (Plasma-EV), EVs purified by ultracentrifugation and plasma of healthy controls and BD patients. (B) LL37 concentration comparison of EVs further purified by sucrose cushion following ultracentrifugation (Left Panel). IL6 induction Healthy PBMCs were incubated with healthy EVs (allo EV), inactive BD EVs (iBD EV) and active BD EVs (aBD EV). IL6 concentration was determined by ELISA. (Right Panel) n=12 for all samples and ** $p<0.001$ for all comparisons. (C) Plots represent the distribution of FPLC fragments collected from healthy control and active BD patients' plasma samples. (D) Each fragment was analyzed by bead-based flow cytometry analysis of EVs against CD9 and CD63 antibodies. Bar graphs show the MFI ratio of specific antibody to its corresponding isotype control. (E) Bar graphs represent the LL37 concentration of different fractions collected by SEC from healthy controls, inactive and active BD patients. (F) Il6 concentrations were determined by ELISA after incubation of healthy PBMCs with different fractions from healthy controls, inactive and active BD patients for 12 hours.

3.3.5. Association of LL37 with EVs mediates cellular internalization and immune activation

After showing plasma level of LL37 increased in BD patients compared to healthy individuals and its association with EVs induces IL6 production, EVs were labeled with lipophilic dye SP-DiOC and healthy PBMCs were incubated as such or LL37 mixed labeled vesicles at 1:2 ratio (cell:EV) for indicated time periods in Fig 3.13A. FACS analysis showed that higher number of EVs mixed with LL37 was internalized by cells compared to only as such EVs and this internalization were consistently higher as incubation time was extended to 8 hours (Fig 3.13A and FigA6.A). In order to investigate the role of this enhanced internalization of EVs with the contribution of LL37 on immune activation, healthy PBMCs were co-cultured with EVs mixed either with different concentrations of LL37 (EV-LL37) or scrambled form of it (EV-SCR) for 12 hours at 1:2 (cell:EV) ratio. ELISA study of supernatants showed that IL6 production was significantly increased in response to

EV-LL37 in a dose dependent manner, whereas combination of EV-SCR induced very little amount of IL6 and EV-LL37 mixture induced 2.2-2.3 fold more IL6 secretion than the free doses of LL37 peptide (Fig 3.13B). To eliminate the possibility that this induction could be due to non-specific association of LL37 with any plasma proteins, same experimental setup was performed with EVs isolated from human monocyte THP1 cells instead of human blood plasma EVs. In this setting, it was found out that EV-SCR induced almost no IL6 secretion, whereas EV-LL37 mixture induced 2.1 fold more IL6 secretion than the free doses of LL37 peptide (Fig 3.13C). To further demonstrate that this immune activation was due to LL37 association, healthy PBMCs were incubated with EV-LL37 mixture in the absence and presence of anti-LL37. Study of IL6 ELISA from cell supernatants revealed that anti-LL37 antibody addition abolished IL6 secretion in a dose dependent manner from cells treated with EV-LL37 mixture (Fig 3.13D). In addition, similar reduction induced by anti-LL37 antibody was observed with cells treated with inactive and active BD EVs (Fig A6.B).

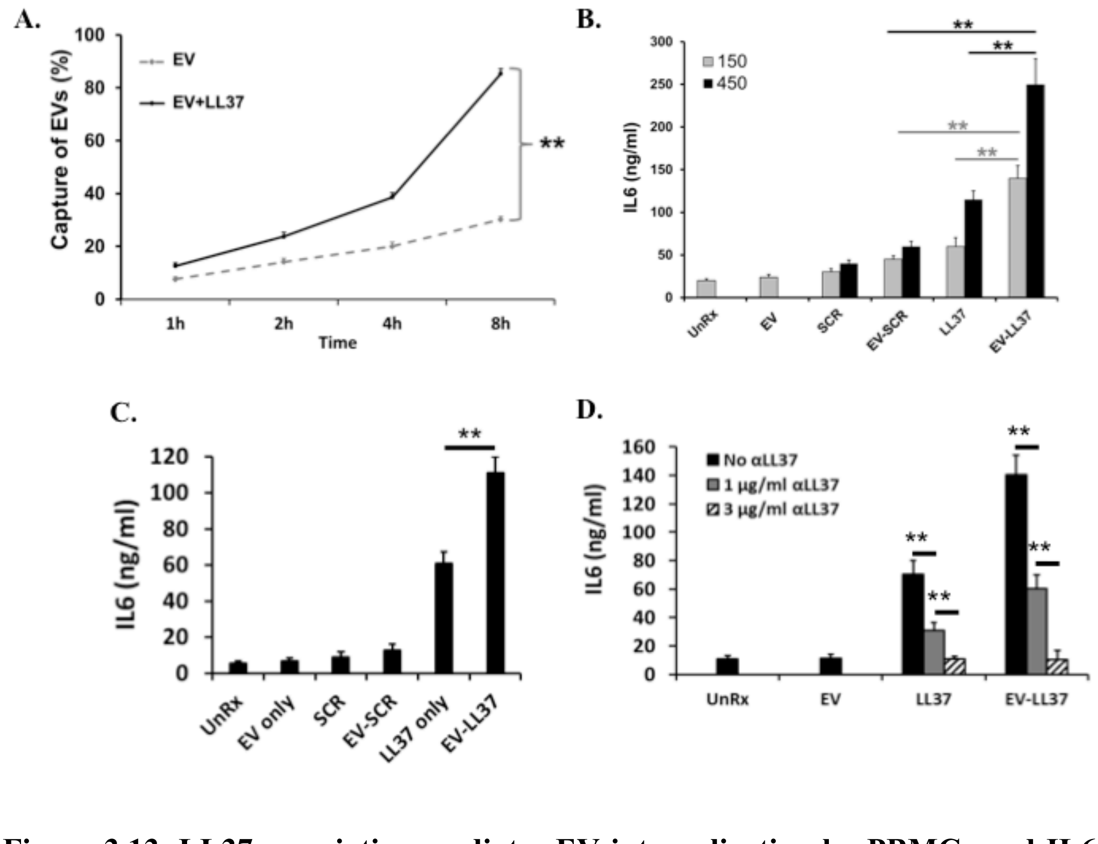

Figure 3.13. LL37 association mediates EV internalization by PBMCs and IL6 production can be abrogated with the addition of anti-LL37 [219, 220].

(A) Healthy PBMCs were treated with SP-DiOC labeled healthy EVs or EV-LL37 mixture at 1:2 (cell:EV) ratio. Line graphs represent the uptake of SP-DiOC labeled as such EVs and EV-LL37 by cells for indicated time periods. (B) Healthy EVs were incubated with LL37 (150 or 450 ng, grey and black bars, respectively). Then, healthy PBMCs were incubated these EVs for 12 hours at 1:2 (cell:EV) ratio. Bar graphs show the IL6 secretion assessed by ELISA from cell culture supernatants. (C) EVs isolated from human THP1 cells were incubated with healthy PBMCs and IL6 concentration was determined by ELISA. (D) Healthy PBMCs were incubated with indicated EV-LL37 a mixtures for 12 hours in the absence and the presence of anti-LL37 antibody. Bar graphs show IL6 secretion mediated by EV-LL37 association following treatment with anti37 antibody.

PART-IV: Effects of TLR Signaling to Immune Dysfunction of Spinal Cord Injured Patients

3.4. Impaired TLR7 and TLR9 Induced Immune Activation in Chronic Spinal Cord Injured Patients Contributes to Immune Dysfunction

3.4.1. Healthy and SCI individuals have similar responses to different immune cell stimulants.

Cytokine ELISA assessment of supernatants from cells stimulated either with R848 (TLR7 ligand) or D35 (TLR9 ligand) showed that there is no impairment in B cell and pDC responses of SCI patients, since level of IL6 and IFNα secretion from SCI PBMCs were similar to those from healthy donors (Fig 3.14A and 3.14B, respectively). Furthermore, IL10 cytokine production in response to PHA-LPS stimulation did not differ between healthy and SCI PBMCs demonstrating that SCI patients does not have any Treg dependent dysregulation (Fig 3.14C). These cytokine ELISA studies revealed that the immune dysfunction in SCI patients is not mainly due to impaired B cell, pDC or $CD4^+$ Treg activity (Fig 3.14).

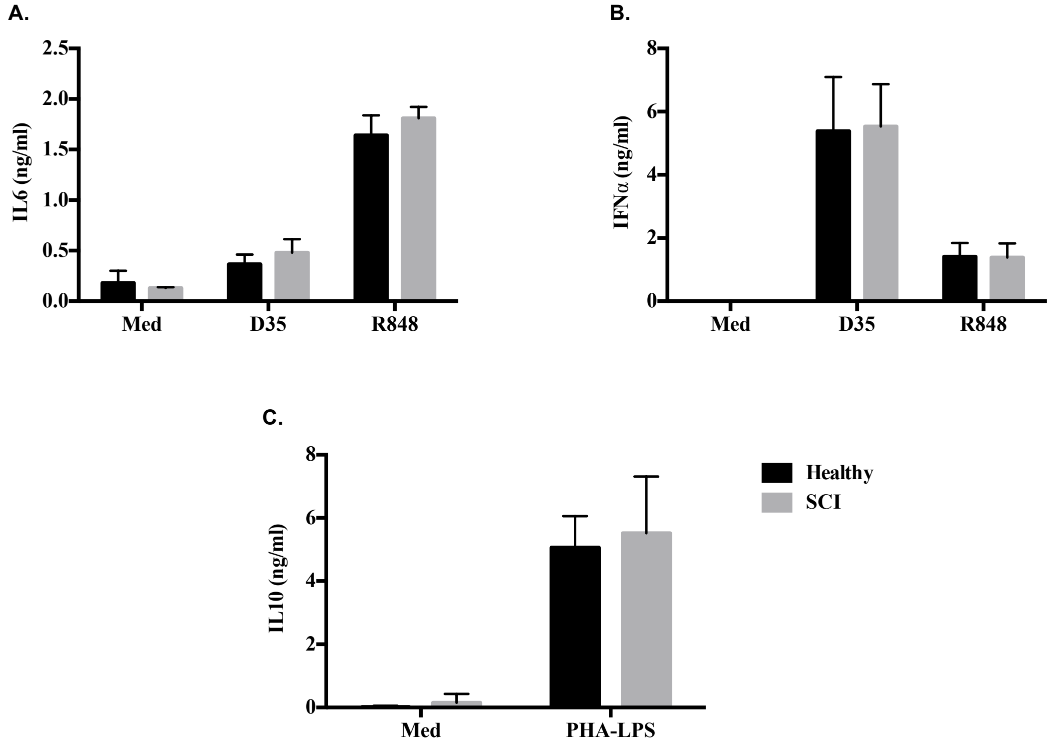

Figure 3.14. Healthy and SCI donors show similar responses to different immune cell stimulants.

PBMCs ($2x10^5$/200µl/well) (n=7) were incubated with different immune stimulatory molecules for 24 hours. (A) IL6 and (B) IFNα cytokine production in response to R848 and D35. (C) IL10 cytokine production in response to PHA-LPS.

3.4.2. Healthy and SCI donor PBMCs respond similarly to PMA-Ionomycin stimulation.

FACS analysis of cells stimulated with PMA-Ionomycin showed that both healthy and SCI PBMCs had significantly increased number of IFNγ producing T cells in response PMA-Ionomycin stimulation (Fig 3.15A and 3.15B, Fig A7). This data demonstrated that dysfunctional immunity is not due to a defect in Th-1 arm of immune activation of SCI patient.

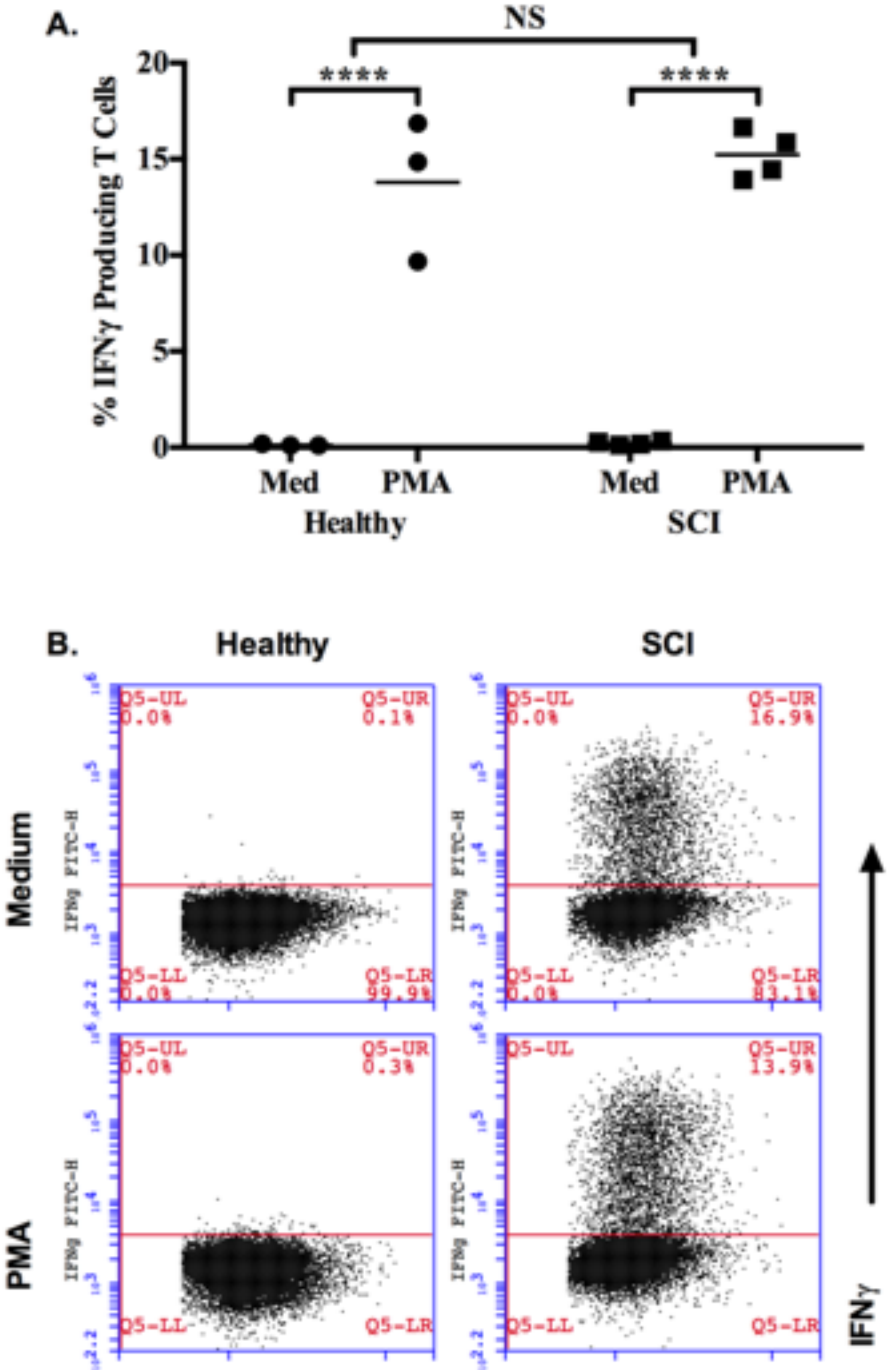

Figure 3.15. Increased number of IFNγ producing T-cells in response to PMA-Ionomycin stimulation by both healthy and SCI donor PBMCs.

PBMCs (10^6/ml) were incubated with PMA-Ionomycin in the presence of Brefeldin A for 6 hours. (A) IFNγ production at cellular of healthy (n=3) and SCI (n=4) donors, (B) Representative dot plots demonstrating % IFNγ producing $CD4^+$ T cells. $5x10^4$ cells were acquired for the analysis. Mann-Whitney test was used to test significance between healthy and SCI responses. Two-way ANOVA with

Bonferroni Correction was used to test the significance when compared to medium alone group. (NS, not significant; ****, p≤0.0001).

3.4.3. SCI patients have altered co-stimulatory and MHCII expression in response to TLR7 and TLR9 ligand stimulation.

Off note, the APC function of 4 SCI and 4 healthy PBMCs were analyzed in response to R848 and D35 (Fig 3.16). Only TLR9 ligand D35 stimulation resulted in significantly higher $CD83^+$/HLA-DR^+ cells both in healthy and SCI PBMCs. There were less CD83/HLA-DR double positive cells % in response to TLR7 and 9 triggering in SCI compared to healthy PBMCs (Fig 3.16A and 3.16B, Fig A8).

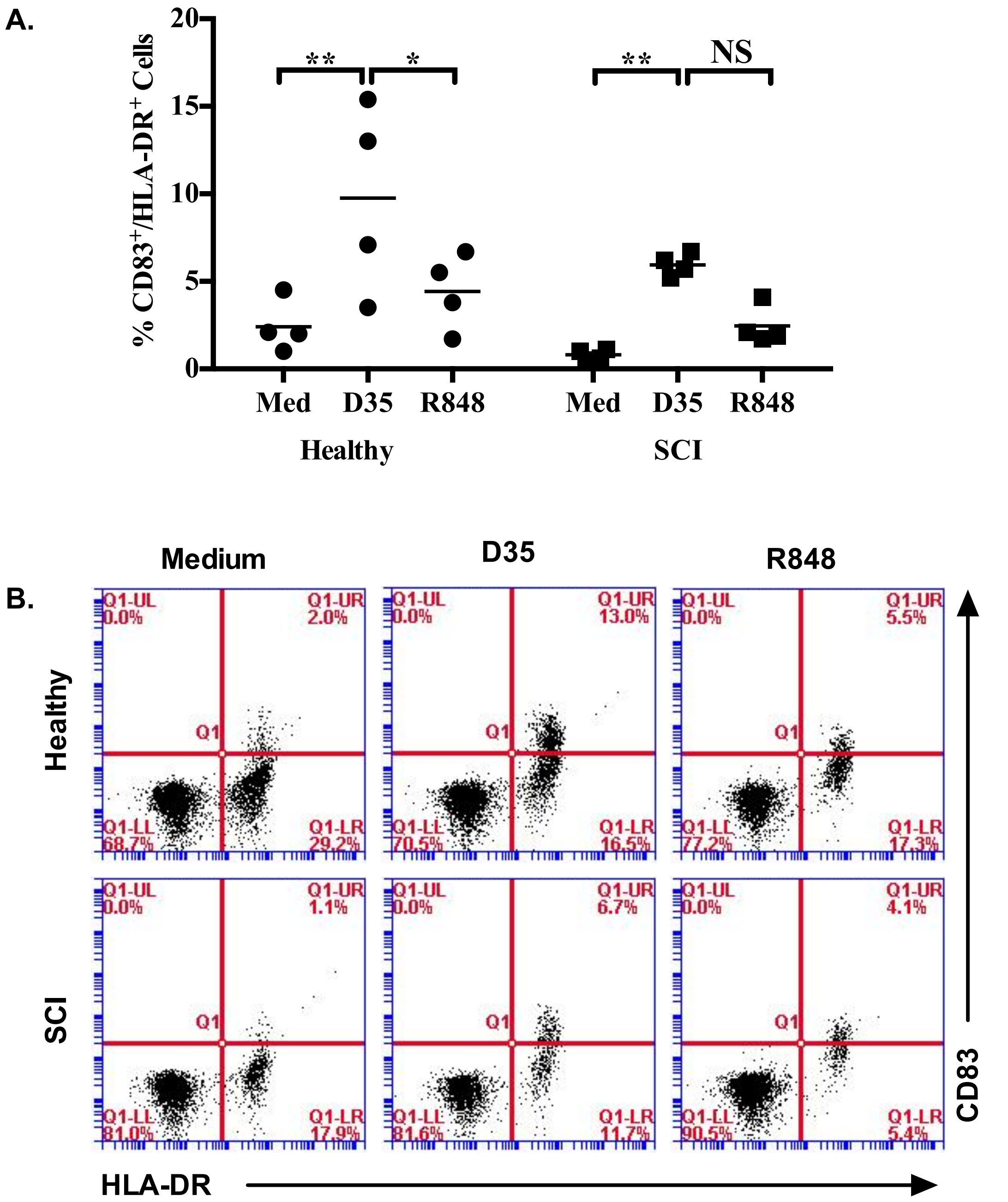

Figure 3.16. SCI patients have altered co-stimulatory and MHCII expression in response to TLR7 and TLR9 ligand stimulation.

PBMCs (10^6/ml) were incubated either with D35 or R848 for 24 hours. (A) Level of $CD83^+$/$HLA\text{-}DR^+$ positive donor PBMCs (n=4), (B) Representative dot plots representing double positive cell percent from PBMCs. During analyses $3x10^4$ cells were acquired. Two-way ANOVA with Bonferroni Correction was used to test the significance when compared to medium alone group. (*, p≤0.05; **, p≤0.01).

3.4.4. SCI patients have altered IFNγ production in response to TLR7 ligand stimulation.

IP10 cytokine ELISA study showed that SCI patients have monocytes with impaired functionality against TLR7 stimulation, since R848 induced 2.7 less IP10 production from SCI PBMCs than the healthy PBMCs (Fig 3.17A). Level of IFNγ cytokine secretion in response to R848 was also 4.2 fold less from SCI donors than healthy groups (Fig 3.17B). Moreover, this altered response was confirmed at cellular level as intracellular cytokine staining implicated that IFNγ producing $CD4^{+}$ T cells in response to R848 by healthy controls were significantly higher compared to SCI patients (Fig 3.17C and 3.17D, Fig A9).

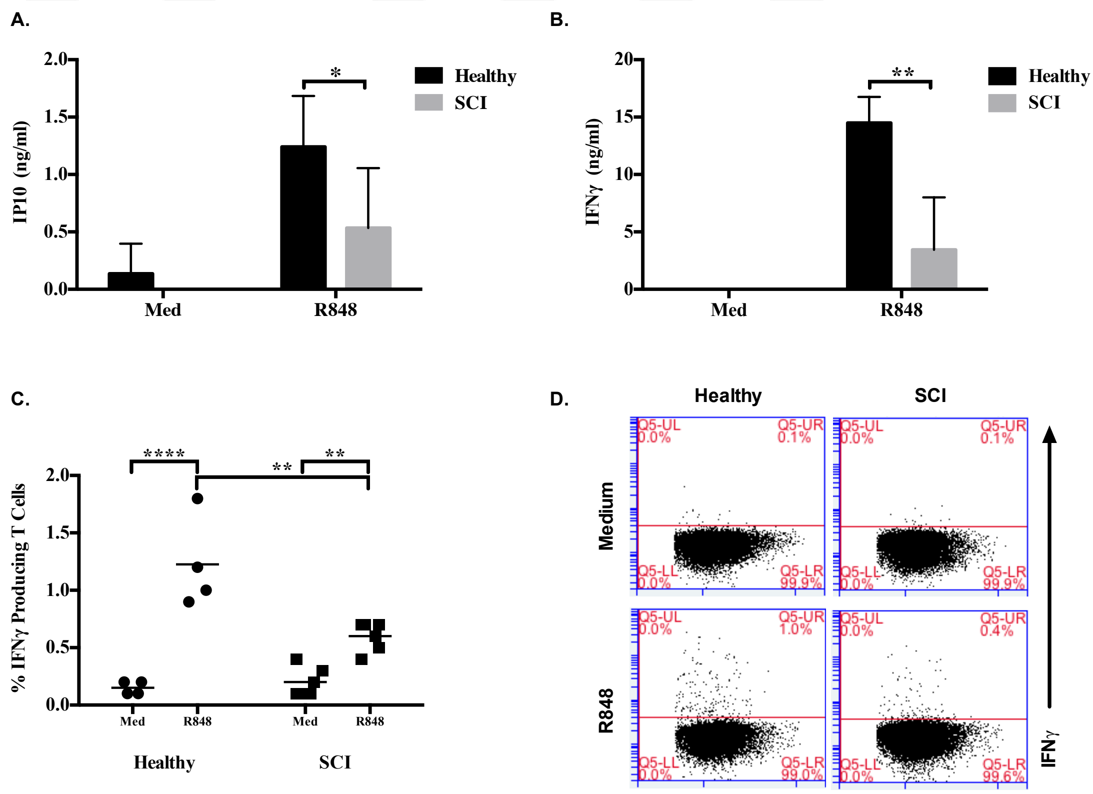

Figure 3.17. IFNγ production by healthy and SCI donor PBMCs is different in response to TLR7 ligand stimulation.

PBMCs ($2x10^{5}$/200µl/well) were incubated with R848 for 24 hours. (A) IP10 and (B) IFNγ secretion level assessment by cytokine ELISA from healthy (n=5) and SCI (n=10) donors. PBMCs (10^{6}/ml) were incubated with R848 for 20 hours, at 12th hour Brefeldin A was added. (C) IFNγ production of healthy (n=4) and SCI (n=6) PBMCs at cellular level, (D) Representative dot plots showing % IFNγ producing $CD4^+$ T cells. During analyses $5x10^4$ cells were acquired. Mann-Whitney test was used to identify significance between healthy and SCI responses to R848. Two-way ANOVA with Bonferroni Correction was used to test the significance of R848 responses compared to medium alone group (*, $p \leq 0.05$; **, $p \leq 0.01$; ****, $p \leq 0.0001$).

3.4.5. SCI donors have impaired monocytes response to TLR9 ligand stimulation.

Healthy and SCI PBMCs were stimulated with D35 and IP10 ELISA study showed that SCI donors have impaired monocytes, since they produced significantly less IP10 cytokine compared to healthy control groups (Fig 3.18A). Moreover, this downtrend was also confirmed at cellular level by FACS analysis showing significantly less IP10 producing $CD14^+$ SCI patient monocytes in response to D35 stimulation (Fig 3.18B and 3.18C, Fig A10).

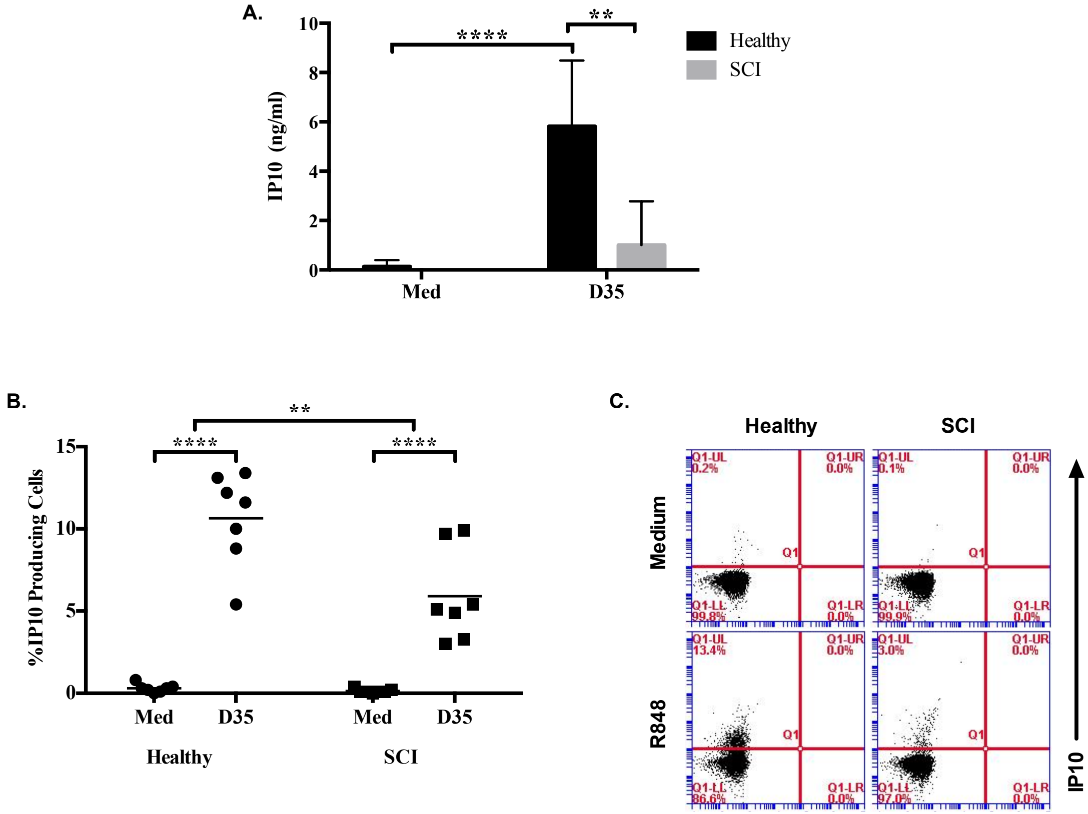

Figure 3.18. Altered SCI patient monocyte response to TLR9 ligand stimulation.

PBMCs ($2x10^5$/200µl/well) were incubated with D35 for 24 hours. (A) IP10 production level of healthy (n=5) and SCI (n=10) individuals assessed by cytokine ELISA. PBMCs (10^6/ml) were incubated with D35for 20 hours, at 12th hour Brefeldin A was added. (B) IP10 production of healthy (n=7) and SCI (n=7) PBMCs at cellular level, (C) Representative dot plots showing IP10 producing $CD14^+$ cells. During analyses $3x10^4$ cells were acquired. Mann-Whitney test was used to test significance between healthy and SCI responses to D35. Two-way ANOVA with Bonferroni Correction was used to test the significance when compared to medium alone group. (*, p≤0.05; **, p≤0.01; ****, p≤0.0001).

Chapter 4

Discussion

4.1. Utilization of exosomes in cancer therapy

Cells are small units but they are unique building blocks with very special properties. They can generate their own sustained release depot systems. Exosomes are naturally occurring nanovesicles secreted from almost all cell types [22]. They can be isolated from all bodily fluids such as plasma, urine, synovial fluid. There is a large body of evidence regarding to their cargo, which is mainly composed of genetic material such as mRNA, miRNA as well as proteins [20, 27]. More importantly, recent reports point in the direction that exosomes play critical roles in cell-to-cell communication and modulation of immune responses since their cargo contents could be functionally active following internalization by recipient cells [20].

Due to their important immunostimulatory activities, CpG ODNs are promising therapeutic agents for cancer therapy, improved response to vaccine, reduced allergic response and protective immunity. However, there are obstacles in their *in vivo* applications due to serum protein adsorption and nuclease attack. There are alternative approaches to overcome these deficiencies. Modifying the backbone chemistry of the ODN is one of the most widely used strategies. However, any great effort is not successful to convert the appreciated immunostimulatory potential of CpG ODNs *in vivo*. Since the main goal is to protect these ODNs and to deliver them to target cells while sparing the dose effect development of an innovative sustained release depot systems might be of utmost interest while bringing successful CpG ODN therapy in to the clinical level. Conventional and widely accepted approach to utilize exosomes as a therapeutic agent involves either engineering cell source that will beget the exosomes or feed the cells directly incubating with the molecule of interest, thereby allowing the release of exosomes with intended cargo enclosed in them [221, 222]. However, none of these approaches are suitable for loading immunostimulatory CpG ODNs within exosomes. Moreover, in these methods exosomes are internalizing the molecules randomly and passively, and cargo distribution could be varying depending on batch to batch and the physiological state of the cells. In the literature exosomes were reported to be loaded via electroporation method, a method leading to vesicle rupture and yielding low level of cargo loading resulting reproducibility problems [223]. Thus, in the first part of this thesis, we developed a novel method based on dehydration-rehydration of vesicles following purification of the exosome from cell supernatant. Our method, furthermore, allow efficient loading of several ligands post-purification at high yield.

Our initial *in vitro* studies conducted with E.G7 derived exosomes supported that lyophilization technique improves the immunostimulatory activity CpG ODNs upon encapsulation within exosomes as evidenced by increased inflammatory cytokine production (Fig 3.1).

To date, there is no study describing the involvement of CpG ODN within exosomes. In one study, exosomes purified from reticulocytes infected with *P.yeoli*, were mixed with CpG ODN and was shown to reduce parasite load by 83% [224]. In another report by the same authors, it was shown that CpG ODN mixed exosomes induce IgG2a and IgG2b response following immunization [225].

When DC exosomes isolated and mixed with 30 μg CpG ODN, and were used as prophylactic or therapeutic vaccine, data suggested that CpG ODN strongly acted as a potent cancer vaccine adjuvant. However, *in vivo* data revealed that only 1.0 ng/ml IFNγ was induced with the exosome CpG ODN mixture. In our hand when we load CpG ODN within exosomes and use at 0.1 μM concentration *in vitro* culture, spleen cells induced ca. 10 ng/ml IFNγ. We did not detect *in vivo* IFNγ in our studies, but determined IgG subtypes. IgG2c is indirectly implicate that a Th-1 biased immune response is developed and support IFNγ production from antigen specific $CD8^+$ T-cells. Higher IgG2c in our hand is indicative of boosted IFNγ response. In the light of our results it is suggested that encapsulation of CpG ODN via lyophilization is a more potent strategy than mixing exosomes harboring antigen epitope with CpG ODN.

It has been reported that both DC-derived exosomes and tumor derived exosomes have potential therapeutic effectiveness as cancer vaccine [44, 123, 130]. Developing *in vitro* DC derived exosomes as a delivery system is expensive and time consuming [49, 124, 125]. Since tumor derived exosomes are also another source of exosomes that carry Major Histocompatibility Complex (MHC) class I molecules, shared tumor antigen, HSPs and other danger molecules [44, 130], they were shown that they can also transfer tumor-shared antigens to DC and improve antigen specific $CD8^+$ T responses [44, 130]. The major limitation of these approaches is that mature DC is required for eliciting antitumor effects from tumor derived exosomes. In one study, exosomes isolated from OVA expressing E.G7 cells were engineered to express IL2 cytokine then tested therapy of E.G7 thymoma model in mice immunized 3 times with 7 days interval. Results showed that IL2 expressing exosomes induced Th1 biased immunity and decreased tumor growth inducing signaling pathways required for DC maturation [225]. In our study, we also used E.G7 exosomes to test against E.G7 thymoma tumor development. However, our CpG ODN loading strategy into exosomes did not require any cell engineering such as stable transfection of IL2 plasmids into E.G7 exosomes. Moreover, in our hand, we provided the protection against tumor development induced $1x10^6$ E.G7 cell inoculation which was almost 3 times higher than used in that experimental setting even after approximately 30 days after the booster injection (Fig 3.3). Our loading strategy provides delivery of both antigen and adjuvant to immature DCs thus inducing more efficient maturation of DCs and eventually more potent antigen specific T cell responses. In those studies APC function was not investigated but in our hands, we demonstrated that APCs significantly upregulated MHC-II+/CD86+ upregulation following CpG ODN loaded exosome treatment.

αGC is a natural glycolipid molecule recognized by CD1d restricted iNKT cells that were identified with important immunomodulatory roles in pathogenesis of diseases as cancer and autoinflammatory disease [227]. Several studies showed that αGC provides profound adjuvant effect for induction of NK cell dependent anti-tumor cytotoxic responses. In one study, mice were vaccinated with αGC loaded MOPC315.BM myeloma cells twice at one-week interval 5 days after intravenous injection of MOPC315.BM myeloma cells. Results showed that αGC loaded cell vaccine contributed to the prevention of tumor growth improving both humoral and cellular responses [228]. There are couple of studies in the literature that investigates the improvement of adjuvant effect of αGC *in vivo* when combined with TLR9 ligand CpG ODNs. In one of these studies, murine colon cancer cells were loaded with αGC via overnight incubation and then mice with established colon tumors were vaccinated with αGC loaded cells with or without CpG ODN. Data showed that combination of αGC and CpG ODN halted the tumor development and increased survival of mice [229]. To our knowledge, there is only one study in the literature that use exosomes as a delivery system to improve anti-tumor activity of αGC *in vivo* [230]. In this study, exosomes were collected from BM-DCs pulsed with OVA (300 μg/ml) and/or αGC (100 ng/ml). *In vivo* proliferation assays showed that loading αGC into exosomes with OVA induced antigen specific $CD8^+$ T cell responses and iNKT cell proliferation as well as antigen specific antibody production. When these formulations were tested in the treatment of OVA expressing B16 established melanoma tumors, data showed that exosomal αGC and OVA decreased tumor growth and increased survival mediated by improved cellular and humoral immunity. In our hand, we also used CpG ODN to improve the anti-tumor activity of αGC loading into macrophage-like cell derived exosomes along with OVA via lyophilization. This technique does not require cell feeding or engineering of cells. We were able to induce proliferation of iNKT cells and moreover, OVA specific CD8+ T cells by just using 30 μg of exosomes loaded with 5μg OVA, 10μg ODN and 0.3μg αGC. Such a low amounts compared to those reported in that study, since cell feeding method does not ensure efficient loading within exosomes researchers choose to include excessive amounts of intended loigand for loading within cell culture environment (Fig 3.6).

It was shown that immature DC derived exosomes have immunosuppressive effect on recipient cells, whereas exosomes derived from mature DCs are potent inducers of antigen specific $CD8^+$ T cell responses mediating tumor clearance [231]. There are several studies discussing how important is to choose suitable cell type for exosome isolation for therapeutic applications, since they might show different immunomodulatory profiles depending on the cells secreting these exosomes . Thus, in our studies, we used murine macrophage like cells RAW264.7 derived exosomes or EG.7 thymoma cells. Irrespective of the cell type loading immunostimulatory ligands via lypohilization converts exosomes to a inflammatory character harboring exosomes which is a feature is not possible by other loading techniques. Furthermore, via lyophilization technique, we were able to overcome the limitations due to batch to bacth variation or altered physiological state of cells that might the loading efficiencies in conventional feeding approach. We also showed that it is not efficient to load exosomes derived from cell lines with antigen molecules via cell feeding (Fig 3.5A) . Since the utmost goal of using tumor derived exosomes is to develop personalized cancer therapy, loading of exosomes via cell feeding could not be as sufficient as it is expected.

Overall our attempts to develop exosome cancer vaccines using lyophilization method to load more than one molecule including antigens and adjuvant showed that lyophilization method is more effective in inducing immunostimulatory and anti-tumor activity when both CpG ODN and αGC is included within exosomes.

4.2. Involvement of EVs in BD Pathogenesis

EVs play crucial role in the communication between the cells [232]. They can circulate in peripheral blood in an intact form and moreover they can transmit important biological mediators/signals from cells that they are originated from to the recipient cells transferring their biologically functional cargos [233]. Thus, they have been implicated as important player in the modulation of even physiological state of the distant cells. Although it was documented that EV numbers in plasma were increased in rheumatologic diseases, such as RA, SLE, primary Sjögren's syndrome, vasculitis and APS [234-238], it is still unclear whether there is a reasonable link between the elevated numbers of EVs and disease pathogenesis. In this thesis, one of our utmost goals was to investigate the involvement of elevated circulating EV levels could have an important contribution to the BD state.

There are several studies implicating that EVs carry biologically active cargos within them such as cytokine, cell or tissue specific antigens, growth factors, and RNA and DNA. In some studies, it was documented that EVs can transfer miRNAs to the recipient cells [239-241]. Moreover, EVs have a profound contribution to the maintenance of cell homeostasis in healthy state and they are also considered to have adverse effects in disease states [242, 243]. The findings in this thesis support the notion that EVs are strongly associated with pathophysiology of BD.

These results are of clinical importance. We demonstrated that the number of EVs in plasma significantly elevated in BD patient compared to healthy controls (Fig 3.10). Moreover, this was associated with the disease severity as active BD patients had much higher EVs in plasma. This correlation between the EV number and disease severity can be used as discriminative approach to diagnose inactive vs active states of the disease and could critically help to better BD pathogenesis management.

There are several studies suggesting that elevated levels of EVs have significant contribution to the disease pathogenesis. For instance, EVs can regulate cellular communications thus modifying the function of target cells [244-246]. In agreement with these finding, our study also revealed that as the number of circulating LL37 associated EVs in BD patients with active disease state the immune activation triggered profound inflammatory effect as evidenced by higher IL6 secretion compared to healthy EVs (Fig 3.11).

LL37 is a cationic anti-microbial peptide that is secreted to prevent the detrimental effects of pathogens [247-249]. In this study, it was revealed that level of LL37 in plasma is highly elevated in BD patients compared to healthy individuals. Another clinical aspect of this study work is to develop a new treatment strategy for BD, Drugs that could abrogate LL37 level could be used to control the symptoms of active BD patients. Moreover, this knowledge could be harnessed to develop a stratification strategy of BD severity. Just by checking LL37 levels could act as a marker to monitor BD severity. To our knowledge, there is only one study in the literature investigating the involvement of LL37 in BD. There, the level of LL37 in saliva of BD patients were reported to be elevated as the occurrence of monthly ulcers were increased [250]. Importantly, in another study unrelated to BD, it was documented that LL37 levels were elevated during sterile inflammation [251]. Of note, LL37 has an important role in production of inflammatory cytokines and chemokine such as IL1β, IL6, MCP-1 and MCP-3 [252]. In concordance with these finding, our study also provided the increased immune activation due to the elevated LL37 levels. These finding could help to develop new treatment strategies for BD targeting LL37.

More importantly, to our knowledge this is the first study showing an association between LL37 and EVs that elicits the cellular delivery of EVs perpetuating immune stimulatory activity. This suggests that increased delivery of EVs to the immune cells, eventually their cargo such as nucleic acids, can contribute to disease severity triggering production of BD-associated cytokines via activation of numerous endosomal and/or cytosolic RNA and DNA-dependent nucleic acid sensors, including TLR7, TLR9, RIG-I, MDA-5, cGAS or AIM-2. The evidence supporting this approach was provided by the study showing that psoriatic patients have TLR9-mediated IFNα response due to the enhanced delivery of DNA to pDCs via complexes formed between LL37 with genomic DNA released from dying cells in psoriatic skin [253].

The anionic charge of EVs provides a surface convenient for complexing with LL37. Our findings implicate that LL37-mediated enhanced delivery of circulating EVs to immune cells contribute to sustain and exacerbate immune activation in active BD. Therefore, targeting this peptide could be of therapeutic value in the management of this complex disease.

4.3. Contribution of impaired TLR7 and TLR9 pathways to immune dysfunction in SCI

In the last section of this thesis, we prompted to investigate whether there is impairment in activation potential of the innate and adaptive immunity in patients with SCI. With this aim, PBMCs collected from 17 patients and 13 healthy control participants were subjected to different experimental evaluations following incubation with different innate and adaptive immune stimulants. The data obtained from this study showed that there is an innate immune dysfunction due to impaired TLR7 and TLR9 mechanisms. Moreover, it was also determined that the diminished T cell response is mediated by impaired Th1-biased IFNγ response not by $CD4^+$ regulatory T-cell mediated IL10 production. In addition, these results propose that B cells can functionally respond to TLR7 and TLR9 ligands, whereas monocytes have deficiency in responding to the production of innate cytokines such as IP-10.

When similar findings from the literature are investigated, none of the human or animal studies are conclusive to explain the mechanisms underlying dysfunction in innate and adaptive immunity of SCI patients [213, 254-256]. To our knowledge, this is the first study conducted to investigate whether there is a link between TLR mediated contribution to the impaired immune responses following established SCI. Immune cells such as monocytes, macrophages, dendritic cells, T- and B-lymphocytes express Toll-like receptors. Following recognition of PAMPs by TLRs, innate immunity is first activated and multiple intracellular signaling pathways are activated subsequently leading to activation of adaptive immunity [257-259]. In addition PAMPs, TLRs can also recognize DAMPs that trigger the sterile inflammation in several pathological conditions [260-262].

In this study, following stimulation with TLR7 and TLR9 ligands, PBMCs of both SCI patients and healthy controls showed similar levels of cytokine production suggesting that immune dysfunction in patients with SCI is not mediated by any impairment in pDC or B cell activation mechanisms (Fig3.14A and 3.14B). Previously, it was shown that number of $ED9^+$ monocytes were decreased in the early phase of the spinal cord injury model developed in rats [255]. However, it was revealed that in the latter stages of the injury (post-day 14 of injury), level of $ED9^+$ monocytes were almost fully recovered to the levels similar to the control group. In addition, level of $HIS48^+$ granulocyte did not differ between rat with SCI and control [255]. In another study in humans conducted by same research group, it was shown that $CD14^+$ monocytes were not as much as higher in patients in first week following injury compared to healthy individuals, where level of monocytes were significantly increased to a number of controls on chronic phase (day 105-136) [263]. Our study showed that monocytes are dysfunctional in producing one of the cardinal monocyte-specific IP10 cytokine in response to R848 and D-type CpG ODN although their levels do change between patient and healthy groups in chronic phase of SCI (Fig 3.17A and Fig 3.18A).

Our findings also provided insight regarding to how T cells respond to different immune stimulations. ELISA studies from supernatants of PBMCs stimulated with R848 and D-type CpG ODN showed that there is no difference in IFNγ production between healthy controls and patients with SCI. Moreover, this similarity was also confirmed at cellular lever by IFNγ intracellular cytokine staining of cells following stimulation with T cell stimulant PMA-Ionomycin as the patients and the healthy individuals almost had the same level of IFNγ-producing T cells (Fig 3.15). This finding is contradictory to the findings of Campagnolo and his friends as they stated that the percent of T cells and helper cells (CD3+, CD4+) in SCI patients significantly increased compared to healthy individuals [213]. Moreover, in our work we and others determined that there is a T cell responsiveness in SCI patients [253, 255, 264]. However, this cannot be regarded as a correct comparison with our investigations. In those reports, patients were either in acute or sub-acute phases following SCI, whereas all patients were in chronic phase of SCI in our study.

Although there are some limitations of this study especially regarding to the sample sizes in each experimental set up, this study is unique in the mean of inclusion and exclusion criteria of patients. In this thesis, SCI patients only in chronic phase were selected to eliminate the possibility of interference that could be caused by the medications such as steroids used during the acute and sub-acute stages to prevent the infections. Also, patients with injury above T-6 level were included to exclude the effect of the autonomic nerve system on the immune responses. Collectively, this study can enlighten the underlying mechanism of the immune dysfunction triggering susceptibility to infection in patients with SCI in chronic phase.

References

[1] Colombo M, Raposo G, Théry C. Biogenesis, secretion, and intercellular interactions of exosomes and other extracellular vesicles. Annual review of cell and developmental biology. 2014 Oct 6;30:255-89.
[2] Anderson HC. Vesicles associated with calcification in the matrix of epiphyseal cartilage. The Journal of cell biology. 1969 Apr 1;41(1):59-72.
[3] Crawford N. The Presence of Contractile Proteins in Platelet Microparticles Isolated from Human and Animal Platelet-free Plasma. Biritis journal of haemataology. 1971 Jul 1;21(1):53-69.
[4] Stegmayr B, Ronquist G. Promotive effect on human sperm progressive motility by prostasomes. Urological research. 1982 Nov 1;10(5):253-7.
[5] Trams EG, Lauter CJ, Salem JN, Heine U. Exfoliation of membrane ecto-enzymes in the form of micro-vesicles. Biochimica et Biophysica Acta (BBA)-Biomembranes. 1981 Jun 6;645(1):63-70.
[6] Dvorak HF, Quay SC, Orenstein NS, Dvorak AM, Hahn P, Bitzer AM, Carvalho AC. Tumor shedding and coagulation. Science. 1981 May 22;212(4497):923-4.
[7] George JN, Thoi LL, McManus LM, Reimann TA. Isolation of human platelet membrane microparticles from plasma and serum. Blood. 1982 Oct 1;60(4):834-40.
[8] Harding C, Heuser J, Stahl P. Receptor-mediated endocytosis of transferrin and recycling of the transferrin receptor in rat reticulocytes. The Journal of cell biology. 1983 Aug 1;97(2):329-39.
[9] Pan BT, Johnstone RM. Fate of the transferrin receptor during maturation of sheep reticulocytes in vitro: selective externalization of the receptor. Cell. 1983 Jul 1;33(3):967-78.
[10] Johnstone RM, Adam M, Hammond JR, Orr L, Turbide C. Vesicle formation during reticulocyte maturation. Association of plasma membrane activities with released vesicles (exosomes). Journal of Biological Chemistry. 1987 Jul 5;262(19):9412-20.
[11] Gould SJ, Raposo G. As we wait: coping with an imperfect nomenclature for extracellular vesicles. Journal of extracellular vesicles. 2013 Feb 15;2.
[12] Kowal J, Tkach M, Théry C. Biogenesis and secretion of exosomes. Current opinion in cell biology. 2014 Aug 31;29:116-25.
[13] Klumperman J, Raposo G. The complex ultrastructure of the endolysosomal system. Cold Spring Harbor perspectives in biology. 2014 Oct 1;6(10):a016857.
[14] Stoorvogel W, Strous GJ, Geuze HJ, Oorschot V, Schwartzt AL. Late endosomes derive from early endosomes by maturation. Cell. 1991 May 3;65(3):417-27.
[15] Jaiswal JK, Andrews NW, Simon SM. Membrane proximal lysosomes are the major vesicles responsible for calcium-dependent exocytosis in nonsecretory cells. J Cell Biol. 2002 Nov 25;159(4):625-35.
[16] Raposo G, Nijman HW, Stoorvogel W, Liejendekker R, Harding CV, Melief CJ, Geuze HJ. B lymphocytes secrete antigen-presenting vesicles. Journal of Experimental Medicine. 1996 Mar 1;183(3):1161-72.
[17] Hanson PI, Cashikar A. Multivesicular body morphogenesis. Annual review of cell and developmental biology. 2012 Nov 10;28:337-62.

[18] Stuffers S, Sem Wegner C, Stenmark H, Brech A. Multivesicular endosome biogenesis in the absence of ESCRTs. Traffic. 2009 Jul 1;10(7):925-37.
[19] Carayon K, Chaoui K, Ronzier E, Lazar I, Bertrand-Michel J, Roques V, Balor S, Terce F, Lopez A, Salomé L, Joly E. Proteolipidic composition of exosomes changes during reticulocyte maturation. Journal of Biological Chemistry. 2011 Sep 30;286(39):34426-39.
[20] Théry C, Ostrowski M, Segura E. Membrane vesicles as conveyors of immune responses. Nature Reviews Immunology. 2009 Aug 1;9(8):581-93.
[21] Robbins PD, Morelli AE. Regulation of immune responses by extracellular vesicles. Nature Reviews Immunology. 2014 Mar 1;14(3):195-208.
[22] Théry C, Amigorena S, Raposo G, Clayton A. Isolation and characterization of exosomes from cell culture supernatants and biological fluids. Current protocols in cell biology. 2006 Apr:3-22.
[23] Muralidharan-Chari V, Clancy J, Plou C, Romao M, Chavrier P, Raposo G, D'Souza-Schorey C. ARF6-regulated shedding of tumor cell-derived plasma membrane microvesicles. Current Biology. 2009 Dec 1;19(22):1875-85.
[24] Baj-Krzyworzeka M, Szatanek R, Węglarczyk K, Baran J, Urbanowicz B, Brański P, Ratajczak MZ, Zembala M. Tumour-derived microvesicles carry several surface determinants and mRNA of tumour cells and transfer some of these determinants to monocytes. Cancer Immunology, Immunotherapy. 2006 Jul 1;55(7):808-18.
[25] Simons M, Raposo G. Exosomes–vesicular carriers for intercellular communication. Current opinion in cell biology. 2009 Aug 31;21(4):575-81.
[26] Keller S, Sanderson MP, Stoeck A, Altevogt P. Exosomes: from biogenesis and secretion to biological function. Immunology letters. 2006 Nov 15;107(2):102-8.
[27] Raposo G, Stoorvogel W. Extracellular vesicles: exosomes, microvesicles, and friends. J Cell Biol. 2013 Feb 18;200(4):373-83.
[28] Van Niel G, Charrin S, Simoes S, Romao M, Rochin L, Saftig P, Marks MS, Rubinstein E, Raposo G. The tetraspanin CD63 regulates ESCRT-independent and-dependent endosomal sorting during melanogenesis. Developmental cell. 2011 Oct 18;21(4):708-21.
[29] Kleijmeer MJ, Stoorvogel W, Griffith JM, Yoshie O, Geuze HJ. Selective enrichment of tetraspan proteins on the internal vesicles of multivesicular endosomes and on exosomes secreted by human B-lymphocytes. Journal of Biological Chemistry. 1998 Aug 7;273(32):20121-7.
[30] Bard MP, Hegmans JP, Hemmes A, Luider TM, Willemsen R, Severijnen LA, van Meerbeeck JP, Burgers SA, Hoogsteden HC, Lambrecht BN. Proteomic analysis of exosomes isolated from human malignant pleural effusions. American journal of respiratory cell and molecular biology. 2004 Jul;31(1):114-21.
[31] Théry C, Regnault A, Garin J, Wolfers J, Zitvogel L, Ricciardi-Castagnoli P, Raposo G, Amigorena S. Molecular characterization of dendritic cell-derived exosomes. The Journal of cell biology. 1999 Nov 1;147(3):599-610.
[32] Kleijmeer MJ, Escola JM, UytdeHaag FG, Jakobson E, Griffith JM, Osterhaus AD, Stoorvogel W, Melief CJ, Rabouille C, Geuze HJ. Antigen loading of MHC class I molecules in the endocytic tract. Traffic. 2001 Jan 1;2(2):124-37.
[33] Masciopinto F, Giovani C, Campagnoli S, Galli-Stampino L, Colombatto P, Brunetto M, Yen TS, Houghton M, Pileri P, Abrignani S. Association of hepatitis C virus envelope proteins with exosomes. European journal of immunology. 2004 Oct 1;34(10):2834-42.

[34] Valadi H, Ekström K, Bossios A, Sjöstrand M, Lee JJ, Lötvall JO. Exosome-mediated transfer of mRNAs and microRNAs is a novel mechanism of genetic exchange between cells. Nature cell biology. 2007 Jun 1;9(6):654-9.
[35] Skog J, Würdinger T, Van Rijn S, Meijer DH, Gainche L, Curry WT, Carter BS, Krichevsky AM, Breakefield XO. Glioblastoma microvesicles transport RNA and proteins that promote tumour growth and provide diagnostic biomarkers. Nature cell biology. 2008 Dec 1;10(12):1470-6.
[36] Rabinowits G, Gerçel-Taylor C, Day JM, Taylor DD, Kloecker GH. Exosomal microRNA: a diagnostic marker for lung cancer. Clinical lung cancer. 2009 Jan 1;10(1):42-6.
[37] Michael A, Bajracharya SD, Yuen PS, Zhou H, Star RA, Illei GG, Alevizos I. Exosomes from human saliva as a source of microRNA bio markers. Oral diseases. 2010 Jan 1;16(1):34-8.
[38] Bellingham SA, Coleman BM, Hill AF. Small RNA deep sequencing reveals a distinct miRNA signature released in exosomes from prion-infected neuronal cells. Nucleic acids research. 2012 Sep 10:gks832.
[39] Nolte EN, Buermans HP, Waasdorp M, Stoorvogel W, Wauben MH, AC't Hoen P. Deep sequencing of RNA from immune cell-derived vesicles uncovers the selective incorporation of small non-coding RNA biotypes with potential regulatory functions. Nucleic acids research. 2012 Jul 19:gks658.
[40] Devaux PF, Herrmann A, Ohlwein N, Kozlov MM. How lipid flippases can modulate membrane structure. Biochim Biophys Acta. 2008 Jul-Aug;1778(7-8):1591-600.
[41] Record M, Carayon K, Poirot M, Silvente-Poirot S. Exosomes as new vesicular lipid transporters involved in cell-cell communication and various pathophysiologies. Biochim Biophys Acta. 2014 Jan;1841(1):108-20.
[42] Nomura S. Extracellular vesicles and blood diseases. International Journal of Hematology. 2017 Jan 27:1-4.
[43] Théry C, Ostrowski M, Segura E. Membrane vesicles as conveyors of immune responses. Nature Reviews Immunology. 2009 Aug 1;9(8):581-93.
[44] Wolfers J, Lozier A, Raposo G, Regnault A, Théry C, Masurier C, Flament C, Pouzieux S, Faure F, Tursz T, Angevin E. Tumor-derived exosomes are a source of shared tumor rejection antigens for CTL cross-priming. Nature medicine. 2001 Mar 1;7(3):297-303.
[45] Andre F, Schartz NE, Movassagh M, Flament C, Pautier P, Morice P, Pomel C, Lhomme C, Escudier B, Le Chevalier T, Tursz T. Malignant effusions and immunogenic tumour-derived exosomes. The Lancet. 2002 Jul 27;360(9329):295-305.
[46] Luketic L, Delanghe J, Sobol PT, Yang P, Frotten E, Mossman KL, Gauldie J, Bramson J, Wan Y. Antigen presentation by exosomes released from peptide-pulsed dendritic cells is not suppressed by the presence of active CTL. The Journal of Immunology. 2007 Oct 15;179(8):5024-32.
[47] Utsugi-Kobukai S, Fujimaki H, Hotta C, Nakazawa M, Minami M. MHC class I-mediated exogenous antigen presentation by exosomes secreted from immature and mature bone marrow derived dendritic cells. Immunology letters. 2003 Oct 31;89(2):125-31.
[48] Hsu DH, Paz P, Villaflor G, Rivas A, Mehta-Damani A, Angevin E, Zitvogel L, Le Pecq JB. Exosomes as a tumor vaccine: enhancing potency through direct loading of antigenic peptides. Journal of immunotherapy. 2003 Sep 1;26(5):440-50.
[49] Chaput N, Schartz NE, André F, Taïeb J, Novault S, Bonnaventure P, Aubert

N, Bernard J, Lemonnier F, Merad M, Adema G. Exosomes as potent cell-free peptide-based vaccine. II. Exosomes in CpG adjuvants efficiently prime naive Tc1 lymphocytes leading to tumor rejection. The Journal of Immunology. 2004 Feb 15;172(4):2137-46.
[50] Admyre C, Johansson SM, Paulie S, Gabrielsson S. Direct exosome stimulation of peripheral humanT cells detected by ELISPOT. European journal of immunology. 2006 Jul 1;36(7):1772-81.
[51] Théry C, Regnault A, Garin J, Wolfers J, Zitvogel L, Ricciardi-Castagnoli P, Raposo G, Amigorena S. Molecular characterization of dendritic cell-derived exosomes. The Journal of cell biology. 1999 Nov 1;147(3):599-610.
[52] Segura E, Nicco C, Lombard B, Véron P, Raposo G, Batteux F, Amigorena S, Théry C. ICAM-1 on exosomes from mature dendritic cells is critical for efficient naive T-cell priming. Blood. 2005 Jul 1;106(1):216-23.
[53] Théry C, Duban L, Segura E, Véron P, Lantz O, Amigorena S. Indirect activation of naïve CD4+ T cells by dendritic cell–derived exosomes. Nature immunology. 2002 Dec 1;3(12):1156-62.
[54] Montecalvo A, Shufesky WJ, Stolz DB, Sullivan MG, Wang Z, Divito SJ, Papworth GD, Watkins SC, Robbins PD, Larregina AT, Morelli AE. Exosomes as a short-range mechanism to spread alloantigen between dendritic cells during T cell allorecognition. The Journal of Immunology. 2008 Mar 1;180(5):3081-90.
[55] Obregon C, Rothen-Rutishauser B, Gitahi SK, Gehr P, Nicod LP. Exovesicles from human activated dendritic cells fuse with resting dendritic cells, allowing them to present alloantigens. The American journal of pathology. 2006 Dec 31;169(6):2127-36.
[56] Baj-Krzyworzeka M, Majka M, Pratico D, Ratajczak J, Vilaire G, Kijowski J, Reca R, Janowska-Wieczorek A, Ratajczak MZ. Platelet-derived microparticles stimulate proliferation, survival, adhesion, and chemotaxis of hematopoietic cells. Experimental hematology. 2002 May 31;30(5):450-9.
[57] Baj-Krzyworzeka M, Szatanek R, Węglarczyk K, Baran J, Zembala M. Tumour-derived microvesicles modulate biological activity of human monocytes. Immunology letters. 2007 Nov 15;113(2):76-82.
[58] Bhatnagar S, Schorey JS. Exosomes released from infected macrophages contain Mycobacterium avium glycopeptidolipids and are proinflammatory. Journal of Biological Chemistry. 2007 Aug 31;282(35):25779-89.
[59] Bhatnagar S, Shinagawa K, Castellino FJ, Schorey JS. Exosomes released from macrophages infected with intracellular pathogens stimulate a proinflammatory response in vitro and in vivo. Blood. 2007 Nov 1;110(9):3234-44.
[60] Quah BJ, O'neill HC. Mycoplasma contaminants present in exosome preparations induce polyclonal B cell responses. Journal of leukocyte biology. 2007 Nov 1;82(5):1070-82.
[61] Klibi J, Niki T, Riedel A, Pioche-Durieu C, Souquere S, Rubinstein E, Le Moulec S, Guigay J, Hirashima M, Guemira F, Adhikary D. Blood diffusion and Th1-suppressive effects of galectin-9–containing exosomes released by Epstein-Barr virus–infected nasopharyngeal carcinoma cells. Blood. 2009 Feb 26;113(9):1957-66.
[62] Liu C, Yu S, Zinn K, Wang J, Zhang L, Jia Y, Kappes JC, Barnes S, Kimberly RP, Grizzle WE, Zhang HG. Murine mammary carcinoma exosomes promote tumor growth by suppression of NK cell function. The Journal of Immunology. 2006 Feb 1;176(3):1375-85.
[63] Clayton A, Mitchell JP, Linnane S, Mason MD, Tabi Z. Human tumor-derived exosomes down-modulate NKG2D expression. The Journal of Immunology.

2008 Jun 1;180(11):7249-58.
[64] Clayton A, Mitchell JP, Mason MD, Tabi Z. Human tumor-derived exosomes selectively impair lymphocyte responses to interleukin-2. Cancer research. 2007 Aug 1;67(15):7458-66.
[65] Valenti R, Huber V, Filipazzi P, Pilla L, Sovena G, Villa A, Corbelli A, Fais S, Parmiani G, Rivoltini L. Human tumor-released microvesicles promote the differentiation of myeloid cells with transforming growth factor-β–mediated suppressive activity on T lymphocytes. Cancer research. 2006 Sep 15;66(18):9290-8.
[66] Wang GJ, Liu Y, Qin A, Shah SV, Deng ZB, Xiang X, Cheng Z, Liu C, Wang J, Zhang L, Grizzle WE. Thymus exosomes-like particles induce regulatory T cells. The Journal of Immunology. 2008 Oct 15;181(8):5242-8.
[67] Xiang X, Poliakov A, Liu C, Liu Y, Deng ZB, Wang J, Cheng Z, Shah SV, Wang GJ, Zhang L, Grizzle WE. Induction of myeloid-derived suppressor cells by tumor exosomes. International journal of cancer. 2009 Jun 1;124(11):2621-33.
[68] Webber J, Yeung V, Clayton A. Extracellular vesicles as modulators of the cancer microenvironment. InSeminars in cell & developmental biology 2015 Apr 30 (Vol. 40, pp. 27-34). Academic Press.
[69] Kim SH, Bianco NR, Shufesky WJ, Morelli AE, Robbins PD. Effective treatment of inflammatory disease models with exosomes derived from dendritic cells genetically modified to express IL-4. The Journal of Immunology. 2007 Aug 15;179(4):2242-9.
[70] Kim SH, Lechman ER, Bianco N, Menon R, Keravala A, Nash J, Mi Z, Watkins SC, Gambotto A, Robbins PD. Exosomes derived from IL-10-treated dendritic cells can suppress inflammation and collagen-induced arthritis. The Journal of Immunology. 2005 May 15;174(10):6440-8.
[71] Smyth LA, Ratnasothy K, Tsang JY, Boardman D, Warley A, Lechler R, et al. CD73 expression on extracellular vesicles derived from CD4+ CD25+ Foxp3+ T cells contributes to their regulatory function. Eur J Immunol. 2013 Sep;43(9):2430-40
[72] Kahraman T, Gucluler G, Gürsel I. Exosomes: Natural nanovesicle candidates used in the diagnosis and treatment [Eksozomlar: Tani ve tedavide kullanilabilen dogal nanokesecik adaylari]. Turkish Journal of Immunology. 2013;2(2):34-40.
[73] Becker A, Thakur BK, Weiss JM, Kim HS, Peinado H, Lyden D. Extracellular Vesicles in Cancer: Cell-to-Cell Mediators of Metastasis. Cancer Cell. 2016 Dec 12;30(6):836-48.
[74] Gan HK, Cvrljevic AN, Johns TG. The epidermal growth factor receptor variant III (EGFRvIII): where wild things are altered. FEBS journal. 2013 Nov 1;280(21):5350-70. [3]
[75] Nazarenko I, Rana S, Baumann A, McAlear J, Hellwig A, Trendelenburg M, Lochnit G, Preissner KT, Zöller M. Cell surface tetraspanin Tspan8 contributes to molecular pathways of exosome-induced endothelial cell activation. Cancer research. 2010 Feb 15;70(4):1668-78.
[76] De Wever O, Demetter P, Mareel M, Bracke M. Stromal myofibroblasts are drivers of invasive cancer growth. International journal of cancer. 2008 Nov 15;123(10):2229-38.
[77] Webber J, Steadman R, Mason MD, Tabi Z, Clayton A. Cancer exosomes trigger fibroblast to myofibroblast differentiation. Cancer research. 2010 Dec 1;70(23):9621-30.

[78] Cho JA, Park H, Lim EH, Lee KW. Exosomes from breast cancer cells can convert adipose tissue-derived mesenchymal stem cells into myofibroblast-like cells. International journal of oncology. 2012 Jan 1;40(1):130-8.
[79] Luga V, Zhang L, Viloria-Petit AM, Ogunjimi AA, Inanlou MR, Chiu E, Buchanan M, Hosein AN, Basik M, Wrana JL. Exosomes mediate stromal mobilization of autocrine Wnt-PCP signaling in breast cancer cell migration. Cell. 2012 Dec 21;151(7):1542-56.
[80] Sung BH, Ketova T, Hoshino D, Zijlstra A, Weaver AM. Directional cell movement through tissues is controlled by exosome secretion. Nature communications. 2015 May 13;6.
[81] Sidhu SS, Mengistab AT, Tauscher AN, LaVail J, Basbaum C. The microvesicle as a vehicle for EMMPRIN in tumor–stromal interactions. Oncogene. 2004 Jan 29;23(4):956-63.
[82] Taraboletti G, D'Ascenzo S, Borsotti P, Giavazzi R, Pavan A, Dolo V. Shedding of the matrix metalloproteinases MMP-2, MMP-9, and MT1-MMP as membrane vesicle-associated components by endothelial cells. The American journal of pathology. 2002 Feb 28;160(2):673-80.
[83] Stein PD, Beemath A, Meyers FA, Skaf E, Sanchez J, Olson RE. Incidence of venous thromboembolism in patients hospitalized with cancer. The American journal of medicine. 2006 Jan 31;119(1):60-8.
[84] Sierko E, Wojtukiewicz MZ. Inhibition of platelet function: does it offer a chance of better cancer progression control?. InSeminars in thrombosis and hemostasis 2007 Oct (Vol. 33, No. 07, pp. 712-721). © Thieme Medical Publishers.
[85] Rak J. Microparticles in cancer. InSeminars in thrombosis and hemostasis 2010 Nov (Vol. 36, No. 08, pp. 888-906). © Thieme Medical Publishers.
[86] Hron G, Kollars M, Weber H, Sagaster V, Quehenberger P, Eichinger S, Kyrle PA, Weltermann A. Tissue factor-positive microparticles: cellular origin and association with coagulation activation in patients with colorectal cancer. Thrombosis and haemostasis. 2007;97(1):119-23.
[87] Tilley RE, Holscher T, Belani R, Nieva J, Mackman N. Tissue factor activity is increased in a combined platelet and microparticle sample from cancer patients. Thrombosis research. 2008 Dec 31;122(5):604-9.
[88] Thomas GM, Panicot-Dubois L, Lacroix R, Dignat-George F, Lombardo D, Dubois C. Cancer cell–derived microparticles bearing P-selectin glycoprotein ligand 1 accelerate thrombus formation in vivo. Journal of Experimental Medicine. 2009 Aug 31;206(9):1913-27.
[89] Yu J, May L, Milsom C, Anderson GM, Weitz JI, Luyendyk JP, Broze G, Mackman N, Rak J. Contribution of host-derived tissue factor to tumor neovascularization. Arteriosclerosis, thrombosis, and vascular biology. 2008 Nov 1;28(11):1975-81.
[90] Abusamra AJ, Zhong Z, Zheng X, Li M, Ichim TE, Chin JL, Min WP. Tumor exosomes expressing Fas ligand mediate CD8+ T-cell apoptosis. Blood Cells, Molecules, and Diseases. 2005 Oct 31;35(2):169-73.
[91] Kim JW, Wieckowski E, Taylor DD, Reichert TE, Watkins S, Whiteside TL. Fas ligand–positive membranous vesicles isolated from sera of patients with oral cancer induce apoptosis of activated T lymphocytes. Clinical Cancer Research. 2005 Feb 1;11(3):1010-20.
[92] Timár CI, Lőrincz ÁM, Csépányi-Kömi R, Vályi-Nagy A, Nagy G, Buzás EI, Iványi Z, Kittel Á, Powell DW, McLeish KR, Ligeti E. Antibacterial effect of

microvesicles released from human neutrophilic granulocytes. Blood. 2013 Jan 17;121(3):510-8.
[93] Turiák L, Misják P, Szabó TG, Aradi B, Pálóczi K, Ozohanics O, Drahos L, Kittel Á, Falus A, Buzás EI, Vékey K. Proteomic characterization of thymocyte-derived microvesicles and apoptotic bodies in BALB/c mice. Journal of proteomics. 2011 Sep 6;74(10):2025-33.
[94] Cloutier N, Tan S, Boudreau LH, Cramb C, Subbaiah R, Lahey L, Albert A, Shnayder R, Gobezie R, Nigrovic PA, Farndale RW. The exposure of autoantigens by microparticles underlies the formation of potent inflammatory components: the microparticle-associated immune complexes. EMBO molecular medicine. 2013 Feb 4;5(2):235-49.
[95] Skriner K, Adolph K, Jungblut PR, Burmester GR. Association of citrullinated proteins with synovial exosomes. Arthritis & Rheumatism. 2006 Dec 1;54(12):3809-14.
[96] Knijff-Dutmer EA, Koerts J, Nieuwland R, Kalsbeek-Batenburg EM, Van De Laar MA. Elevated levels of platelet microparticles are associated with disease activity in rheumatoid arthritis. Arthritis & Rheumatism. 2002 Jun 1;46(6):1498-503.
[97] Boilard E, Nigrovic PA, Larabee K, Watts GF, Coblyn JS, Weinblatt ME, Massarotti EM, Remold-O'Donnell E, Farndale RW, Ware J, Lee DM. Platelets amplify inflammation in arthritis via collagen-dependent microparticle production. Science. 2010 Jan 29;327(5965):580-3.
[98] Sellam J, Proulle V, Jüngel A, Ittah M, Richard CM, Gottenberg JE, Toti F, Benessiano J, Gay S, Freyssinet JM, Mariette X. Increased levels of circulating microparticles in primary Sjögren's syndrome, systemic lupus erythematosus and rheumatoid arthritis and relation with disease activity. Arthritis research & therapy. 2009 Oct 15;11(5):R156.
[99] György B, Szabó TG, Turiák L, Wright M, Herczeg P, Lédeczi Z, Kittel Á, Polgár A, Tóth K, Dérfalvi B, Zelenák G. Improved flow cytometric assessment reveals distinct microvesicle (cell-derived microparticle) signatures in joint diseases. PloS one. 2012 Nov 20;7(11):e49726.
[100] Berckmans RJ, Nieuwland R, Tak PP, Böing AN, Romijn FP, Kraan MC, Breedveld FC, Hack CE, Sturk A. Cell-derived microparticles in synovial fluid from inflamed arthritic joints support coagulation exclusively via a factor VII–dependent mechanism. Arthritis & Rheumatology. 2002 Nov 1;46(11):2857-66.
[101] Wang H, Wang ZH, Kong J, Yang MY, Jiang GH, Wang XP, Zhong M, Zhang Y, Deng JT, Zhang W. Oxidized low-density lipoprotein-dependent platelet-derived microvesicles trigger procoagulant effects and amplify oxidative stress. Mol Med. 2012 Mar 27;18(1):159-66.
[102] Rautou PE, Vion AC, Amabile N, Chironi G, Simon A, Tedgui A, Boulanger CM. Microparticles, vascular function, and atherothrombosis. Circulation research. 2011 Aug 19;109(5):593-606.
[103] Berckmans RJ, Nieuwland R, Kraan MC, Schaap MC, Pots D, Smeets TJ, Sturk A, Tak PP. Synovial microparticles from arthritic patients modulate chemokine and cytokine release by synoviocytes. Arthritis research & therapy. 2005 Mar 1;7(3):R536.
[104] Reich N, Beyer C, Gelse K, Akhmetshina A, Dees C, Zwerina J, Schett G, Distler O, Distler JH. Microparticles stimulate angiogenesis by inducing ELR+ CXC-chemokines in synovial fibroblasts. Journal of cellular and molecular medicine. 2011 Apr 1;15(4):756-62.

[105] Østergaard O, Nielsen CT, Iversen LV, Tanassi JT, Knudsen S, Jacobsen S, Heegaard NH. Unique protein signature of circulating microparticles in systemic lupus erythematosus. Arthritis & Rheumatism. 2013 Oct 1;65(10):2680-90.
[106] Parker B, Al-Husain A, Pemberton P, Yates AP, Ho P, Gorodkin R, Teh LS, Alexander MY, Bruce IN. Suppression of inflammation reduces endothelial microparticles in active systemic lupus erythematosus. Annals of the rheumatic diseases. 2013 May 5:annrheumdis-2012.
[107] Guiducci S, Distler JH, Jüngel A, Huscher D, Huber LC, Michel BA, Gay RE, Pisetsky DS, Gay S, Matucci-Cerinic M, Distler O. The relationship between plasma microparticles and disease manifestations in patients with systemic sclerosis. Arthritis & Rheumatism. 2008 Sep 1;58(9):2845-53.
[108] Sgonc R, Gruschwitz MS, Dietrich H, Recheis H, Gershwin ME, Wick G. Endothelial cell apoptosis is a primary pathogenetic event underlying skin lesions in avian and human scleroderma. Journal of Clinical Investigation. 1996 Aug 1;98(3):785.
[109] Kim HK, Song KS, Park YS, Kang YH, Lee YJ, Lee KR, Ryu KW, Bae JM, Kim S. Elevated levels of circulating platelet microparticles, VEGF, IL-6 and RANTES in patients with gastric cancer: possible role of a metastasis predictor. European Journal of Cancer. 2003 Jan 31;39(2):184-91. [2]
[110] Helley D, Banu E, Bouziane A, Banu A, Scotte F, Fischer AM, Oudard S. Platelet microparticles: a potential predictive factor of survival in hormone-refractory prostate cancer patients treated with docetaxel-based chemotherapy. European urology. 2009 Sep 30;56(3):479-85.
[111] Tesselaar ME, Romijn FP, Van Der Linden IK, Prins FA, Bertina RM, Osanto S. Microparticle-associated tissue factor activity: a link between cancer and thrombosis?. Journal of Thrombosis and Haemostasis. 2007 Mar 1;5(3):520-7.
[112] Baran J, Baj-Krzyworzeka M, Weglarczyk K, Szatanek R, Zembala M, Barbasz J, Czupryna A, Szczepanik A, Zembala M. Circulating tumour-derived microvesicles in plasma of gastric cancer patients. Cancer Immunology, Immunotherapy. 2010 Jun 1;59(6):841-50.
[113] Nilsson J, Skog J, Nordstrand A, Baranov V, Mincheva-Nilsson L, Breakefield XO, Widmark A. Prostate cancer-derived urine exosomes: a novel approach to biomarkers for prostate cancer. British journal of cancer. 2009 May 19;100(10):1603-7.
[114] Redman CW, Tannetta DS, Dragovic RA, Gardiner C, Southcombe JH, Collett GP, Sargent IL. Review: does size matter? Placental debris and the pathophysiology of pre-eclampsia. Placenta. 2012 Feb 29;33:S48-54.
[115] Ohno SI, Ishikawa A, Kuroda M. Roles of exosomes and microvesicles in disease pathogenesis. Advanced drug delivery reviews. 2013 Mar 31;65(3):398-401.
[116] Heldring N, Mager I, Wood MJ, Le Blanc K, Andaloussi SE. Therapeutic Potential of Multipotent Mesenchymal Stromal Cells and Their Extracellular Vesicles. Hum Gene Ther. 2015 Aug;26(8):506-17.
[117] Lai RC, Arslan F, Lee MM, Sze NS, Choo A, Chen TS, et al. Exosome secreted by MSC reduces myocardial ischemia/reperfusion injury. Stem Cell Res. 2010 May;4(3):214-22.
[118] Bruno S, Grange C, Deregibus MC, Calogero RA, Saviozzi S, Collino F, et al. Mesenchymal stem cell-derived microvesicles protect against acute tubular injury. J Am Soc Nephrol. 2009 May;20(5):1053-67.

[119] Zhang B, Yin Y, Lai RC, Tan SS, Choo AB, Lim SK. Mesenchymal stem cells secrete immunologically active exosomes. Stem Cells Dev. 2014 Jun 1;23(11):1233-44.
[120] Kordelas L, Rebmann V, Ludwig AK, Radtke S, Ruesing J, Doeppner TR, et al. MSC-derived exosomes: a novel tool to treat therapy-refractory graft-versus-host disease. Leukemia. 2014 Apr;28(4):970-3.
[121] Zhou X, Bailey-Bucktrout SL, Jeker LT, Penaranda C, Martinez-Llordella M, Ashby M, et al. Instability of the transcription factor Foxp3 leads to the generation of pathogenic memory T cells in vivo. Nat Immunol. 2009 Sep;10(9):1000-7.
[122] Yu X, Huang C, Song B, Xiao Y, Fang M, Feng J, et al. CD4+CD25+ regulatory T cells-derived exosomes prolonged kidney allograft survival in a rat model. Cell Immunol. 2013 Sep-Oct;285(1-2):62-8.
[123] Zitvogel L, Regnault A, Lozier A, Wolfers J, Flament C, Tenza D, et al. Eradication of established murine tumors using a novel cell-free vaccine: dendritic cell-derived exosomes. Nat Med. 1998 May;4(5):594-600.
[124] Escudier B, Dorval T, Chaput N, Andre F, Caby MP, Novault S, et al. Vaccination of metastatic melanoma patients with autologous dendritic cell (DC) derived-exosomes: results of thefirst phase I clinical trial. J Transl Med. 2005 Mar 2;3(1):10.
[125] Morse MA, Garst J, Osada T, Khan S, Hobeika A, Clay TM, et al. A phase I study of dexosome immunotherapy in patients with advanced non-small cell lung cancer. J Transl Med. 2005 Feb 21;3(1):9.
[126] Lamparski HG, Metha-Damani A, Yao JY, Patel S, Hsu DH, Ruegg C, et al. Production and characterization of clinical grade exosomes derived from dendritic cells. J Immunol Methods. 2002 Dec 15;270(2):211-26.
[127] Viaud S, Ploix S, Lapierre V, Thery C, Commere PH, Tramalloni D, et al. Updated technology to produce highly immunogenic dendritic cell-derived exosomes of clinical grade: a critical role of interferon-gamma. J Immunother. 2011 Jan;34(1):65-75.
[128] S ELA, Mager I, Breakefield XO, Wood MJ. Extracellular vesicles: biology and emerging therapeutic opportunities. Nat Rev Drug Discov. 2013 May;12(5):347-57.
[129] Andre F, Chaput N, Schartz NE, Flament C, Aubert N, Bernard J, et al. Exosomes as potent cell-free peptide-based vaccine. I. Dendritic cell-derived exosomes transfer functional MHC class I/peptide
[130] Thery C, Zitvogel L, Amigorena S. Exosomes: composition, biogenesis and function. Nat Rev Immunol. 2002 Aug;2(8):569-79.
[131] Wahlgren J, Karlson TD, Brisslert M, Vaziri Sani F, Telemo E, Sunnerhagen P, et al. Plasma exosomes can deliver exogenous short interfering RNA to monocytes and lymphocytes. Nucleic Acids Res. 2012 May 22.
[132] Alvarez-Erviti L, Seow Y, Yin H, Betts C, Lakhal S, Wood MJ. Delivery of siRNA to the mouse brain by systemic injection of targeted exosomes. Nat Biotechnol. 2011 Apr;29(4):341-5.
[133] [131] Sun D, Zhuang X, Xiang X, Liu Y, Zhang S, Liu C, et al. A novel nanoparticle drug delivery system: the anti-inflammatory activity of curcumin is enhanced when encapsulated in exosomes. Mol Ther. 2010 Sep;18(9):1606-14.
[134] Zhuang X, Xiang X, Grizzle W, Sun D, Zhang S, Axtell RC, et al. Treatment of brain inflammatory diseases by delivering exosome encapsulated anti-inflammatory drugs from the nasal region to the brain. Mol Ther. 2011 Oct;19(10):1769-79.

[135] Akao Y, Iio A, Itoh T, Noguchi S, Itoh Y, Ohtsuki Y, et al. Microvesicle-mediated RNA molecule delivery system using monocytes/macrophages. Mol Ther. 2011 Feb;19(2):395-9.
[136] Kosaka N, Iguchi H, Yoshioka Y, Takeshita F, Matsuki Y, Ochiya T. Secretory mechanisms and intercellular transfer of microRNAs in living cells. J Biol Chem. 2010 Jun 4;285(23):17442-52.
[137] Fang Y, Wu N, Gan X, Yan W, Morrell JC, Gould SJ. Higher-order oligomerization targets plasma membrane proteins and HIV gag to exosomes. PLoS Biol. 2007 Jun;5(6):e158.
[138] Shen B, Wu N, Yang JM, Gould SJ. Protein targeting to exosomes/microvesicles by plasma membrane anchors. J Biol Chem. 2011 Apr 22;286(16):14383-95.
[139] Krieg AM, Yi AK, Matson S, Waldschmidt TJ, Bishop GA, Teasdale R, et al. CpG motifs in bacterial DNA trigger direct B-cell activation. Nature. 1995 Apr 6;374(6522):546-9.
[140] Hemmi H, Takeuchi O, Kawai T, Kaisho T, Sato S, Sanjo H, et al. A Toll-like receptor recognizes bacterial DNA. Nature. 2000 Dec 7;408(6813):740-5.
[141] Klinman DM, Currie D, Gursel I, Verthelyi D. Use of CpG oligodeoxynucleotides as immune adjuvants. Immunol Rev. 2004 Jun;199:201-16.
[142] Verthelyi D, Ishii KJ, Gursel M, Takeshita F, Klinman DM. Human peripheral blood cells differentially recognize and respond to two distinct CPG motifs. J Immunol. 2001 Feb 15;166(4):2372-7.
[143] Krug A, Rothenfusser S, Hornung V, Jahrsdorfer B, Blackwell S, Ballas ZK, et al. Identification of CpG oligonucleotide sequences with high induction of IFN-alpha/beta in plasmacytoid dendritic cells. Eur J Immunol. 2001 Jul;31(7):2154-63.
[144] Hartmann G, Krieg AM. Mechanism and function of a newly identified CpG DNA motif in human primary B cells. J Immunol. 2000 Jan 15;164(2):944-53.
[145] Williams R (2006) The endosome effect J. Exp. Med 203:1834
[146] Takeshita F, Leifer CA, Gursel I, Ishii KJ, Takeshita S, Gursel M, et al. Cutting edge: Role of Toll-like receptor 9 in CpG DNA-induced activation of human cells. J Immunol. 2001 Oct 1;167(7):3555-8.
[147] Klinman DM, Yi AK, Beaucage SL, Conover J, Krieg AM. CpG motifs present in bacteria DNA rapidly induce lymphocytes to secrete interleukin 6, interleukin 12, and interferon gamma. Proc Natl Acad Sci U S A. 1996 Apr 2;93(7):2879-83.
[148] Kobayashi H, Horner AA, Takabayashi K, Nguyen MD, Huang E, Cinman N, et al. Immunostimulatory DNA pre-priming: a novel approach for prolonged Th1-biased immunity. Cell Immunol. 1999 Nov 25;198(1):69-75.
[149] Davis HL, Weeratna R, Waldschmidt TJ, Tygrett L, Schorr J, Krieg AM. CpG DNA is a potent enhancer of specific immunity in mice immunized with recombinant hepatitis B surface antigen. J Immunol. 1998 Jan 15;160(2):870-6.
[150] Klinman DM. Adjuvant activity of CpG oligodeoxynucleotides. Int Rev Immunol. 2006 May-Aug;25(3-4):135-54.
[151] von Hunolstein C, Mariotti S, Teloni R, Alfarone G, Romagnoli G, Orefici G, et al. The adjuvant effect of synthetic oligodeoxynucleotide containing CpG motif converts the anti-Haemophilus influenzae type b glycoconjugates into efficient anti-polysaccharide and anti-carrier polyvalent vaccines. Vaccine. 2001 Apr 30;19(23-24):3058-66.

[152] Chu RS, Targoni OS, Krieg AM, Lehmann PV, Harding CV. CpG oligodeoxynucleotides act as adjuvants that switch on T helper 1 (Th1) immunity. J Exp Med. 1997 Nov 17;186(10):1623-31.
[153] Astcott JW, Holmberg CJ, Dewhirst FE, Esch TR, Smith DJ, Taubman MA. Oligonucleotide containing CpG motifs enhances immune response to mucosally or systemically administered tetanus toxoid. Vaccine. 2001 Feb 8;19(13-14):1636-42.
[154] Xie H, Gursel I, Ivins BE, Singh M, O'Hagan DT, Ulmer JB, et al. CpG oligodeoxynucleotides adsorbed onto polylactide-co-glycolide microparticles improve the immunogenicity and protective activity of the licensed anthrax vaccine. Infect Immun. 2005 Feb;73(2):828-33.
[155] Cerundolo V, Silk JD, Masri SH, Salio M. Harnessing invariant NKT cells in vaccination strategies. Nature Reviews Immunology. 2009 Jan 1;9(1):28-38.
[156] Brennan PJ, Brigl M, Brenner MB. Invariant natural killer T cells: an innate activation scheme linked to diverse effector functions. Nature Reviews Immunology. 2013 Feb 1;13(2):101-17.
[157] Kumar V, Delovitch TL. Different subsets of natural killer T cells may vary in their roles in health and disease. Immunology. 2014 Jul 1;142(3):321-36.
[158] Kawano T, Cui J, Koezuka Y, Toura I, Kaneko Y, Motoki K, Ueno H, Nakagawa R, Sato H, Kondo E, Koseki H. CD1d-restricted and TCR-mediated activation of Vα14 NKT cells by glycosylceramides. Science. 1997 Nov 28;278(5343):1626-9.
[159] Godfrey DI, Kronenberg M. Going both ways: immune regulation via CD1d-dependent NKT cells. The Journal of clinical investigation. 2004 Nov 15;114(10):1379-88.
[160] Dhodapkar MV, Richter J. Harnessing natural killer T (NKT) cells in human myeloma: progress and challenges. Clinical immunology. 2011 Aug 31;140(2):160-6.
[161] Exley MA, Nakayama T. NKT-cell-based immunotherapies in clinical trials.
[162] Berzins SP, Smyth MJ, Baxter AG. Presumed guilty: natural killer T cell defects and human disease. Nature Reviews Immunology. 2011 Feb 1;11(2):131-42.
[163] Smyth MJ, Crowe NY, Pellicci DG, Kyparissoudis K, Kelly JM, Takeda K, Yagita H, Godfrey DI. Sequential production of interferon-γ by NK1. 1+ T cells and natural killer cells is essential for the antimetastatic effect of α-galactosylceramide. Blood. 2002 Feb 15;99(4):1259-66.
[164] Giaccone G, Punt CJ, Ando Y, Ruijter R, Nishi N, Peters M, von Blomberg BM, Scheper RJ, van der Vliet HJ, van den Eertwegh AJ, Roelvink M. A phase I study of the natural killer T-cell ligand α-galactosylceramide (KRN7000) in patients with solid tumors. Clinical Cancer Research. 2002 Dec 1;8(12):3702-9.
[165] Konishi J, Yamazaki K, Yokouchi H, Shinagawa N, Iwabuchi K, Nishimura M. The characteristics of human NKT cells in lung cancer—CD1d independent cytotoxicity against lung cancer cells by NKT cells and decreased human NKT cell response in lung cancer patients. Human immunology. 2004 Nov 30;65(11):1377-88.
[166] Parekh VV, Wilson MT, Olivares-Villagómez D, Singh AK, Wu L, Wang CR, Joyce S, Van Kaer L. Glycolipid antigen induces long-term natural killer T cell anergy in mice. The Journal of clinical investigation. 2005 Sep 1;115(9):2572-83.
[167] Chang DH, Osman K, Connolly J, Kukreja A, Krasovsky J, Pack M, Hutchinson A, Geller M, Liu N, Annable R, Shay J. Sustained expansion of NKT cells and antigen-specific T cells after injection of α-galactosyl-ceramide loaded mature dendritic cells in cancer patients. Journal of Experimental Medicine. 2005 May 2;201(9):1503-17.

[168] Fujii SI, Shimizu K, Kronenberg M, Steinman RM. Prolonged IFN-γ–producing NKT response induced with α-galactosylceramide–loaded DCs. Nature immunology. 2002 Sep 1;3(9):867-74.
[169] Nieda M, Okai M, Tazbirkova A, Lin H, Yamaura A, Ide K, Abraham R, Juji T, Macfarlane DJ, Nicol AJ. Therapeutic activation of Vα24+ Vβ11+ NKT cells in human subjects results in highly coordinated secondary activation of acquired and innate immunity. Blood. 2004 Jan 15;103(2):383-9.
[170] Toura I, Kawano T, Akutsu Y, Nakayama T, Ochiai T, Taniguchi M. Cutting edge: inhibition of experimental tumor metastasis by dendritic cells pulsed with α-galactosylceramide. The Journal of Immunology. 1999 Sep 1;163(5):2387-91.
[171] Ko HJ, Kim YJ, Kim YS, Chang WS, Ko SY, Chang SY, Sakaguchi S, Kang CY. A combination of chemoimmunotherapies can efficiently break self-tolerance and induce antitumor immunity in a tolerogenic murine tumor model. Cancer research. 2007 Aug 1;67(15):7477-86.
[172] Fukushima S, Hirata S, Motomura Y, Fukuma D, Matsunaga Y, Ikuta Y, Ikeda T, Kageshita T, Ihn H, Nishimura Y, Senju S. Multiple Antigen-targeted Immunotherapy With α-Galactosylceramide–loaded and Genetically Engineered Dendritic Cells Derived From Embryonic Stem Cells. Journal of Immunotherapy. 2009 Apr 1;32(3):219-31.
[173] Matsuyoshi H, Hirata S, Yoshitake Y, Motomura Y, Fukuma D, Kurisaki A, Nakatsura T, Nishimura Y, Senju S. Therapeutic effect of α-galactosylceramide-loaded dendritic cells genetically engineered to express SLC/CCL21 along with tumor antigen against peritoneally disseminated tumor cells. Cancer science. 2005 Dec 1;96(12):889-96.
[174] Barral P, Polzella P, Bruckbauer A, Van Rooijen N, Besra GS, Cerundolo V, Batista FD. CD169+ macrophages present lipid antigens to mediate early activation of iNKT cells in lymph nodes. Nature immunology. 2010 Apr 1;11(4):303-12.
[175] Barral P, Sánchez-Niño MD, Van Rooijen N, Cerundolo V, Batista FD. The location of splenic NKT cells favours their rapid activation by blood-borne antigen. The EMBO journal. 2012 May 16;31(10):2378-90.
[176] Fernandez EM, Chang J, Fontaine J, Bialecki E, Rodriguez F, Werkmeister E, Krieger V, Ehret C, Heurtault B, Fournel S, Frisch B. Activation of invariant Natural Killer T lymphocytes in response to the α-galactosylceramide analogue KRN7000 encapsulated in PLGA-based nanoparticles and microparticles. International journal of pharmaceutics. 2012 Feb 14;423(1):45-54.
[177] Thapa P, Zhang G, Xia C, Gelbard A, Overwijk WW, Liu C, Hwu P, Chang DZ, Courtney A, Sastry JK, Wang PG. Nanoparticle formulated alpha-galactosylceramide activates NKT cells without inducing anergy. Vaccine. 2009 May 26;27(25):3484-8.
[178] Behcet H. Uber rezidivierende, aphtose, durch ein Virus verursachte Geschwure am Mund, am Auge und an den Genitalien. Dermatologische Wochenschr. 1937;105:1152-7.
[179] Sallakci N, Bacanli A, Coskun M, Yavuzer U, Alpsoy E, Yegin O. CTLA-4 gene 49A/G polymorphism in Turkish patients with Behçet's disease. Clinical and experimental dermatology. 2005 Sep 1;30(5):546-50.
[180] Yurdakul S. Epidemiology of Behçet’s syndrome and regional differences in disease expression. InBehçet’s syndrome 2010 (pp. 35-52). Springer New York.
[181] Alpsoy E, Zouboulis CC, Ehrlich GE. Mucocutaneous lesions of Behçet's disease. Yonsei medical journal. 2007 Aug 1;48(4):573-85.

[182] Kural-Seyahi E, Fresko I, Seyahi N, Ozyazgan Y, Mat C, Hamuryudan V, Yurdakul S, Yazici H. The long-term mortality and morbidity of Behçet syndrome: a 2-decade outcome survey of 387 patients followed at a dedicated center. Medicine. 2003 Jan 1;82(1):60-76.
[183] Gül A, Ohno S. Genetics of Behçet's disease. InBehçet's syndrome 2010 (pp. 265-276). Springer New York.
[184] Emmi G, Silvestri E, Squatrito D, D'Elios MM, Ciucciarelli L, Prisco D, Emmi L. Behçet's syndrome pathophysiology and potential therapeutic targets. Internal and emergency medicine. 2014 Apr 1;9(3):257-65.
[185] Verity DH, Marr JE, Ohno S, Wallace GR, Stanford MR. Behçet's disease, the silk road and HLA-B51: Historical and geographical perspectives. Tissue antigens. 1999 Sep 1;54(3):213-20.
[186] Meguro A, Inoko H, Ota M, Katsuyama Y, Oka A, Okada E, Yamakawa R, Yuasa T, Fujioka T, Ohno S, Bahram S. Genetics of Behçet's disease inside and outside the MHC. Annals of the rheumatic diseases. 2009 Aug 13.
[187] Remmers EF, Cosan F, Kirino Y, Ombrello MJ, Abaci N, Satorius C, Le JM, Yang B, Korman BD, Cakiris A, Aglar O. Genome-wide association study identifies variants in the MHC class I, IL10, and IL23R-IL12RB2 regions associated with Behcet's disease. Nature genetics. 2010 Aug 1;42(8):698-702.
[188] Hou S, Yang Z, Du L, Jiang Z, Shu Q, Chen Y, Li F, Zhou Q, Ohno S, Chen R, Kijlstra A. Identification of a susceptibility locus in STAT4 for Behçet's disease in Han Chinese in a genome-wide association study. Arthritis & Rheumatism. 2012 Dec 1;64(12):4104-13.
[189] Direskeneli H. Autoimmunity vs autoinflammation in Behcet's disease: do we oversimplify a complex disorder? Rheumatology (Oxford, England). 2006 Dec;45(12):1461-5.
[190] Hamzaoui K, Hamzaoui A, Guemira F, Bessioud M, Hamza M, Ayed K. Cytokine profile in Behcet's disease patients. Relationship with disease activity. Scandinavian journal of rheumatology. 2002;31(4):205-10.
[191] Melikoglu M, Uysal S, Krueger JG, Kaplan G, Gogus F, Yazici H, et al. Characterization of the divergent wound-healing responses occurring in the pathergy reaction and normal healthy volunteers. J Immunol. 2006 Nov 1;177(9):6415-21.
[192] Pay S, Şimşek İ, Erdem H, Dinç A. Immunopathogenesis of Behçet's disease with special emphasize on the possible role of antigen presenting cells. Rheumatology international. 2007 Mar 1;27(5):417-24.
[193] Zhou ZY, Chen SL, Shen N, Lu Y. Cytokines and Behcet's disease. Autoimmunity reviews. 2012 Aug 31;11(10):699-704.
[194] Chambrun MP, Wechsler B, Geri G, Cacoub P, Saadoun D. New insights into the pathogenesis of Behcet's disease. Autoimmunity reviews. 2012 Aug 31;11(10):687-98.
[195] Lopalco G, Lucherini OM, Vitale A, Talarico R, Lopalco A, Galeazzi M, Lapadula G, Cantarini L, Iannone F. Putative Role of Serum Amyloid-A and Proinflammatory Cytokines as Biomarkers for Behcet's Disease. Medicine. 2015 Oct;94(42).
[196] Chari A, Hentall ID, Papadopoulos MC, Pereira EA. Surgical Neurostimulation for Spinal Cord Injury. Brain Sciences. 2017 Feb 10;7(2):18.
[197] Held KS, Lane TE. Spinal cord injury, immunodepression, and antigenic challenge. InSeminars in immunology 2014 Oct 31 (Vol. 26, No. 5, pp. 415-420). Academic Press.

[198] Popa C, Popa F, Grigorean VT, Onose G, Sandu AM, Popescu M, Burnei G, Strambu V, Sinescu C. Vascular dysfunctions following spinal cord injury. Journal of medicine and life. 2010 Jul 1;3(3):275.
[199] Bonner S, Smith C. Initial management of acute spinal cord injury. Continuing Education in Anaesthesia, Critical Care & Pain. 2013 Jul 12:mkt021.
[200] Furlan JC, Fehlings MG. Cardiovascular complications after acute spinal cord injury: pathophysiology, diagnosis, and management. Neurosurgical focus. 2008 Nov;25(5):E13.
[201] Lo V, Esquenazi Y, Han MK, Lee K. TRAUMA SURGERY. J Neurosurg Sci. 2013;57:281-92.
[202] Dumont RJ, Okonkwo DO, Verma S, Hurlbert RJ, Boulos PT, Ellegala DB, Dumont AS. Acute spinal cord injury, part I: pathophysiologic mechanisms. Clinical neuropharmacology. 2001 Sep 1;24(5):254-64.
[203] Hagg T, Oudega M. Degenerative and spontaneous regenerative processes after spinal cord injury. Journal of neurotrauma. 2006 Apr 1;23(3-4):263-80.
[204] Cruse JM, Lewis Jr RE, Bishop G, Kliesch WF, Gaitan E, Britt R. Decreased immune reactivity and neuroendocrine alterations related to chronic stress in spinal cord injury and stroke patients. Pathobiology. 1993 Jul 1;61(3-4):183-92.
[205] Nash MS. Known and plausible modulators of depressed immune functions following spinal cord injuries. The journal of spinal cord medicine. 2000 Jan 1;23(2):111-20.
[206] DeVivo MJ, Kartus PL, Stover SL, Rutt RD, Fine PR. Cause of death for patients with spinal cord injuries. Archives of internal medicine. 1989 Aug 1;149(8):1761-6.
[207] Soden RJ, Walsh J, Middleton JW, Craven ML, Rutkowski SB, Yeo JD. Causes of death after spinal cord injury. Spinal Cord. 2000 Oct 1;38(10):604.
[208] Sekhon LH, Fehlings MG. Epidemiology, demographics, and pathophysiology of acute spinal cord injury. Spine. 2001 Dec 15;26(24S):S2-12.
[209] Grau AJ, Buggle F, Schnitzler P, Spiel M, Lichy C, Hacke W. Fever and infection early after ischemic stroke. Journal of the neurological sciences. 1999 Dec 15;171(2):115-20.
[210] Yu CG, Jagid J, Ruenes G, Dietrich WD, Marcillo AE, Yezierski RP. Detrimental effects of systemic hyperthermia on locomotor function and histopathological outcome after traumatic spinal cord injury in the rat. Neurosurgery. 2001 Jul 1;49(1):152-9.
[211] Kwan J, Hand P. Infection after acute stroke is associated with poor short-term outcome. Acta neurologica scandinavica. 2007 May 1;115(5):331-8.
[212] Campagnolo DI, Bartlett JA, Keller SE, Sanchez W, Oza R. Impaıred Phagocytosıs of Staphylococcus Aureus In Complete Tetraplegics. American journal of physical medicine & rehabilitation. 1997 Jul 1;76(4):276-80.
[213] Campagnolo DI, Dixon D, Schwartz J, Bartlett JA, Keller SE. Altered innate immunity following spinal cord injury. Spinal Cord. 2008 Jul 1;46(7):477-81.
[214] Cruse JM, Lewis RE, Dilioglou S, Roe DL, Wallace WF, Chen RS. Review of immune function, healing of pressure ulcers, and nutritional status in patients with spinal cord injury. The journal of spinal cord medicine. 2000 Jan 1;23(2):129-35.
[215] Cano G, Sved AF, Rinaman L, Rabin BS, Card JP. Characterization of the central nervous system innervation of the rat spleen using viral transneuronal tracing. Journal of Comparative Neurology. 2001 Oct 8;439(1):1-8.
[216] Teasell RW, Arnold JM, Krassioukov A, Delaney GA. Cardiovascular consequences of loss of supraspinal control of the sympathetic nervous system after

spinal cord injury. Archives of physical medicine and rehabilitation. 2000 Apr 30;81(4):506-16.
[217] Iversen PO, Hjeltnes N, Holm B, Flatebø T, Strøm-Gundersen I, Rønning W, Stanghelle J, Benestad HB. Depressed immunity and impaired proliferation of hematopoietic progenitor cells in patients with complete spinal cord injury. Blood. 2000 Sep 15;96(6):2081-3.
[218] Lucin KM, Sanders VM, Jones TB, Malarkey WB, Popovich PG. Impaired antibody synthesis after spinal cord injury is level dependent and is due to sympathetic nervous system dysregulation. Experimental neurology. 2007 Sep 30;207(1):75-84.
[219] Kahraman T, Gucluler G, Simsek I, Yagci FC, Yildirim M, Ozen C.et al. Circulating LL37 targets plasma extracellular vesicles to immune cells and intensifies Behçet's disease severity. Journal of Extracellular Vesicles. 2017 Feb 6:1, 1284449.
[220] Kahraman T. Therapeutic and Diagnostic Applications of Extracellular Vesicles, PhD Thesis, 2017.
[221] Cho JA, Yeo DJ, Son HY, Kim HW, Jung DS, Ko JK, et al. Exosomes: a new delivery system for tumor antigens in cancer immunotherapy. Int J Cancer. 2005 Apr 20;114(4):613-22.
[222] Kim SH, Bianco N, Menon R, Lechman ER, Shufesky WJ, Morelli AE, et al. Exosomes derived from genetically modified DC expressing FasL are anti-inflammatory and immunosuppressive. Mol Ther. 2006 Feb;13(2):289-300.
[223] Villarroya-Beltri C, Baixauli F, Gutierrez-Vazquez C, Sanchez-Madrid F, Mittelbrunn M. Sorting it out: regulation of exosome loading. Semin Cancer Biol. 2014 Oct;28:3-13.
[224] Martín-Jaular L, de Menezes-Neto A, Monguió-Tortajada M, Elizalde-Torrent A, Díaz-Varela M, Fernández-Becerra C, Borras FE, Montoya M, Del Portillo HA. Spleen-Dependent Immune Protection Elicited by CpG Adjuvanted Reticulocyte-Derived Exosomes from Malaria Infection Is Associated with Changes in T cell Subsets' Distribution. Frontiers in Cell and Developmental Biology. 2016;4.
[225] Martin-Jaular L, Nakayasu ES, Ferrer M, Almeida IC, del Portillo HA. Exosomes from Plasmodium yoelii-infected reticulocytes protect mice from lethal infections. PloS one. 2011 Oct 26;6(10):e26588.
[226] Yang Y, Xiu F, Cai Z, Wang J, Wang Q, Fu Y, Cao X. Increased induction of antitumor response by exosomes derived from interleukin-2 gene-modified tumor cells. Journal of cancer research and clinical oncology. 2007 Jun 1;133(6):389-99.
[227] Macho-Fernandez E, Brigl M. The extended family of CD1d-restricted NKT cells: sifting through a mixed bag of TCRs, antigens, and functions. Frontiers in immunology. 2015 Jul 28;6:362.
[228] Hong S, Lee H, Jung K, Lee SM, Lee SJ, Jun HJ, Kim Y, Song H, Bogen B, Choi I. Tumor cells loaded with α-galactosylceramide promote therapeutic NKT-dependent anti-tumor immunity in multiple myeloma. Immunology letters. 2013 Dec 31;156(1):132-9.
[229] Dong T, Yi T, Yang M, Lin S, Li W, Xu X, Hu J, Jia L, Hong X, Niu W. Co-operation of α-galactosylceramide-loaded tumour cells and TLR9 agonists induce potent anti-tumour responses in a murine colon cancer model. Biochemical Journal. 2016 Jan 1;473(1):7-19.
[230] Gehrmann U, Hiltbrunner S, Georgoudaki AM, Karlsson MC, Näslund TI, Gabrielsson S. Synergistic induction of adaptive antitumor immunity by codelivery

of antigen with α-galactosylceramide on exosomes. Cancer research. 2013 Jul 1;73(13):3865-76.
[231] Romagnoli GG, Zelante BB, Toniolo PA, Migliori IK, Barbuto JA. Dendritic Cell-Derived Exosomes may be a Tool for Cancer Immunotherapy by Converting Tumor Cells into Immunogenic Targets. Front Immunol. 2014;5:692.
[232] Distler JH, Huber LC, Gay S, Distler O, Pisetsky DS. Microparticles as mediators of cellular cross-talk in inflammatory disease. Autoimmunity. 2006 Jan 1;39(8):683-90.
[233] Knijff-Dutmer EA, Koerts J, Nieuwland R, Kalsbeek-Batenburg EM, Van De Laar MA. Elevated levels of platelet microparticles are associated with disease activity in rheumatoid arthritis. Arthritis & Rheumatism. 2002 Jun 1;46(6):1498-503.
[234] Berckmans RJ, Nieuwland R, Tak PP, Böing AN, Romijn FP, Kraan MC, Breedveld FC, Hack CE, Sturk A. Cell-derived microparticles in synovial fluid from inflamed arthritic joints support coagulation exclusively via a factor VII–dependent mechanism. Arthritis & Rheumatology. 2002 Nov 1;46(11):2857-66.
[235] Brogan PA, Dillon MJ. Endothelial microparticles and the diagnosis of the vasculitides. Internal medicine. 2004;43(12):1115-9.\
[236] Combes V, Simon AC, Grau GE, Arnoux D, Camoin L, Sabatier F, Mutin M, Sanmarco M, Sampol J, Dignat-George F. In vitro generation of endothelial microparticles and possible prothrombotic activity in patients with lupus anticoagulant. The Journal of clinical investigation. 1999 Jul 1;104(1):93-102.
[237] Larkin M. Raised endothelial microparticles an early marker for multiple sclerosis?. (2001): 1679.
[238] Sellam J, Proulle V, Jüngel A, Ittah M, Richard CM, Gottenberg JE, Toti F, Benessiano J, Gay S, Freyssinet JM, Mariette X. Increased levels of circulating microparticles in primary Sjögren's syndrome, systemic lupus erythematosus and rheumatoid arthritis and relation with disease activity. Arthritis research & therapy. 2009 Oct 15;11(5):R156.
[239] Cocucci E, Racchetti G, Meldolesi J. Shedding microvesicles: artefacts no more. Trends in cell biology. 2009 Feb 28;19(2):43-51.
[240] Hunter MP, Ismail N, Zhang X, Aguda BD, Lee EJ, Yu L, Xiao T, Schafer J, Lee ML, Schmittgen TD, Nana-Sinkam SP. Correction: Detection of microRNA Expression in Human Peripheral Blood Microvesicles. PLoS ONE. 2010;5(3).
[241] Reich CF, Pisetsky DS. The content of DNA and RNA in microparticles released by Jurkat and HL-60 cells undergoing in vitro apoptosis. Experimental cell research. 2009 Mar 10;315(5):760-8.
[242] Hugel B, Martínez MC, Kunzelmann C, Freyssinet JM. Membrane microparticles: two sides of the coin. Physiology. 2005 Feb 1;20(1):22-7.
[243] Yáñez-Mó M, Siljander PR, Andreu Z, Zavec AB, Borràs FE, Buzas EI, Buzas K, Casal E, Cappello F, Carvalho J, Colás E. Biological properties of extracellular vesicles and their physiological functions. Journal of extracellular vesicles. 2015 May 14;4.
[244] Danielson KM, Das S. Extracellular vesicles in heart disease: excitement for the future?. Exosomes and microvesicles. 2014 Jan 1;2:1.
[245] Gaceb A, Martinez MC, Andriantsitohaina R. Extracellular vesicles: new players in cardiovascular diseases. The international journal of biochemistry & cell biology. 2014 May 31;50:24-8.
[246] Beyer C, Pisetsky DS. The role of microparticles in the pathogenesis of rheumatic diseases. Nature Reviews Rheumatology. 2010 Jan 1;6(1):21-9.

[247] Dean SN, Bishop BM, Van Hoek ML. Susceptibility of Pseudomonas aeruginosa biofilm to alpha-helical peptides: D-enantiomer of LL-37. Front. Microbiol. 2011 Jan 1;2.
[248] Wong JH, Ng TB, Legowska A, Rolka K, Hui M, Cho CH. Antifungal action of human cathelicidin fragment (LL13–37) on Candida albicans. Peptides. 2011 Oct 31;32(10):1996-2002.
[249] Barlow PG, Svoboda P, Mackellar A, Nash AA, York IA, Pohl J, Davidson DJ, Donis RO. Antiviral activity and increased host defense against influenza infection elicited by the human cathelicidin LL-37. PloS one. 2011 Oct 21;6(10):e25333.
[250] Mumcu G, Cimilli H, Karacayli U, Inanc N, Ture-Ozdemir F, Eksioglu-Demiralp E, Ergun T, Direskeneli H. Salivary levels of antimicrobial peptides Hnp 1-3, Ll-37 and S100 in Behcet's disease. Archives of oral biology. 2012 Jun 30;57(6):642-6.
[251] Vandamme D, Landuyt B, Luyten W, Schoofs L. A comprehensive summary of LL-37, the factotum human cathelicidin peptide. Cellular immunology. 2012 Nov 30;280(1):22-35.
[252] Yu J, Mookherjee N, Wee K, Bowdish DM, Pistolic J, Li Y, Rehaume L, Hancock RE. Host defense peptide LL-37, in synergy with inflammatory mediator IL-1β, augments immune responses by multiple pathways. The Journal of Immunology. 2007 Dec 1;179(11):7684-91.
[253] Lande R, Gregorio J, Facchinetti V, Chatterjee B, Wang YH, Homey B, Cao W, Wang YH, Su B, Nestle FO, Zal T. Plasmacytoid dendritic cells sense self-DNA coupled with antimicrobial peptide. Nature. 2007 Oct 4;449(7162):564-9.
[254] Campagnolo DI, Keller SE, DeLisa JA, Glick TJ, Sipski ML, Schleifer SJ. Alteration of Immune System Function in Tetraplegics: A Pilot Study. American journal of physical medicine & rehabilitation. 1994 Nov 1;73(6):387-93.
[255] Campagnolo DI, Bartlett JA, Keller SE. Influence of neurological level on immune function following spinal cord injury: a review. The journal of spinal cord medicine. 2000 Jan 1;23(2):121-8.
[256] Riegger T, Conrad S, Liu K, Schluesener HJ, Adibzahdeh M, Schwab JM. Spinal cord injury-induced immune depression syndrome (SCI-IDS). European Journal of Neuroscience. 2007 Mar 1;25(6):1743-7.
[257] Mills KH. TLR-dependent T cell activation in autoimmunity. Nature Reviews Immunology. 2011 Dec 1;11(12):807-22.
[258] Ozinsky A, Underhill DM, Fontenot JD, Hajjar AM, Smith KD, Wilson CB, Schroeder L, Aderem A. The repertoire for pattern recognition of pathogens by the innate immune system is defined by cooperation between toll-like receptors. Proceedings of the National Academy of Sciences. 2000 Dec 5;97(25):13766-71.
[259] Medzhitov R. Toll-like receptors and innate immunity. Nature Reviews Immunology. 2001 Nov 1;1(2):135-45.
[260] Imai Y, Kuba K, Neely GG, Yaghubian-Malhami R, Perkmann T, van Loo G, Ermolaeva M, Veldhuizen R, Leung YC, Wang H, Liu H. Identification of oxidative stress and Toll-like receptor 4 signaling as a key pathway of acute lung injury. Cell. 2008 Apr 18;133(2):235-49.
[261] West XZ, Malinin NL, Merkulova AA, Tischenko M, Kerr BA, Borden EC, Podrez EA, Salomon RG, Byzova TV. Oxidative stress induces angiogenesis by activating TLR2 with novel endogenous ligands. Nature. 2010 Oct 21;467(7318):972-6.

[262] Takeuchi O, Akira S. Pattern recognition receptors and inflammation. Cell. 2010 Mar 19;140(6):805-20.
[263] Riegger T, Conrad S, Schluesener HJ, Kaps HP, Badke A, Baron C, Gerstein J, Dietz K, Abdizahdeh M, Schwab JM. Immune depression syndrome following human spinal cord injury (SCI): a pilot study. Neuroscience. 2009 Feb 6;158(3):1194-9.
[264] Cruse JM, Lewis RE, Bishop GR, Kliesch WF, Gaitan E. Neuroendocrine-immune interactions associated with loss and restoration of immune system function in spinal cord injury and stroke patients. Immunologic research. 1992 Jun 1;11(2):104-16.

Appendix

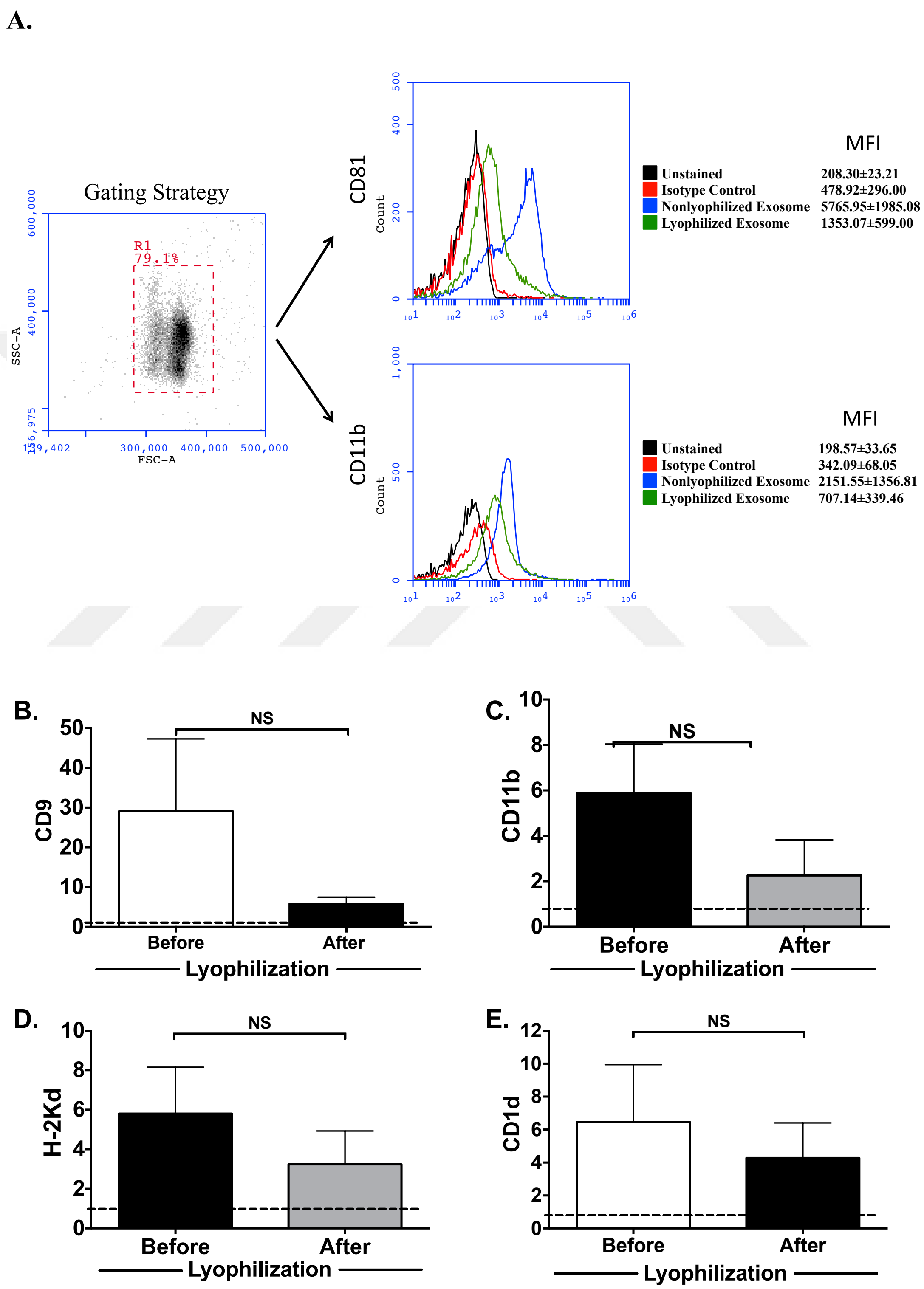

Figure A1. Exosomes retain cardinal exosomal markers after lyophilization.

(A) Gating strategy to determine bead conjugated exosomes by FACS and representative MFI plots. Bar graphs showing MFI ratio of (B) CD9 and (C) CD11b (D) MHCII (E) CD1d molecules to their specific isotype controls. Mann-Whitney test was used to test statistical significance. NS: Non-significant.

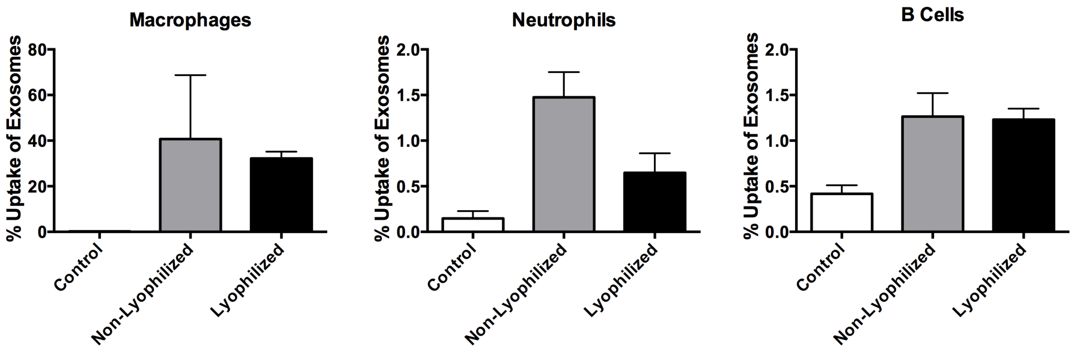

Figure A2. Non-lyophilized and lyophilized exosomes are taken up by PECs at similar levels.

Mice were intraperitoneally injected with non-lyophilized and lyophilized exosomes 4 days after thioglycolate injection to mice. Bar graphs show (A) PKH-26$^+$ and CD11b$^+$ macrophages, (B) PKH-26$^+$ and Ly-6G$^+$ neutrophils and (C) PKH-26$^+$ and B220$^+$ B cells within PEC population of mice treated with exosomes 4 hours before sacrifice.

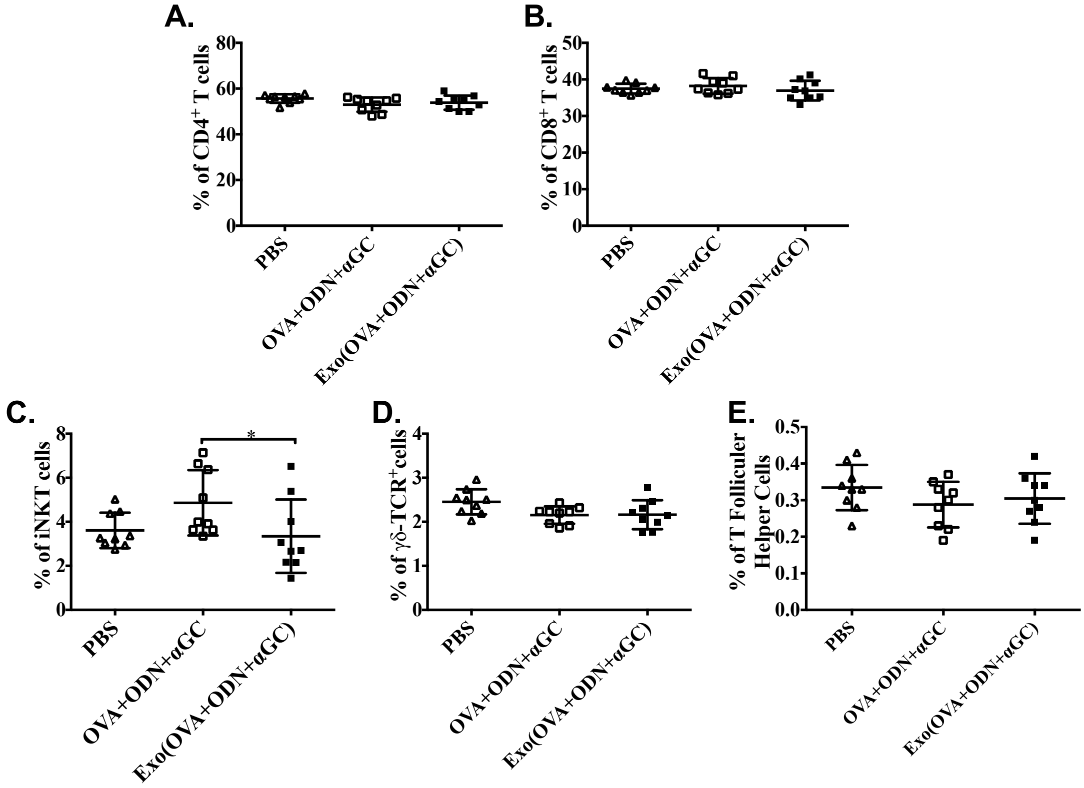

Figure A3. Percent of immune cells 7 days after immunization with free and exosomal form of OVA+ODN+αGC.

FACS analysis of splenic (A) $CD4^+$ cells (defined as live cells, $B220^-$, TCR-β^+, $CD4^+$ cells) (B) $CD8^+$ cells (defined as live cells, $B220^-$, TCR-β^+, $CD8^+$ cells), (C) iNKT cells (defined as live cells, $B220^-$, TCR-β^+, $DimerX^+$ live cells), D. γδ-TCR cells (E) T follicular helper cells (defined as live cells, $B220^-$, TCR-β^+, $CD4^+$ PD-1^+, $CXCR5^+$ cells). Statistical significance was tested using Kruskal-Wallis test. *, $p<0.05$.

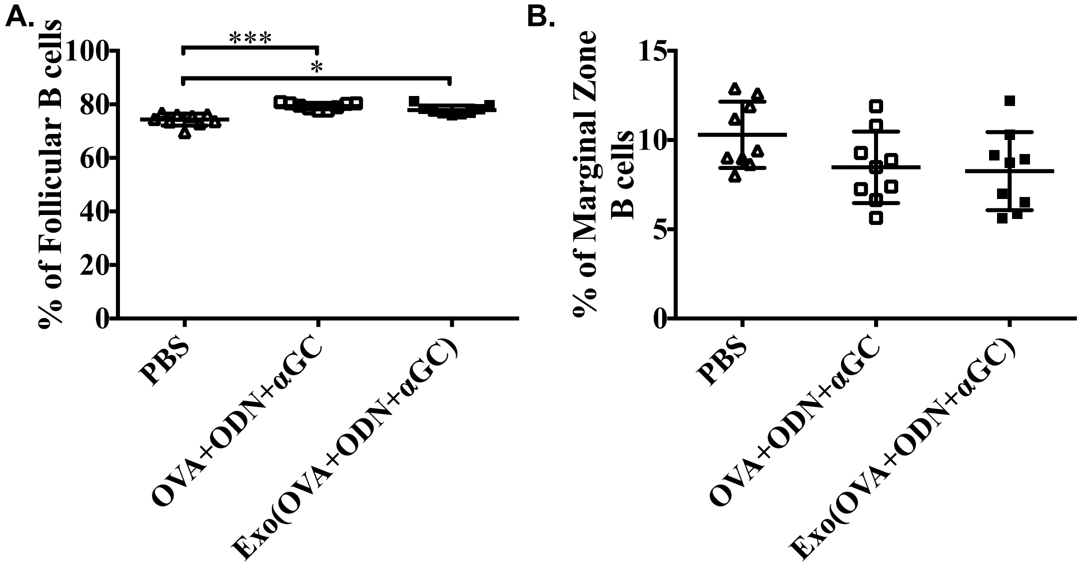

Figure A4. Percent number of B cell subtypes 7 days after immunization with free and exosomal form of OVA+ODN+αGC.

FACS analysis of splenic (A) Follicular B cells (defined as live cells, $B220^{+}$, $CD21^{lo}$, $CD23^{hi}$ cells) and (B) Marginal Zone B cells (defined as live cells, $B220^{+}$, $CD21^{+}$, $CD23^{lo}$ cells). Statistical significance was tested by using Kruskal-Wallis test. *, $p<0.05$; **, $p<0.001$; ***, $p<0.001$.

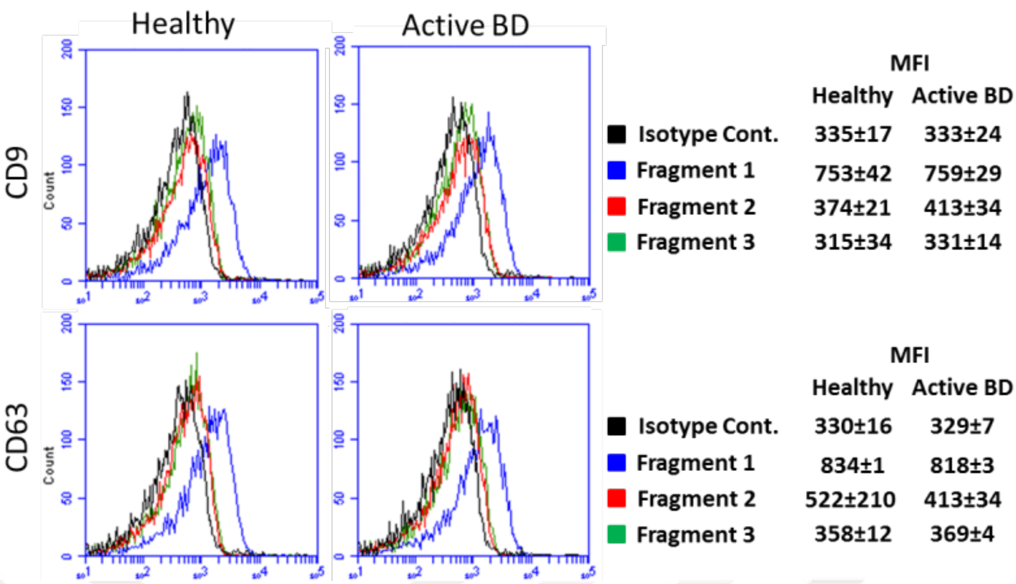

Figure A5. Characterization of EV fractions obtained by FPLC Separation [220].

Each fragment was analyzed by bead-based flow cytometry analysis of EVs against CD9 and CD63 antibodies. Left panel represents the histograms of bead-based flow cytometer analysis of EVs.

A

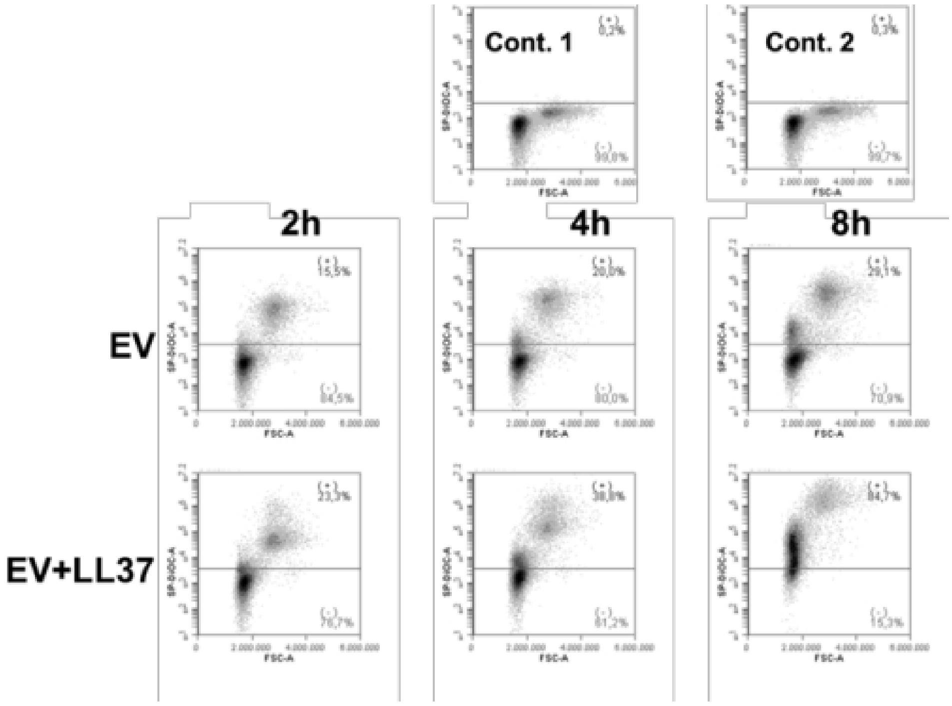

B

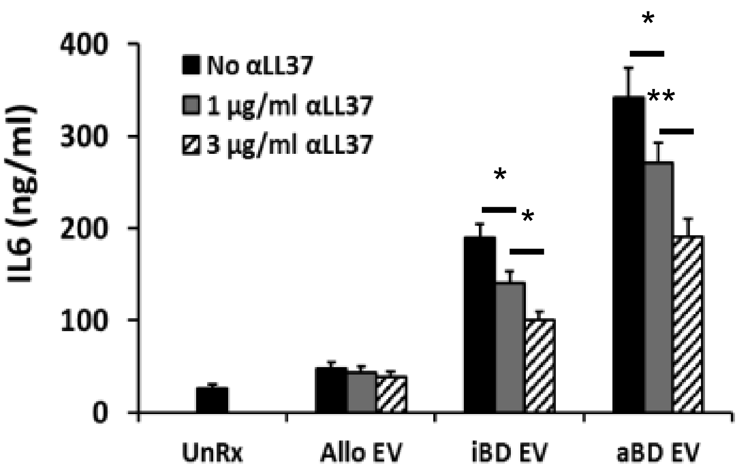

Figure A6. Different immune cells internalize EV/LL37 complex at different levels [219, 220].

(A) Dot plots represent EV internalization by healthy PBMCs at different time points. As a negative control, PBMCs were incubated in the absence of stained EVs (denoted as "Cont. 1", top left panel) as well as ultracentrifuged SP-DiOC pellet to rule out any noise or dye contamination (denoted as "Cont. 2", top right panel, respectively. (B) Dose dependent inhibition of BD EV mediated IL6 secretion from PBMCs following incubation for 12 h. *p<0.01, and **p<0.001 for all comparisons.

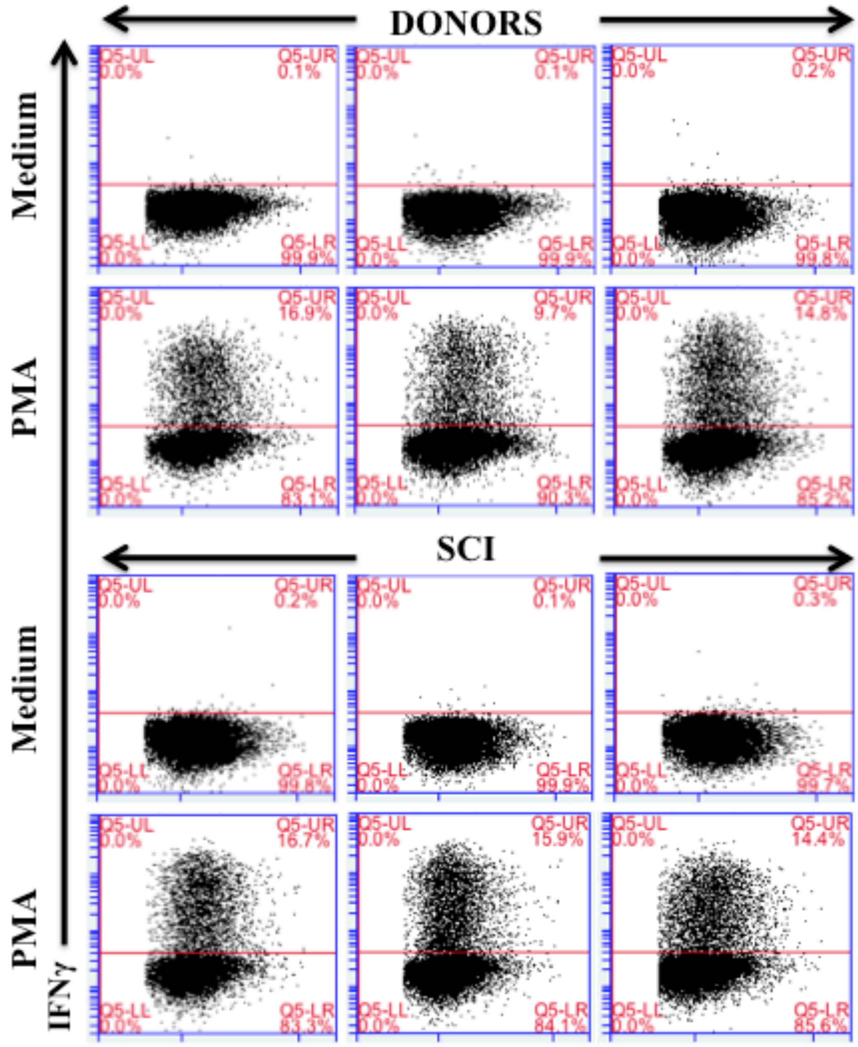

Figure A7. Representative FACS analysis plots of IFNγ producing T cells. Healthy donor (upper panels) and SCI patient (lower panels) PBMCs were incubated in either medium only or PMA-Ionomycin. IFNγ signal was detected from CD4$^+$positive T cells.

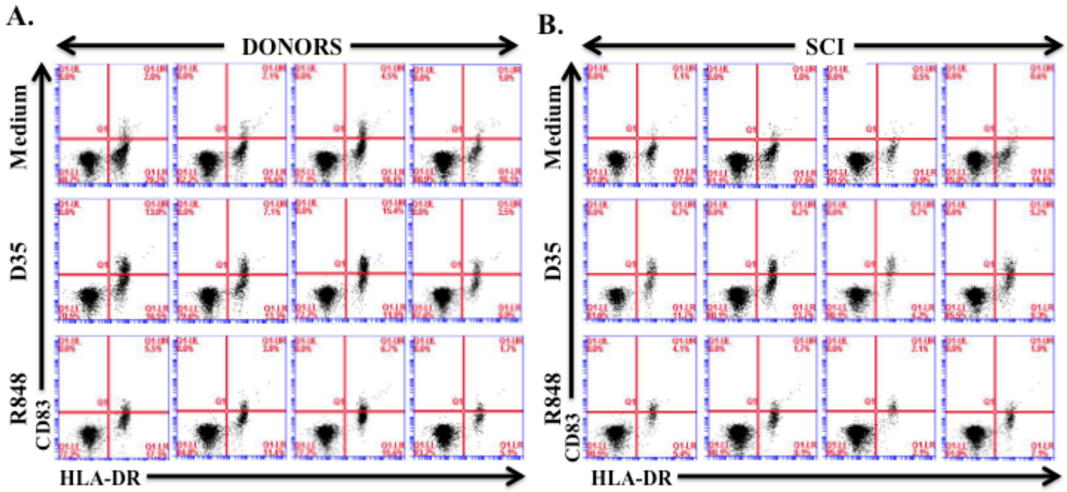

Figure A8. Representative FACS analysis plots of CD83$^+$ and HLA-DR$^+$ cells. (A) Healthy donor and (B) SCI patient PBMCs were stimulated either with D35 or R848.

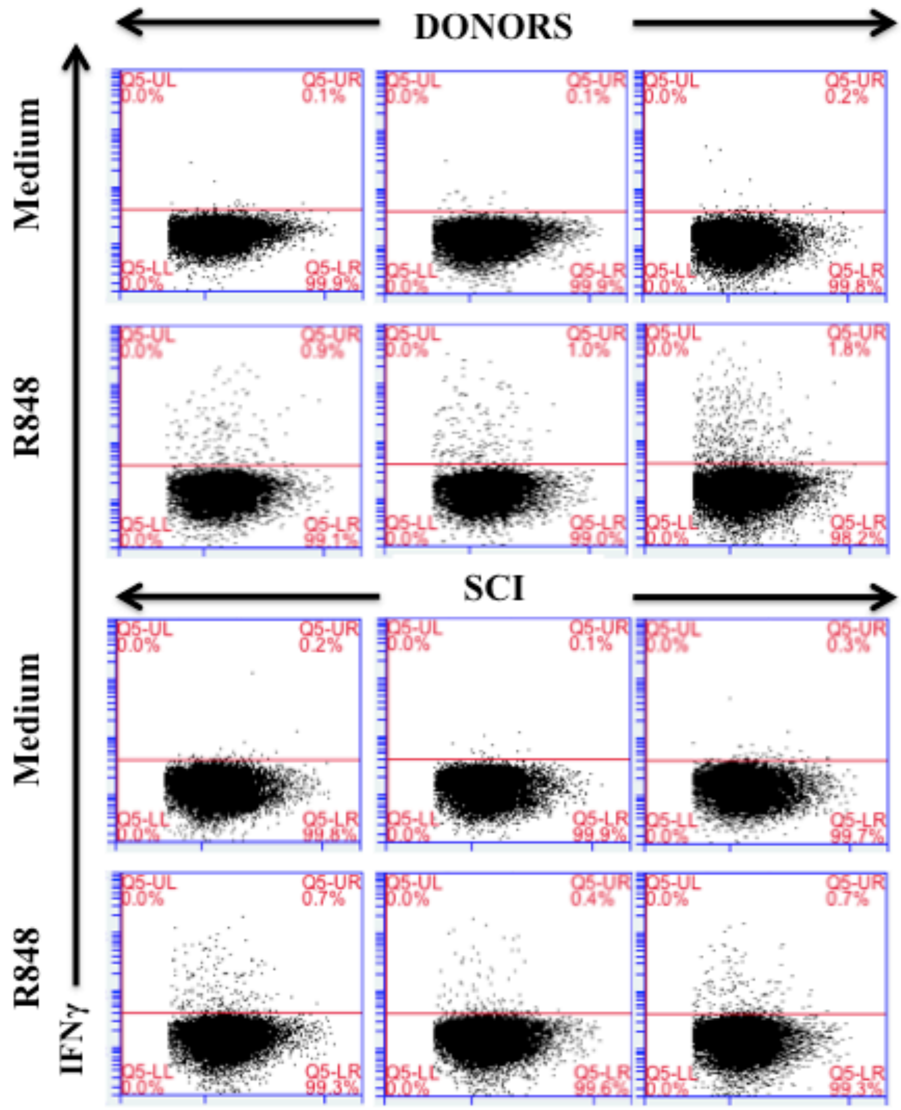

Figure A9. Representative FACS analysis plots of IFNγ producing T-cells.

Healthy donor (upper panels) and SCI patient (lower panels) PBMCs were incubated in either medium only or R848. IFNγ signal was detected from $CD4^+$ positive T cells.

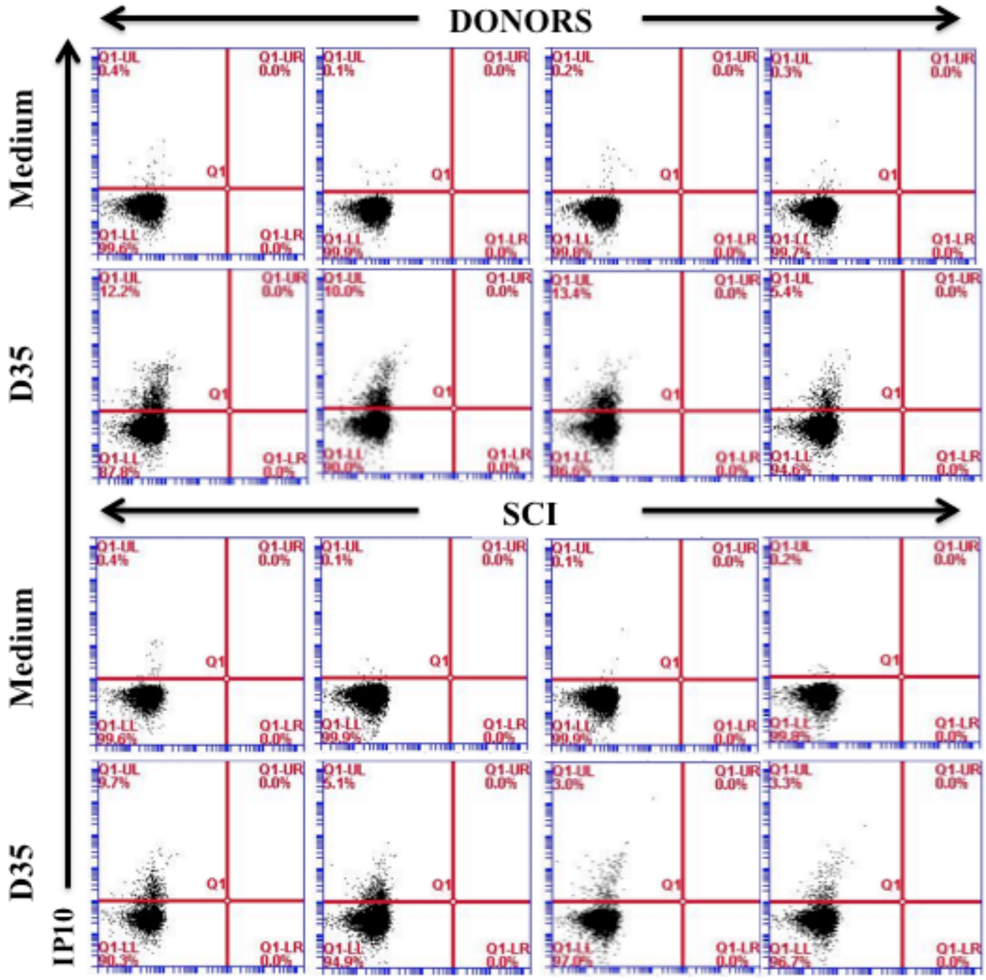

Figure A10. Representative FACS analysis plots of IP10 producing monocytes. Healthy donor (upper panels) and SCI patient (lower panels) PBMCs were incubated in either medium only or D35. IP10 signal was detected from $CD14^{+}$.

Curriculum Vitae and Publications

PERSONAL INFORMATION

Name Surname	Gözde Güçlüler
Date of Birth	01. July. 1987
Nationality	Turkish
Languages spoken	Turkish (Mother tongue) English (Fluent)
Address	ThorLab, Molecular Biology and Genetics, Bilkent University, Ankara, Turkey www.thorlab.bilkent.edu.tr
Phone	Mobile phone: +90-506-361-9232 Work phone: +90 312 290 2396
E-mail	gucluler@bilkent.edu.tr, gozdegucluler@gmail.com

EDUCATION

2010-	**Bilkent University,** Department of Molecular Biology and Genetics, Ankara, Turkey (PhD Degree)
2006-2010	**Izmir Institute of Technology,** Department of Molecular Biology and Genetics, Izmir, Turkey (B.Sc. Degree, 2nd place among Molecular Biology and Genetics Department Students)

PEER REVIEWED PUBLICATIONS

1. T. Kahraman*, **G. Gucluler***, P. Larssen. Gursel, M. Gursel, S. Gabrielsson, I. Gursel, Lyophilization of exosomes results in efficient antigen loading and a functional cancer vaccine (*in preparation for **Nature Communications***) **Equal Contribution*

2. T. Kahraman*, **G. Gucluler***, I. Simsek, F.C. Yagci, M. Yildirim, C. Ozen, A. Dinc, M. Gursel, L. Ikromzoda, T. Sutlu, S. Gay, I. Gursel. Circulating LL37 Targets Plasma Extracellular Vesicles to Immune Cells and Intensifies Behçet's Disease Severity, **Journal of Extracellular Vesicles**, 2017 Feb 6:1, 1284449. **Equal Contribution*

3. G. Gucluler, E. Adiguzel, B. Gungor, T. Kahraman, M. Gursel, B. Yilmaz, I. Gursel. Impaired toll like receptor-7 and 9 induced immune activation in chronic spinal cord injured patients contributes to immune dysfunction. **PloS One**, 2017, 7;12(2):e0171003

4. S. Yalcin, I. Gursel, G. Bilgen, B. H. Horuluoglu, **G. Gucluler,** G.T. Izzetoglu. Effect of egg storage duration and brooding temperatures on chick growth, intestine morphology and nutrient transporters. **Animal**. 2017, DOI: 10.1017/S1751731117000404 (Epub ahead of print)

5. S. Yalcin, I. Gursel, G. Bilgen, G.T. Izzetoglu, B. H. Horuluoglu, **G. Gucluler**. Egg storage duration and hatch window affect gene expression of nutrient transporters and intestine morphological parameters of early hatched broiler chicks. **Animal,** 2016 ,1;10(05):805-11

6- T. Kahraman, **G. Gucluler**, I. Gursel. Exosomes: Natural Nanovesicle Candidates Used in the Diagnosis and Treatment. **Turkish J. Immunol.,** 2014, 2(2): 34-40

7- G. Gucluler, O. Piskin, Y. Baran. The roles of antiapoptotic sphingosine kinase-1 and glucosylceramide genes in drug induced cell death of MCF-7 breast cancer cells. **J BUON**, 2011, 16(4): 646-51

8- G. Gucluler, Y. Baran. Docetaxel Enhances The Cytotoxic Effects Of Imatinib On Philadelphia Positive Human Chronic Myeloid Leukemia Cells. **Hematology**, 2009**,** 14(3): 139-144

ABSTRACT PUBLICATIONS

1. G. Gucluler, T. Kahraman, P. Larssen, M. Eld, M. Yildirim, S. Gabrielsson, I. Gursel

Encapsulation of TLR9 and iNKT cell ligands into exosomes induces immune responses and prevents tumor development. 3rd Molecular Immunology&Immunogenetics Congress, Antalya, Turkey, April 2016 (Oral Presentation)

2- E. Vezir, D. Azkur, **G. Gucluler,** T. Kahraman, E. Civelek, M. Capanoglu, H. Guvenir, I. Gursel, C. N. Kocabaş. Investigation of effects of allergen specific immunotherapy on cytokine profile, exosomes and T lymphocytes, 22. Turkish Congress of Allergy and Clinical Immunology, Belek, Antalya, Turkey, November 2015 (Oral Presentation)

3- G. Gucluler, T. Kahraman, D. Bayik, S. Gabrielsson, I. Gursel. Improved Immunostimulatory Activity of D-Type CpG Oligonucleotides Encapsulated Into Exosomes In Cancer Treatment, KIIM Retreat, Sånga Säby Stockholm, Sweden, October 2015

4- D. Bayik, T. Kahraman, **G. Gucluler**, D. Klinman, I. Gursel. Targeting and sub-cellular localization of cell-derived microparticles to macrophages, ISEV 2015 Annual Meeting, Washington DC, USA, April 2015

5- G. Gucluler, M. Sahin, T. Kahraman, A. Gursel, I. Gursel. Enhanced Immunostimulatory Properties of Extracellular Vesicles Harboring Different TLR Ligands, 2nd Molecular Immunology&Immunogenetics Congress, Antalya, Turkey, April 2014 (Oral Presentation)

6- G. Gucluler, T. Kahraman, D. Bayik, B. H. Horuluoglu, A. Gursel, I. Gursel. CpG ODN Loaded Extracellular Nanovesicles: Enhanced Immunotherapeutic Activity. ILS Liposome Advances Conference, London, United Kingdom, December 2013 (Oral Presentation)

7- G. Gucluler, T. Kahraman, D. Bayik, A. Gursel, M. Gursel, I. Gursel. D type CpG oligonucleotide loaded EG7 exosomes act as strong vaccine adjuvant and anti-cancer agent. 15th International Congress of Immunology, Milan, Italy, August 2013

8- T. Kahraman, **G. Gucluler**, D. Bayik, A, Gursel, I. Gursel. EXOLIGOS: a CpG oligonucleotide loaded exosome nanovesicle delivery platform suitable for effective immune modulation. 15th International Congress of Immunology, Milan, Italy, August 2013

9- S. Yildiz, E. Alpdundar, B. Bayyurt, M. Ozcan, **G. Gucluler**, D. Bayik, B. Gungor, I. Gursel, M. Gursel. Cyclic-di-GMP based immune stimulatory formulations as novel vaccine adjuvants and anti-cancer agents. 15th International Congress of Immunology, Milan, Italy, August 2013

10- E. Alpdundar, S. Yildiz, B. Bayyurt, M. Ozcan, **G. Gucluler**, D. Bayik, B. Gungor, I. Gursel, M. Gursel. Commensal bacteria-derived membrane vesicles suppress Th-1 dominated immune responses in vaccinated and tumor-bearing mice. 15th International Congress of Immunology, Milan, Italy, August 2013
11- G. Gucluler, T. Kahraman, D. Bayik, A. Gursel, M. Gursel, I. Gursel. D type CpG oligonucleotide loaded EG7 exosomes act as strong vaccine adjuvant and anti-cancer agent. 22th Turkish Congress of Immunology, Çesme, Izmir, Turkey, April 2013
12- G. Gucluler, T. Kahraman, I. Gursel. ODN-loaded exosome nanovesicles: A novel anticancer and vaccine delivery platform. Innate Immunity 2012:from Evolution to Revolution, Sorrento, Italy, November 2012
13- F. C. Yagci, **G. Gucluler**, F. Kiran, I. Gursel. Bacteriocin DNA nanocomplexes as immunotherapeutic carriers. 10th Annual Meeting of CIMT, Mainz, Germany, May 2012
14- T. Kahraman, **G. Gucluler**, I. Gursel. A novel ODN delivery platform: CpG-ODN-loaded exosome nanovesicles. 10th Annual Meeting of CIMT, Mainz, Germany, May 2012
15- G. Gucluler, T. Kahraman, I. Gursel. Immunostimulatory activity of CpG-ODN is enhanced via encapsulation into nanovesicles. New Perspective on Immunity to Infection. Heidelberg, Germany, May 2012
16- G. Gucluler, T. Kahraman, I. Gursel. CpG ODN Loaded Exosome Nanovesicles:
Enhanced Immunostımulatory Activity. Molecular Immunology&Immunogenetics Congress, Antalya, Turkey, April 2012
17- T. Kahraman**, G. Gucluler**, E. Alpdundar, M. Gursel, I. Gursel. Encapsulating CpG-ODNs into nanovesicles enhances their immunostimulatory action. BIOMED, Ankara, Turkey, November, 2011
18- T. Kahraman, **G. Gucluler**, M. Gursel, C. Ozen, I. Gursel. Transfer of CpG Oligos to cells via exosome. 21th Turkish Congress of Immunology, Marmaris, Turkey, April, 2011

AWARDS

1. Partial EFIS Fellowship, EFIS, EFIS-EJI Advanced course Metchnikoff's Legacy: Tissue Phagocytes and Functions, Naples, Italy, October, 2016
2. Registration and Accommodation Award, EFIS, 2nd Molecular Immunology&Genetics Congress, Antalya, Turkey, April 2016
3- EFIS-IL Short Term Fellowship, EFIS, Translational Immunology Unit Karolinska Institutet, Stockholm, Sweden, 01 August- 27 October 2015
4- ME-HAD EV Training School Trainee, COST Action BM1202, Siena, Italy, 26 March- 28 March 2014.
5- Registration and Accommodation Award, EFIS, 2nd Molecular Immunology&Genetics Congress, Antalya, Turkey, April 2014
6- The Best Podium Presentation Award, International Liposome Society, ILS Liposome Advances Conference, London, United Kingdom, December 2014
7- Travel Award, Turkish Society of Immunology, 15th International Congress of Immunology, Milan, Italy, August 2013
8- EFIS Travel Award, 15th International Congress of Immunology, Milan, Italy, August 2013

9- Travel Award, Amgen Scholars Alumni Support Scheme, 15th International Congress of Immunology, Milan, Italy, August 2013
10- Registration and Travel Award by EMBO (EMBL Symposium: New Perspectives on Immunity to Infection, Heidelberg, Germany, May 2012
11- Best Poster Award by Turkish Society of Immunology (**G. Gucluler**, T. Kahraman, I. Gursel. CpG ODN Loaded Exosome Nanovesicles: Enhanced Immunostımulatory Activity. Molecular Immunology&Immunogenetics Congress, Antalya, Turkey, April 2012).
12- Registration and accommodation awards by Turkish Society of Immunology. (Molecular Immunology&Immunogenetics Congress, Antalya, Turkey, April 2012).
13- Registration and accommodation awards by Turkish Society of Immunology. (21th National Immunology Congress, Marmaris, Turkey, April 2011).

SCHOLARSHIPS

1- Project bursary, Ministry of Industry and Trade (SANTEZ grant, 1414 STZ.2012-1), "Development of Oligodeoxynucleotide Based Adjuvants for FMD Vaccine Formulation", January 2013-January 2015 (Duration: 24 months)
2- Registration scholarship by the European Federation of Immunological Societies (EFIS). EFIS-EJI Course on Innate Immunity 2012: From Evolution to Revolution, Sorrento, Naples, Italy, October 2012
3- Full scholarship**,** Graduate education, Bilkent University, Molecular Biology and Genetics Department (2010 – …)
4- "Amgen Scholar 2009" Scholarship by AMGEN (Ludwig-Maximilians-Universitat München, Germany, July-September 2009)

CONGRESS, SYMPOSIUM AND WORKSHOP PARTICIPATIONS

1- EFIS-EJI Advanced course Metchnikoff's Legacy: Tissue Phagocytes and Functions, Naples, Italy, 12-14 October, 2016
2- 3rd Molecular Immunology&Immunogenetics Congress, Antalya, Turkey, 27-30 April 2016
3- Turkish Congress of Allergy and Clinical Immunology, Belek, Antalya, Turkey, 28 November- 01. December 2015
4- Karolinska Institutet Inflammation and Immunology Network (KIIM) Retreat 2015, Sånga Säby Stockholm, Sweden, 15-16 October 2015
5- IMTAC Summer School in Immunology, Rastaborg Ljusterö, Stockholm, Sweden, 17-19 August 2015
6- ISEV 2015 Annual Meeting, Washington DC, USA, 23-26 April 2015
7- ME-HAD EV Training School, Siena, Italy, 26-28 March 2015
8- Technology Profiling of R&D Projects Based On Patent Research and Analysis Workshop, Ankara, Turkey, 5-6 February 2015
9- 2nd Molecular Immunology & Immunogenetics Congress, Antalya, Turkey, 27-30 April 2014
10- ILS Liposome Advances Conference, London, United Kingdom, 13-17 December 2013
11- 15th International Congress of Immunology, Milan, Italy, 23-27 August 2013
12- 22th Turkish Congress of Immunology, Cesme, Izmir, Turkey, 27-30 April 2013
13- Course on Innate Immunity 2012: From Evolution to Revolution, Sorrento, Naples, Italy, October 2012

14- 10^{th} Annual meeting of CIMT, Mainz, Germany, 23-25 May 2012
15- New Perspectives on Immunity to Infection, Heidelberg, Germany, 19-22 May 2012
16- Molecular Immunology & Immunogenetics Congress, Antalya, Turkey, 27-29 April 2012
17- 17^{th} International Symposium on Biomedical Science and Technology, Ankara, Turkey, 23–25 November, 2011
18- Advances in Immunology and Cancer Biology Workshop, Istanbul, Turkey, 15–17 April 2011.
19- 21^{st} National Immunology Congress, Marmaris, Turkey, 6–9 April, 2011.
20- Cancer Workshop**,** Ege University, Izmir, Turkey, 8 March, 2010
21- Amgen Scholars European Symposium, University of Cambridge, Cambridge, 16-18 September, 2009

NATIONAL AND INTERNATIONAL PATENTS/PENDINGS

"A Method of Loading D-Type CpG ODNs in Exosome Nanovesicles", in preparation for PCT application.

CERTIFICATES

1- 'Expertise in Patent and Trademark Management Certification Program', 01 October 2015-31 October 2015, University of Sakarya, (Online Education Exam Grade: 78/100)
2. ' Ethical Certificate in Laboratory Animals', 31 August 2011- 13 September 2011, Bilkent University Animal Ethics Committee

SOCIETY MEMBERSHIPS

Turkish Society of Immunology
International Society for Extracellular Vesicles (ISEV)

Journal of Extracellular Vesicles

ISSN: (Print) 2001-3078 (Online) Journal homepage: http://www.tandfonline.com/loi/zjev20

Circulating LL37 targets plasma extracellular vesicles to immune cells and intensifies Behçet's disease severity

Tamer Kahraman, Gozde Gucluler, Ismail Simsek, Fuat Cem Yagci, Muzaffer Yildirim, Can Ozen, Ayhan Dinc, Mayda Gursel, Lolai Ikromzoda, Tolga Sutlu, Stephen Gay & Ihsan Gursel

To cite this article: Tamer Kahraman, Gozde Gucluler, Ismail Simsek, Fuat Cem Yagci, Muzaffer Yildirim, Can Ozen, Ayhan Dinc, Mayda Gursel, Lolai Ikromzoda, Tolga Sutlu, Stephen Gay & Ihsan Gursel (2017) Circulating LL37 targets plasma extracellular vesicles to immune cells and intensifies Behçet's disease severity, Journal of Extracellular Vesicles, 6:1, 1284449

To link to this article: http://dx.doi.org/10.1080/20013078.2017.1284449

Published online: 28 Feb 2017.

JOURNAL OF EXTRACELLULAR VESICLES, 2017
VOL. 6, 1284449
http://dx.doi.org/10.1080/20013078.2017.1284449

Taylor & Francis
Taylor & Francis Group

ORIGINAL RESEARCH ARTICLE

OPEN ACCESS

Circulating LL37 targets plasma extracellular vesicles to immune cells and intensifies Behçet's disease severity

Tamer Kahraman[a*], Gozde Gucluler[a*], Ismail Simsek[b], Fuat Cem Yagci[a], Muzaffer Yildirim[a], Can Ozen[c], Ayhan Dinc[b], Mayda Gursel[d], Lolai Ikromzoda[e], Tolga Sutlu[e], Stephen Gay[f] and Ihsan Gursel[a]

[a]Science Faculty, Department of Molecular Biology and Genetics, Bilkent University, Ankara, Turkey; [b]Division of Rheumatology, Gulhane School of Medicine, Ankara, Turkey; [c]Department of Biotechnology, Middle East Technical University, Ankara, Turkey; [d]Department of Biological Sciences, Middle East Technical University, Ankara, Turkey; [e]Nanotechnology Research and Application Center, Sabanci University, Istanbul, Turkey; [f]Department of Rheumatology, University Hospital Zurich, Zurich, Switzerland

ABSTRACT

Behçet's disease (BD) activity is characterised by sustained, over-exuberant immune activation, yet the underlying mechanisms leading to active BD state are poorly defined. Herein, we show that the human cathelicidin derived antimicrobial peptide LL37 associates with and directs plasma extracellular vesicles (EV) to immune cells, thereby leading to enhanced immune activation aggravating BD pathology. Notably, disease activity was correlated with elevated levels of circulating LL37 and EV plasma concentration. Stimulation of healthy PBMC with active BD patient EVs induced heightened IL1β, IFNα, IL6 and IP10 secretion compared to healthy and inactive BD EVs. Remarkably, when mixed with LL37, healthy plasma-EVs triggered a robust immune activation replicating the pathology inducing properties of BD EVs. The findings of this study could be of clinical interest in the management of BD, implicating LL37/EV association as one of the major contributors of BD pathogenesis.

Abbreviations: BD: Behçet's disease; EV: extracellular vesicle; BB: binding buffer; AnV: annexin V; autologEV: autologous extracellular vesicles; alloEV: allogeneic extracellular vesicles

ARTICLE HISTORY
Received 4 March 2016
Revised 28 November 2016
Accepted 3 December 2016

RESPONSIBLE EDITOR
Edit Buzás, Semmelweis University, Hungary

KEYWORDS
Extracellular vesicles; Behçet's disease; autoimmune; immune activation; LL37; cytokine

Introduction

Behçet's disease (BD) is a complex multi-organ chronic inflammatory condition of unknown etiology wherein the genetic background and environmental factors are thought to be important contributors for disease pathogenesis.[1–5] Recent findings suggest that a predominance of Th1/Th17-type immune polarisations and elevated levels of associated cytokines correlate with disease activity.[6–9] In this context, plasmapheresis has been shown to induce rapid short-term remission suggesting that an unidentified plasma-associated factor could be a trigger of flare-ups.[10] Herein, we hypothesised that one such plasma-related factor contributing to disease activity and severity could be the circulating extracellular vesicles (EV).

EVs are small vesicles (diameter of 30 nm to 1 μm) constitutively released from various cell types and are considered as key players mediating cell-to-cell communication.[11–13] Accumulating evidence suggests that plasma EV levels are altered during disease states.[12] For instance, the number of EVs released from cultured immune cells increases dramatically upon stimulation with TNFα or IL1β. Moreover, several apoptosis inducers contribute to EV secretion.[13–17] In addition, stimulation of RAW 264.7 cells by TLR ligands intensify EV release.[18] EVs have several roles in immune modulation along with stimulation of coagulation, and modulation of vascular functions.[19–25] In general, their cargo is loaded with an array of bioactive molecules capable of regulating target cell behaviour.[23–27] Recent studies revealed that numbers of circulating EVs were elevated in several rheumatologic diseases, such as rheumatoid arthritis, systemic lupus erythematosus, primary Sjögren's syndrome, vasculitis and anti-phospholipid syndrome.[20–31] The implications of elevated EV levels were not fully understood.

Since inflammation, endothelial dysfunction, and thrombotic tendency are collectively regarded as cardinal features of BD, we speculated that the levels and source of EVs along with their cargo might influence the course of BD in terms of disease activity and severity.

In this study, we report that circulating EV numbers correlate with BD severity. Furthermore, we show that

CONTACT Ihsan Gursel ihsangursel@bilkent.edu.tr
*These authors contributed equally.
Supplemental data for this article can be accessed here.

the human cathelicidin group of anti-microbial peptide LL37 associates with EVs, enhancing their internalisation by immune cells, initiating a robust pro-inflammatory cytokine milieu.

Materials and methods

Patients and controls

Consecutive patients, who were regularly examined at the Department of Rheumatology and had an established diagnosis of BD (according to the criteria of the International Study Group for Behçet's Disease [32]), were referred for the study after they had their last clinical evaluation to determine clinical disease status (see Table 1). For this study, plasma of 72 BD patients (active; n = 35, inactive; n = 37) and 22 healthy control individuals were included. Patients having active disease was defined by the presence of two and more clinical characteristics, such as oral ulcers, genital ulcers, papulopustular or pseudo-follicular cutaneous lesions, active vascular disease and active ocular involvement. The patients who had no symptoms related with BD at the time of sampling and receiving steady medication for at least one month were classified as having an inactive disease. All patients were further categorised according to their organ of involvement as (i) mucocutaneous, (ii) ocular, and (iii) vascular. With regard to the classification of those patients with inactive disease, patients' detailed clinical history was investigated with respect to either deep vein thrombosis or arterial aneurysm and evidence for uveitis was sought. Subjects with hypertension, diabetes mellitus, renal disease or a previous history of coronary artery disease or myocardial infarction were excluded. The healthy control group included 22 individuals, matched for age and sex. Baseline characteristics of patients with BD and healthy subjects at inclusion are summarised in Table 1. The study was approved by the Institutional Review Board, and all participants provided their informed consents.

Table 1. Clinical evaluations of the BD patients.

	Healthy (n = 22)	Inactive BD (n = 37)	Active BD (n = 35)
Sex (M)	22	37	35
Age (year, mean ± SD)	22 ± 5	22 ± 5	19 ± 6
Disease duration (year, mean ± SD)	N/A	11 ± 5	8 ± 2
Disease progression			
Mucosa	N/A	9	16
Vein	N/A	12	7
Eye	N/A	16	12
Treatment			
Colchicine	N/A	21	24
Azathioprine	N/A	14	11
Cyclophophamide	N/A	2	0

Collection of platelet poor plasma from PBMCs

Fresh blood samples collected into sodium citrate containing vacutainers were centrifuged at 400g for 10 min; plasma was separated and further centrifuged at 1500g for 10 min to obtain platelet poor plasma (PPP). The PPP was collected and divided into 1.5 ml aliquots, which were snap-frozen in liquid nitrogen and kept at −80°C.

Isolation of EVs by differential centrifugation

EV isolation from PPP was based on the differential centrifugation method.[33] All reagents used throughout the purification were filtered using 0.2 µm filters and then centrifuged at 100,000g for two hours. Briefly, PPPs were thawed centrifuged at 10,000g for 10 min to remove cell debris. One ml of the supernatant was 35× diluted by PBS-citrate buffer (10 mM tri-sodium citrate in Ca^{2+}/Mg^{2+} free PBS, pH = 7.4) and centrifuged at 100,000g for 1 h (XL90 Beckman ultracentrifuge with a SW28 rotor with 6 × 38.5 ml polyallomer tubes, Beckman Instruments, Fullerton, CA, USA). The supernatant was discarded, and the pellet was washed once with PBS-citrate buffer. The pellet (containing EV fraction) was then dissolved in 150 µl of buffer, either 1× PBS or binding buffer (BB) (10× BB was composed of 0.1 M HEPES, 1.4 M NaCl and 25 mM $CaCl_2$, pH = 7.4).

Purification of EVs by sucrose cushion

Purification of EVs using sucrose cushion was performed as described elsewhere.[33] The isolated EV pellet, after the final ultracentrifugation step, was dissolved in 2 ml 1× PBS. The EVs were then added to 30% (w/v) sucrose solution in 15 ml ultracentrifuge UC polyallomer tubes and centrifuged for 2 h at 100,000g. After centrifugation, 3–4 ml of supernatant (including purified EVs) from the top of the sucrose solution was collected and transferred into 38.5 ml UC polyallomer tubes. Up to 35 ml 1× PBS was added onto the solution and centrifuged for 2 h at 100,000g. The EV pellet was collected by using 150 µl 1× PBS for subsequent analysis.

Characterisation of EVs by western blotting

EVs for western blotting was prepared with RIPA lysis buffer and protein concentration was determined using BCA Protein Assay Reagent Kit (Thermo Scientific, Waltham, MA, USA). An amount of 25 µg of protein was loaded and separated by SDS-polyacrylamide gel electrophoresis, transferred to PVDF membrane and probed with 1:1000 diluted primary antibodies against Alix (Cell Signaling, Denver, CO, USA) and Grp94 (Cell

Signaling). Blots were visualised by Amersham Imager 600 (GE, Amersham, UK) after incubating membranes with 1:10,000 diluted HRP linked secondary antibodies as anti-mouse IgG (Cell Signaling) and anti-rabbit IgG (Cell Signaling) for Alix and Grp94 blotting, respectively.

Characterisation of EV markers with bead assay using flow cytometer

In order to characterise exosomal surface antigens by flow cytometer, initially, 10 µl carboxyl modified latex beads (bead diameter: 3.9 µm, Invitrogen, Carlsbad, CA, USA) were incubated with 10 µg LEAF purified anti-human CD63 antibody (Biolegend, San Diego, CA, USA) for 30 min at RT and then rotated overnight at RT after bringing the volume to 500 µl with 1× PBS. Afterwards, latex bead/anti-CD63 complex were blocked with 5% BSA (Roche, Basel, Switzerland) containing 1× PBS for 4 h at RT. Coated and blocked beads were washed twice with 1× PBS by centrifuging at 3000 g for 10 min at RT. The coated beads were stored in 1× PBS containing 0.1% glycine and 0.1% NaN3 (@pH; 7.2) at a final concentration of 3 × 10-^{5} beads µl^{-1} at 4°C until analysis. Then, 1 µg exosomal protein containing intact EVs were incubated with 1 µl of anti-CD63 coated beads in 100 µl FACS Buffer (FB; 1× PBS containing 5% BSA and 0.05% Tween 20) with gentle mixing for 30 min at RT. EV bound beads were centrifuged at 3000×g for 10 min and supernatant was removed. Beads were washed twice with FB. After that exosome/bead complex were incubated with anti-CD9-PE, CD63-PE antibody (Biolegend) or Annexin V-PE (AnV, Becton Dickenson, Franklin Lakes, NJ, USA) in FB or in 1× BB, respectively, for 30 min with gentle mixing at RT. At the end of incubation period, EV/bead complexes were centrifuged, washed twice and analysed by BD Accuri C6 (Becton Dickinson) flow cytometer.

Determination of size distribution of EVs by dynamic light scattering

Hydrated sizes of EVs isolated from healthy donors and BD patient plasmas were 100× diluted with 1× PBS and analysed by dynamic light scatter method on Zetasizer (Nano ZS, Malvern Instruments, Malwern, UK).

Isolation of exosomes from blood plasma with size exclusion chromatography

For isolation of exosomes with size exclusion chromatography (SEC), plasma samples (1–1.5 ml) from Behçet's patients or healthy donors were diluted up to 2 ml with PBS and centrifuged at 10,000g for 20 min to get rid of debris and precipitates. The supernatants were collected, filtered through 0.22 µm filters and subsequently loaded on a HiPrep 16/60 Sephacryl S-400 HR SEC column (GE Healthcare, Uppsala, Sweden) with a 120 ml bed volume connected to an ÄKTA FPLC system (GE Healthcare). The separation was done at a 0.5 ml min^{-1} flow rate using PBS as the eluent while the chromatogram was recorded using absorbance at 280 nm and 2 ml fractions were collected. After separation, the indicated fractions were pooled and concentrated using ultracentrifugation as described above.

Flow cytometer analyses of labelled EVs

For the identification and quantification of EVs, samples were double-stained with AnV (-PE or FITC conjugated, Biolegend) and an antibody against one of the following cell surface markers: PE-CD42a (platelet, BD Pharmingen, Franklin Lakes, NJ, USA), FITC-CD31 (endothelial cells, Biolegend), PE-CD69 (early activated cells, Biolegend) PE-CD105 (epithelial/endothelial cells, Biolegend), PE-CD3 (T-cells, BD Pharmingen) and PE-CD14 (monocytes, BD Pharmingen). Then 25 µl EVs aliquots were incubated with a staining cocktail containing of 5 µl AnV (as instructed in the manufacturers protocol) and 1 µg ml^{-1} of one of the indicated cell surface markers) for 30 min at RT in dark. Following staining, EVs were washed by ultracentrifugation and then dissolved in 500 µl of 1× BB, particles were counted on a FACS Calibur (Becton Dickinson) flow cytometer using a 60 s acquisition time at a "medium-flow" setting and data evaluation was performed using the CellQuest Pro Software (Becton Dickinson) . Of note, in order to gate-out air bubbles, electrical noise and contaminating particles, a very stringent FSC-SSC gating strategy was used as indicated by the "EV-associated particle gate" (Supplementary Figure 2). In addition, to gate out particles >1 µm, latex beads (Sigma LB-11, St. Louis, MO, USA) with 1.1 µm diameter were used to define our EV associated gate. The optimised acquisition settings were controlled weekly. In some experiments, data acquisition was performed on an Accuri C6 Flow cytometer with similar results to those obtained using the FACS Calibur.

Calculation of EV number in one ml plasma

Our initial optimisation studies were performed with standard calibration beads of known concentration (1×10^{7} beads ml^{-1}, Sigma LB-11, 1.1 µm in diameter). We acquired the # of events (@ 1 min) and determined the volume utilised for that run. After verification, we acquired AnV positive EVs and multiplied with the dilution factor to determine the # of EVs ml^{-1} plasma.

Binding and uptake of EVs by PBMCs

Purified EVs were stained with the lipophilic cell tracers of CM-Dil (for confocal studies) and SP-DiOC (for binding and uptake studies) at 1 µM concentration by incubating for 30 min at 37°C and then washed two times in 35 ml PBS and centrifuged at 100,000g for 1 h. As a negative control, 1 µM dye, both for CM-Dil and SP-DiOC, was incubated in the absence of EVs and then washed twice. Following re-suspension in 200 µl of endotoxin-free PBS, labelled EVs were incubated with 2×10^6 ml^{-1} PBMCs at the at 1:2 cell:EV ratio. For binding and uptake studies, cells were incubated with SP-DiOC labelled EVs for various time points and cells were analysed by Accuri C6 flow cytometer. For confocal microscopy studies, cells were incubated on cover slips with CM-Dil labelled EVs for 8 h (at 1:2 cell:EV ratio), washed, fixed and studied using a Zeiss LSM5 (Carl Zeiss, Oberkochen, Germany) confocal microscope.

Human ELISA studies

EVs from active BD, inactive BD and healthy subjects were incubated with healthy PBMCs and autologous PBMCs (1.25×10^6 per ml) for 12 h at a ratio of 1:2 (Cell:EV) in 96-well flat bottom culture plates. In some experiments, healthy EVs were mixed with recombinant LL37 (AnaSpec, Freemont, CA, USA) overnight and incubated with autologous PBMCs ifor 12h. In neutralization studies anti-LL37 mAb (HyCult Biotech, Uden, Netherlands) were incubated with EV treated PBMCs at indicated concentrations. LPS (5 µg ml^{-1}) and PGN (5 µg ml^{-1}) were used as positive controls throughout these assays. Culture supernatants were collected and IL6 production was determined by ELISA.[34] The concentration of LL37 from plasma and EV samples was measured by a human LL37 ELISA kit (HyCult Biotech), according to the manufacturer's protocol.

Intracellular cytokine staining

Healthy EVs with or without LL37 were used to stimulate healthy PBMCs for determining IP10, IL1β and IFNα positive cells. Healthy PBMCs were stimulated with EV or EV/LL37 complex for 6 h and 16 h in the presence of Brefeldin-A (5 µg ml^{-1}, Biolegend, Cat#420601) for IL1β and IP10 analysis, respectively. Of note, Brefeldin-A was added at t = 0 and t = 6th hour of incubation for IL1β and for IP10, respectively. The cells were then fixed with Fix & Perm Medium A (Invitrogen, Cat# GAS001S100). Cells were first stained with CD14-PE (Biolegend, Cat#325606) and then to detect the level of intracellular IL1β or IP10 were stained wither with IL1β-FITC (e-Biosciences, Cat# 12-7018-81) or IP10-Biotin (BD, Cat# 555048) then SA-FITC (Biolegend, Cat# 405202) in the presence of saponin (0.1%).

IFNα secreting cells were analysed with Miltenyi Biotech's (San Diego, CA, USA) IFNα Secretion Assay and Detection Kit (PE-labelled, Miltenyi, Cat# 130-094-161) from PBMCs in accordance with kit instructions. Additionally, in order to identify IFNα secreting pDCs, cells were stained with BDCA-2-FITC (Biolegend, Cat# 354208) and then analysed by BD Accuri C6 flow cytometer.

Statistical analysis

All statistical data analyses were carried out using the Sigma Stat 3.5 (Systat Software Inc., London, UK). In order to assess significance between active BD, inactive BD and healthy groups, one-way ANOVA test was used, while Student's t-test was applied to analyse significance between sub-groups of active BD vs. inactive BD. p-values ≤0.05 were set to be statistically significant.

Results

Characterisation of EVs from blood plasma

We collected EVs following either ultracentrifugation or sucrose cushion and conducted Western blotting analyses. The exosome marker proteins Alix, and Grp94 were detected in EVs purified from plasma (Supplementary Figure 1(a)). Furthermore, via bead-based flow cytometric analysis, we demonstrated that EVs express cardinal markers such as CD9 and CD63 (Supplementary Figure 1(b)). Moreover, isolated EVs were subjected to dynamic light scattering analyses to determine the size distribution. DLS investigation revealed that the size of the purified EVs from healthy or BD patient plasmas following ultracentrifugation or sucrose cushion were in the expected size range (ranging between ~30 and 1000 nm, Supplementary Figure 1(c)).

BD patients have elevated circulating EV numbers

To assess whether plasma EV concentrations correlated with BD severity, EV numbers in plasma of 72 BD patients (active; n = 35, inactive; n = 37) and 22 healthy controls were determined by flow cytometry. Results presented in Figure 1 show that total plasma EV concentrations (number of EV ml^{-1} plasma) were significantly higher in active BD ($3.9 \pm 0.77 \times 10^5$) and inactive BD ($2.05 \pm 0.46 \times 10^5$) compared to healthy plasma EVs ($0.78 \pm 0.25 \times 10^5$, $p < 0.001$, active vs. healthy, and inactive vs. healthy). Total EV numbers in active BD were consistently higher

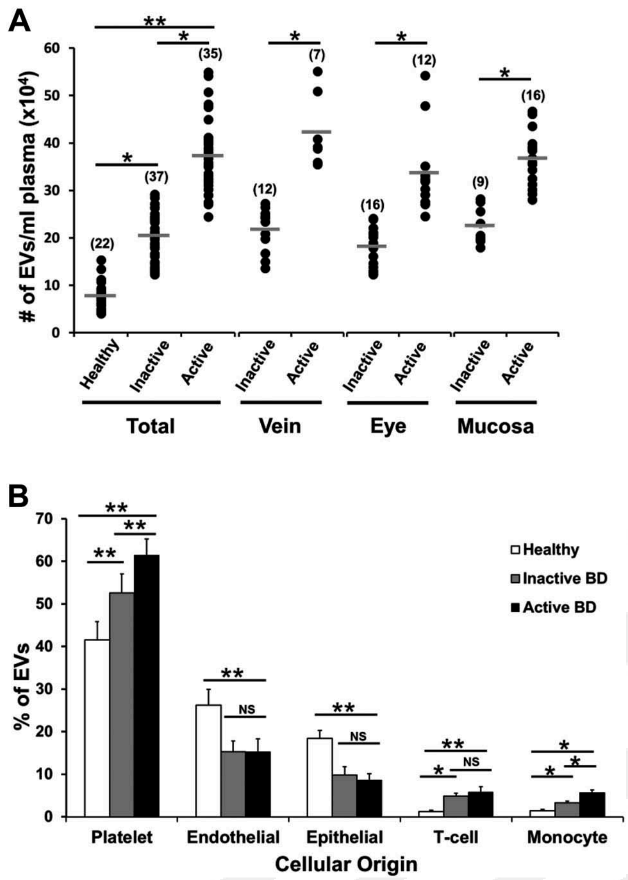

Figure 1. Differential levels and cellular origin of EVs in BD plasma. (a) Plasma EVs were purified and stained with AnV-FITC as described in the Materials and Methods section. Number of EVs per ml plasma was calculated following flow analyses of AnV positive EV signals. Numbers in parentheses represent number of subjects studied. (b) EVs were stained with corresponding cell type specific surface markers as well as AnV. Data are represented as the mean percentage of AnV positive EVs derived from each cell type ± SD for all samples. Individual dot-plots were used to calculate CD3 (T-cells), CD14 (monocytes), CD42a (platelets), CD31 (endothelial cells) and CD105 (epithelial cells) derived EV ratios over total EVs from healthy (n = 22), inactive BD (n = 37) and active BD (n = 35) donors. *$p < 0.01$ and **$p < 0.001$ for comparison groups based on Student's t-test analyses of healthy vs. inactive BD, healthy vs. active BD and inactive BD vs. active BD. NS indicates not significant.

than the inactive BD group ($p < 0.01$) and this increase (1.75–2.2-fold) was valid in all patient sub-groups, suggesting that elevated EV levels was a common feature of active disease and was not dependent on organ involvement (Figure 1(a), $p < 0.01$ for all tested sub-groups).

Platelet derived EVs constitute the majority of circulating EVs in BD plasma

EVs are believed to be secreted from multiple cell types, including platelets, endothelial cells, monocytes, and T cells. However, contribution of each population to the circulating EV pool can vary depending on disease activity. To elucidate whether source of EVs varied with respect to BD severity, isolated particles from healthy (n = 22), inactive (n = 35) and active BD patients (n = 37) were stained with different cell specific markers and their relative ratios were confirmed by flow cytometry. The gating strategy for flow cytometric analysis and representative dot-plots of individual plasma EV staining are detailed in Supplementary Figure 2 and Supplementary Figure 3. Flow cytometric analysis of stained EV populations revealed that platelets were the most common source of EV population in all groups (Figure 1(b)). Platelet-derived EV percentages correlated with disease state and were found to be significantly elevated in BD patients (52.6 ± 4.5% and 65.4 ± 3.8%, inactive and active BD, respectively) when compared to healthy controls (41.5 ± 4.3%, $p < 0.001$ for all comparisons). Similarly, significant increases were found for EVs derived from T cells (Figure 1(b), 1.49 ± 0.36, 4.14 ± 0.77 and 5.25 ± 1.24% for healthy, inactive and active BD, respectively; $p < 0.001$) and monocytes (Figure 1(b), 1.39 ± 0.32, 3.27 ± 0.42 and 5.7 ± 0.56% for healthy, inactive and active BD, respectively; $p < 0.001$). In contrast, endothelial and/or epithelial derived EVs in BD plasma were lower than those observed in healthy controls ($p < 0.001$ for all comparisons).

EVs are internalised by PBMCs triggering IL6 secretion

The underlying reasons for the heightened and sustained immune activation in BD patients remain elusive. We established that circulating EV concentrations are elevated, especially in active BD plasmas. We next attempted to explore the role of heightened EV concentration as a culprit in sustained immune activation in BD patients. To test this possibility, we investigated the EV internalisation using fluorescently labelled extracellular vesicles. For this, lipophilic CM-DiI dye labelled EVs were incubated with healthy PBMCs and their associations were analysed by confocal microscopy (Figure 2(a)). Photomicrographs revealed that BD EVs were effectively associated with immune cells (Figure 2(a)). This association is not mediated by non-specific binding of EVs to PBMCs because there was no cellular staining following incubation of EVs with cells at 4°C. The signal was EV specific as there was no non-specific dye binding to cells upon incubating centrifuged CM-DiI dye pellet with cells (Figure 2(a), middle and lower panels). We next attempted to explore

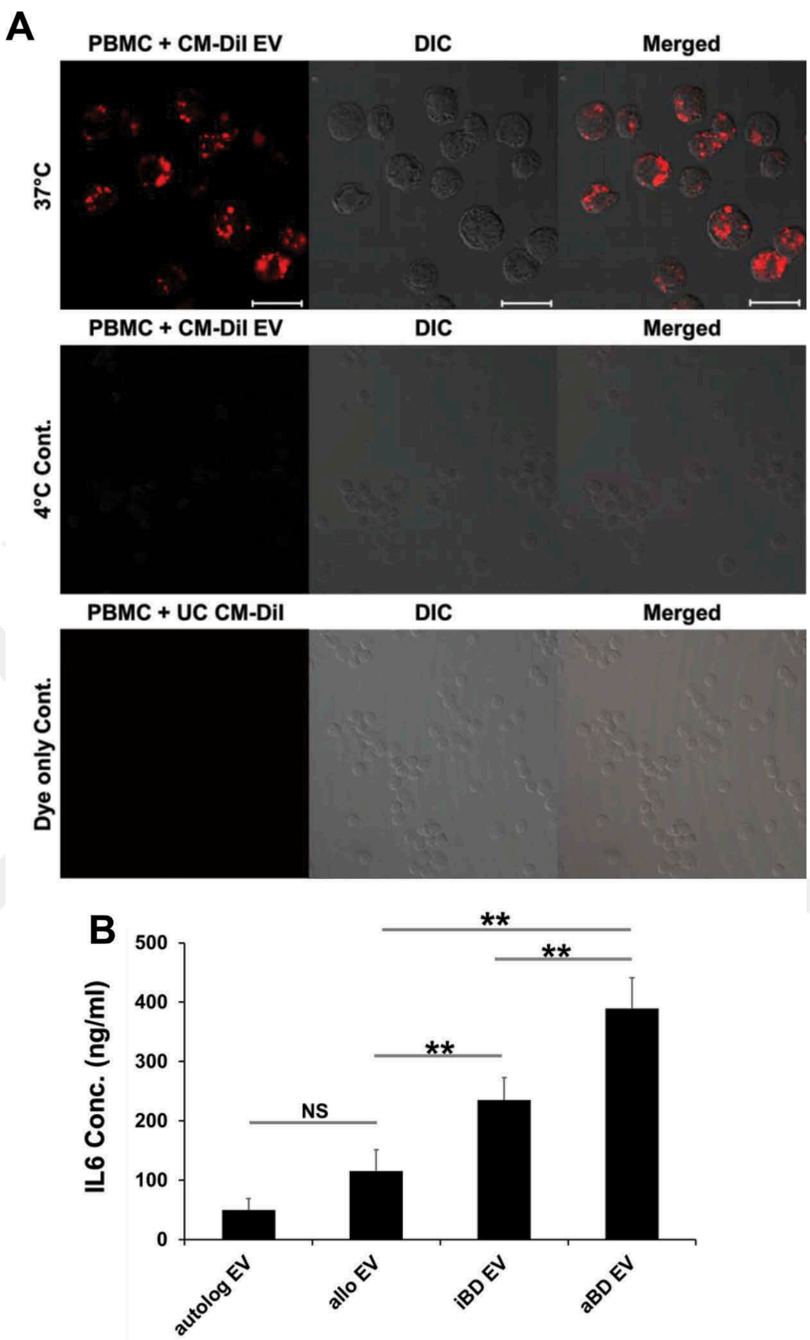

Figure 2. BD EV binding and IL6 secretion by PBMCs. (a) Confocal images showing interaction of EVs following 8 h of incubation with PBMCs. The upper panel shows incubation at 37°C. The middle panel is the interaction of stained EVs with cells at 4°C. The lower panel is the negative control which indicates there is no interaction of the precipitated dye following ultracentrifugation. The left panel represents CM-DiI positive signal; the middle panel represents DIC images of the cells and the right panel shows merged images (scale bar = 20 µm). (b) Healthy PBMCs were incubated with autologous or allogeneic EVs at a cell:EV ratio of 1:2 for 12 h. IL6 production was assessed from the culture supernatants by ELISA. (autolog EV; autologous EVs from healthy donor; allo EV; allogeneic EVs from healthy donor; iBD EV; inactive BD EVs and aBD EV; active BD EVs). n = 12 samples, $^{**}p < 0.001$ for all comparisons.

whether active BD EVs were capable of triggering an immune response. We incubated EVs isolated from healthy, inactive or active BD with healthy PBMCs for 12 h and determined EV-induced cytokine secretion from culture supernatants. Results revealed that autologous and allogeneic healthy plasma-derived EVs triggered lower but detectable levels of IL6 production from healthy PBMC (Figure 2(b), 49.9 ± 19.0 and 116.1 ± 35.4 ng ml^{-1}, respectively). In contrast, inactive and active BD patients' EVs triggered 2-fold and 3.3-

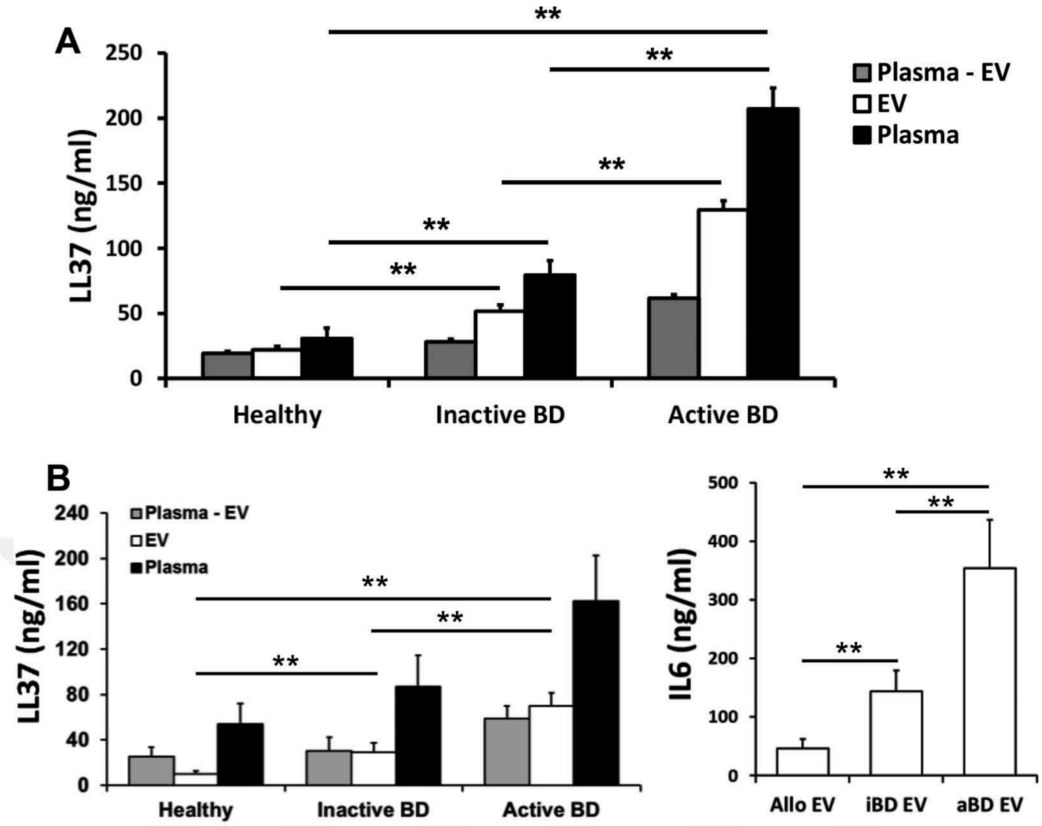

Figure 3. Elevated levels of antimicrobial peptide LL37 are mostly associated with EVs in BD patients. (a) LL37 concentrations (ng ml^{-1}) in EV depleted plasma, EV fraction and in plasma of BD patients and control healthy subjects were assessed by LL37 ELISA kit. (b) LL37 levels of EVs and IL6 induction capacities of EVs (alloEV-healthy EVs; iEV-inactive BD EVs and aEV-active BD EVs) from healthy PBMCs after sucrose cushion purification (n = 12 for all samples and **$p \leq 0.001$ for all comparisons).

fold more IL6 (Figure 2(b), 235.1 ± 38.0 and 384.9 ± 51.3 ng ml^{-1}, respectively) when compared to allogeneic healthy EVs ($p < 0.001$ for all comparisons). These findings demonstrate that EVs can interact with and are internalised by human PBMCs and this interaction leads to a more pronounced IL6 production when EVs were of BD origin.

Active BD patient plasma LL37 levels are elevated and majority of LL37 is associated with EVs

After establishing that circulating EVs are elevated in active BD plasma and are mediating exaggerated cytokine secretion from PBMCs, we embarked on identifying the factor(s) that might contribute to BD EV-associated immune activation. For this, we analysed the plasma levels of LL37, an anti-microbial peptide associated with the pathogenesis of several autoimmune/inflammatory diseases, including psoriasis, systemic lupus erythematosus, rheumatoid arthritis and atherosclerosis.[35] LL37 concentrations were found to be 39 ± 8, 80 ± 11 and 207 ± 16 ng ml^{-1} in healthy, inactive and active BD plasma samples, respectively (Figure 3(a)), representing a 2-fold (inactive) and 5-fold (active) increase.

Considering that LL37 is a cationic peptide and EVs are enriched in negatively charged phospholipids such as phosphatidyl serine [36], we next analysed the possibility of EV/LL37 interaction and determined the levels of LL37 in EV-depleted plasma and in the EV fraction following ultracentrifugation of donor plasmas. Strikingly, ~2/3 of LL37 was found to be associated with EVs in active BD (Figure 3(b)).

To further purify EV preparations, we applied EV pellets (following ultracentrifugation) onto sucrose cushion. From this fraction, LL37 detection by ELISA was performed. As seen in Figure 3(c), LL37 level of EVs isolated from active BD plasma were significantly higher than inactive BD EVs or healthy plasma EVs (9.8 ± 3; 29.1 ± 8.6, and 70.6 ± 11.2 ng ml^{-1} LL37 in healthy, inactive BD and active BD EVs, respectively, n = 12 for each samples, $p < 0.001$). Furthermore, consistent with previous findings provided in Figure 2 (b), active BD EVs induced significantly higher IL6 secretion than inactive BD EVs and healthy EVs (Figure 3(c), right panel, $p < 0.001$). Collectively, these findings implied that EVs are associated with LL37 and are capable of inducing IL6 secretion from healthy PBMCs (Figure 3(c)).

In order to further rule out contribution of unassociated LL37 aggregates to observed immune activation, we additionally subjected plasma from healthy and active BD patients to size exclusion chromatography purification (SEC) (Supplementary Figure 4(a)). The SEC fractions were then analysed for expression of cardinal EV markers via the bead method and each fraction was analysed by flow cytometer (Supplementary Figure 4 (b)). As expected, EV markers such as CD9 and CD63 were highly abundant only in fraction #1 (>2–2.5-fold more marker expression) coinciding only to the EV fraction, compared to other fractions as expected, suggesting the presence of EVs in this fraction (Supplementary Figure 4(b)). Furthermore, LL37 levels of each fraction was analysed by ELISA and found to be significantly higher in the SEC fraction #1, thereby coinciding with the EVs (Supplementary Figure 4(c), SEC Fraction #1: 58.9 ± 7.1; SEC Fraction #2: 5.7 ± 1.9, and SEC Fraction #3: 21.6 ± 2.7 ng ml^{-1}), Lastly, we checked the IL6 induction potential of each SEC fraction. Following incubation of fractions with healthy PBMCs for 12 h in culture, data revealed that significantly higher levels of IL6 was obtained only from cell supernatants that was treated with active BD derived plasma fraction #1 compared to healthy EV fractions. Furthermore, only fraction #1 of active BD plasma induced IL6 secretion compared to fraction #2 and fraction #3 (185.4 ± 30.9 ng ml^{-1}, 28.6 ± 7.5 ng ml^{-1}, and 49.1 ± 14.1 ng ml^{-1}, for SEC Fraction #1, #2, and #3, respectively) (Supplementary Figure 4(d), $p < 0.001$).

LL37 association with EV governs cellular internalisation and cytokine induction

LL37 was previously shown to interact with and enhance delivery of nucleic acids to immune cells.[37] To assess whether a similar mechanism could operate for EVs, SP-DiOC labelled healthy EVs were either used as such or mixed with LL37 peptide (endotoxin free) prior to incubation with healthy donor PBMCs (Figure 4). Binding of EVs was significantly enhanced when PBMCs were incubated with LL37 associated EVs. This enhanced binding was much pronounced when incubation period was extended to 8 h (Figure 4(a) and Supplementary Figure 5, $p < 0.001$, EV vs. EV + LL37 comparison).

Next, to establish whether this enhanced LL37-mediated cellular internalisation had an impact on subsequent cytokine induction, healthy EVs were mixed with increasing concentrations of LL37 or its scrambled-control prior to co-culture with healthy PBMCs. As seen in Figure 4(b), LL37/EV combination induced significantly higher IL6 secretion from PBMCs in a dose dependent manner ($p < 0.001$). This induction was specific to LL37 since the scrambled peptide (SCR/EV) combination did not yield appreciable amounts of IL6 (Figure 4(b)). Although free LL37 also triggered IL6 release at these doses, EV/LL37 combination triggered 2.2–2.3-fold more IL6 than the free peptide at both doses (150 and 450 ng, respectively, Figure 4(b)). To further demonstrate that any contaminating LL37 aggregate together with EVs does not contribute to IL6 production by PBMCs, we conducted an additional experiment using THP1 cell derived EVs. We isolated EVs from THP1 cell supernatants that were devoid of any plasma components and complexed with LL37 as described earlier and incubated with PBMCs. As done previously, IL6 production by PBMCs was assessed by ELISA. As seen in Figure 4(c), EV/LL37 treated PBMCs secreted more IL6, representing a 2.1-fold higher cytokine production compared to cells that were treated with free LL37 (Figure 4(c)). Consistently, scrambled peptide mixed EVs failed to secrete any appreciable levels of IL6. To further prove that indeed LL37 association to EVs regulates cytokine induction by PBMCs, next, we treated cells with EV/LL37 complex in the presence and absence of anti-LL37 antibody and detected IL6 levels from cell supernatants. As seen in Figure 4(d), in a dose-dependent manner anti-LL37 addition onto LL37-EV treated cells significantly abrogated IL6 secretion from PBMCs suggesting that LL37/EVs regulate IL6 secretion from PBMCs (Figure 4(d)). Of important note, IL6 secretion capacity of EVs isolated from inactive and active BD patient plasmas significantly reduced when increasing doses of anti-LL37 antibody was incubated with healthy PBMCs (Supplementary Figure 5(b)).

Active BD EVs triggers IFNa from pDC, IL1β and IP10 from monocytes/macrophages

Our findings implicated that LL37 associated EVs are capable of inducing elevated immune activation. To identify the cell types activated by LL37/EV complexes, healthy donor EVs were mixed with LL37, (mimicking active BD EVs) and subsequently incubated with healthy PBMCs. LL37-free and LL37 associated-EV binding profiles in dendritic cell (DC), macrophage and T-cell populations were assessed with flow cytometer 1 h after co-incubation (Figure 5 and Supplementary Figure 5(a)). Results showed that EV delivery to macrophages, DCs and to a lesser extent to T-cells were significantly enhanced in the presence of LL37 (Figure 5(a)).

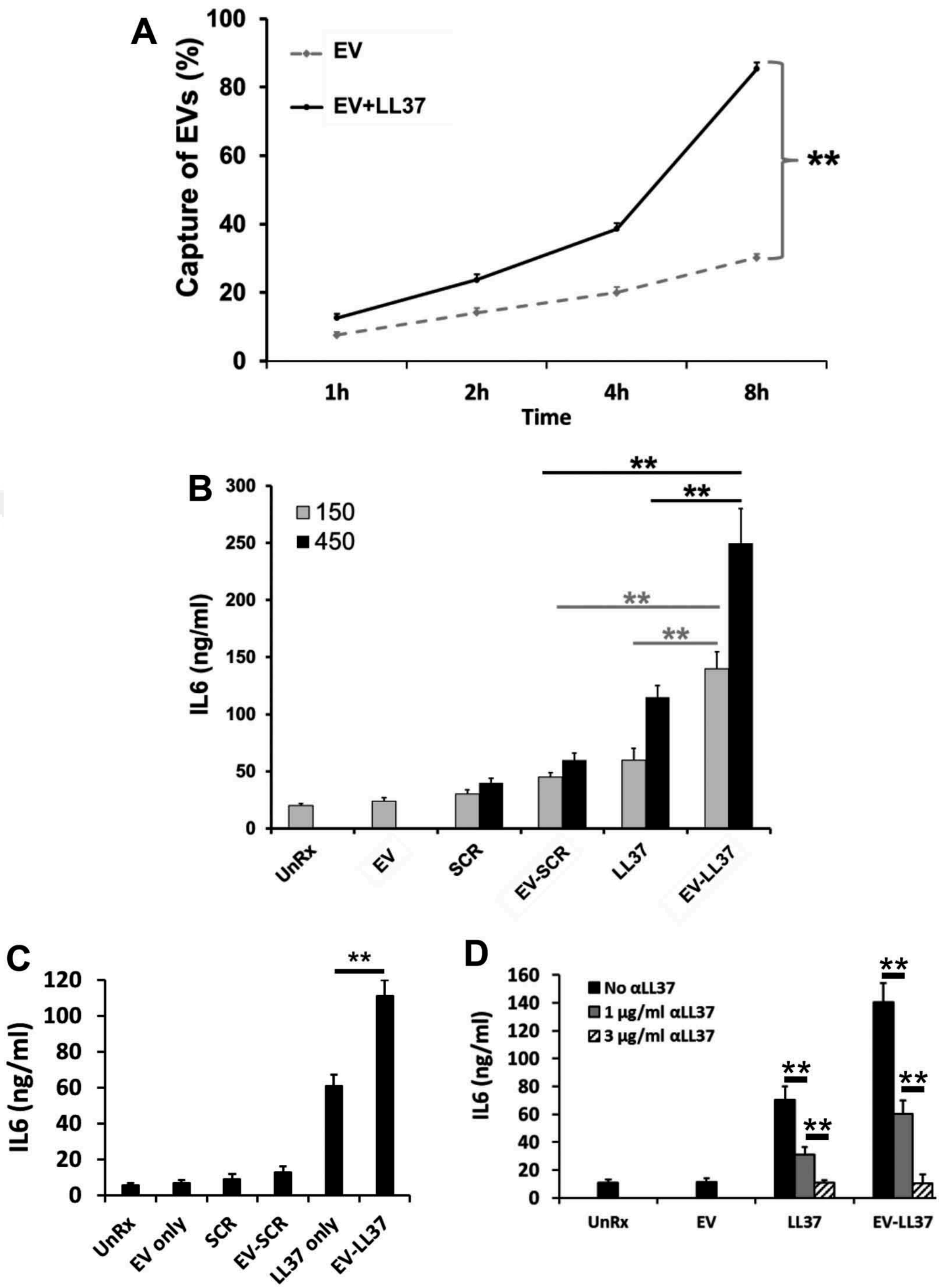

Figure 4. LL37 promotes EVs uptake and IL6 induction by immune cells can be suppressed by LL37 antibody. (a) SP-DiOC labelled healthy EVs or LL37/EV complexes were incubated with healthy PBMCs at 1:2 ratio (cell:EV) for indicated time periods. The line graph shows the kinetic of EVs association by cells in the presence or absence of LL37. (b) EVs isolated from healthy plasma were complexed overnight at 4°C either with 150 ng (grey bars) or with 450 ng (black bars) LL37, and then incubated with healthy PBMCs for 12 h at 1:2 (cell:EV) ratio. IL6 levels were assessed from culture supernatants by ELISA. (c) IL6 induction capacity of EVs isolated from THP-1 cells that is devoid of any plasma contamination. (d) Dose-dependent suppression of LL37/EV mediated IL6 production by PBMCs following treatment with anti-LL37 antibody for 12 h in culture. $^{**}p < 0.001$ for all comparisons.

Next, EV mediated immune activation by blood peripheral cells were investigated. As expected, healthy EVs devoid of LL37 failed to induce any detectable IFNα or IL1β (Figure 5(b), and Supplementary Figure 6). However, LL37/EV complexes induced >2-fold more IL1β, and >20-fold more IFNα production from monocytes and plasmacytoid dendritic cells (pDC), respectively. Similarly, IP10 production from monocytes was

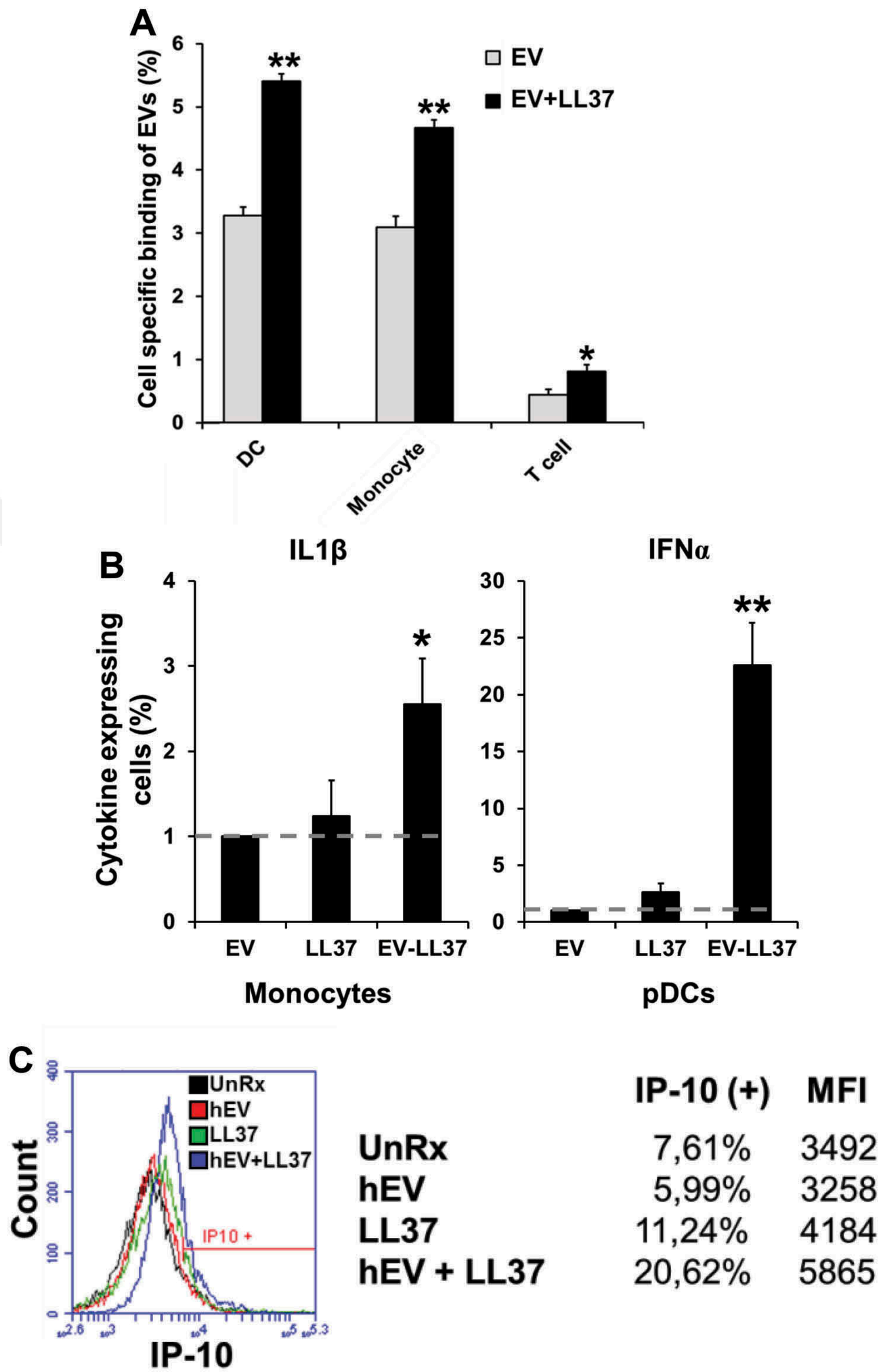

Figure 5. EVs associated with LL37 can be taken up by immune cells and boost IL1β and IP10 from monocytes and IFNα from pDCs. (a) Cell specific binding of LL37-free and LL37-associated EVs. SP-DiOC stained EVs were incubated with PBMCs for 1 h and analysed by flow cytometer following cell-specific surface marker staining. (b) IL1β and IFNα secreting monocytes and pDCs, respectively, were assessed by intracellular cytokine staining technique. (c) Histogram of IP10 secreting monocytes were shown following treatment of cells either with EVs or free LL37 and LL37/EV complex.

elevated only in response to LL37-EV (Figure 5(c), >2-fold more IP10 was secreted). Of note, IFNα, IL1β and IP10 productions from pDC and monocytes were dependent on LL37-EV complex since treatment of cells only with LL37 failed to reproduce similar immune stimulatory activity.

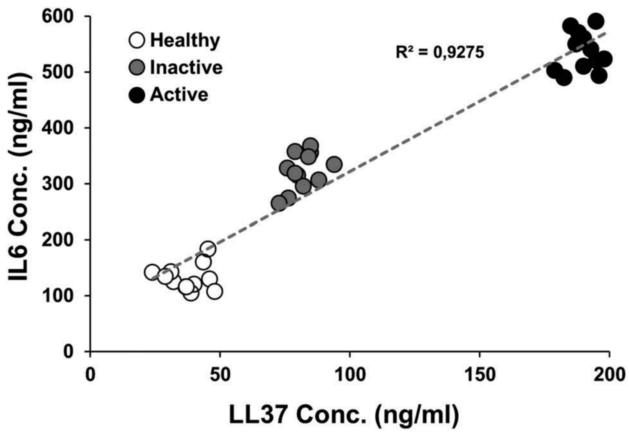

Figure 6. Disease activity strongly correlates with LL37 and IL6 concentrations. Healthy, inactive and active BD patient EVs were analysed for LL37 association levels and subsequent IL6 production by healthy PBMCs. The correlation plot was prepared from these two independent data to determine the correlation coefficient between disease states IL6 secretion and LL37 levels. R^2 = coefficient of correlation (*n* = 12 for all sample plasmas).

When taken together, these findings demonstrated that (i) LL37 levels, (ii) EVs concentration and (iii) pathological cytokine production are well correlated with disease severity (Figure 6, R^2: 0.9275, and Supplementary Figure 7(a) and 7(b)).

Collectively, our findings established that active BD patient plasmas contain elevated numbers of circulating EVs, and majority of LL37 does not co-exist in the EV pellet as a contaminating aggregate but are physically associated with LL37. The EV-LL37 complex drives EVs specifically and efficiently to immune cells, probably inducing robust and sustained immune activation.

Discussion

EVs have recently been implicated as novel extracellular mediators of distant intercellular communication. [11] Since EVs circulate and remain intact in peripheral blood, they are capable of transferring labile cargo to distant targets, thereby altering the physiology of the recipient cells. This study is the first to demonstrate that EVs are elevated in the peripheral blood of BD patients, suggesting their potential involvement in disease pathogenesis.

Several studies demonstrated that EVs not only possess bioactive materials on their surface but also harbour biologically active cargo within their lumen. These include nucleic acids (both RNA and DNA) or proteins, such as cytokines, growth factors and cell or tissue specific antigens. Recently, miRNAs were also reported to be delivered via these structures.[38–40] EVs are considered to have important functions in establishment of homeostasis in health and could play potentially detrimental roles during disease states.[41,42] Data presented herein are in support of these observations and extend our current knowledge of EV-disease associations.

Several concerns could be raised during working with plasma in an EV related study, such as contamination of EVs during the isolation step with several other unrelated proteins or protein aggregates that ultimately overshadow the anticipated results. Importantly, the presence of negatively charged apolipoproteins in EV pellets as a contaminant could facilitate association of cationic plasma LL37 with apolipoproteins. However, according to two studies, this association abrogates LL37 inherent immune related activity.[43,44] Since we purified EVs also on a sucrose cushion, we consider it unlikely that apolipoprotein mediated LL37 complexes contributed to the activities observed by EV-LL37.

Our findings could be of clinical interest for several reasons. First, plasma EV numbers were found to be elevated in BD patients, which correlated with disease severity (higher EV numbers in active BD patients). It is conceivable that a plasma EV number-based stratification of BD could more precisely identify inactive and active disease states and could aid in pharmacological management of this disease.

Second, although LL37 is a cationic anti-microbial peptide generally known to be secreted during pathogenic insult,[45–47] the data presented here demonstrate that plasma LL37 levels are elevated in BD. As in the case of EVs, this information could be of value to follow patient responses to treatment. Of interest, the only published data that investigated a role of LL37 in BD revealed elevated LL37 levels in saliva of BD patients which correlated with the number of monthly oral ulcers.[48] Consistent with this observation, our results also revealed a correlation between LL37 levels and disease severity. Of note, LL37 levels were reported to be higher during sterile inflammation.[49] In addition, this cationic peptide was demonstrated to contribute to IL-1β, IL6, MCP-1 and MCP-3 production.[50] In this context, our results also established a link between elevated LL37 levels and enhanced cytokine production.

Third, to our knowledge this paper is the first to show that LL37 can interact with EVs, enhancing their cellular delivery and immune stimulatory activity. As stated before, EVs are known carriers of self-nucleic acids. It is conceivable that LL37-mediated enhanced EV delivery to immune cells could activate several endosomal and/or cytosolic RNA and DNA-dependent nucleic acid sensors, including TLR7, TLR9, RIG-I, MDA-5, cGAS or AIM-2, leading to production of

BD-associated cytokines (i.e. IL6, IL-1β and IFNα), contributing to disease severity. Supporting this view, it was shown that high levels of LL37 present in psoriatic skin formed complexes with genomic DNA liberated from dying cells, and enhanced DNA delivery to pDCs, triggering a TLR9-mediated interferon alpha response in psoriatic patients.[51]

The anionic charge of EVs provides a surface convenient for complexing with LL37. Our findings imply that LL37-mediated enhanced delivery of circulating EVs to immune cells contributes to sustaining and exacerbating immune activation in active BD. Therefore, targeting this peptide could be of therapeutic value in the management of this complex disease.

Acknowledgements

Dr Gizem Tincer Konig and Deniz C. Kahraman are sincerely acknowledged for their critical reading of the manuscript and feedback during the study.

Disclosure statement

No potential conflict of interest was reported by the authors.

Funding

This work is partially supported by a TUBITAK grant [SBAG: 108S316]. Tamer Kahraman received scholarship from Scientific and Technological Research Council of Turkey [TUBITAK grant number 108S316).

References

[1] Comarmond C, Wechsler B, Bodaghi B, et al. Biotherapies in Behcet's disease. Autoimmun Rev. 2014;13:762–769.
[2] Hatemi G, Merkel PA, Hamuryudan V, et al. Outcome measures used in clinical trials for Behcet syndrome: a systematic review. J Rheumatol. 2014;41:599–612.
[3] Direskeneli H. Autoimmunity vs autoinflammation in Behcet's disease: do we oversimplify a complex disorder? Rheumatology. 2006;45:1461–1465.
[4] Emmi G, Silvestri E, Squatrito D, et al. Behcet's syndrome pathophysiology and potential therapeutic targets. Intern Emerg Med. 2014;9:257–265.
[5] Yazici Y, Yurdakul S, Yazici H. Behcet's syndrome. Curr Rheumatol Rep. 2010;12:429–435.
[6] Hamzaoui K, Hamzaoui A, Guemira F, et al. Cytokine profile in Behcet's disease patients. Relationship with disease activity. Scand J Rheumatol. 2002;31:205–210.
[7] Hatemi G, Yazici Y, Yazici H. Behcet's syndrome. Rheum Dis Clin North Am. 2013;39:245–261.
[8] Melikoglu M, Uysal S, Krueger JG, et al. Characterization of the divergent wound-healing responses occurring in the pathergy reaction and normal healthy volunteers. J Immunol. 2006;177:6415–6421.
[9] Raziuddin S, Al-Dalaan A, Bahabri S, et al. Divergent cytokine production profile in Behcet's disease. Altered Th1/Th2 cell cytokine pattern. J Rheumatol. 1998;25:329–333.
[10] Raizman MB, Foster CS. Plasma exchange in the therapy of Behcet's disease. Graefes Arch Clin Exp Ophthalmol. 1989;227:360–363.
[11] Distler JH, Huber LC, Gay S, et al. Microparticles as mediators of cellular cross-talk in inflammatory disease. Autoimmunity. 2006;39:683–690.
[12] Théry C, Ostrowski M, Segura E. Membrane vesicles as conveyors of immune responses. Nat Rev Immunol. 2009;9:581–593.
[13] Distler JH, Jungel A, Huber LC, et al. The induction of matrix metalloproteinase and cytokine expression in synovial fibroblasts stimulated with immune cell microparticles. Proc Natl Acad Sci U S A. 2005;102:2892–2897.
[14] Barry OP, Praticò D, Savani RC, et al. Modulation of monocyte-endothelial cell interactions by platelet microparticles. J Clin Invest. 1998;102:136–144.
[15] Duval A, Helley D, Capron L, et al. Endothelial dysfunction in systemic lupus patients with low disease activity: evaluation by quantification and characterization of circulating endothelial microparticles, role of anti-endothelial cell antibodies. Rheumatology (Oxford). 2010;49:1049–1055.
[16] Ullal AJ, Pisetsky DS. The release of microparticles by Jurkat leukemia T cells treated with staurosporine and related kinase inhibitors to induce apoptosis. Apoptosis. 2010;15:586–596.
[17] VanWijk MJ, VanBavel E, Sturk A, et al. Microparticles in cardiovascular diseases. Cardiovasc Res. 2003;59:277–287.
[18] Gauley J, Pisetsky DS. The release of microparticles by RAW 264.7 macrophage cells stimulated with TLR ligands. J Leukoc Biol. 2010;87:1115–1123.
[19] Beyer C, Pisetsky DS. The role of microparticles in the pathogenesis of rheumatic diseases. Nat Rev Rheumatol. 2010;6:21–29.
[20] Berckmans RJ, Nieuwland R, Kraan MC, et al. Synovial microparticles from arthritic patients modulate chemokine and cytokine release by synoviocytes. Arthritis Res Ther. 2005;7:R536–R544.
[21] Berckmans RJ, Nieuwland R, Tak PP, et al. Cell-derived microparticles in synovial fluid from inflamed arthritic joints support coagulation exclusively via a factor VII-dependent mechanism. Arthritis Rheum. 2002;46:2857–2866.
[22] Brogan PA, Shah V, Brachet C, et al. Endothelial and platelet microparticles in vasculitis of the young. Arthritis Rheum. 2004;50:927–936.
[23] Brogan PA, Dillon MJ. Endothelial microparticles and the diagnosis of the vasculitides. Intern Med. 2004;43:1115–1119.
[24] Combes V, Simon AC, Grau GE, et al. In vitro generation of endothelial microparticles and possible prothrombotic activity in patients with lupus anticoagulant. J Clin Invest. 1999;104:93–102.
[25] Guiducci S, Distler JH, Jungel A, et al. The relationship between plasma microparticles and disease manifestations in patients with systemic sclerosis. Arthritis Rheum. 2008;58:2845–2853.

[26] Knijff-Dutmer EA, Koerts J, Nieuwland R, et al. Elevated levels of platelet microparticles are associated with disease activity in rheumatoid arthritis. Arthritis Rheum. 2002;46:1498–1503.
[27] Larkin M. Raised endothelial microparticles an early marker for multiple sclerosis? Lancet. 2001;357:1679.
[28] Minagar A, Jy W, Jimenez JJ, et al. Elevated plasma endothelial microparticles in multiple sclerosis. Neurology. 2001;56:1319–1324.
[29] Sellam J, Proulle V, Jungel A, et al. Increased levels of circulating microparticles in primary Sjogren's syndrome, systemic lupus erythematosus and rheumatoid arthritis and relation with disease activity. Arthritis Res Ther. 2009;11:R156.
[30] van Eijk IC, Tushuizen ME, Sturk A, et al. Circulating microparticles remain associated with complement activation despite intensive anti-inflammatory therapy in early rheumatoid arthritis. Ann Rheum Dis. 2010;69:1378–1382.
[31] Dye JR, Ullal AJ, Pisetsky DS. The role of microparticles in the pathogenesis of rheumatoid arthritis and systemic lupus erythematosus. Scand J Immunol. 2013;78:140–148.
[32] Criteria for diagnosis of Behcet's disease. International study group for Behcet's disease. Lancet. 1990;335:1078–1080.
[33] Thery C, Amigorena S, Raposo G, et al. Isolation and characterization of exosomes from cell culture supernatants and biological fluids. Curr Protoc Cell Biol. 2006;Chapter 3:Unit 3 22.
[34] Gursel I, Gursel M, Yamada H, et al. Repetitive elements in mammalian telomeres suppress bacterial DNA-induced immune activation. J Immunol. 2003;171:1393–1400.
[35] Kahlenberg JM, Kaplan MJ. Little peptide, big effects: the role of LL-37 in inflammation and autoimmune disease. J Immunol. 2013;191:4895–4901.
[36] Lynch SF, Ludlam CA. Plasma microparticles and vascular disorders. Br J Haematol. 2007;137:36–48.
[37] Hurtado P, Peh CA. LL-37 promotes rapid sensing of CpG oligodeoxynucleotides by B lymphocytes and plasmacytoid dendritic cells. J Immunol. 2010;184:1425–1435.
[38] Cocucci E, Racchetti G, Meldolesi J. Shedding microvesicles: artefacts no more. Trends Cell Biol. 2009;19:43–51.
[39] Hunter MP, Ismail N, Zhang X, et al. Detection of microRNA expression in human peripheral blood microvesicles. PLoS One. 2008;3:e3694.
[40] Reich CF 3rd, Pisetsky DS. The content of DNA and RNA in microparticles released by Jurkat and HL-60 cells undergoing in vitro apoptosis. Exp Cell Res. 2009;315:760–768.
[41] Hugel B, Martínez MC, Kunzelmann C, et al. Membrane microparticles: two sides of the coin. Physiology (Bethesda). 2005;20:22–27.
[42] Yáñez-Mó M, Siljander PR, Andreu Z, et al. Biological properties of extracellular vesicles and their physiological functions. J Extracell Vesicles. 2015;4:27066.
[43] Wang YQ, Johansson J, Agerberth B, et al. The antimicrobial peptide LL-37 binds to the human plasma protein apolipoprotein A-I. Rapid Commun Mass Spectrom. 2004;18:588–589.
[44] Wang Y, Agerberth B, Löthgren A, et al. Apolipoprotein A-I binds and inhibits the human antibacterial/cytotoxic peptide LL-37. J Biol Chem. 1998;273:33115–33118.
[45] Dean SN, Bishop BM, van Hoek ML. Susceptibility of Pseudomonas aeruginosa biofilm to alpha-helical peptides: D-enantiomer of LL-37. Front Microbiol. 2011;2:128.
[46] Wong JH, Ng TB, Legowska A, et al. Antifungal action of human cathelicidin fragment (LL13-37) on Candida albicans. Peptides. 2011;32:1996–2002.
[47] Barlow PG, Svoboda P, Mackellar A, et al. Antiviral activity and increased host defense against influenza infection elicited by the human cathelicidin LL-37. PLoS One. 2011;6:e25333.
[48] Mumcu G, Cimilli H, Karacayli U, et al. Salivary levels of antimicrobial peptides Hnp 1-3, Ll-37 and S100 in Behcet's disease. Arch Oral Biol. 2012;57:642–646.
[49] Vandamme D, Landuyt B, Luyten W, et al. A comprehensive summary of LL-37, the factotum human cathelicidin peptide. Cell Immunol. 2012;280:22–35.
[50] Yu J, Mookherjee N, Wee K, et al. Host defense peptide LL-37, in synergy with inflammatory mediator IL-1beta, augments immune responses by multiple pathways. J Immunol. 2007;179:7684–7691.
[51] Lande R, Gregorio J, Facchinetti V, et al. Plasmacytoid dendritic cells sense self-DNA coupled with antimicrobial peptide. Nature. 2007;449:564–569.

PLOS ONE

RESEARCH ARTICLE

Impaired toll like receptor-7 and 9 induced immune activation in chronic spinal cord injured patients contributes to immune dysfunction

Gozde Gucluler[1☯], Emre Adiguzel[2☯], Bilgi Gungor[3], Tamer Kahraman[1], Mayda Gursel[3], Bilge Yilmaz[2,4]*, Ihsan Gursel[1]*

1 THORLAB, Department of Molecular Biology and Genetics, Bilkent University, Ankara, Turkey, **2** Gaziler Physical Medicine and Rehabilitation Education and Research Hospital, Ankara, Turkey, **3** Department of Molecular Biology and Genetics, Middle East Technical University, Ankara, Turkey, **4** University of Health Sciences, Gulhane Medical School, Department of Physical Medicine and Rehabilitation, Gaziler Physical Medicine and Rehabilitation Education and Research Hospital, Ankara, Turkey

☯ These authors contributed equally to this work.
* ihsangursel@bilkent.edu.tr(IG); biyilmaz@gata.edu.tr, bilgeyilmaztr@hotmail.com (BY)

Abstract

Reduced immune activation or immunosuppression is seen in patients withneurological diseases. Urinary and respiratory infections mainly manifested as septicemia and pneumonia are the most frequent complications following spinal cord injuries and they account for the majority of deaths. The underlying reason of these losses is believed to arise due to impaired immune responses to pathogens. Here, we hypothesized that susceptibility to infections of chronic spinal cord injured (SCI) patients might be due to impairment in recognition of pathogen associated molecular patterns and subsequently declining innate and adaptive immune responses that lead to immune dysfunction. We tested our hypothesis on healthy and chronic SCI patients with a level of injury above T-6. Donor PBMCs were isolated and stimulated with different toll like receptor ligands and T-cell inducers aiming to investigate whether chronic SCI patients display differential immune activation to multiple innate and adaptive immune cell stimulants. We demonstrate that SCI patients' B-cell and plasmacytoid dendritic cells retain their functionality in response to TLR7 and TLR9 ligand stimulation as they secreted similar levels of IL6 and IFNα. The immune dysfunction is not probably due to impaired T-cell function, since neither $CD4^+$ T-cell dependent IFNγ producing cell number nor IL10 producing regulatory T-cells resulted different outcomes in response to PMA-Ionomycin and PHA-LPS stimulation, respectively. We showed that TLR7 dependent IFNγ and IP10 levels and TLR9 mediated APC function reduced substantially in SCI patients compared to healthy subjects. More importantly, IP10 producing monocytes were significantly fewer compared to healthy subjects in response to TLR7 and TLR9 stimulation of SCI PBMCs. When taken together this work implicated that these defects could contribute to persistent complications due to increased susceptibility to infections of chronic SCI patients.

OPEN ACCESS

Citation: Gucluler G, Adiguzel E, Gungor B, Kahraman T, Gursel M, Yilmaz B, et al. (2017) Impaired toll like receptor-7 and 9 induced immune activation in chronic spinal cord injured patients contributes to immune dysfunction. PLoS ONE 12 (2): e0171003. doi:10.1371/journal.pone.0171003

Editor: Michael G. Fehlings, University of Toronto, CANADA

Received: September 2, 2016

Accepted: January 13, 2017

Published: February 7, 2017

Data Availability Statement: All relevant data are within the paper and its Supporting Information files.

Funding: This study is partly supported by Bilkent University account to IG. The funders had no role in study design, data collection and analysis, decision to publish, or preparation of the manuscript.

Competing Interests: The authors have declared that no competing interests exist.

Introduction

Infectious complications, predominantly septicemia and pneumonia are the most common causes of death in the years following spinal cord injury (SCI) [1,2]. Urinary and respiratory infections are the most abundant problems of re-hospitalizations of these patients. Therefore, it is likely that there is an increased susceptibility to infections in patients with chronic SCI due to impaired sensing of pathogen associated molecular patterns (PAMPs) of the microbial world [3].

This increased susceptibility to infections following SCI has prompted the researchers to consider the reasons leading to reduced immune response in this patient group. Indeed, studies revealed that there are several abnormalities in immune system that might increase the rate and severity of infections in patients with SCI. Natural killer cell counts and cytotoxicity levels were found to be decreased [4], whereas there were contradictory reports about the relationship between the level of injury and immune dysfunction [5,6].

When the possible contribution of the level of injury to immune dysfunction is taken into account, possible effect of another important factor-autonomic nervous system dysfunction-has to be kept in mind. Although there was some effort to clarify this issue, it is still unresolved [7].

In most of the central nervous system diseases (i.e. multiple sclerosis, Alzheimer's disease, stroke, and HIV encephalitis), notable activation of innate immunity occurs [8, 9]. In SCI, strikingly beside activation of innate immunity, an immune impairment is also present. Increased levels of circulating pro-inflammatory cytokines and autoantibodies have been reported which supports these immune changes [10, 11, 12]. Despite elevated inflammatory processes, patients with chronic SCI frequently show a state of immune suppression and a susceptibility to infections [13, 14].

Accordingly, we aimed to define the role of nucleic acid sensors triggering innate immune response from SCI PBMC in this cross-sectional study. We found that SCI patients with level of injury above T-6 displayed impaired TLR7 and TLR9 mediated immune activation.

Materials and methods

Patients and controls

Subjects were recruited from spinal cord injury rehabilitation unit of a national rehabilitation center and healthy controls were included from the same hospital employee. Patients inclusion criteria were as follows: 1) neurologically complete spinal cord injury (AIS A, as defined by the American Spinal Injury Association, Atlanta, GA, USA) occurring 6 or more months prior to the study [15], 2) level of injury above T-6, 3) 18 years of age or older. Exclusion criteria were fever in 7 days preceding study procedures; current pressure ulcers; having vaccine therapy in the last three months; use of substances that may influence the immune system such as corticosteroids, alcohol and chemotherapies in the last nine months. All patients have received corticosteroid treatment in acute injury for anti-edema purpose when they were first admitted to the hospital. To these patients, administration of methylprednisolone was done according to the NASCIS 2 protocol. All patients underwent a general examination and a full American Spinal Injury Association (ASIA) examination were conducted before they were included the study. Written informed consent was obtained from each participant and the study protocol was approved by Keçiören Training and Research Hospital Ethical Committee with the decision number 249 on 13.03.2013. Venous blood samples were drawn under non-fasting conditions between 7:00–8:00 am from all subjects. Laboratory personnel were blinded to the case-control identification.

PBMC isolation

Blood samples were transferred to 15ml falcon tubes containing lymphocyte separation medium (Lonza, 17-829F) and immediately centrifuged at 1500 RPM for 30 minutes with the break off. At the end of the centrifuge, three layers were obtained. The lymphocyte fraction was gently transferred into new tubes and washed twice with fresh media (1500 RPM for 10 min). The supernatant was discarded and the cells were adjusted to 1x10^6/ml before further analysis.

Treatment of cells with stimulants

Isolated PBMCs were seeded (2x10^5/well/200μl) in 96-well plate and incubated with i) R848 (5μg/ml, Enzo), ii) D-type CpG ODN (3μM, ID: D35 sequence, Alpha DNA, `5′ggTGCATCG ATGCAGGGGgg-3′`, lower letters represents phosphodiester linkages, capital letters phosphorothioate linkages, hereafter D35), iii) PHA (5μg/ml, Roche) and iv) LPS (1μg/ml, Sigma) for 24 hours for cytokine ELISA studies. The cell supernatants were analyzed for human IL6, IL10, IFNα, IFNγ and IP10 production.

For human IFNγ and IP10 intracellular cytokine studies by flow cytometry (BD Accuri C6 Flow Cytometry, Becton Dickenson), 10^6/ml PBMCs were incubated with R848 (5μg/ml)or D35 (3μM) for 12 hours. Then, Brefeldin A (10μl/ml, Sigma) was added onto each sample and the cells were further incubated for eight hours.

To assess T-cell function via IFNγ intracellular staining in response to PMA-Ionomycin, 10^6/ml PBMCs were incubated with PMA (10ng/ml, Sigma), Ionomycin (0,5μM, Sigma) and Brefeldin A (10μg/ml) for 6 hours in 1ml media. Then, the cells were collected for intracellular cytokine staining analysis by FACS.

ELISA studies

2HB 96-well plates (ThermoFisher Scientific) were coated with Abs specific for human IL6, IL10, IFNα, IFNγ and IP10 for 4 h at RT or o/n at 4˚C. In S1A Table, specificities and concentrations of each antibody used for ELISA analyses were listed. The plates were blocked with 1x PBS-5% BSA for 2h at RT, washed 5x with 1x PBS-0.025% Tween 20 and then cell supernatants were layered onto the wells, recombinant standard proteins (S1B Table) in duplicates were plated via serial dilutions (1/2x dilution, 11 series). Following incubation at 4˚C o/n, plates were washed and biotin-labeled anti-cytokine Abs (S1A Table) were added and incubated for 2h at RT. Streptavidin-Alkaline Phosphatase (1:1000x diluted, ThermoFisher Scientific) was added after washing the plates. Following incubation 1h at RT and washing, ELISA plates were developed with the addition of Phosphatase substrate (1:5000x, ThermoFisher Scientific). Optical density values for samples and standard cytokines were detected on a Spectramax ELISA reader (Molecular Devices) at 405nm.

Intracellular cytokine staining studies

For IFNγ and IP10 intracellular cytokine staining studies, cells were incubated with the respective ligands as indicated above. Following centrifugation, supernatants were discarded and cell pellets were resuspended in fixation medium A (100μl, ThermoFisher Scientific) and incubated in dark at RT for 15 mins. PBS-BSA-Sodium azide buffer (2 ml) was added into each tube and then washed twice. At the end of the second washing step, permeabilization medium B (50μl, ThermoFisher Scientific) containing anti-IFNγ-FITC and anti-CD4-PE cocktail were added onto cells. For IP10 staining, anti-CD14-FITC and anti-IP10-PE (S1A Table) were added and the samples were incubated in dark for 30 mins. Cells were washed twice, resuspended in 500μl

PBS-BSA-Sodium azide buffer, transferred to FACS tubes and analyzed in BD Accuri 6 Flow Cytometry.

CD83/HLA-DR studies

Healthy and SCI PBMCs (10^6 /ml) were treated with R848 (5μg/ml) or D35 (3μM) in 1ml final volume of media for 24h. Cells were fixed and washed as described above and stained with anti-CD83-PE and anti-HLA-DR- FITC Ab. Cells were washed twice, resuspended in 500μl PBS-BSA-Sodium azide, and analyzed in BD Accuri 6 Flow Cytometry.

Statistical analysis

Statistical analysis was performed using GraphPad Software (GraphPad Inc.). All continuous variables were presented as mean and standard deviation. Categorical data was presented using number and percent. Mann-Whitney U test was used for comparison of between group results and two-way ANOVA with Bonferroni's correction was used for comparison of within-group results. Categorical variables were compared with the X2 test. $p<0.05$ was considered to be significant.

Results

Seventeen patients with SCI and thirteen healthy controls were included in the study. Age and sex distributions of patients and healthy participants and etiologies of the injuries are shown in Table 1 and S1 Fig. There was no statistically significant difference in age and sex distribution between the SCI group and the healthy controls (Mann-Whitney U test, p = 0.16, Chi-square test, p = 0.98, respectively). All patients were complete (AIS A) spinal cord injured individuals. Complete blood counts of the SCI and healthy control group were shown in Table 2. There was no statistical significance between blood counts of the groups (p>0.05, Mann-Whitney U test).

Cytokine ELISA results revealed that SCI patients'B cells and pDCs compared to healthy control cells had no significant difference in response to R848 (TLR7 ligand, 5μg/ml) and D35 (TLR9 ligand, 3μM) stimulation, since they induced similar levels of IL6 and IFNα (Fig 1A and 1B, respectively). Moreover, the ability of $CD4^+$ T-cells to secrete immunomodulatory cytokine IL10 in response to PHA+LPS implicated that SCI patients does not have any Treg dependent dysregulation compared to healthy PBMCs (Fig 1C), indicating that the cell sources

Table 1. Baseline characteristics of the patients and control group.

	SCI Patients (n = 17)	Healthy Controls (n = 13)	p
Age (median, (min-max))	37.0 (21.0–45.0)	29.0 (24.0–49.0)	0,14*
Sex (%male; %female)	82.4; 17.6	53.8; 46.2	0,09**
Months from injury (median, (min-max))	72.0 (10.0–288.0)	NA	
Etiology (%)			
Motor vehicle collisions	47.0	NA	
Fall from an elevated height	29.4	NA	
Gunshot wound	11.8	NA	
Diving into shallow water	11.8	NA	

Abbreviation: NA, not applicable

* Mann-Whitney U test

**Chi-square test

doi:10.1371/journal.pone.0171003.t001

Table 2. Hematological characteristics of the patients and the control group.

Blood variable	SCI patients	Healthy control	p
Haemoglobin (g/dl)	12.9±1.2	14.1±1.4	>0.05*
Erythrocytes (X10^6/μL)	4.5±0.4	4.8±0.3	>0.05*
Trombocytes (X10^3/μL)	255.8±43.7	269.8±79.5	>0.05*
Leukocytes (X10^3/μL)	6.3±1.1	6.9±2.3	>0.05*
Leukocytes subsets (X10^3/μL)			
Lymphocytes	2.4±0.6	2.4±0.9	>0.05*
Neutrophils	3.2±0.8	3.6±1.4	>0.05*
Eosinophils	0.2±0.1	0.2±0.1	>0.05*
Monocytes	0.5±0.1	0.5±0.1	>0.05*

* Mann-Whitney U test

doi:10.1371/journal.pone.0171003.t002

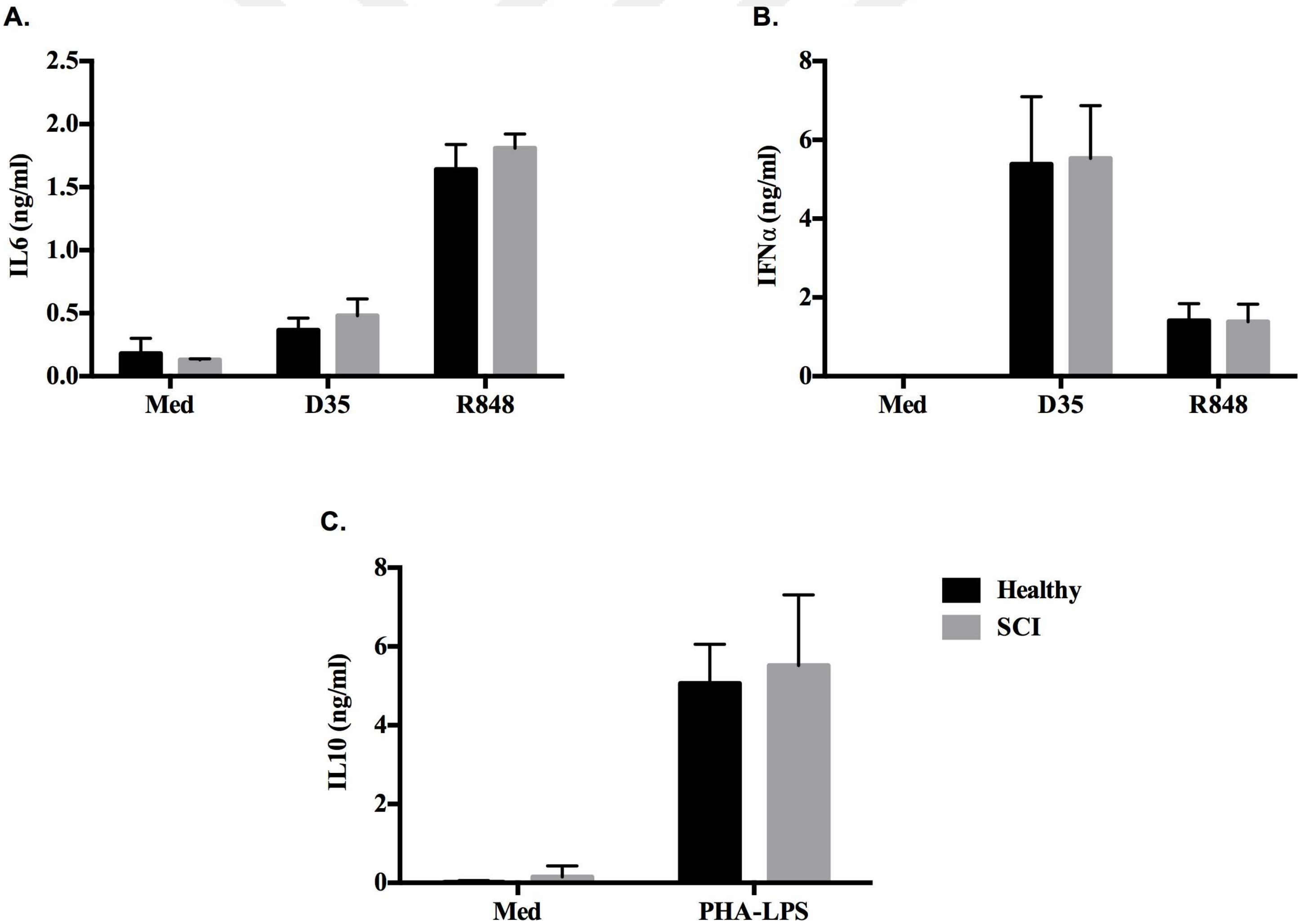

Fig 1. Healthy and SCI donor PBMCs respond similarly to different immune cell stimulants. PBMCs (2x10^5/200μl/well) were incubated with different immune stimulants for 24h. (A) IL6 and (B) IFNα secretion in response to R848 (5μg/ml) and D35 (3μM), (**C**) IL10 production in response to PHA-LPS (5μg/ml-1μg/ml).

doi:10.1371/journal.pone.0171003.g001

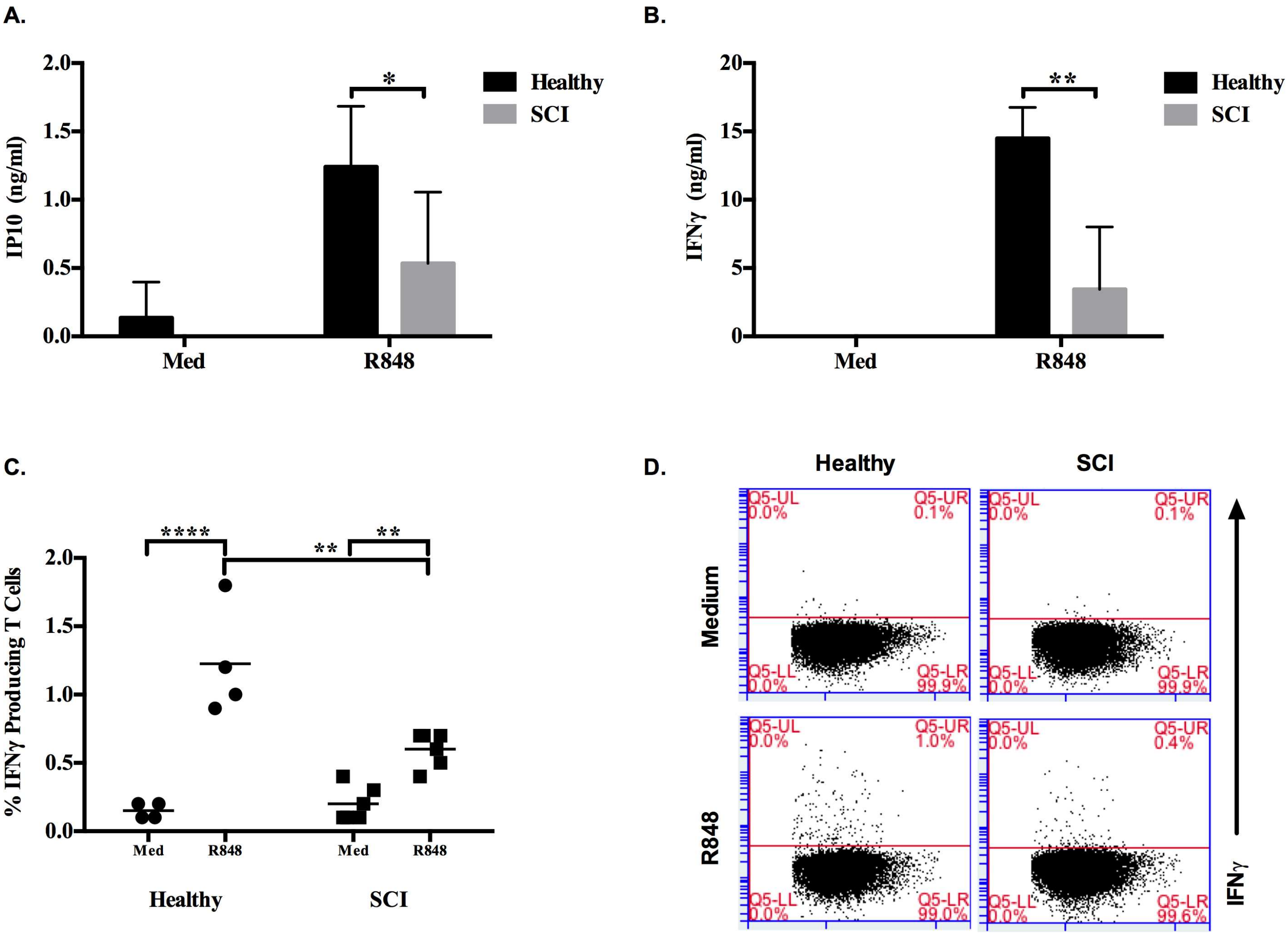

Fig 2. Healthy and SCI individuals show discrepant IFNγ production in response to TLR7 ligand stimulation. PBMCs ($2x10^5$/200µl/well) were incubated with R848 (5µg/ml) for 24h. (A) IP10 and (B) IFNγ secretion levels as assessed by ELISA from healthy (n = 5) and SCI (n = 10) donors. PBMCs (10^6/ml) were stimulated with R848 (5µg/ml) for 20h, at 12h Brefeldin A (10µl/ml) was added. (C) Intracellular IFNγ levels of healthy (n = 4) and SCI (n = 6) donors, (D) Representative dot plots demonstrating IFNγ+/CD4$^+$ T cells. During analyses 50000 cells were acquired. Mann-Whitney test was used to identify significance between healthy and SCI responses to R848. Two-way ANOVA with Bonferroni Correction was used to test the significance of R848 responses compared to medium alone group (*, p≤0.05; **, p≤0.01; ****, p≤0.0001).

doi:10.1371/journal.pone.0171003.g002

of suspected immune dysfunction is not mainly due to impaired B cell, pDC or altered CD4$^+$ Treg activity (Fig 1).

When IP10 secretion levels between healthy and SCI PBMCs in response to R848 were compared, there was 2.3 fold less IP10 production from SCI PBMCs (Fig 2A). Strikingly, secreted IFNγ was 4.2 fold less from SCI patients compared to healthy control groups (Fig 2B). Moreover, this downtrend was confirmed at cellular level by intracellular cytokine staining as healthy controls had significantly higher IFNγ producing T cells then SCI patients in response to TLR7 ligand stimulation (Fig 2C and 2D, S2 Fig).

Off note, the APC function of 4 SCI and 4 healthy PBMCs were analyzed in response to R848 and D35 (Fig 3). Only TLR9 ligand D35 stimulation resulted significantly higher CD83 +/HLA-DR+ cells both in healthy and SCI PBMCs. There were less CD83/HLA-DR double positive cells % in response to TLR7 and 9 triggering in SCI compared to healthy PBMCs (Fig 3A and 3B, S3 Fig).

Next, function of T cells was evaluated at cellular level by treating PMBCs from 3 healthy and 4 SCI donors with PMA-Ionomycin in the presence of Brefeldin-A. FACS analysis revealed that both healthy and SCI PBMCs had significantly increased number of IFNγ

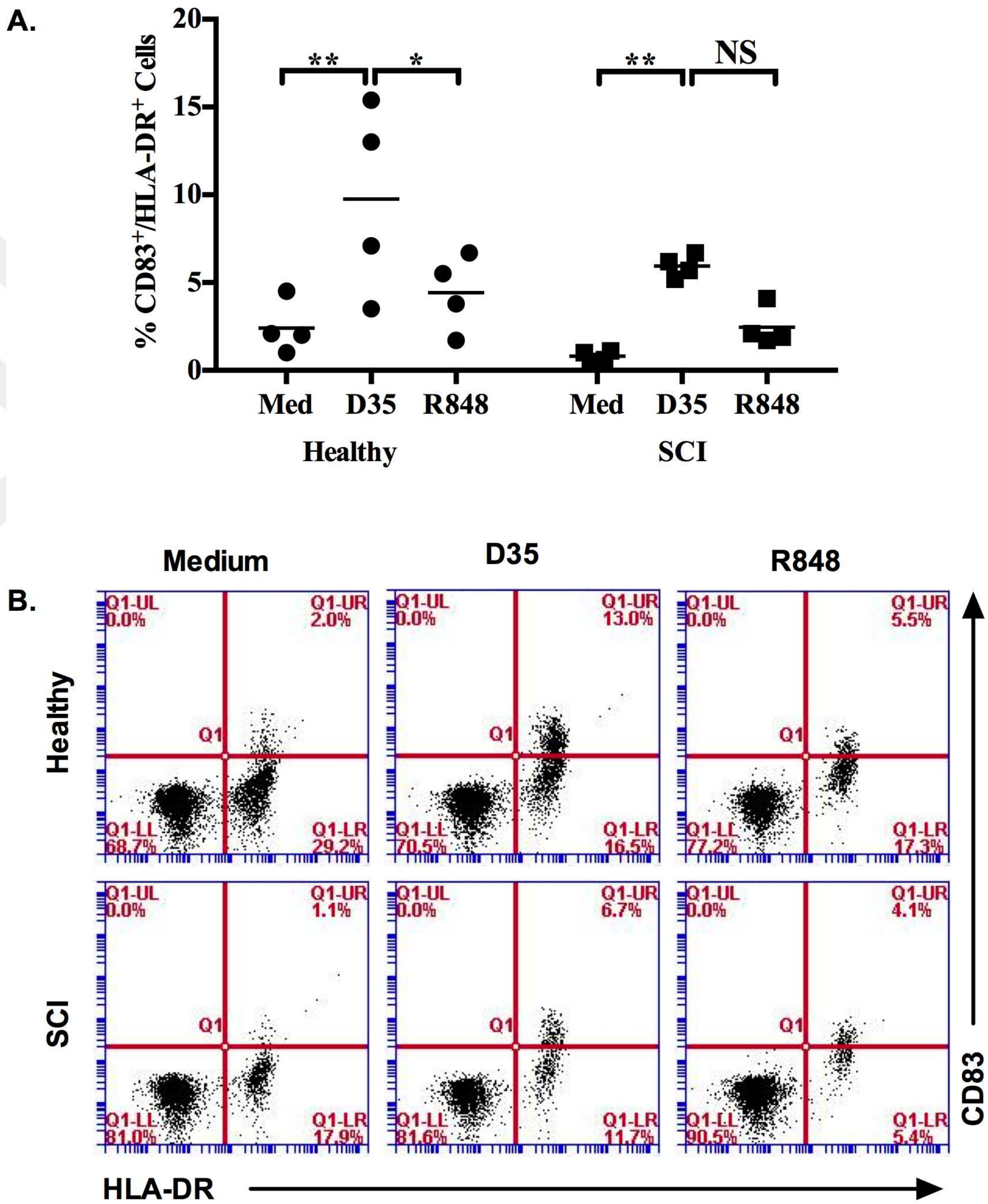

Fig 3. Co-stimulatory molecule and MHC-II expressions altered in response to TLR ligand stimulation of healthy and SCI PBMCs. PBMCs (10^6/ml) were stimulated with R848 (5μg/ml) or D35 (3μM) for 24h. (A) Average levels of CD83/HLA-DR double positive cells (n = 4), (B) Representative dot plots demonstrating double positive cell percent from PBMCs. During analyses 30000 cells were acquired. Two-way ANOVA with Bonferroni Correction was used to test the significance when compared to medium alone group. (*, $p \leq 0.05$; **, $p \leq 0.01$).

doi:10.1371/journal.pone.0171003.g003

producing T cells (Fig 4A and 4B, S4 Fig). This data demonstrated that dysfunctional immunity is not due to a defect in Th-1 arm of immune activation of SCI patient.

Moreover, from these PBMCs, we identified that the ability of monocytes to secrete IP10 was significantly impaired in response to D35 treatment. ELISA study suggested that IP10

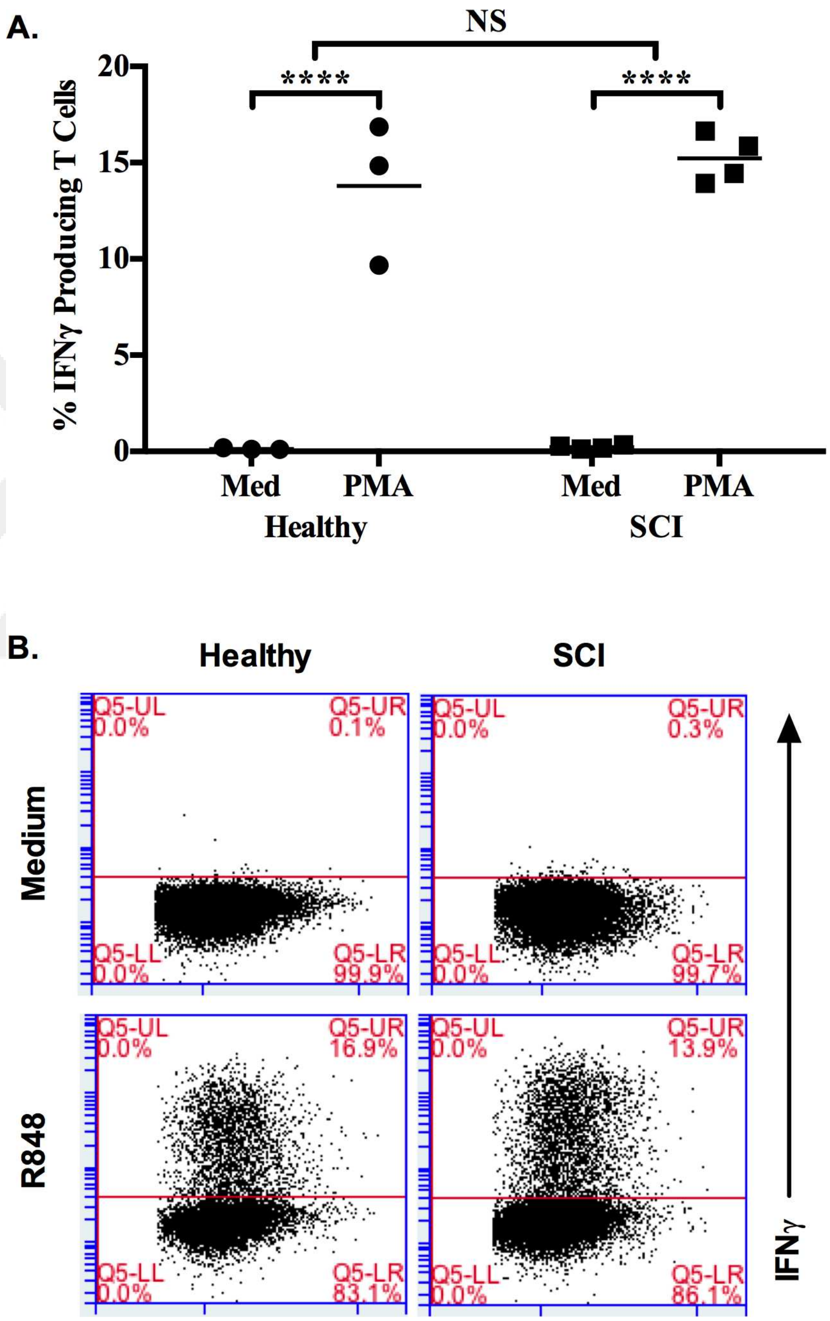

Fig 4. PMA-Ionomycin stimulation induced similar IFNγ producing T cells from healthy and SCI PBMCs. PBMCs (10^6/ml) were incubated with PMA-Ionomycin for 6h in the presence of Brefeldin A (10μl/ml). (A) % IFNγ producing T cell number by FACS analysis (Healthy = 3, SCI = 4), (B) Representative dot plots showing IFNγ$^+$/CD4$^+$ T cells. 50000 cells were acquired for the analysis. Mann-Whitney test was used to test significance between healthy and SCI responses. Two-way ANOVA with Bonferroni Correction was used to test the significance when compared to medium alone group. (NS, not significant; ****, $p \leq 0.0001$).

doi:10.1371/journal.pone.0171003.g004

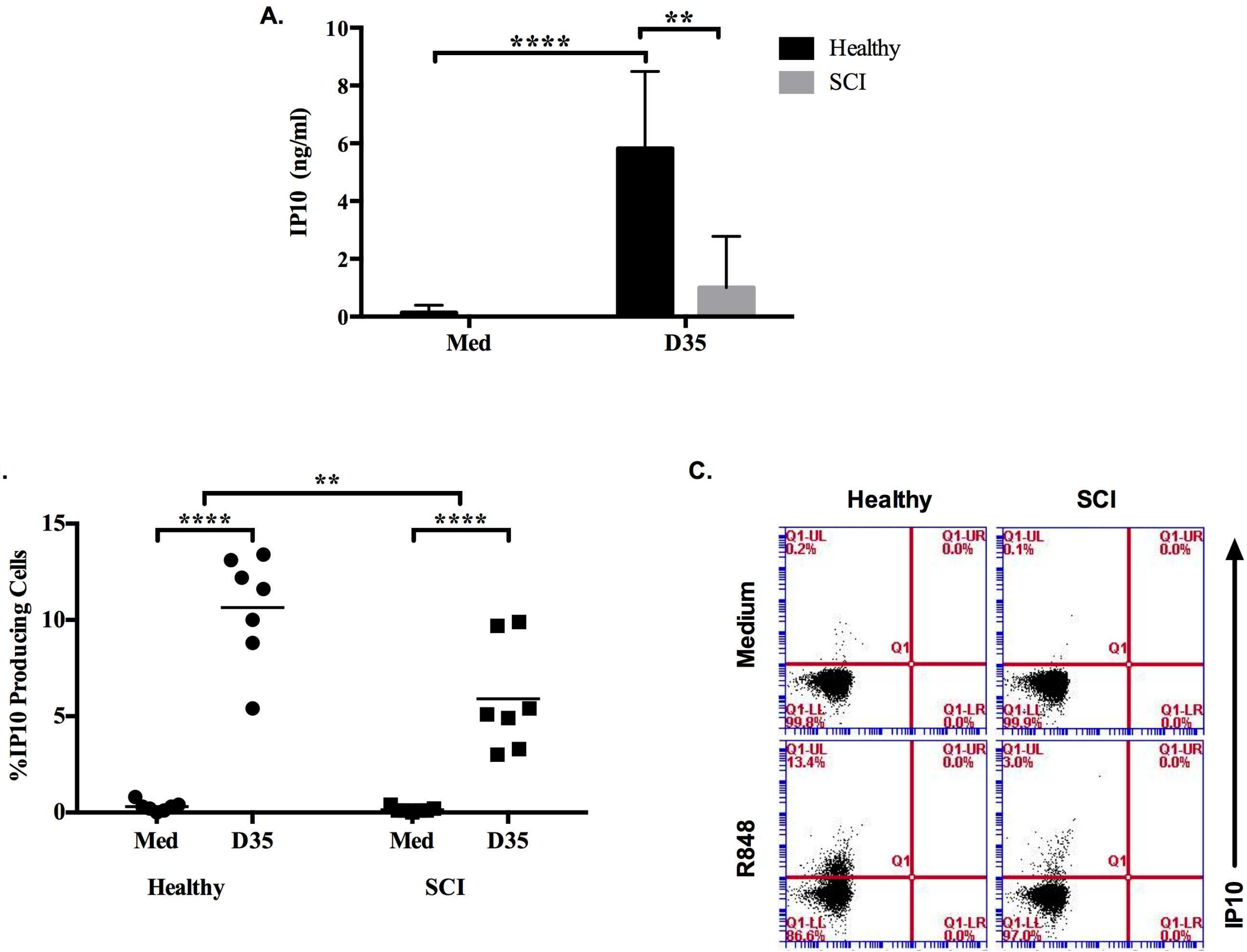

Fig 5. SCI monocytes are defective in IP10 production in response to D35 stimulation. PBMCs (2x10^5/200μl/well) were incubated with D35 (3μM) for 24h. (A) IP10 secretion levels of healthy (n = 5) and SCI (n = 10) PBMC supernatants. PBMCs (10^6/ml) were stimulated with D35 (3μM) for 20h, at 12h Brefeldin A (10μl/ml) was added. (B) Percent IP10 producing cells following intracellular cytokine staining of healthy (n = 7) and SCI (n = 7) PBMCs, (C) Representative dot plots showing IP10 producing monocytes. 30000 cells were acquired during the analysis. Mann-Whitney test was used to test significance between healthy and SCI responses to D35. Two-way ANOVA with Bonferroni Correction was used to test the significance when compared to medium alone group. (*, p≤0.05; **, p≤0.01; ****, p≤0.0001).

doi:10.1371/journal.pone.0171003.g005

production by healthy PBMCs but not SCI was significantly increased in response to D35 (Fig 5A). This increased IP10 production was further confirmed at cellular level by FACS analysis. The percentage of CD14$^+$/IP10$^+$ healthy monocytes significantly increased in response to TLR9 ligand stimulation (Fig 5B and 5C, S5 Fig).

When taken together our results revealed that although chronic SCI patient T cell responses to PMA-Ionomycin stimuli is functional, their monocytes are impaired in in response to both TLR7 and TLR9 ligand stimulations. These defects could contribute to persistent complications due to increased susceptibility to infections.

Discussion

In this study, we analyzed the status of innate and adaptive immune activation capacities of SCI patient PBMCs. The results revealed that there is a TLR7 and TLR9 mediated innate immune dysfunction in chronic phase of spinal cord injury. We further demonstrated that the diminished T-cell response is not due to the increase in CD4+ regulatory T-cells mediated IL10, but due to impaired Th1-biased IFNγ response. Furthermore, our findings suggested that although there is no significant reduction in response to TLR7 and 9 ligands by B-cells and pDCs, the ability of monocytes to get activated is defective (as evidenced by reduced IP10) in response to the existing innate cytokine milieu.

When animal and human data from the literature is taken into account, immune system dysfunction studies concerning innate and adaptive immune function of SCI patients are ambiguous [4–7, 16]. Furthermore, to our knowledge, there is no study attempted to establish the connection between 'TLR' mediated activation and their contribution to the immune dysfunction. Toll-like receptors are expressed on monocytes/macrophages, dendritic cells, T and B-lymphocytes of immune system cells. Stimulation of TLRs via PAMPS triggers multiple intracellular signaling cascades and establishes an inflammatory cytokine/chemokine milieu and contributes to shape adaptive immune responses [17, 18, 19]. In addition, TLRs are able to recognize endogenous molecules, which are called as danger-associated molecular patterns (DAMPs) [20, 21, 22]. This recognition results with sterile inflammatory processes in various pathological states [23].

In our study, SCI patients and healthy donors presented similar response to TLR7 and TLR9 ligands which implicates that the dysfunction in SCI patients is not due impaired pDC or B cell functions (Fig 1A and 1B). In previous studies regarding innate immune responses of SCI patients, Riegger et al, showed a decrease in $ED9^+$ monocytes on early stages of experimental spinal cord injury rat model. But they reported that, on the following days of the injury (day 14), $ED9^+$ monocytes recovered to almost control levels. Also, in the same study, HIS 48^+ granulocyte levels of animals were not different from sham operated controls on day 14 [16]. Riegger et al [24] performed another study in humans and demonstrated that $CD14^+$ monocytes decreased on the first week of spinal cord injury but on chronic stages (day 105–136), monocyte number reached a plateau control levels and there is no decrease in $CD15^+$ granulocyte number. Here, we demonstrated that although the numbers of monocytes are similar between SCI vs. healthy subjects, their ability to secrete one of the cardinal monocyte-specific IP10 cytokine is impaired in response to R848 and D35 (Fig 2A and Fig 5A and 5B).

Impaired natural killer (NK) cell function is another difference demonstrated in patients with SCI. Cruse et al [25] and Campagnolo et al [4] showed NK cell dysfunction in their studies. In the study of Campagnolo et al [4], the patients were divided into two groups according to level of injury. Although they did not find statistically significant difference between the groups above and below T-6 level, they showed reduction in NK cell numbers and cytotoxicity when compared with healthy group. In present study, reduced IFNγ levels in response to TLR ligand stimulation could support this view, although we did not elaborated on NK-specific interferon production. Further studies are planned to understand this issue.

Here, additionally we checked T cell response rates of both groups via intracellular cytokine staining method. The patient group demonstrated similar increase in T cell response against healthy control group (Fig 1D). This finding was also supported at the cellular level since both SCI patients and healthy donors had almost same level of increase in IFNγ producing T cells in response PMA-Ionomycin (Fig 4A). This finding is in contrast to the data of Campagnolo et al [4]. They showed a significant increase in the percent of T cells and helper cells ($CD3^+$, $CD4^+$) in SCI patients when compared with healthy controls. Furthermore, T cell responsiveness was emphasized in several other studies [5, 16, 25], however, in these reports, patients were predominantly in acute or sub-acute stages of spinal cord injury limiting accurate comparison with regard to the findings in the present study.

There are some limitations of our study. The sample size of each experiment was different and in some experiments, sample size of patient and healthy subjects was relatively limited. But the unique strengths of the present study rely on the patient inclusion criteria. Here, we intentionally included only complete SCI patients above level of T-6 to exclude the potential impact of the autonomic nerve system on the immune system and included only chronic SCI patients in order to exclude the effects of both infections of the acute and sub-acute stages and the obscuring contributions of medication such as steroids.

Conclusion

These results might explain the underlying cause for infection susceptibility in the chronic phase of spinal cord injury, especially concerning the innate immune mediated immune activations. More detailed analyses should be planned to explore potential therapeutic targets, thereby helping chronic SCI patients to alleviate susceptibility to infection.

Supporting information

S1 Fig. Plot Illustrating post injury time of SCI patients (n = 17).
(TIFF)

S1 Table. Detailed information about the antibodies used throughout the study. (A) ELISA and FACS antibodies, (B) Recombinant standard antibodies used in the ELISA studies.
(TIFF)

S2 Fig. Representative FACS analysis plots of IFNγ producing T cells. Healthy donor (upper panels) and SCI patient (lower panels) PBMCs were incubated in either medium only or R848. IFNγ signal was detected from $CD4^+$ positive T cells.
(TIFF)

S3 Fig. Representative FACS analysis plots of $CD83^+$ and $HLA\text{-}DR^+$ cells. (A) Healthy donor and (B) SCI patient PBMCs were stimulated with either D35 or R848.
(EPS)

S4 Fig. Representative FACS analysis plots of IFNγ producing T cells. Healthy donor (upper panels) and SCI patient (lower panels) PBMCs were incubated in either medium only or PMA-Ionomycin. IFNγ signal was detected from $CD4^+$positive T cells.
(TIFF)

S5 Fig. Representative FACS analysis plots of IP10 producing monocytes. Healthy donor (upper panels) and SCI patient (lower panels) PBMCs were incubated in either medium only or D35. IP10 signal was detected from $CD14^+$ positive cells.
(TIFF)

Author contributions

Conceptualization: IG BY MG.

Data curation: GG EA IG.

Formal analysis: EA GG.

Funding acquisition: IG.

Investigation: GG EA BG TK.

Methodology: IG BY MG GG EA.

Project administration: IG.

Resources: IG BY MG.

Software: EA GG BG TK.

Supervision: IG BY MG.

Validation: GG EA BG TK IG BY MG.

Visualization: GG EA.

Writing – original draft: IG BY GG EA.

Writing – review & editing: IG GG EA.

References

1. DeVivo MJ, Krause JS, Lammertse DP. Recent trends in mortality and causes of death among persons with spinal cord injury. Arch Phys Med Rehabil. 1999; 80:1411–1419. PMID: 10569435
2. Lidal IB, Snekkevik H, Aamodt G, Hjeltnes N, Biering-Sørensen F, Stanghelle JK. Mortality after spinal cord injury in Norway.J Rehabil Med. 2007; 39:145–51. doi: 10.2340/16501977-0017 PMID: 17351697
3. Takeda K, Kaisho T, Akira S. Toll-like Receptors. Annu. Rev. Immunol. 2003; 21:335–76. doi: 10.1146/annurev.immunol.21.120601.141126 PMID: 12524386
4. Campagnolo DI, Dixon D, Schwartz J, Barlett JA, Keller SE. Altered innate immunity following spinal cord injury. Spinal Cord. 2008; 46:477–481. doi: 10.1038/sc.2008.4 PMID: 18268516
5. Campagnolo DI, Keller SE, DeLisa JA, Glick TJ, Sipski ML, Schleifer SJ. Alteration of immune system function in tetraplegics. A pilot study. Am J Phys Med Rehabil. 1994; 73:387–393. PMID: 7993612
6. Campagnolo DI, Bartlett JA, Keller SE. Influence of neurological level on immune function following spinal cord injury: a review. J Spinal Cord Med. 2000; 23:121–128. PMID: 10914353
7. Allison DJ, Ditor DS. Immune dysfunction and chronic inflammation following spinal cord injury. Spinal Cord. 2015; 53:14–18 doi: 10.1038/sc.2014.184 PMID: 25366531
8. Fallarino F, Gargaro M, Mondanell G, Downer EJ, Hossain MJ, Gran B. Delineating the Role of Toll-Like Receptors in the Neuro-inflammation Model EAE. Methods Mol Biol. 2016; 1390:383–411 doi: 10.1007/978-1-4939-3335-8_23 PMID: 26803641
9. Leszek J, Barreto GE, Gąsiorowski K, Koutsouraki E, Ávila-Rodrigues M, Aliev G. Inflammatory Mechanisms and Oxidative Stress as Key Factors Responsible for Progression of Neurodegeneration: Role of Brain Innate Immune System. CNS Neurol Disord Drug Targets. 2016; 15(3):329–36 PMID: 26831258
10. Davies AL, Hayes KC, Dekaban GA. Clinical correlates of elevated serum concentrations of cytokines and autoantibodies in patients with spinal cord injury. Arch Phys Med Rehabil 2007; 88: 1384–1393. doi: 10.1016/j.apmr.2007.08.004 PMID: 17964877
11. Gibson a E, Buchholz C, Martin Ginis K. C-Reactive protein in adults with chronic spinal cord injury: increased chronic inflammation in tetraplegia vs paraplegia. Spinal Cord 2008; 46: 616–621 doi: 10.1038/sc.2008.32 PMID: 18414426
12. Liang H, Mojtahedi MC, Chen D, Braunschweig CL. Elevated C-reactive protein associated with decreased high-density lipoprotein cholesterol in men with spinal cord injury. Arch Phys Med Rehabil 2008; 89: 36–41 doi: 10.1016/j.apmr.2007.08.121 PMID: 18164328
13. Held KS, Steward O, Blanc C, Lane TE. Impaired immune responses following spinal cord injury lead to reduced ability to control viral infection. Exp Neurol 2010; 226: 242–253 doi: 10.1016/j.expneurol.2010.08.036 PMID: 20832407
14. Lucin KM, Sanders VM, Jones TB, Malarkey WB, Popovich PG. Impaired antibody synthesis after spinal cord injury is level dependent and is due to sympathetic nervous system dysregulation. Exp Neurol 2007; 207: 75–84 doi: 10.1016/j.expneurol.2007.05.019 PMID: 17597612

15. Rowland JW, Hawr yluk GWJ, Kwon B, Fehlings MG. Current status of acute spinal cord injury pathophysiology and emerging therapies: promise on the horizon. Neurosurg. Focus 2008; 25(5), E2. doi: 10.3171/FOC.2008.25.11.E2 PMID: 18980476

16. Riegger T, Conrad S, Liu K, Schluesener HJ, Adibzahdeh M, Schwab JM. Spinal cord injury-induced immune depression syndrome (SCI-IDS). European Journal of Neuroscience. 2007; 25:1743–1747. doi: 10.1111/j.1460-9568.2007.05447.x PMID: 17432962

17. Mills KH. TLR-dependent T cell activation in autoimmunity. Nat Rev Immunol. 2011, 11: 807–822 doi: 10.1038/nri3095 PMID: 22094985

18. Ozinsky A, Underhill DM, Fontenot JD, Hajjar AM, Smith KD, Wilson CB, et al. The repertoire for pattern recognition of pathogens by the innate immune system is defined by cooperation between toll-like receptors. Proc Natl Acad Sci. 2000; 97:13766–13771. doi: 10.1073/pnas.250476497 PMID: 11095740

19. Medzhitov R. Toll-like receptors and innate immunity. Nat Rev Immunol. 2001; 1:135–145. doi: 10.1038/35100529 PMID: 11905821

20. Imai Y, Kuba K, Neely GG, Yaghubian-Malhami R, Perkmann T, van LG, et al. Identification of oxidative stress and Toll-like receptor 4 signaling as a key pathway of acute lung injury. Cell 2008, 133: 235–249 doi: 10.1016/j.cell.2008.02.043 PMID: 18423196

21. Midwood K, Sacre S, Piccinini AM, Inglis J, Trebaul A, Chan E, et al. Tenascin-C is an endogenous activator of Toll-like receptor 4 that is essential for maintaining in ammation in arthritic joint disease. Nat Med 2009, 15: 774–780. doi: 10.1038/nm.1987 PMID: 19561617

22. West XZ, Malinin NL, Merkulova AA, Tischenko M, Kerr BA, Borden EC, et al. Oxidative stress induces angiogenesis by activating TLR2 with novel endogenous ligands. Nature 2010, 467: 972–976 doi: 10.1038/nature09421 PMID: 20927103

23. Takeuchi O, Akira S. Pattern recognition receptors and inflammation. Cell 2010, 140: 805–820 doi: 10.1016/j.cell.2010.01.022 PMID: 20303872

24. Riegger T, Conrad S, Schluesener HJ, Kaps H-P, Badke A, Baron C, et al. Immune depression syndrome following human spinal cord injury (SCI): a pilot study. Neuroscience. 2009; 158:1194–1199. doi: 10.1016/j.neuroscience.2008.08.021 PMID: 18790013

25. Cruse JM, Lewis RE, Bishop GR, Kliesch WF, Gaitan E. Neuroendocrine-immune interactions associated with loss and restoration of immune system dysfunction in spinal cord injury and stroke patients. Immunol Res. 1992; 11:104–116. PMID: 1331272

Title:	Membrane vesicles as conveyors of immune responses	Logged in as: Gozde Gucluler
Author:	Clotilde Thery, Matias Ostrowski and Elodie Segura	LOGOUT
Publication:	Nature Reviews Immunology	
Publisher:	Nature Publishing Group	
Date:	Jun 5, 2009	

Order Completed

Thank you for your order.

This Agreement between Gozde Gucluler ("You") and Nature Publishing Group ("Nature Publishing Group") consists of your license details and the terms and conditions provided by Nature Publishing Group and Copyright Clearance Center.

Your confirmation email will contain your order number for future reference.

Printable details.

License Number	4057670428791
License date	Feb 28, 2017
Licensed Content Publisher	Nature Publishing Group
Licensed Content Publication	Nature Reviews Immunology
Licensed Content Title	Membrane vesicles as conveyors of immune responses
Licensed Content Author	Clotilde Thery, Matias Ostrowski and Elodie Segura
Licensed Content Date	Jun 5, 2009
Licensed Content Volume	9
Licensed Content Issue	8
Type of Use	reuse in a dissertation / thesis
Requestor type	academic/educational
Format	print and electronic
Portion	figures/tables/illustrations
Number of figures/tables/illustrations	1
High-res required	no
Figures	Different types of secreted membrane vesicles
Author of this NPG article	no
Your reference number	
Title of your thesis / dissertation	IMMUNOTHERAPEUTIC ACTION OF EXTRACELLULAR VESICLES AND EFFECTS OF TLR SIGNALING TO IMMUNE DYSFUNCTION OF SCI PATIENTS
Expected completion date	Mar 2017
Estimated size (number of pages)	200
Requestor Location	Gozde Gucluler Bilkent Universitesi Fen FAkultesi MBG Departmani Ankara, 06800 Turkey Attn: Gozde Gucluler
Billing Type	Invoice
Billing address	Gozde Gucluler Bilkent Universitesi Fen FAkultesi MBG Departmani

Ankara, Turkey 06800
Attn: Gozde Gucluler

Total	0.00 USD

ORDER MORE CLOSE WINDOW

ANNUAL REVIEWS

Title: Biogenesis, Secretion, and Intercellular Interactions of Exosomes and Other Extracellular Vesicles

Author: Marina Colombo, Graça Raposo, Clotilde Théry

Publication: Annual Review of Cell and Developmental Biology

Publisher: Annual Reviews

Date: Oct 11, 2014

Permission Not Required

Material may be republished in a thesis / dissertation without obtaining additional permission from Annual Reviews, providing that the author and the original source of publication are fully acknowledged.